THE UNIVERSITY of EDINBURGH

Title	Biochemical studies on gelsolin : actin complexes and experiments to form a minimal, defined-length actin filament
Author	Wear, Martin Alexander
Qualification	PhD
Year	2000

Biochemical studies on gelsolin:actin complexes and experiments to form a minimal, defined-length actin filament

Martin Alexander Wear

Ph. D. Thesis

The University of Edinburgh

2000

Declaration

This thesis was composed and written by myself and I personally carried out the work described.

Martin Wear

This thesis is dedicated to my wife Elaine for her love, support and a never-ending supply of patience. (We'll always have those memories!!!)

Acknowledgements

I owe my supervisor, Dr. Paul McLaughlin, a very large debt of gratitude, for two reasons. Firstly, for giving me the opportunity of gaining my Ph. D. and secondly (and more importantly), for the unstinting patience and support he has furnished me with, right from the very beginning. Without such understanding, completing my thesis would have been a much more arduous and time-consuming endeavour.

I would also like to thank Dr. Sutherland Maciver for sharing his extensive experience and knowledge of the actin cytoskeleton field, and for his numerous invaluable and informative discussions. Similarly, my thanks are extended to Dr. Steve Winder and Dr. Lindsay Sawyer for encouragement and helpful suggestions during the course of my thesis.

I am further indebted to Dr. Holger Husi, and would like to acknowledge (with much appreciation) the help and direction he supplied me with and also for the divulgence of some priceless unwritten "tricks-of-the-trade" for survival in the lab.

Gratitude is also extended to a large number of other individuals (too numerous to name) who gave me huge amounts of encouragement during my studies, and helped keep me sane (especially Nathan Cowieson and Dr. Janice Bramham; cheers guys!).

Finally, thanks to all my family and friends who supported me throughout with lots of love and encouragement.

Abstract

A number of important eukaryotic cellular processes (including movement, endocytosis and generation of cytokinetic forces) are mediated by the dynamic turnover of the actin cytoskeleton. Many actin-binding proteins control this turnover of actin filaments; e.g. gelsolin, a Ca^{2+} and PIP_2 regulated actin filament severing and capping protein.

In this thesis we report the formation of a putative "capped-actin-minifilament" complex. This was created by combining the gelsolin:$actin_2$ ternary ($G:A_2$) and the actin:DNaseI binary (A:D) complexes together (1:1 molar ratio) under polymerising conditions (100mM KCl; 2mM $MgCl_2$ in the presence of 0.2mM $CaCl_2$). Size-exclusion data indicates the formation of a significantly larger species (in relation to $G:A_2$), with an apparent stoichiometry of **$G:A_3:D$** (gelsolin:actin:DNaseI, respectively).

Kinetic and modelling evidence (Weber et al, 1994) suggests that the binding of *two* DNaseI molecules at the pointed-end of filaments is not possible due to a steric clash. Using DNaseI's ability to bind at the pointed-ends of actin monomers, we have probed the disposition of the monomers in the $G:A_2$ complex. Size-exclusion, native-PAGE and fluorescence enhancement data (performed with NBD-Actin) indicate the formation of a stable, co-operative complex with a stoichiometry of **$G:A_2:D_2$** (gelsolin:actin:DNaseI, respectively). The apparent K_d of A:D binding to the gelsolin:actin binary complex (G:A) is ~ 50nM, and is equivalent to the binding of G-Actin alone (K_d ~ 39nM). Our data are consistent with DNaseI having *no* effect on the interaction of actin monomers with gelsolin, and with the spatial orientation of monomers in $G:A_2$ being *different* to those at the barbed-end of filaments.

In contrast to this, data from fluorescence enhancement experiments with rhodamine-phalloidin (an actin *filament specific* binding molecule) provide evidence for the actin monomers, within the putative "minifilament", being in a filamentous-like conformation. We observe a specific binding, with significant levels of fluorescence enhancement (~ 3 – 4 fold), of rhodamine-phalloidin to the putative "minifilament", with an apparent K_d of ~ 4.6μM.

We have also examined the possibility of replacing gelsolin (as the barbed-end capping protein) with a cloned polypeptide fragment derived from tensin, a component of focal adhesions. This polypeptide spans the region of tensin that contains the sequence of "insertin", previously identified as possessing a controversial high-affinity barbed-end capping activity (Ruhnau et al, 1989). Our results are consistent with this polypeptide not binding to monomeric actin, and it therefore not being a suitable alternative to gelsolin, for further analysis of the putative "minifilament". However, we have studied its interaction with filamentous actin. We report data that is consistent with the *tight* capping of the barbed-end (K_{cap} of ~ 6 - 8nM). Our construct causes a shift in the steady-state critical monomer concentration towards that of the pointed-end, consistent with it possessing a *non*-"insertin-like" activity. We also report a novel F-Actin side-binding activity for this polypeptide, with an apparent K_d of ~ 10μM.

Abbreviations

2xTY:	2 x yeast-tryptone extract
ABD:	Actin-binding domain
A_{280}/Abs_{280}:	Absorbance at a given wavelength in nm
ABPs:	Actin-binding proteins
A:D:	Actin:DNaseI binary complex
A_{nbd}:D:	Actin:DNaseI binary complex, with the actin labelled with NBD
ADP:	Adenosine diphosphate
AMP:	Ampicillin
APS:	Ammonium persulphate
ATP:	Adenosine triphosphate
BCA:	Bicinchoninic acid
BSA:	Bovine serum albumin
$[C_c]$:	Actin critical monomer concentration
Da.:	Dalton
DEAE:	Diethylaminoethyl
ΔF_{max}:	Maximal difference in fluorescence intensity (arbitrary units)
DMF:	Dimethylformamide
DMSO:	Dimethylsulphoxide
DNaseI:	Deoxyribonuclease I
DTT:	Dithiothreitol
ECM:	Extra-cellular matrix
EDTA:	Ethylenediamine-tetra-acetic acid
EGTA:	Ethylene glycol-bis-[β-aminoethyl ether]-N,N,N',N'-tetra-acetic acid
EM:	Electron microscopy
F.:	Fluorescence intensity (arbitrary units)
F-Actin:	Filamentous actin
FPLC:	Fast protein liquid chromatography
G1 – G6:	Gelsolin domains (numbered G1, G2, G3, G4, G5 and G6).
G:A:	Gelsolin:actin binary complex
G:A_2:	Gelsolin:$actin_2$ ternary complex
G-Actin:	Monomeric actin
GA_2:D_2:	Gelsolin:$actin_2$:$DNaseI_2$ complex
GA_3D:	Gelsolin:$actin_3$:DNaseI – putative "minifilament" complex
HGS:	Human cytoplasmic gelsolin
IPTG:	Isopropyl-β-D-thio-galactopyranside
K_{cap}:	Concentration of capping protein that causes a 50% inhibition in the initial rate of actin polymerisation
kDa.:	Kilodaltons
λem:	emission wavelength, in nm
λex:	excitation wavelength, in nm
Mr.:	Molecular weight, in daltons or kilodaltons
NBD:	4-chloro-7-nitro-2,1,3-benzoxadiazole
NBD-Actin:	4-chloro-7-nitro-2,1,3-benzoxadiazole labelled monomeric actin
NEM:	N-ethylmaleimide
NHS:	N-hydroxysuccinamide
P:	Pellet fraction

PIP_2:	Phosphatidylinositol-4,5-bisphosphate
PMSF:	Phenylmethylsulfonyl fluoride
S200:	Sephacryl 200 size-exclusion resin
S-1:	Myosin sub-fragment 1
SD:	Standard deviation
SDS-PAGE:	Sodium dodecylsulphate polyacrylamide gel electrophoresis
SEM:	Standard error of the mean
S/N:	Supernatant fraction
S/N50:	Supernatant fraction following centrifugation for 1hr at 50,000 xg
STREP:	Streptomycin
TEMED:	N,N,N',N'-tetramethyl-ethylenediamine
THI:	Thiamine
Tris:	2-Amino-2-(hydroxymethyl)-1,3-propanediol
V_t:	total resin-bed volume, in ml

Table of contents

Table of figures

1. Introduction

1.1 Overview

Our knowledge of the structure of actin filaments is only at low resolution and the details of the intermolecular contacts at the atomic level are, at best, only approximate. We consider here approaches to form a minimal stable unit, representative of these contacts, using well defined actin monomer-binding proteins as tools in the controlled definition of this minimal complex, with the ultimate aim being to crystallise such a complex. Development of this argument is discussed in the proceeding sections; we first introduce the biochemistry and cell biology of actin in order to clarify why knowledge of the filament structure (at atomic detail) is an important biological problem; we further describe the properties of the actin-binding proteins (ABPs) we use; finally we describe our hypothesis and rationale to attempt to produce a mono-disperse molecular complex representative of the subunit:subunit contacts within an actin filament.

1.2 An introduction to actin

Actins comprise a highly conserved family of cytoplasmic proteins found in all eukaryotes and can constitute upwards of ~ 10 – 15% of the total cellular protein. No actin has been found, so far, in any prokaryotes. Large numbers of isoforms have been identified and purified from animal, plant, protozoan and fungal sources and are often differentially expressed in tissue specific as well as specific intracellular locations (Vandekerckhove and Weber, 1979; Herman, 1993; Sheterline et al, 1995).

Early experiments analysing the various aspects of eukaryotic cell motility, and the role actin played in this function, utilised potent actin-binding toxins isolated from several sources including fungi (e.g. the cytochalasins and phalloidin) and marine sponges (the latrunculins) (Cooper, 1987; Sampath and Pollard, 1991; Faulstich and Wieland, 1996; Ayscough, 1998). It was clear from the action of these drugs on the actin cytoskeleton, that the actin structures within the cell were highly *dynamic*,

(cycling between populations of polymers and monomers), and played central roles in a number important cellular processes, e.g. maintaining cell size and shape, motility, cytokinesis, competent vesicular traffic (Sheterline et al, 1995; Stossel et at al 1999; Goode et al, 2000; Rogers and Gelfand, 2000; Borisy and Svitkina, 2000). The functional form of actin *in vivo* is a non-covalent filamentous polymer (F-Actin). Under physiological ionic conditions (~ 50 - 100mM KCl, pH ranging from 7.0 - 8.0 and 1 - 2mM free Mg^{2+}) F-Actin assembles spontaneously *in vitro* from pools of the monomer (G-Actin), a globular protein of approximately 42kDa.

1.3 Actin polymerisation

The first steps of the spontaneous polymerisation process for actin can be described as indicated in fig. 1.1. Polymerisation is initiated by the activation of actin monomers. This probably takes place by the binding of Mg^{2+} at a high-affinity site (see fig. 1.5) and also by the binding of mono- and divalent cations to several low affinity sites on the monomer. This activated monomer appears to undergo subtle conformational changes that result in nucleation and then subsequent polymerisation (Rich and Estes, 1976; Rouayrenc and Travers, 1981; Frieden, 1982; Shu et al, 1992). The nucleus for polymerisation is usually defined as the smallest actin oligomer that is more likely to remain stable long enough for another monomer to add than to dissociate into monomers. Kinetic analysis of polymerisation curves (Frieden, 1985; Pollard and Cooper, 1986) and solution scattering studies (Matsudaira et al, 1987) appear to indicate that this nucleus is a trimer.

Nucleation is the rate-limiting step in the spontaneous polymerisation of actin. Diffusion limited association rate constants ($10^7 M^{-1}.s^{-1}$) and dissociation rate constants in the range of $10^6 - 10^7 s^{-1}$ mean that the intermediates of the nucleation stage are very unstable, and this energetically unfavourable stage gives rise to the lag phase seen during polymerisation (Pollard and Cooper, 1986). During spontaneous polymerisation of 10 – 20μM actin, the concentrations of dimers and trimers is expected to be very low («nM) and their lifetimes very short (Freiden, 1985).

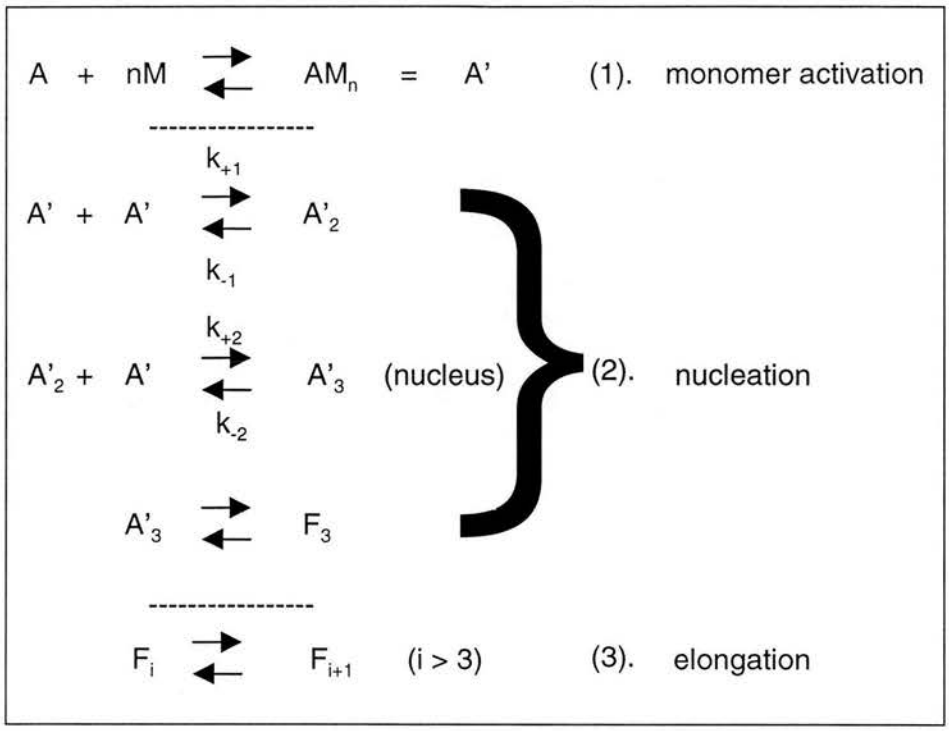

Fig. 1.1. ***Kinetic scheme describing the first steps of the polymerisation process.*** The polymerisation of actin can be divided into four steps (steps 1 – 3 are illustrated above): 1. activation (the actin monomer is "activated" probably by the binding of Mg-ATP at the tight nucleotide binding-site and the binding of mono- or divalent cations to several low affinity sites; Carlier, 1991); 2. nucleation (the formation of oligomers that have a higher probability of growing into filaments rather than dissociating into monomers); 3. elongation (the end-wise addition of monomers onto both ends of polymers); 4. annealing (the end-to-end joining of two filaments). A' represents the "activated" monomer (either Ca-ATP-Actin or Mg-ATP-Actin) and M represents the various cations (e.g. Na^+, Mg^{2+}, K^+, Ca^{2+}), that bind to several low affinity sites, resulting in "activation" of that monomer. Activation is followed by the formation of an energetically unfavourable trimer nucleus. This is then subsequently followed by elongation of the nuclei by end-wise addition of actin monomers onto both ends of the polymer. The association rate constants for the formation of the trimer nucleus appear to be diffusion limited (e.g. k_{+1} and $k_{+2} \approx 10^7 M^{-1}.s^{-1}$) with the dissociation rate constants in the range of $10^6 - 10^7 s^{-1}$. Thus, nucleation is the rate-limiting step in the spontaneous polymerisation of actin because the reactions are so unfavourable, with dissociation constants of ~ 0.1 – 1.0M. ($K_{d1} = k_{-1}/k_{+1}$ ~ 0.1M; $K_{d2} = k_{-2}/k_{+2}$ ~ 0.1M, Frieden, 1985; Pollard and Cooper, 1986). These large dissociation rates emphasise the instability of the intermediates of nucleation, and the formation of these trimer-nuclei is responsible for the lag-phase at the outset of polymerisation.

In vitro under physiological ionic conditions (~ 100mM KCl, pH ~ 7.0 - 8.0, ~ 2mM free Mg^{2+}) the critical concentration (below which filaments dissociate or do not form) of the Mg^{2+}-ATP bound monomer is ~ 0.1μM or greater (Pollard, 1986; Carlier, 1991; Sheterline et al, 1995). The ionic composition of the buffer solution

(variations in salt concentration, the type and concentration of mono- and divalent cations present, and pH) used to initiate actin polymerisation, has *very* marked effects on the kinetics of assembly and disassembly and on the monomer critical concentration (Frieden, 1982; Brenner and Korn, 1983; Gershman et al, 1984; Coué and Korn, 1985; Pollard, 1986; Zimmerle and Frieden, 1988a/b/c; Wang et al, 1989; Kinosian et al, 1993; Sheterline et al, 1995). Typical purification procedures, usually involving the extraction of actin from rabbit muscle acetone powders (Spudich and Watt, 1971), take advantage of the higher critical concentration of Ca^{2+}-ATP-Actin to aid recovery of the monomeric form (G-Actin).

Actin filaments in non-muscle cells undergo rapid turnover, with cycles of assembly and disassembly occurring over a period of minutes. Actins possess an intrinsic ATPase activity and bound ATP (under physiological conditions Mg^{2+}-ATP is bound at the high affinity site) becomes hydrolysed after incorporation into the filament (Korn et al, 1987; Pollard et al, 1992). Hydrolysis lags behind polymerisation and as a result elongating filaments possess an evolving population of monomers. Typically this involves a cap of ATP-Actin at the *barbed-end* (see section 1.5 and fig. 1.4), a section of ADP.Pi-actin (due to the relatively slow release of the hydrolysed phosphate), followed by a *pointed-end* consisting only of ADP-Actin (Carlier, 1991; Sheterline et al, 1995). The net result of ATP hydrolysis is a difference in the kinetics of association and disassociation at either end of the actin filament; actin filaments therefore possess *polarity* (see fig. 1.4). ATP hydrolysis acts as a chemical switch that maintains the dynamic nature of F-Actin.

Due to the differences in the kinetics of monomer addition and dissociation at each end filament growth is unidirectional, with overall elongation occurring by the rapid addition of ATP-Actin to the *faster* growing *barbed-end* and loss of ADP-Actin from the *slower* growing *pointed-end* (Frieden, 1985; Pollard and Cooper, 1986; Pollard, 1986; Korn et al, 1987; Carlier, 1991; Sheterline et al, 1995). At steady-state the phenomenon of "treadmilling" occurs (Wanger et al, 1985). During treadmilling the net length of the filaments remains constant but a cycling of actin subunits occuring, essentially with the loss of ADP-Actin from the pointed-ends and addition of ATP-

Actin to the barbed-ends. It appears that the main consequence of ATP hydrolysis in F-actin is to destabilise actin:actin interactions in the filament and facilitate depolymerisation. This destabilisation probably occurs due to slight changes in the actin monomer structure conformation, thus causing loss of binding energy (Bremer et al, 1991; Orlova and Egelman, 1992).

1.4 The cortical actin cytoskeleton

In eukaryotic cells the actin cytoskeleton consists of a gel-like cortex of actin filaments that underlies the plasma membrane. Dynamic changes in the organisation of this actin cytoskeleton have been closely linked to a large number of important cellular processes, including changes in the size and shape of cells, the formation and regulation of focal contacts (see below), generation of cytokinetic forces (a process mediated by myosin in an ATP dependent manner; Sellers and Goodson, 1995) and the mobility of cells in response to signalling events (Burridge and Chrzanowska-Wodnicka, 1996; Taylor et al, 1998; Stossel et al, 1999; Critchley, 2000; Rogers and Gelfand, 2000; Borisy and Svitkina, 2000).

Within this cytoplasmic cortex individual arrays of assembled actin filaments are further organised into three-dimensional networks by a large collection (~ 80) of Actin-Binding Proteins (ABPs) (Pollard, 1993; Sheterline et al, 1995; Van Troys et al, 1999). Several broad (and sometimes over-lapping) groups of ABPs have been defined depending on the type of interaction they exhibit with actin filaments. The major categories of ABP function include; motor proteins (myosins, see section 1.5), filament-stabilising proteins (tropomyosins), filament de-stabilising proteins (cofilins), cross-linking proteins (e.g. villin, fimbrin and α-Actinin; Matsudaira, 1991), anchorage proteins that link the actin cytoskeleton to the plasma membrane (e.g. talin, tensin; Taylor et al, 1998), end-binding proteins (capping protein; Schafer and Cooper, 2000) and severing proteins (gelsolin and the numerous member of the gelsolin family; Maciver and Weeds, 1993). Actin filaments, along with the unpolymerised cytosolic actin - associated with monomer sequestering proteins in the cytoplasm, principally β4-thymosin and profilin (Theriot and Mitchison, 1993;

Sun et al, 1996) - are in a constant state of flux in response to interaction and regulation by these ABPs, and ultimately signal transduction pathways initiated at the surface of the cell. It is these ABPs that allow non-muscle cells to transmit force *per se* and exert spatial and temporal control over the three-dimensional actin cytoskeleton. This allows for vesicle translocation along the filaments, cytoplasmic streaming and the generation of movement and the associated myosin mediated forces involved in cytokinesis (Stossel et al, 1999; Rogers and Gelfand, 2000).

Although this actin cortex lacks the highly ordered structure of the acto-myosin array in muscle (see section 1.5), it nevertheless presents several characteristic higher-order actin structures that arise due to the interaction of numerous ABPs with the actin filaments (Sheterline et al, 1995). These higher-order actin structures include focal contacts (complex multi-protein arrays that act as attachment sites and mediate signals between the actin cytoskeleton and the plasma membrane; Critchley, 2000), anti-parallel arrays of actin filaments that form stress fibres (the cytoplasmic homologue of myofibrils) and less obvious bundles and parallel arrays of F-actin that form dynamic protrusive structures (e.g. microspikes or filopodia) at the surface of the cell, see fig. 1.2 (Furukawa and Fechheimer, 1997).

The actin cytoskeleton also attaches to transmembrane proteins in the bilayer (e.g. $\alpha\beta$ integrins and the EGFR; epidermal growth factor receptor) often via the adapter-like mediation of ABPs in specialised areas of the cell called focal contacts (see below) that allow the cells to initiate myosin mediated movement. Focal contacts (also called adhesion plaques or focal adhesions) are specialised areas of the plasma membrane where cells (especially cultured cell-lines like fibroblasts) attach to the underlying substratum (see fig. 1.3). These areas are of great interest because of their roles in actin:membrane association, cell-substrate adhesion, and in signal transduction, both internally and externally directed, that regulate cell growth and apoptosis (Burridge et al, 1988; Geiger, 1989; Luna and Hitt, 1992; Hynes, 1992; Jockusch et al 1995; Burridge and Chrzanowska-Wodnicka, 1996; Gilmore and Burridge, 1996; Lauffenberger and Horwitz, 1996; Yamada and Geiger, 1997; Taylor et al, 1998; Stossel et al, 1999; Critchley, 2000).

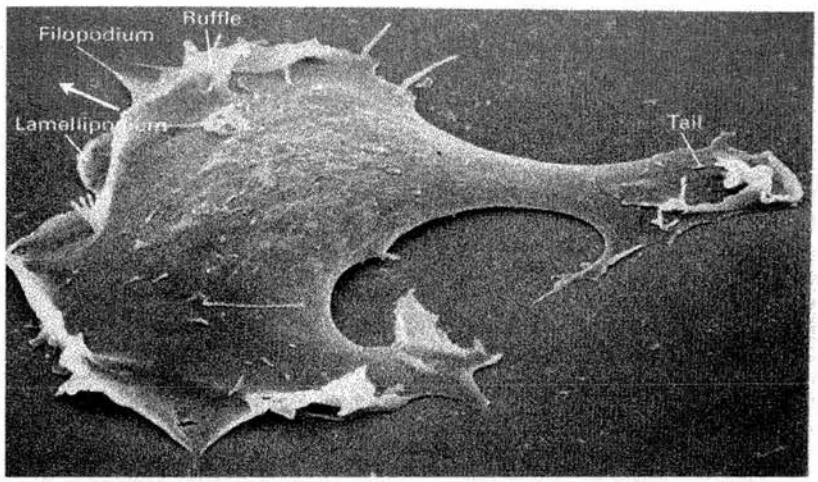

A

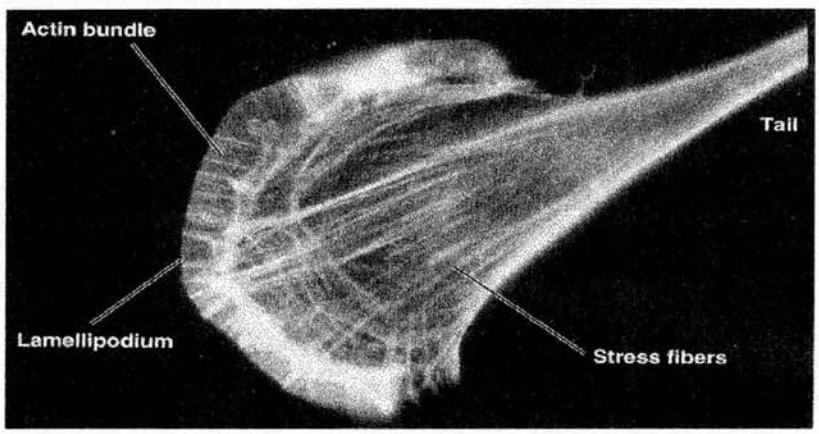

B

Fig. 1.2. ***Actin structures in a moving Fibroblast.*** (A) Scanning EM micrograph of a motile cultured fibroblast. At the cell front, filopodia, lamellipodia, and ruffles project from the cell membrane, while at the rear of the cell the tail is firmly attached to the substratum. (B) A Fluorescence micrograph of a fibroblast stained with Rhodamine-Phalloidin (a fluorescent F-Actin *specific* binding molecule) showing some of the higher-order actin structures of the cortical cytoskeleton in a moving fibroblast. (Figure was reproduced from Darnell et al, 1995).

The number of proteins that have been identified and localised at focal contacts is growing rapidly. These include vinculin (Geiger, 1979; Feramisco and Burridge, 1980), α-Actinin (Lazarides and Burridge, 1975), talin (Burridge and Connell, 1983), paxillin (Turner et al, 1990), zyxin (Crawford and Beckerle, 1991), radixin (Sato et al, 1991), Src (Rorschneider, 1980), focal adhesion kinase (FAK) (Schaller et al, 1992), tensin (Tsukita and Itoh, 1989), fimbrin/APB120 (Feramisco and Burridge, 1980), vasodilator-stimulated phosphoprotein (Reinhard et al, 1992), fibronectin, and

integrin (Chen et al, 1986; Horwitz et al, 1990), see fig. 1.3. The roles for many of these proteins are relatively unknown. However, the identification of the components of focal contacts that are involved in the linkage of actin filaments to the integral constituents of the plasma membrane (e.g. tensin) has proved critical in elucidating the function of both the proteins themselves and also the function, composition and regulation of focal contacts as dynamic multimeric protein complexes.

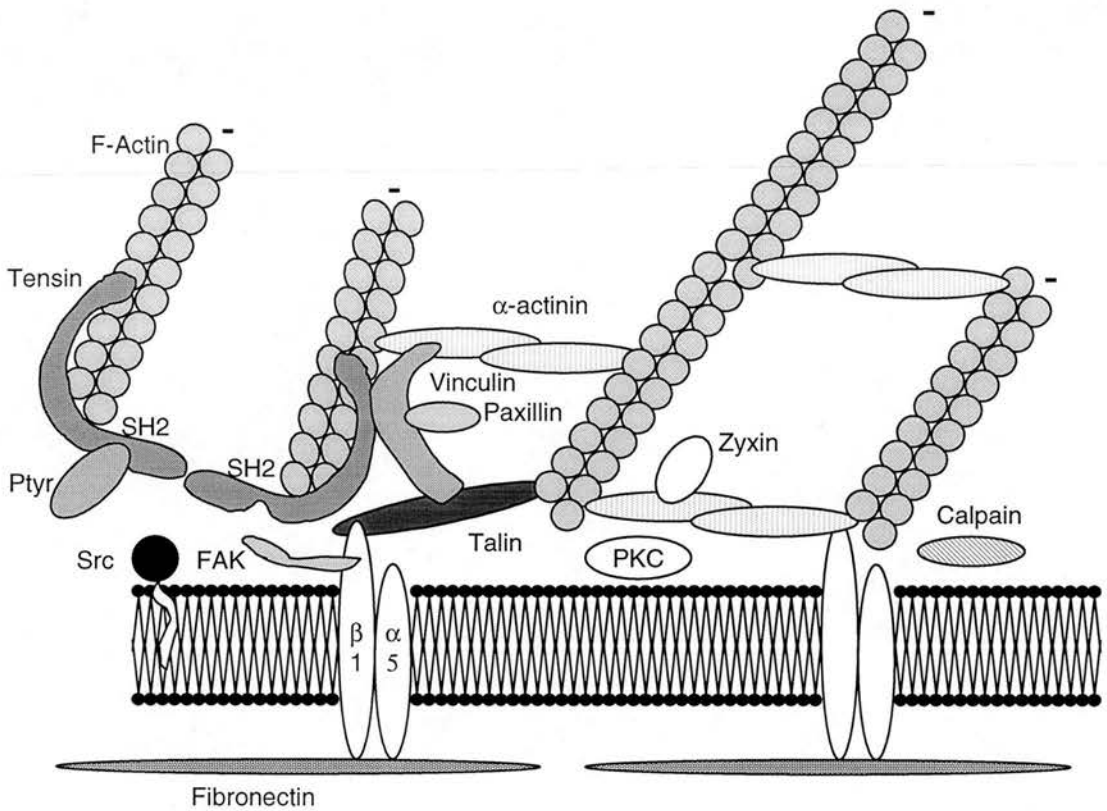

Fig. 1.3. ***Schematic diagram of a focal adhesion.*** The figure above shows a model of the structural arrangements for some of the components of a focal adhesion. Many of the known protein:protein interactions are illustrated, based on *in vitro* binding (see Taylor et al, 1998 for review). The putative tensin-dimer is also shown. Abbreviations: PKC, protein kinase C; FAK, focal adhesion kinase; SH2, Scr homology domain; Src, non-receptor tyrosine kinase; Ptyr, phosphotyrosine; α5β1, integrin receptor (cell-matrix adhesion molecule). This figure was reproduced from Lo et al, (1994b).

1.5 The acto-myosin interaction

Most of our knowledge of the structure of the actin filament and the structure of myosin has arisen from a huge body of work performed on skeletal muscle, mainly due to the highly ordered structure and the ease of purification of both actin and myosin from such specialised tissue (Sellers and Goodson, 1995). The α-skeletal isoform of actin (in invertebrate muscle it constitutes ~ 20% of the total cellular protein) and myosin are the two major constituents found in myofibrils and form part of the interlocking parallel array of stable thin actin filaments and thick myosin II fibrils that gives rise to the characteristic light and dark bands seen by EM at low magnification (Amos, 1985). These basic components mediate the shortening of the sarcomere, the contractile unit of muscle fibre, by sliding over each other in an ATP dependent manner.

Myosins form a large and very diverse super-family of proteins that act as ATP dependent molecular motors. These motors are capable of translocating actin filaments or of the polar translocation of vesicles and other cargo along fixed "tracks" of filamentous actin (Sellers and Goodson, 1995; Rogers and Gelfand, 2000). The most familiar and well-studied member of this family is the myosin II from skeletal muscle. There are now ~ 15 distinct classes of myosin based on sequence homology (Goodson and Spudich, 1993; Cheney et al, 1993; Sellers and Goodson, 1995; Cope et al, 1996). These myosin II molecules form thick filaments at low ionic strength and become soluble at high ionic strength. This feature is utilised in the purification of vertebrate skeletal myosin II, most commonly from rabbit skeletal muscle.

All myosins examined to date have the ability to bind actin and hydrolyse Mg-ATP. There are very large differences in the hydrolysis activities of different classes of myosin and the myosin II (from skeletal muscle) appears to have an unregulated ATPase activity when assayed in the presence of purified actin filaments *in vitro* (Sellers and Goodson, 1995). The regulation of myosin II *in vivo* (in skeletal muscle

fibres) appears to result solely from the action of the troponin-tropomyosin system on the thin actin filaments.

All types of myosin purified to date are multimeric complexes and appear to possess at least three functional domains, a head, neck and tail. Members of the class II myosins are hexameric complexes, comprised of two heavy chains (Mr. ~ 171 – 241kDa) and two pairs of light chains (Mr. ~ 14 – 30kDa). The N-terminal sequence of the heavy chain forms the head region of the molecule, while the C-terminal sequences of the heavy chains form an elongated coiled-coil α-helical rod structure. Between these two regions are the binding sites for the two light chains and each head of myosin is associated with an essential and a regulatory type light chain.

Myosin II can be cleaved into separate and functional fragments using controlled proteolysis. Various proteases cleave the myosin at a site that is typically ~ 130kDa from the N-terminus and produce two fragments, heavy meromyosin (HMM) and light meromyosin (LMM). HMM can be further divided by proteolysis, which occurs just after the regulatory chain-binding region of the neck, to generate sub-fragments S-1 and S-2. The S-1 fragment is enzymatically active and is associated with either both of the light chains or just the essential light chain (under some conditions the regulatory light chain is lost), dependent on the type of protease used in the cleavage.

The S-1 head has been used extensively in kinetic and actin-binding studies and most of the knowledge of the kinetic cycle of myosin has been performed using the soluble S-1 head fragment (see Sellers and Goodson, 1995; Vale and Milligan, 2000 and Volkmann and Hanein, 2000 for reviews of the structural and kinetic considerations of the acto-myosin interaction). Actin filaments typically activate the Mg-ATPase activity of myosin by a factor of 50 – 100 (depending on the solution ionic conditions). In the absence of ATP, actin and myosin are tightly complexed (the association constant, in the absence of ATP is ~ 10^7 – 10^8 M^{-1} for acto-S1, Marston and Weber, 1975; Margossian and Lowey, 1978). ATP binds rapidly to the S-1 head, as it does with myosin alone, and has the resultant effect of lowering the affinity of actin for myosin to about 10^4 – 10^5 M^{-1} (Chalovich et al, 1984).

The three-dimensional structure of the S-1 head region, from chicken fast skeletal muscle, has been solved to a resolution of 2.8Å (Rayment et al, 1993b). Myosin S-1 has a very asymmetric structure; ~ 165Å long, ~ 65Å wide and up to 40Å thick. The globular head (also referred to as the motor region) contains a nucleotide-binding site and the actin-binding site, oriented on opposite sides of the globular head domain (Rayment et al, 1993a/b).

It is important to know the structure of the acto-mysoin complex, both to elucidate the molecular details of this reaction and also to provide data at the molecular level for the interaction that take place between actin monomers in the filament. A low resolution structure of the acto-myosin complex has been obtained by helical reconstruction of electron micrographs of actin filaments completely decorated with the S-1 myosin heads, see fig. 1.4 (Milligan and Flicker, 1987; Milligan et al, 1990; Schroder et al, 1993). These images indicated and highlight the polar nature of the actin filament, supporting the kinetic observations. I.e. polymerising filaments have fast- and slow-growing ends, defined as the *barbed-* and *pointed-ends*, respectively, (see fig. 1.4)

A model for the interaction of myosin with the actin filament was constructed by computer fitting of the electron density of the S-1 myosin head and the F-Actin model (Rayment et al, 1993a/b). Overall, this fit was good but it was clear that there were subtle changes in the actin monomer structure, upon incorporation into the filament, as well as for the structure of the S-1 head and its interaction with the filament (Rayment et al, 1993a/b). In a similar manner the crystal structure of the G-Actin:DNaseI complex (Kabsch et al, 1990) was used to build a model of the actin filament (Holmes et al, 1990). However, the data used in the construction of these models extend to only ~ 7Å. As a result we have *limited* knowledge of the molecular details of the numerous protein:protein interactions involved in both actin filaments and the acto-myosin complex at the atomic level, and given the importance of the actin cytoskeleton in eukaryotic cells knowing the structure of the actin filament at atomic resolution is necessary to further our understanding of how the actin

cytoskeleton is controlled and modulated. The model of the actin filament (Holmes et al, 1990) is described in more detail in section 1.6.

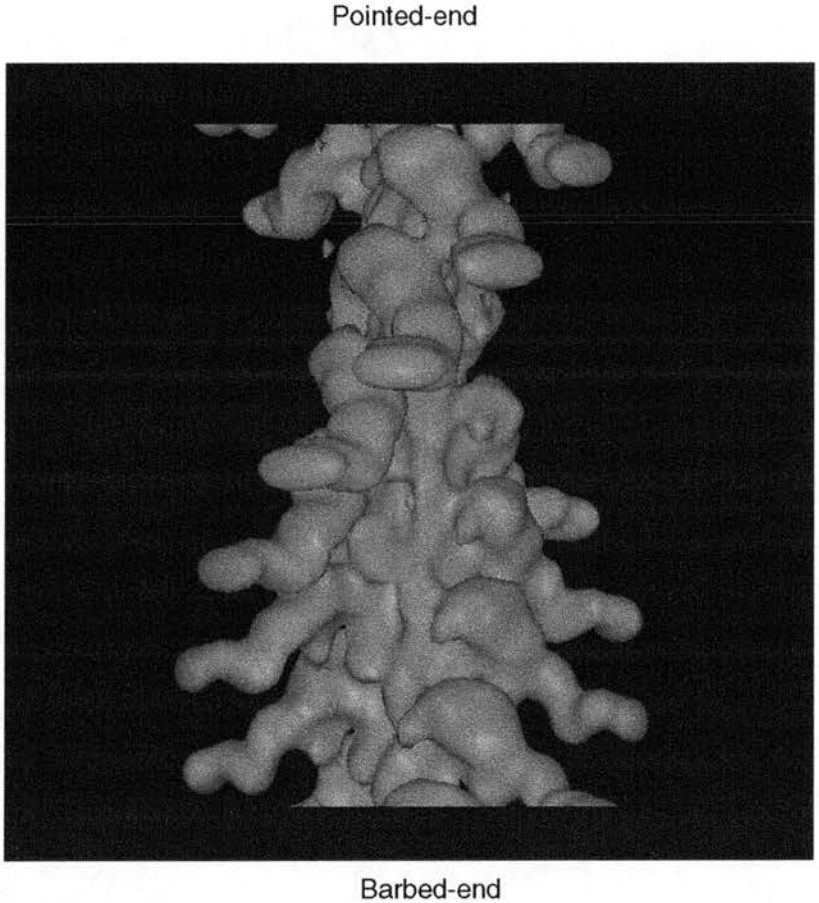

Fig. 1.4. ***The actin filament has a polar nature.*** The figure above shows an image reconstruction from EM micrographs of an actin filament decorated with the myosin S-1 head, bound along the long axis of the filament (Milligan and Flicker, 1987; Milligan et al, 1990; Schroder et al, 1993). This image accentuates the polar nature of the filament - the fast growing *barbed-end* and the slower growing *pointed-end* - demarcated by the arrow head appearance of the structure.

1.6 G- and F-Actin structure

F-actin is *not* amenable to crystallisation and subsequent determination to atomic resolution, due to the uncontrollable distribution of polymer lengths and their relative flexibility. However, the atomic structure of monomeric actin (G-Actin) has been determined, in 3 separate complexes: bovine DNaseI (Kabsch et al, 1990; see fig.

1.10) and gelsolin segment 1 (McLaughlin et al, 1993, see fig. 1.8) in complex with rabbit skeletal muscle actin, while the structure of bovine profilin was solved complexed with Bovine β-actin (Schutt et al, 1993). From the three dimensional structures, the actin monomer resembles a "box" of dimensions 67x40x37Å and is divided into two roughly equal domains separated by a cleft containing the high-affinity nucleotide and divalent-cation binding site (see fig. 1.5). Each of these domains can be further split into two domains (termed subdomains I, II, III, IV) with a hinge region that runs below the cleft, connecting the domains I and III via two strands of the polypeptide chain (Kabsch et al, 1990).

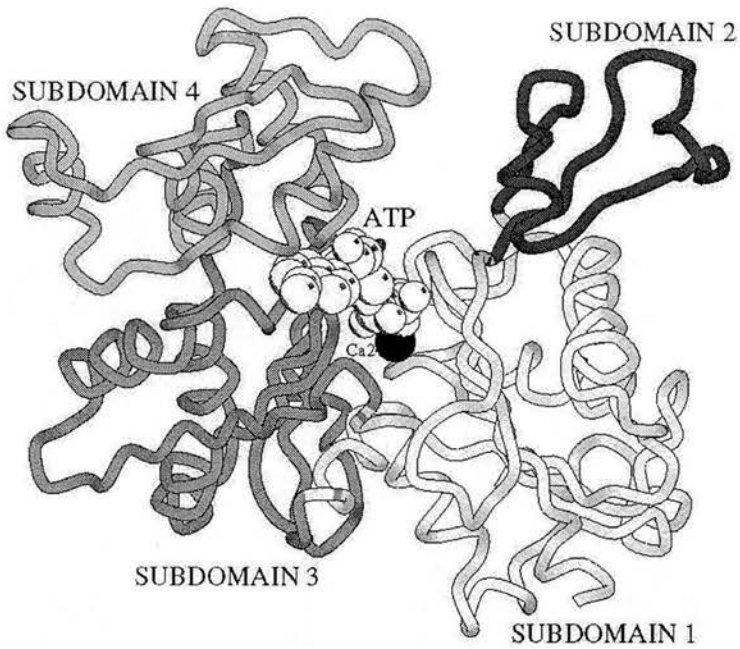

Fig. 1.5. ***Actin monomer structure.*** Schematic view of the chain trace of G-Actin (375 residues, Mr. ~ 42kDa) highlighting the subdomains (I – IV, numbered 1 – 4, respectively) of the monomer, and Ca^{2+}-ATP bound at the high affinity site (as described by Kabsch et al, 1990 and McLaughlin et al, 1993). (The figure was created using MOLSCRIPT, Kraulis, 1991).

The crystal structure of the G-Actin:DNaseI complex (Kabsch et al, 1990) has been used to build a model of the actin filament using data from X-ray diffraction patterns of oriented F-Actin gels (Holmes et al, 1990; Lorenz et al, 1993). The fibre symmetry has two descriptions. One is of a single start, left handed helix with a 13 subunit repeating every 6 turns in roughly 360Å up the long axis. The orientation that

relates subsequent monomers is a then rotation of -166° and a translation of 27.5Å, half the height of the monomer along the axis. Two such operations give the third subunit lying on top of the first, related to each other by a rotation of 28° in the opposite sense. This gives the alternate description; a right handed, two-strand helix with a half pitch of 360Å (see fig. 1.6).

The major problem with this model is that the experimental observations extend to *only* 7-8 Å, at best (Holmes et al, 1990; Lorenz et al, 1993; Schmid et al, 1993). Although a unique solution was found, the resolution of the experimental data were insufficient to allow further refinement of the input model. Thus, if there had been any conformational changes in surface loops, or even rigid rotations of subdomains within the monomer, the observation to parameter ratio was insufficient to reliably estimate these by least squares fitting of the model to the data.

Furthermore, low-resolution data is more susceptible to bias towards the input model. Thus difference map techniques, such as those used in high-resolution crystallography, less reliably show differences between the input model and the true structure. At low resolution the input model is reinforced and the differences are down weighted.

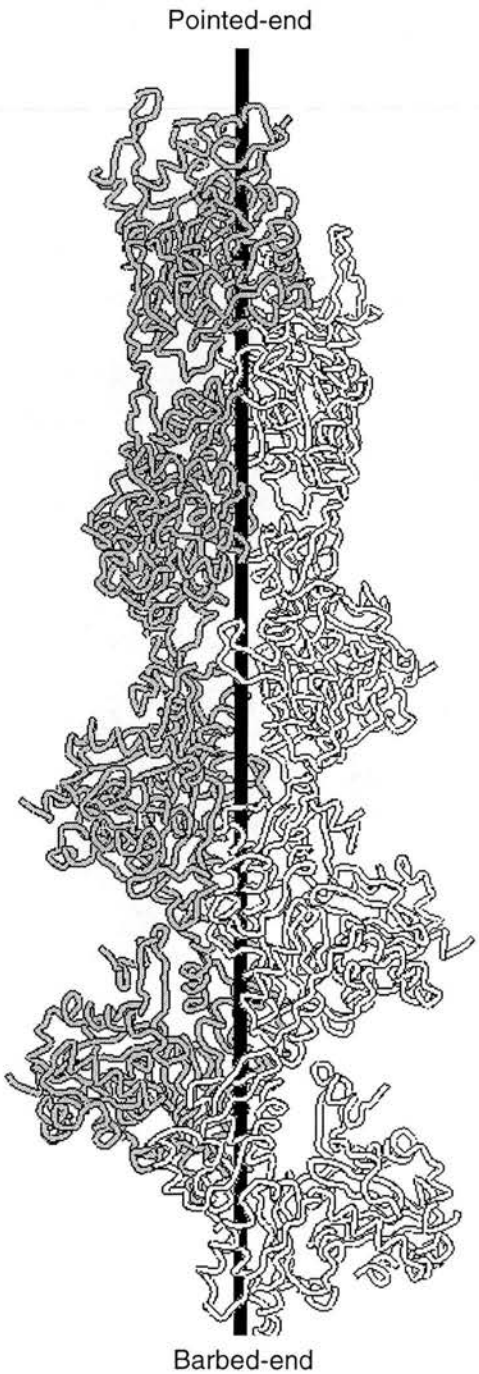

Fig. 1.6. ***Model of the actin filament.*** The figure to the right shows eight actin subunits oriented in the filament as described by Holmes et al (1990). The differential shading indicates the two strands of the right-handed, two-start helix description of the filament. (The figure was created by MOLSCRIPT, Kraulis, 1991).

However, in its favour, the model is consistent with crosslinking and esr-spin probe data and both the low resolution EM reconstruction (Milligan et al, 1990) and X-ray models (Holmes et al, 1990; Lorenz et al, 1993) agree (Mendelson and Morris, 1994). Nevertheless, despite this agreement, due to the low resolution of the current model we are far from understanding the atomic contacts that hold the filament together, the interactions involved when myosin uses the actin polymer as a track during muscle contraction, and also how the many ABPs that control the actin cytoskeleton, bind to and interact with the filament at the atomic level. Thus, given the pivotal role that actin plays in a host of important cellular processes, knowledge of the structure of the actin filament at the atomic level is crucial to aid our understanding of the molecular details of the subunit:subunit contacts within the filament, but also in elucidating the interactions between the filament and the numerous actin binding protein at the atomic level.

If some form of control could be placed on the length of the filament, attempts could be made to crystallise, and determine the atomic interactions of F-actin and bound proteins. Several actin-binding proteins, **gelsolin**, **DNaseI** and **tensin**, present us with an opportunity to control the two ends of the filament. We propose a different approach in an attempt to solve the resolution problem of the current F-Actin model; this is to form a **capped-actin-"minifilament"**, utilising the actin-binding properties of these three proteins (see below).

Before describing this proposal in detail, it is necessary to explain the properties of these ABPs (gelsolin and DNaseI) and the details of their interaction with actin. The actin-binding properties of tensin are described separately in chapter 5.

1.7 Gelsolin, a Ca^{2+} activated, PIP_2 regulated actin filament severing and barbed-end capping protein

Gelsolin severs actin filaments and remains tightly bound to the severed-end. It also forms a ternary complex with two actin monomers under depolymerising conditions. This gelsolin:actin ternary complex ($G:A_2$) may represent a cap between gelsolin and

two actin subunits, one from each strand in the filament. Kinetic evidence suggests that the complex is at the faster growing barbed-end of the actin filament.

Gelsolin was first identified as a calcium-dependent actin filament destabilising protein found as a component of blood plasma (with an additional 25-residue leader sequence) and in the cytoplasm of macrophages (Chaponnier et al, 1979; Yin and Stossel, 1979; Harris et al, 1980; Kwiatkowski et al, 1986). The cytosolic form of gelsolin (Mr. ~ 82kDa) is one of the primary candidates implicated in the regulation of the cortical F-actin network in response to a wide range of extra- and intracellular signals (Sun et al, 1999 and Kwiatkowski, 1999). While gene knockout experiments (Witke et al, 1995) have shown that gelsolin is not essential, it is required for the rapid movement of dynamic cell like fibroblasts. Over expression of gelsolin in fibroblasts results in increased motility (Cunningham et al, 1991).

Gelsolin is a ubiquitous actin filament-severing, -capping and nucleating protein, and these multiple activities allow gelsolin to regulate the architecture and mobility of cells (Yin, 1987). Gelsolin is a member of a family of proteins that is defined by either a three (e.g. fragmin, severin) or a six (e.g. gelsolin, villin and adsevrin) repeat sequence motif that spans 125 – 150 residues, see fig. 1.7 (Vandekerckhove, 1990; Hartwig and Kwiatkowski, 1991; Weeds and Maciver, 1993). The crystal structures of whole, Ca^{2+}-free gelsolin (Burtnick et al, 1997) and the actin:G4 – 6 complex (Robinson et al, 1999) have shown that this motif folds up into functionally distinct domains with the same basic fold topology (originally identified on the basis of their sequence homology; Kwiatkowski et al, 1986; Way and Weeds, 1988; Way et al, 1989), and conserved residues present in all segments of the gelsolin family contribute to the apolar core of the molecule, possibly indicating the selective evolutionary pressures involved in maintaining a tightly folded globular domain (Matsudaira, 1988). See figs. 1.7, 1.8 and 1.9 for details.

From these studies it is apparent that the segments G1 and G4 are the most similar and the X-ray crystal structures of the G1:actin complex (McLaughlin et al, 1993) and of the actin:G4 – 6 complex (Robinson et al, 1999) have revealed the details of

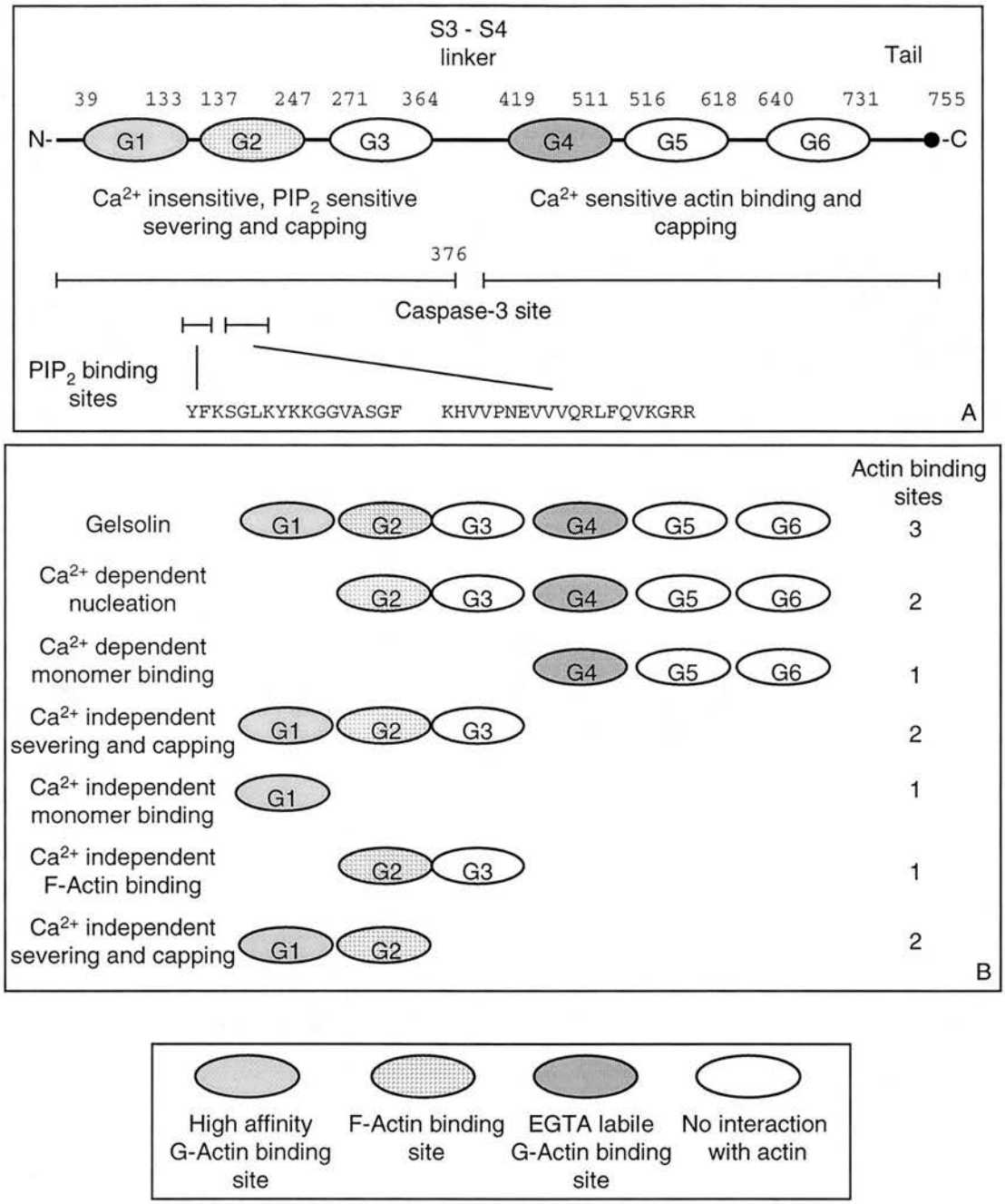

Fig. 1.7. ***Gelsolin structure-function domains.*** (A) A schematic diagram illustrating the segmental boundaries of the six-fold domain repeat of gelsolin (as defined by the Ca^{2+}-free structure, described by Burtnick et al, 1997), with the amino acid residues (shown at the boundary of each of the individual domains) numbered as in human plasma gelsolin (Kwiatkowski et al, 1986) is shown above. The sequences of the putative PIP_2-binding sites are also illustrated (Janmey et al, 1992; Yu et al, 1992; see Janmey, 1995 for review). (B) A schematic diagram correlating the actin-binding and functional activities (Ca^{2+} dependence, F-Actin-binding, severing and capping) with the six-fold segmental repeat of gelsolin (Way and Weeds, 1988; Way et al, 1989; see Weeds and Maciver, 1993 and Sun et al, 1999 for reviews).

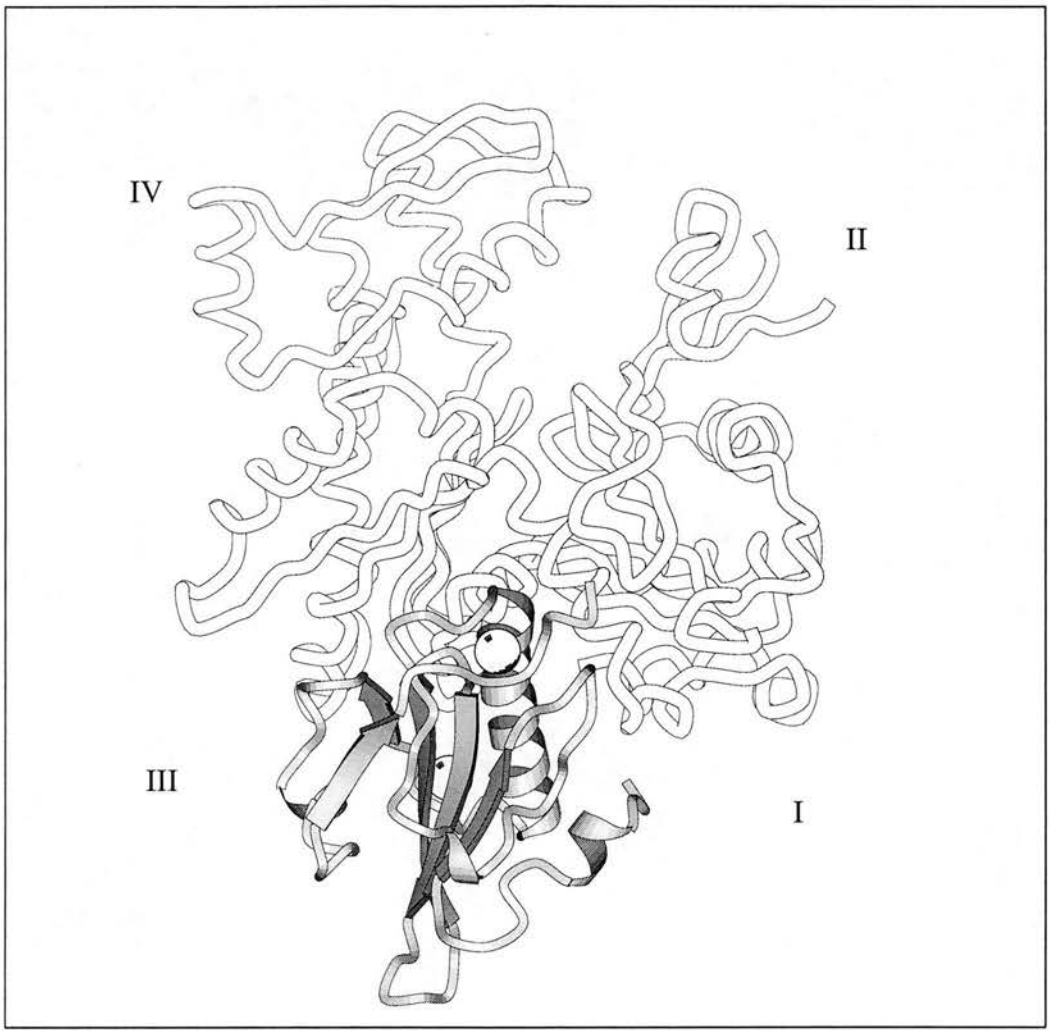

Fig. 1.8. ***The actin:gelsolin segment 1 binary complex.*** A schematic representation of the actin:gelsolin segment 1 (G1 is shaded) binary complex is shown (the Ca^{2+} ions are shown as spheres) as described by McLaughlin et al (1993). G1 forms a globular domain of dimensions 13x26x25Å and is composed of a 3 layered structure. A central 4 stranded β-sheet is sandwiched between a 4-turn α-helix (termed the long helix) roughly parallel to the strands and a second α-helix perpendicular to the strands. This figure clearly shows the binding interaction between the long α-helix from G1 at the cleft between the subdomains I and III of the actin monomer. (The figure was produced using MOLSCRIPT; Kraulis, 1991).

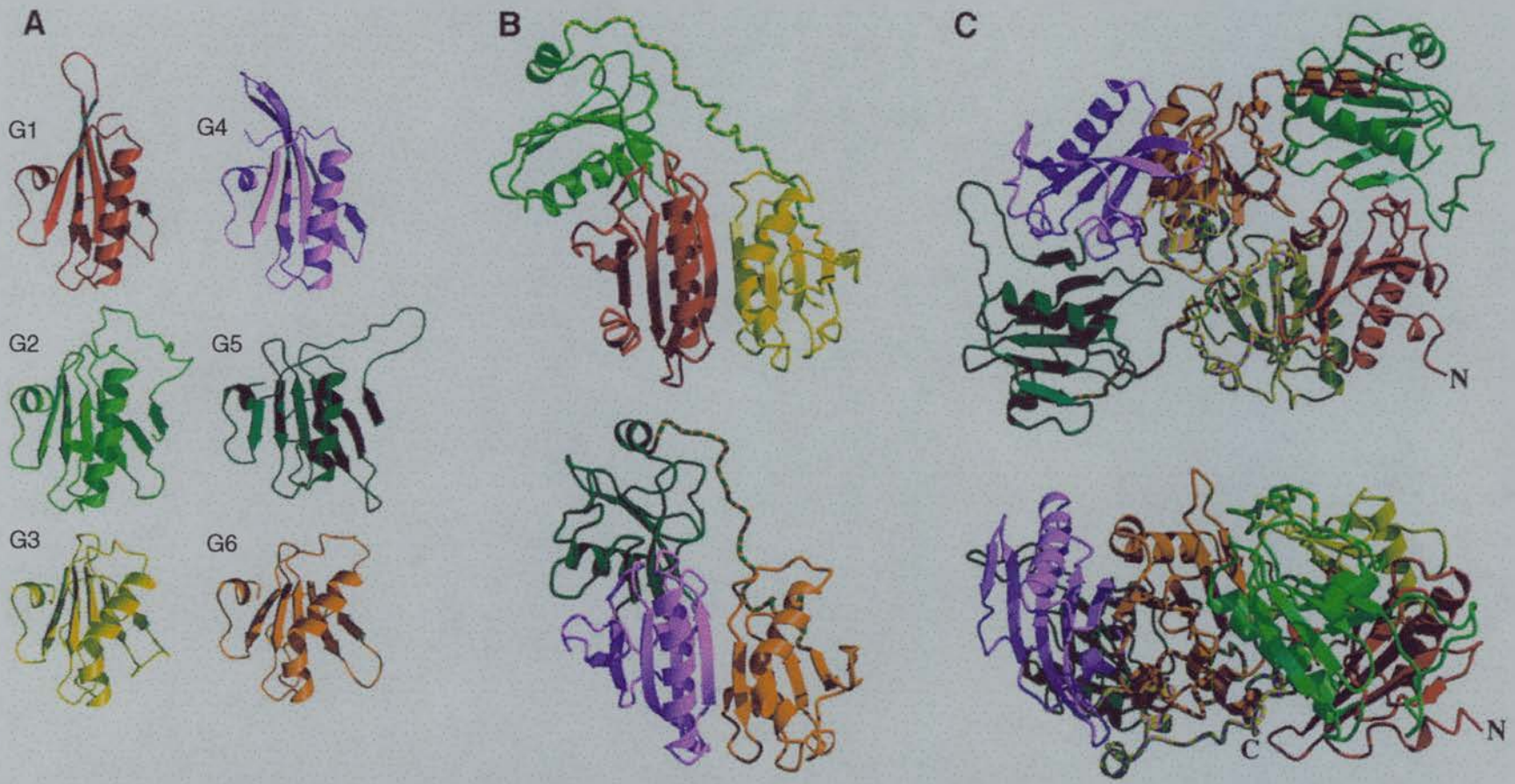

Fig. 1.9. ***The structure of the Ca^{2+}-free (inactive) form of gelsolin.*** (A) A schematic representation of the six domains of gelsolin (G1 - 6), with the individual domains in a similar orientation. All six domains share a similar folding topology, consisting of a central five- or six-stranded β-sheet sandwiched between a 3.5-to-4.5 turn α-helix (termed the long helix in discussions of the structure) running roughly parallel to the strands in the sheet, and a 1-to-2 turn α-helix running approximately perpendicular to the strands. Colouring of the segments is: G1, red; G2 light green; G3, yellow; G4, pink; G5, dark green; G6, orange. (B) A schematic representation of the relative organisation of G1 - 3 (upper panel) and G4 - 6 (lower panel), with both in approximately the same orientation. The linker regions between the various domains are striped with the colours of the segments they connect. (C) A schematic representation of the structure of whole gelsolin (Ca^{2+}-free form). The upper panel is a 90° clockwise rotation around the horizontal, with respect to the view shown in the lower panel. The C-terminal extension is striped orange and black. (The figure was reproduced from Burtnick et al, 1997).

the interaction between the two monomer-binding domains in gelsolin, G1 and G4, and the actin monomer (see fig. 1.8). This association involves the long α-helix present in the gelsolin domains binding in a cleft (between subdomains I and III) at the barbed-end of the actin monomer (see fig. 1.8).

The activation of gelsolin requires calcium ions. The levels of calcium, reported in the literature, required for activation, nucleation, filament severing and actin monomer (G-Actin) binding show a large amount of variation (Bryan and Kurth, 1984; Weeds et al, 1986; Pope et al, 1986; Janmey and Stossel, 1986; Selve and Wegner, 1986; Patkowski et al, 1991; McLaughlin et al, 1993; Hellweg et al, 1993; Lamb et al, 1993; Ditsch and Wegner, 1995; Pope et al, 1995). However, it appears that while gelsolin has several high affinity binding sites for calcium (K_d in the nM range) in the C-terminal half, that may be involved in the activation and the subsequent large scale conformational changes associated with the opening of the molecule, calcium concentrations in the μM range are required for actin binding, severing and nucleation activities (Weeds et al, 1986; Way et al, 1989; Way et al, 1992; Hellweg et al, 1993; Sun et al, 1994; Ditsch and Wegner, 1995; Pope et al, 1995; Pope et al, 1997; Burtnick et al, 1997; Robinson et al, 1999).

In response to elevated calcium concentrations gelsolin severs actin filaments, and remains tightly bound to the barbed-end of the filament, capping it and preventing further monomer addition at that end (K_{cap} ~ 10pM; Selve and Wegner, 1986). PIP_2 dissociates the gelsolin cap *in vitro*, and its severing ability is inhibited (Janmey and Stossel, 1987; Janmey and Stossel, 1989; Janmey et al, 1992; Yu et al, 1992). The barbed-end of the actin filament is the preferred end to which monomers bind as new filaments extend during re-arrangement of the actin cytoskeleton in response to signalling events (Cooper and Schafer, 2000). Thus, it has been proposed that as the levels of polyphosphoinositides (PIP_2) are altered at the plasma membrane (by activation of receptors and signalling cascades) such interactions would localise the growth of new filaments close to the site of action of these extra-cellular signals. This model provides a possible means for the rapid control of severing and nucleation of F-actin (Janmey, 1995; Stossel et al, 1999).

Much of the work that has ascribed functional properties to the six domains of gelsolin was performed by studies on truncated domains of the protein (following limited proteolysis or using expressed recombinant constructs) and chimeric constructs (Bryan and Hwo, 1986; Bryan, 1988; Yin et al, 1988; Kwiatkowski et al, 1989; Way et al, 1989; Way et al, 1990; Pope et al, 1991; Weber et al, 1991; Way et al, 1992; McLaughlin et al, 1993; Sun et al, 1994; Pope et al, 1995; Pope et al, 1997; McGough et al, 1998; Robinson et al, 1999; Puius et al, 2000). This body of work has established that there are three distinct actin-binding sites, *unevenly* distributed, within the six-fold segmental repeat of gelsolin (see below and fig. 1.7 for a summary of the current picture of gelsolins domain structure-function relationships).

In summary: gelsolin has two binding sites for monomeric actin, a high-affinity calcium-independent monomer-binding site in G1 (K_d ~ 5pM) and a calcium-dependent site in G4 (K_d ~ 1.8μM in G4 alone, but ~ 25nM in the G4 – 6 construct; Bryan, 1988; Pope et al, 1995). G2 contains the calcium independent F-Actin binding site (K_d ~ 5μM; Way et al, 1992; Sun et al, 1994; Puius et al, 2000). While it is apparent that the F-Actin binding domain of gelsolin (G2) localises the protein to the sides of actin filaments, it also contributes to the severing activity of G1 (Sun et al, 1994). The severing and capping activity of gelsolin are both highly dynamic processes that require the participation and co-operation of several domains (if not all six). The minimal actin severing domain is G1 – 2 (Way et al, 1992; Sun et al, 1994), while full nucleating ability requires the two actin binding sites in G2 – 6 (Way et al, 1989). The former construct is calcium independent while the latter is calcium dependent, indicating the calcium regulation of actin binding, of all three of the sites is mediated via the C-terminal half of gelsolin. Calcium regulation of whole gelsolin appears to be modulated by several sites in the C-terminal (G4 – 6) domains, with a high affinity Ca^{2+}-binding site located in G6 (Hellweg et al, 1993; Ditsch and Wegner, 1995; Pope et al, 1995; Pope et al, 1997).

Despite the extensive functional analysis of the various domains of gelsolin and the structural information these crystal structures have provided, the molecular details of the modulation and regulation of the cellular F-Actin architecture by gelsolin are still

relatively unclear. However, the formation of a ternary complex between gelsolin and two actin monomers may provide a tool to address some of these problems.

Gelsolin forms two complexes with monomeric actin (in a calcium dependent manner), a binary (**G:A**) complex and a ternary (**G:A_2**) complex (Weeds et al, 1986). G:A_2 caps the barbed-end (K_{cap} ~ 20nM; Coué and Korn, 1985) and also nucleates the rapid polymerisation of actin, in the pointed-end direction. Data from cross-linking studies (Doi et al, 1991; Doi, 1992) has indicated that the two monomers, bound by G1 and G4 in the G:A_2 ternary complex, are related to one another across the *short-pitch helix* of the filament (akin to the two terminal, laterally related monomers at the barbed-end of the filament) and *not* longitudinally up the long axis. The chelation of the Ca^{2+} ions with EGTA results in the dissociation of only one of the actin monomers, leaving a binary complex that has lost the nucleating ability (Bryan and Kurth, 1984; Bryan, 1988; Way et al, 1989). Dissociation of the G:A binary complex can be induced by PIP_2 (Janmey et al, 1987; Janmey and Stossel, 1989), with the binding sites for this interaction located to G2 (Yu et al, 1992; Janmey et al, 1992).

Gelsolins ability to form a very tight cap at the barbed-end of an actin filament, and its ability to form a stable ternary complex with two actin monomers, provides us with a tool to ***control*** the *definition* of one end (the barbed-end) of the actin filament. **GA_2** ternary complexes could be combined with a pointed-end capped actin species to give a larger complex, hopefully with the actin in an F-conformation. A candidate pointed-end capping species is the **actin:DNaseI** (A:D) binary complex, used in the co-crystallisation and determination of the actin monomer structure (Kabsch et al, 1990).

1.8 The actin:DNaseI binary complex

Bovine pancreatic deoxyribonuclease I (DNaseI) is a glycoprotein that binds to, and subsequently cleaves double stranded DNA to yield 5'-oligonucleotides (Moore, 1981). As well as possessing these enzymatic activities DNaseI is also a high-affinity

actin-sequestering protein (Lazarides and Lindberg, 1974; Mannherz et al, 1975; Hitchcock et al, 1976; Hitchcock, 1980) which forms a 1:1 binary complex (A:D) with actin. DNaseI binds to subdomains II and IV of monomeric actin (Kabsch et al, 1990; see fig. 1.10) with a K_d ~ 0.1 – 1.0nM (Mannherz et al, 1980). It has also been reported to bind with similar affinity (K_d ~ 1nM) to the pointed-ends of actin filaments (Podolski et al, 1988; Weber et al, 1994), and this leads to a blockage of filament elongation. This inhibition is conferred by the binding of only one DNaseI molecule to the pointed-end of a single strand of the F-Actin two-start helix. (One DNaseI molecule bound per filament; Podolski et al, 1988). The binding of this DNaseI appears to have *no* significant effect on the affinity of the attached actin for the pointed-end of the filament (Weber at al, 1994). DNaseI has also filament side-binding activity (Hitchcock et al, 1976) but this is of much lower affinity (K_d ~ 0.1mM; Mannherz et al, 1980). It is agreed that this interaction is probably *not* physiological; nevertheless it has been used extensively as a tool in the study of actin.

Work carried out by Weber and co-workers (Weber et al, 1994) indicated that the binding of two DNaseI molecules was not possible at the pointed-ends of gelsolin-capped actin filaments. At higher concentrations of DNaseI, 1 – 100μM (three orders of magnitude higher than that required for the blockage of elongation), an increase in the rate of depolymerisation from the pointed-ends of gelsolin-capped filaments was observed. The $K_{50\%}$ for this effect was ~ 5μM DNaseI (Weber et al, 1994). The explanation proposed for this was a steric clash between two DNaseI molecules at the pointed-end. This prevented the stable binding of both DNaseI molecules and resulted in an increase in the k_{off} rate for the actin monomer, as a 1:1 binary complex with DNaseI (Weber et al, 1994). Modelling of DNaseI molecules onto the pointed-ends of two subunits in the Holmes filament model (Holmes et al, 1990) indicates that DNaseI would sterically interfere with each other.

In a similar manner to the G:A_2 ternary complex, the tight, stable and easily purified A:D binary complex provides us with a tool that allows us to ***define*** and ***control*** the pointed-end of the actin filament.

1.9 A capped-actin-"minifilament" presents a different approach to attempt to address the resolution problem of the current filament model

We propose to take a different approach to attempt to address the resolution problem of the current actin filament model: this is to form a **capped-actin-"minifilament"**, with a view to crystallographic studies. This species has a defined length and composition, and contains three actin subunits forming a "minifilament", blocked at both ends by specific binding proteins with **gelsolin** binding at the barbed-end and **DNaseI** at the pointed-end of the filament (see fig. 1.10).

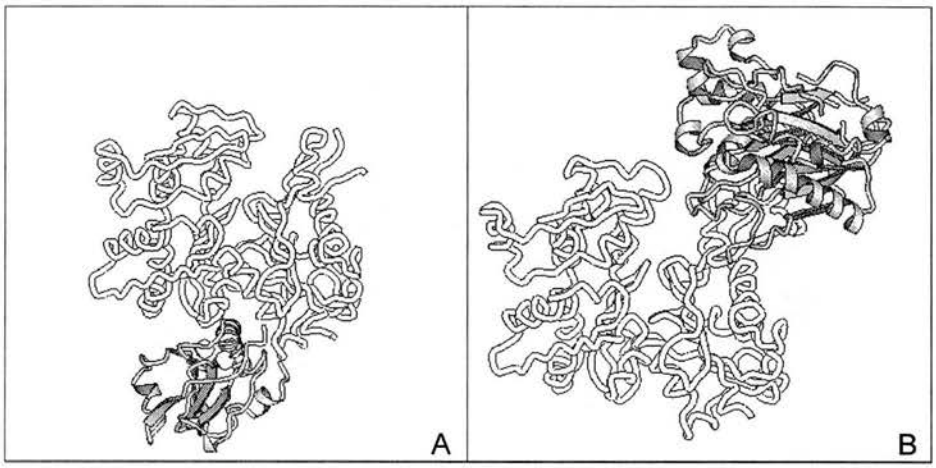

Fig. 1.10. ***G-Actin in complex with two opposite end-opposed binding proteins.*** (A) A schematic view of the actin-gelsolin segment 1 (shaded) complex (the Ca^{2+} ions are shown as spheres) as described by McLaughlin et al (1993). (B) A schematic view of the actin-DNaseI (shaded) complex as described by Kabsch et al (1990). This side-by-side orientation clearly indicates the binding of the two proteins at opposite ends of the actin monomer. (Diagrams were created using MOLSCRIPT; Kraulis, 1991).

Combining the G:A_2 ternary complex and the A:D binary complex under polymerising conditions may result in an association between the free ends of the actin monomers, hopefully giving rise to a larger species with the actin monomers oriented as they are in a filament. As described above, two actin:DNaseI binary complexes (A:D) cannot be accommodated at the pointed-ends of filaments due to a significant steric clash consistent with modelling and kinetic data (Weber et al, 1994). Our proposed "minifilament" model (see fig. 1.11) with the actin monomers oriented in a filamentous conformation (as described by the Holmes filament model;

Holmes et al, 1990) acknowledges this argument. It is not possible to accommodate *two* DNaseI molecules at the pointed-ends of the putative "minifilament", giving our model a predicted stoichiometry of **G:A_3:D** (see fig. 1.11).

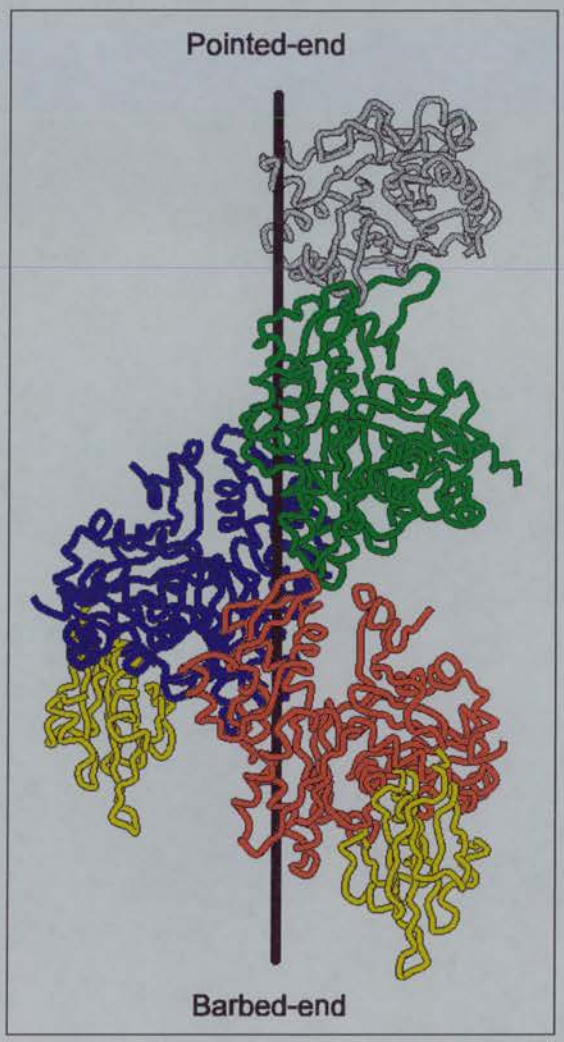

Fig. 1.11. ***Model of the putative "minifilament".*** A schematic representation of a putative model of the capped-actin-"minifilament", with stoichiometry of **G:A_3:D** (gelsolin:$actin_3$:DNaseI), is shown. DNaseI is coloured grey, the three actin monomer subunits, oriented as described by the Holmes filament model (Holmes et al, 1990), are coloured red, green and blue. Only segment 1 (G1) and a putatively positioned segment 4 (G4) – by analogy – from gelsolin are shown, coloured yellow. Kinetic and modelling evidence suggests that only one DNaseI molecule can be bound at the pointed-end (Weber et al, 1994). (The diagram was created using MOLSCRIPT; Kraulis, 1991).

1.10 Thesis rationale

This thesis is primarily concerned with the analysis of the formation of a putative "minifilament". As we are proposing to use the G:A_2 ternary complex as the barbed-end capping species in our analysis of the formation of a putative "minifilament" we first address the question of whether the actin subunits within this complex are held in a filamentous conformation, akin to that for those at the barbed-end of the filament, or in an alternative orientation (chapter 3). The G:A_2 complex is a potent nucleator of actin polymerisation and tightly caps the barbed-end, but the spatial orientation of the actin subunits is still unknown. We propose to use the ability of DNaseI to bind at the pointed-ends of actin monomers to probe the actin subunits in G:A_2. Acknowledging the kinetic and modelling arguments that indicate that *two* DNaseI molecules cannot be accommodated at the pointed-end of actin filament, we similarly propose that *two* DNaseI molecules cannot be accommodated at the pointed-end of the actin monomers within G:A_2 if they are bound with a filamentous orientation.

We then address the possibility of forming a putative "minifilament" complex by combining G:A_2 and A:D together under polymerising conditions (chapter 4). As part of this analysis we also examine the possibility of using the protein tensin (an actin-binding protein localised to focal contacts, discussed in chapter 5) as an alternative to gelsolin as the barbed-end capping molecule due to its smaller size.

2. Materials and methods

2.1 Rabbit muscle actin acetone powder preparation

The method for the preparation of rabbit muscle acetone powder is based on that described by Spudich and Watt (1971). Modifications are described below.

Stock solutions

Guba Straub buffer:	0.3M NaCl;
	0.1M NaH_2PO_4;
	50mM Na_2HPO_4;
	1.0mM NaN_3;
	50mM PMSF;
	1mM $MgCl_2$;
	1mM $Na_4P_2O_7$;
	2.0mM ATP;
	Made up to 4 L with dH_2O, adjusted to pH 6.5.
Solution (i):	50mM $NaHCO_3$;
	0.1mM $CaCl_2$.
	(The above solution is a x10 concentrate and was stored at 4°C).
Solution (ii):	10mM $NaHCO_3$;
	10mM Na_2CO_3;
	0.1mM $CaCl_2$.
	(The above solution was stored at 4°C).
Solution (iii):	Analar acetone, stored at 4°C.

The soleus and upper leg muscles from a large (~ 3kg) newly killed rabbit were excised as quickly as possible. The tissue was placed on ice immediately, to preserve the endogenous ATP, and left to cool for 30min. Following cooling, the fat and connective tissue were removed and the remaining muscle tissue minced. 3 volumes of Guba Straub buffer were added to the minced tissue and left stirring for 15min at

room temperature. The tissue extract was then centrifuged at 3000 xg, for 20min at 4°C, to pellet the residue. The tissue residue pellet is used for the preparation of actin, while the supernatant is used for the preparation of myosin (see section 2.1.2).

2.1.1 Actin preparation

The tissue residue pellet was re-suspended in 10 volumes of solution (i), and stirred for 15min at 4°C. The tissue residue was then filtered through cheesecloth.

This filtered residue was re-suspended in one volume of solution (ii), and stirred for 10min at 4°C. The residue was again filtered through cheesecloth, and the residue then diluted into 10 volumes of dH_2O. This suspension was thoroughly mixed, quickly filtered through cheesecloth and then re-suspended in 2.5L of cold acetone. This was mixed and left to stand at room temperature for 15min. Rounds of filtration, through cheesecloth, and washing with cold acetone were repeated until the supernatant became clear. The residue was then left over-night to dry in a fume hood.

Typical yields of acetone powder were 0.5 – 2.0% (w/w) of the starting muscle tissue.

2.1.2 Myosin preparation

The supernatant fraction (see section 2.1) was filtered through a bed (15cm x 3cm) of 3MM filter paper in Guba Straub buffer. Myosin was then precipitated by the addition of 10 volumes of dH_2O, at 4°C, while stirring. The precipitated myosin was left to settle overnight, at 4°C, and then the clear supernatant carefully decanted off. The settled myosin precipitate was then subjected to centrifugation at 1000 xg for 30min at 4°C.

The resulting pellet was re-dissolved in 10mM $NaPO_4$, pH 7.0 and 0.6M NaCl and stirred for 30min, at 4°C. (The pellet was weighed and NaCl was added to exactly 0.6M). The resultant suspension was then carefully diluted to 0.3M NaCl at pH 6.5 –

6.8, and subjected to centrifugation to pellet any remaining acto-myosin. (Myosin is less soluble at lower pH, but denatures below pH 5.5).

The myosin was re-precipitated in 10 volumes of dH_2O, at 4°C. This mixture was then centrifuged immediately at 15,000 xg, for 15min at 4°C. The resultant pellet was re-dissolved in 10mM $NaPO_4$, pH 7.0; 0.6M NaCl as before and subjected to high-speed centrifugation at 35,000 xg, for 2hrs at 4°C, in a preparative Beckman XL100/70Ti rotor. The supernatant was carefully removed and the concentration of myosin recorded; A_{280} of a 1%(w/v) solution of myosin = 5.6. NaCl, $NaPO_4$, NaN_3, and glycerol were added to give a final buffer composition of 10mM $NaPO_4$, pH 7.0; 0.6M NaCl; 1mM NaN_3; 50% glycerol. The protein was stored in the above buffer at minus 20°C, at a concentration of ~ 10mg.ml^{-1}.

2.1.2.1 Myosin sub-fragment 1 preparation

Myosin (~ 10mg.ml^{-1}) stored in 10mM $NaPO_4$, pH 7.0; 0.6M NaCl; 1mM NaN_3; 50% glycerol, at minus 20°C, was rapidly thawed and dialysed overnight against 10mM imidazole, pH 6.5; 20mM NaCl; 5mM $MgCl_2$, at 4°C. (Myosin forms filaments at low ionic strength. In these myosin filaments, the rods are protected from cleavage, with only the heads, which stick out, being cut. Glycerol is removed, as it tends to reduce the size of the myosin aggregates that form at low ionic strength, and makes them difficult to spin down). The dialysed myosin solution was diluted 2 – 3 times with dialysis buffer and subjected to centrifugation at 50,000 xg, for 30min at 4°C. The resultant pellet was then resuspended in 120mM $NaPO_4$, pH 7.0; 120mM NaCl; 2mM $MgCl_2$; 1mM DTT.

Prior to proteolysis the myosin solution was incubated at 25°C. Papain (a cysteine protease, made up as a 100mM stock solution in 200mM $NaPO_4$, pH 7.0) was added at 1:700 - 800 (w/w) to the myosin solution and the mixture incubated for 7min. The reaction was quenched by the addition of iodoacetamide to 1mM. (Iodoacetamide reacts covalently with the cysteine group at the active site and irreversibly inhibits the enzyme).

This reaction mixture was immediately subjected to dialysis against 50mM Tris, pH 6.8; 2mM $MgCl_2$; 2mM DTT, for 2hrs at 4°C. (This reduces the salt to 20 – 30mM). The sample was then centrifuged at 40,000 xg, for 30min at 4°C, to clarify the myosin solution (rod sections and undigested heads remain insoluble, and so sediment) leaving essentially only the soluble S-1 head in the supernatant fraction.

Prior to storage or use in further experiments, myosin is frequently subjected to further purification by anion-exchange chromatography, on DEAE-Sepharose columns equilibrated in 10mM imidazole, pH 6.8; 2mM $MgCl_2$; 2mM DTT. Elution is typically achieved with a gradient of 0 – 100mM NaCl, in the same buffer, over 6 column volumes.

The appropriate fractions were then dialysed against 50mM Tris, pH 6.8; 2mM $MgCl_2$; 2mM DTT prior to use. Myosin was stored in 50mM Tris, pH 6.8; 2mM $MgCl_2$; 2mM DTT; 20% sucrose (w/v) at minus 80°C.

2.2 Extraction and purification of G-Actin using 1M Tris, pH 8.0: ATP-G-Buffer

The G-Actin extraction and purification protocol was adapted from those of Spudich and Watt (1971) and Pinder at al (1995). Modifications are as follows.

ATP-G-Buffer

5mM Tris, pH 8.0; 0.5mM DTT; 0.2mM $CaCl_2$; 0.2mM ATP; 1.0mM NaN_3.

1.0M Tris, pH 8.0; ATP-G-Buffer

1.0M Tris, pH 8.0; 0.5mM DTT; 0.2mM $CaCl_2$; 0.2mM ATP; 1.0mM NaN_3.

40ml of ATP-G-Buffer, at 4°C, was added to each gram of rabbit muscle acetone powder. The mixture was stirred gently for 1½ – 2hrs at 4°C. The extract was then filtered sequentially, under suction, through Whatman No. 54 filter paper, 8µm

cellulose membranes and finally 0.22μm cellulose membranes. (The filtrate should be clear at this stage). KCl was then added to 0.8M, while gently stirring. When most of the KCl had dissolved $MgCl_2$ and EGTA were added to 2mM and 0.1mM, respectively. This mixture was left to polymerise for 1hr at room temperature.

The polymerised solution was then subjected to high-speed centrifugation at 160,000xg, for 2hrs at 4°C, in a preparative Beckman XL100/70Ti rotor. This pellets essentially only F-actin. The supernatant was discarded and the gelatinous F-Actin pellet removed and homogenised in ~ 20ml of 1.0M Tris, pH 8.0; ATP-G-Buffer, at 4°C. Following homogenisation the suspension was diluted with 1.0M Tris, pH 8.0; ATP-G-Buffer, at 4°C, so the final actin concentration was ~ 0.5 – 1.0 $mg.ml^{-1}$. (We worked on the assumption that we extract ~ 30mg of actin from every gram of acetone powder). This solution was dialysed overnight against 1L of 1.0M Tris, pH 8.0; ATP-G-Buffer, at 4°C. The dialysate was then clarified by high-speed centrifugation at 160,000 xg, for 2hr at 4°C, in a preparative Beckman XL100/70Ti rotor, and the supernatant carefully removed. The depolymerised G-Actin was stored in this solution, at 4°C, until required. Every 2 weeks the G-Actin solution was dialysed against 1L of 1.0M Tris, pH 8.0; ATP-G-Buffer, at 4°C, and then filtered through a 0.22μm filter.

Prior to use in other experiments ~ 10 – 15ml of the 1M Tris-G-Actin solution was filtered through a 0.22μm filter and concentrated to ~ 2ml (~ $5mg.ml^{-1}$). This sample was then subjected to gel-filtration chromatography on an S200 size-exclusion column (V_t ~ 135ml; 65cm x 1.6cm), pre-equilibrated in ATP-G-Buffer, with a flow rate of $0.5ml.min^{-1}$. Proteins were detected by A_{280nm} and analysis by SDS-PAGE. The relevant fractions were pooled and the G-Actin concentrated to ~ $1mg.ml^{-1}$, (based on the absorption coefficient of 0.63 at 290nm for a $1mg.ml^{-1}$ solution with a 1cm path-length).

This high concentration Tris buffer enabled us to store G-actin in native and an active state for over 4 months, in comparison to 2 – 3 weeks for conventional ATP-G-Buffer. See appendix A for details of the viability of 1.0M Tris, pH 8.0; ATP-G-

Buffer, at 4°C, for the long term storage of G-Actin with native activity, as judged by critical concentration ([Cc]) assay with 5% pyrene labelled actin.

2.3 Pyrene-actin preparation

Pyrene-actin was prepared from pre-purified G-Actin and modified by the coupling of N-pyrenyl iodoacetamide (Molecular Probes Inc.) to residue Cys-374, based on the method of Kouyama and Mihashi (1981). Modifications are described below.

Approximately 15mg of G-actin, concentrated to ~ 2mg.ml^{-1} was dialysed over night, at 4°C, against 25mM Tris, pH 8.0; 0.2mM ATP; 1mM NaN_3; 100mM KCl; 2mM $MgCl_2$, at a 1:100 volume ratio for sample:dialysis buffer, respectively. The concentration of polymerised actin was then adjusted to 1mg.ml^{-1} (based on the absorption coefficient of 0.63 at 290nm for a 1mg.ml^{-1} solution with a 1cm path-length). This solution was then transferred to a suitable container (~ 25ml volume) and N-pyrenyl iodoacetamide (stock solution of 10mM in Dimethylformamide, DMF) was added at a molar ratio of 7:1 N-pyrenyl iodoacetamide:actin, while gently stirring. Following addition of N-pyrenyl iodoacetamide, the solution is covered in foil and left overnight at 4°C.

The sample was then subjected to low speed centrifugation at 3000 xg, for 5min at 4°C, to pellet any precipitated dye. The clarified supernatant was carefully removed and subjected to centrifugation at 160,000 xg, for 2hrs at 4°C, in a preparative Beckman XL100/70Ti rotor, to precipitate the filamentous actin. The supernatant was discarded and the gelatinous F-Actin pellet removed and homogenised in ~ 10ml of ATP-G-Buffer. The sample was subjected to dialysis against ATP-G-Buffer, at a 1:100 volume ratio for sample:dialysis buffer, respectively, for 48 hrs in the dark, at 4°C, with several buffer changes.

Following exhaustive dialysis the G-Actin solution was clarified by centrifugation at 160,000 xg, for 2hrs at 4°C, in a preparative Beckman XL100/70Ti rotor. The resulting supernatant was then concentrated to ~ 2ml (~ 5mg.ml^{-1}) and then subjected to size-exclusion chromatography on an S200 column, (V_t ~ 135ml; 65cm x 1.6cm), pre-equilibrated in ATP-G-Buffer, with a flow rate of 0.5ml.min^{-1}. The relevant fractions were pooled, concentrated to ~ 1mg.ml^{-1}, and either used immediately or 0.5ml aliquots were flash frozen with liquid nitrogen, in ATP-G-Buffer, and stored at minus 70°C until needed. Prior to use the pyrene-actin aliquots were rapidly thawed and then centrifuged at 160,000 xg, for 30min at 4°C, in a preparative Beckman XL100/70Ti rotor. The supernatant was carefully removed and the extent of labelling measured.

The extent of pyrene labelling was calculated using the extinction coefficients listed below:

$$\%\text{Label} = [\text{Pyrene-Actin}] / [\text{Actin}]_{total}$$

$$[\text{Pyrene-Actin}] = A_{344nm} / 2.2 \times 10^4\ (M^{-1})$$

$$[\text{Actin}]_{total} = (A_{290nm} - ((A_{344nm} \times 0.127)) / 2.66 \times 10^4\ (M^{-1})$$

Typical labelling was between 65 – 95% with a ~ 60% yield of the total actin initially used.

2.4 N-ethylmaleimide/4-chloro-7-nitro-2,1,3-benzoxadiazole-Actin (NEM/NBD)-Actin preparation

NEM/NBD-Actin was prepared from pre-purified G-Actin based on the method of Detmers et al (1981). Modifications are described below.

Modified ATP-G-Buffer for NEM labelling

5mM Tris, pH 8.0; 0.2mM $CaCl_2$; 0.2mM ATP.

N-ethylmaleimide (NEM) labelling of Cys-374. Approximately 15mg of G-actin (~ 2mg.ml^{-1}) was dialysed over night, at 4°C, against 5mM Tris, pH 8.0; 0.2mM $CaCl_2$; 0.2mM ATP; 0.2mM DTT, at a 1:100 volume ratio for sample:dialysis buffer, respectively. The dialysate was filtered through a 0.22µm filter and NEM, (stock solution of 100mM in dH_2O), was added to a final concentration of 1.0mM. Immediately following NEM addition NaCl and $MgCl_2$ were added to 100mM and 2mM, respectively. The mixture was left to polymerise at room temperature for 30min and then DTT was added to 1mM, to quench the reaction. The sample was then subjected to high-speed centrifugation at 160,000 xg, for 2hr at 4°C, in a preparative Beckman XL100/70Ti rotor. The supernatant was discarded and the gelatinous F-actin pellet resuspended in ~10ml of modified ATP-G-Buffer. The sample was subjected to dialysis against modified ATP-G-Buffer, at a 1:100 volume ratio for sample:dialysis buffer, respectively, for 48 hrs in the dark at 4°C, with several buffer changes.

4-chloro-7-nitro-2,1,3-benzoxadiazole (NBD) labelling of Lys-373. Following exhaustive dialysis the NEM-G-Actin solution was clarified by high-speed centrifugation at 160,000 xg, for 1hr at 4°C, in a preparative Beckman XL100/70Ti rotor and the concentration then adjusted to 1mg.ml^{-1} (based on the absorption coefficient of 0.63 at 290nm for a 1mg.ml^{-1} solution with a 1cm path-length). NBD was then added to the supernatant to 0.6mM, (stock solution of 20mM in 95% ethanol), and NaCl and $MgCl_2$ immediately added to 100mM and 2mM respectively. This mixture was left for 5hrs, at room temperature, in the dark, while *gently* stirring. Following this the F-Actin solution was centrifuged at 160,000 xg, for 2hrs at 4°C, in a preparative Beckman XL100/70Ti rotor. The supernatant was discarded and the gelatinous F-actin pellet resuspended in ~10ml of modified ATP-G-Buffer. The sample was subjected to dialysis ATP-G-Buffer, at a 1:100 volume ratio for sample:dialysis buffer, respectively, for 48 hrs in the dark at 4°C, with several buffer changes. Finally, the NBD-G-Actin was filtered through a 0.22µm filter before use. The shelf life of NBD-Actin is ~ 2 - 3 weeks, and all experiments carried out with NBD-Actin were performed within this time.

The extent of labelling was calculated using the extinction coefficients listed below:

$$\% \text{ labelling} = [\text{NBD-Lys-373}] / [\text{Actin}]_{total}$$
$$[\text{NBD-Lys-373}] = A_{480nm} / 26{,}000\ (M^{-1})$$
$$[\text{Actin}]_{total} = A_{290nm} / 26{,}000\ (M^{-1})$$

Typical labelling was between 40 – 70% with a ~ 40 – 60% yield of the total actin initially used.

2.5 Actin critical concentration assay ($[C_c]$)

The protocol used was based on that described by Kouyama and Mihashi (1981). Modifications are described below.

Pre-purified G-Actin and pyrene-actin are required. A dilution series of actin (5% pyrene labelled) was set up, with actin concentrations typically ranging from 0.1, 0.2, 0.3, 0.4, 0.5, 0.6, 0.7, 0.8, 1.0, 1.2, 1.5, 1.8, 2.0μM. One dilution series was incubated under depolymerising conditions (ATP-G-Buffer) while the other was incubated under polymerising conditions (ATP-F-Buffer). Upon incorporation of pyrene actin into the filament, a ~ 20 – 25 fold fluorescence enhancement (linearly dependent on the actin concentration), over that of a similar concentration of 5% pyrene labelled G-actin, is observed. Linear extrapolation of the G and F-Actin series, to the intersection point, gives the $[C_c]$ for that particular actin preparation, or set of conditions, (see example in fig. 2.1).

Method

Typically, a 12μM/5% pyrene G-Actin stock solution was first prepared. From this, a 6μM/5% pyrene F-Actin solution was prepared by the addition of KCl and $MgCl_2$ to 100mM and 2mM, respectively. This was left for 2hrs, at 20°C in the dark, to polymerise. Following polymerisation, the sample was subjected to brief

ultrasonication (a single 20sec burst, at 4°C). Each individual sample in the F-Actin dilution series was then prepared by diluting the appropriate amount of 6μM/5% pyrene F-Actin to the appropriate concentration with ATP-F-Buffer, to a final reaction volume of 500μl. A similar dilution series was also prepared using the 12μM/5% pyrene G-Actin stock solution and ATP-G-Buffer. Both the F and G-Actin dilution series were then incubated for 24hrs, at 20°C in the dark.

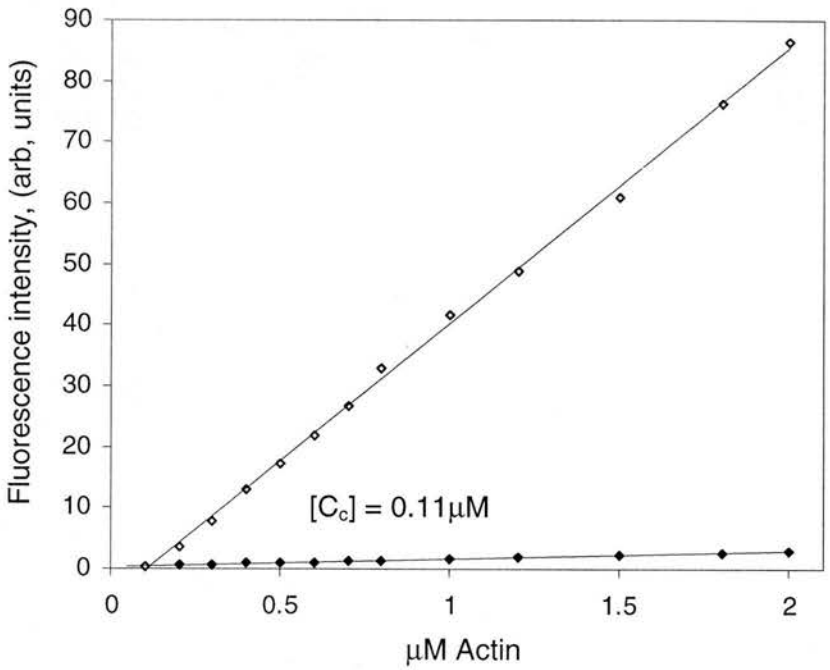

Fig. 2.1 ***Actin critical concentration ([C_c]) assay.*** [C_c] assay performed after a 24hr incubation, at 20°C in the dark. *Closed squares* indicate the fluorescence intensity of the G-Actin dilution series. *Open squares* indicate the fluorescence intensity enhancement of the F-Actin dilution series, under polymerising conditions; 100mM KCl; 2mM $MgCl_2$. The solid lines represent a linear regression and the intersect of the two series reports the [C_c] of the actin; 0.11μM in this particular preparation. The excitation wavelength was 366nm, the emission wavelength was 384nm, with a 5nm slit for both.

Following this incubation, the fluorescence of each sample was measured. Fluorescence measurements were carried out in a Perkin-Elmer LS50B spectrofluorimeter at 20°C, with a Grant LTD6 temperature control unit. The excitation wavelength for pyrene actin was 366nm and the emission wavelength was 384nm, using a 5nm slit width for both. A quartz fluorimeter cuvette with a 1cm-path length and a 400μl working volume was used. F-Actin containing samples were

removed from the incubation tubes, and added to the cuvette using a truncated tip, to prevent breakage of the filaments due to shearing forces. The fluorescence intensity is reported in arbitrary units.

2.6 Actin polymerisation/depolymerisation assays

The ability of proteins to influence actin assembly/disassembly was determined by their effect on the initial rate and extent of the fluorescence intensity increase, caused by polymerisation of pyrene labelled actin monomers. The basis of this assay is described by Kouyama and Mihashi (1981) and Walsh et al (1984). Modifications are as follows.

2.6.1 Polymerisation assay

G-Actin (20% pyrene labelled) was prepared at a concentration of 1.0μM in ATP-G-Buffer. F-Actin, used as seeds for nucleation, was prepared by polymerising 20 – 30μM actin (unlabelled), in ATP-G-Buffer, by the addition of KCl and $MgCl_2$ to 100mM and 2mM, respectively. This mixture was left for 30min at room temperature, and then ATP-F-Buffer was used to dilute the polymerised actin to 3.0μM. The F-Actin solution was equilibrated at 20°C for 2hrs before subsequent use.

Method

The final reaction volume was 500μl. A solution containing 2M KCl, 40mM $MgCl_2$ ("20x salt") was added to 250μl of 1.0μM G-Actin so the final concentrations were 100mM KCl and 2mM $MgCl_2$. This was incubated for 60sec, at 20°C, before the addition of F-Actin seeds (0.1μM) to nucleate polymerisation. Aliquots of 3.0μM F-Actin were vortexed for 20sec, then mixed with the appropriate amount/volume of protein (T-cap-protein or Gelsolin, in ATP-F-Buffer). Following a subsequent 20sec incubation ATP-F-Buffer was added to a final volume of 250μl. The F-Actin seeds

were then added to the G-Actin solution, to nucleate polymerisation, and following a further 20sec incubation, 400µl of the reaction mixture was removed and placed in a quartz fluorescence cuvette (1cm path length) and the rate of polymerisation measured. (The total incubation time was 90sec. This includes ~ 10sec for the transfer of the reaction mixture into the cuvette and the transfer of the cuvette into the holding cell of the fluorimeter). The initial rate of polymerisation was measured by monitoring the increase in the fluorescence intensity of pyrene actin. Fluorescence measurements were carried out in a Perkin-Elmer LS50B spectrofluorimeter at 20°C, with a Grant LTD6 temperature control unit. The excitation wavelength for pyrene actin was 366nm and the emission wavelength was 384nm, using a 5nm slit width for both. The fluorescence signal was typically measured for 400, 800 or 1000 sec.

The initial rate of polymerisation can be directly measured from the initial increase in the fluorescence intensity of pyrene labelled actin, which is proportional to the rate of incorporation of monomers into filaments. d[F-Actin] / dt can be calculated from the relationship:

$$d[F\text{-}Actin] / dt = df / dt \cdot \{[total\ actin] / (fF - fG)\},$$

where fF is the fluorescence of the pyrene-actin when it is all polymerised, fG is the fluorescence when all the pyrene-actin is monomeric and df / dt is the time dependent fluorescence. df / dt can be calibrated, from the mean fluorescence intensity values from a range of concentrations of G-Actin and F-Actin, obtained from critical concentration assays, to give d[F-actin] / dt in $nM.s^{-1}$.

2.6.2 Depolymerisation assay

Method

20 – 30µM G-Actin (20% pyrene), in ATP-G-Buffer, was polymerised by the addition of KCl and $MgCl_2$ to 100mM and 2mM, respectively. This mixture was left

for 30min at room temperature, and then further diluted to 3.0μM by the addition of ATP-F-Buffer. The F-Actin solution was equilibrated at 20°C for 2hrs before subsequent use.

Aliquots of F-Actin were vortexed for 20sec and then the appropriate amount/volume of protein (T-cap-protein or Gelsolin) was added and mixed and incubated for a further 10secs. ATP-G-Buffer or ATP-F-Buffer was then added to give a final concentration of actin of 0.5μM, in a total reaction mixture volume of 500μl. 400μl of the reaction mixture was then removed and placed in a quartz fluorescence cuvette (1cm path length) and the rate of polymerisation measured. The initial rate of polymerisation was measured by monitoring the increase in the fluorescence intensity of pyrene actin. Fluorescence measurements were carried out in a Perkin-Elmer LS50B spectrofluorimeter at 20°C, with a Grant LTD6 temperature control unit. The excitation wavelength for pyrene actin was 366nm and the emission wavelength was 384nm, using a 5nm slit width for both. The fluorescence signal was typically measured for 400, 800 or 1000 sec.

2.7 Actin co-sedimentation assay

The protocol used was based on that described by Winder and Walsh (1990). Modifications are described below.

The assay volume used was 50 or 100μl (the amount of available protein dictates the actual volume used). 20 – 30μM G-Actin, in ATP-G-Buffer, was polymerised by the addition of KCl and $MgCl_2$ to 100mM and 2mM, respectively. This was left to incubate at room temperature for 1hr before use in the co-sedimentation assays. The protein under examination (e.g. T-cap-protein) was concentrated to ~ 1000μM, in ATP-F-Buffer. A dilution series of the F-Actin binding protein under examination, was then set up (typically with the range of concentrations of 0, 2, 5, 10, 20, 50, 80, 100, 200, 400, 1000μM). Additionally an incubation containing the highest

concentration of ligand alone and 10μM F-Actin alone were also set up. The appropriate amount of the F-Actin binding protein was then diluted to the appropriate final concentration, in a final volume of 50 or 100μl, with ATP-F-Buffer, and gently mixed. The final concentration of actin was 10μM in every reaction mixture. The samples were then incubated for 15min at room temperature, and then subsequently centrifuged at 386,000 xg, in a TL100 Ultracentrifuge rotor (Beckman), for 15min at 4°C.

Following the high-speed centrifugation, the supernatant was carefully removed and added to an equal volume of 2x SDS-PAGE sample buffer. 50 or 100μl (whatever the assay volume used) of 2x SDS-PAGE sample buffer was then added to the F-Actin pellet fraction. This was incubated at room temperature for 30min, to allow the pellet to completely dissolve. The pellet fraction was then transferred to a fresh tube and the original washed with an equal volume of ATP-F-Buffer. This was then added to the pellet fraction. Equal volumes of the supernatant and pellet fractions were then subjected to SDS-PAGE analysis. Typically 10% (w/v) polyacrylamide gels were used and run as described. The gels were stained with SYPRO™ Red protein stain and the intensities of the bands analysed as described in ImageQuant™, performed as described. Following analysis in ImageQuant™ the gels were re-stained with R250 Coomassie Blue to visualise the proteins normally.

Typically the amount of ligand bound to the F-Actin fraction is calculated from the difference between the two intensities of the supernatant and pellet fractions (where the sum of the two intensities corresponds to the total ligand concentration used in the incubation). Corrections need to be made to the values obtained for the band intensities. The amount of ligand that pellets in the absence of any actin (% of insoluble material) is obtained from the incubation tube containing the highest concentration of ligand alone, in the absence of F-Actin. This value was typically 1 – 2% of the concentration added. The amount of ligand "trapped" by the F-Actin filament network, in a non-specific way also needs to be determined empirically, with a protein of similar size that does not bind to actin (e.g. ovalbumin was used for T-cap-protein). Typically this value was ~ 1%. The corrections reduced the mean

apparent ligand in the pellet by ~ 2%. The 10μM F-Actin incubation tube provide a reference for the quality of the actin and provides a monitor for any change in the critical concentration due to ligand binding (any change in the amount of actin recovered in the supernatant fractions).

Typically the binding data is analysed by Scatchard plots, plotting:

[Bound ligand] / [Free ligand] vs [Bound ligand] / [F-Actin]

The K_d can be derived from 1/gradient and maximum ligand bound per F-Actin monomer (i.e. the stoichiometry of binding) from the intersection on the x-axis. Alternatively, non-linear least squares fitting of the data to equation below can be performed;

$$[\text{Bound ligand}] = B_{max} * [\text{ligand}] / ([\text{ligand}] + K_d),$$

where B_{max} is equal to the maximal amount of ligand bound and K_d is equilibrium dissociation constant.

2.8 Recipes for *E. coli* growth media

The recipes used were based on those described by Sambrook et al (1989), in *Molecular Cloning. A laboratory manual.*

Stock solutions

Ampicillin (AMP), 50mg.ml^{-1} in dH_2O.

Streptomycin (STREP), 40mg.ml^{-1}, in dH_2O.

Thiamine (THI), 1mg.ml^{-1}, in dH_2O.

20% Glucose.

Isopropyl-β-D-thio-galactopyranside (IPTG), 1M in dH_2O.

(All of the above were sterile filtered through a 0.22µm filter and stored at minus 20°C).

1M $MgSO_4$.

1M $CaCl_2$.

1 litre of x4 M9 salts:	$Na_2HPO_4.7H_2O$	64g;
	KH_2PO_4	15g;
	NaCl	2.5g;
	NH_4Cl	5.0g.

(All of the above were autoclaved separately).

2xTY agar plates

15g.L^{-1} Bacto-Agar;

31g.L^{-1} 2x yeast-tryptone powder (2xTY).

The media was autoclaved in a suitable sterile vessel, and cooled to below 50°C before the addition of any antibiotic/heat sensitive compound.

2xTY/Ampicillin (AMP) agar plates

Ingredients are identical to those listed above, except with the addition of ampicillin to 50µg.ml^{-1}.

M9 minimal media agar plates

6g Bacto-Agar;

100ml of x4 M9 salts;

0.8ml of 1M $MgSO_4$;

40µl of 1M $CaCl_2$;

dH_2O added to final volume of 400ml.

The media was autoclaved in a suitable sterile vessel, and cooled to below 50°C. After cooling the following were added:

THI, to 1µg.ml^{-1};

8ml of 20% glucose;

STREP, to 25µg.ml^{-1}.

2xTY liquid growth media

31g.L^{-1} 2x yeast-tryptone powder (2xTY).

The media was autoclaved in a sterile 2L conical shaker flask, and cooled to below 50°C before the addition of any antibiotic/heat sensitive compound.

2xTY/AMP liquid growth media

Ingredients are identical to those listed above, except with the addition of ampicillin to 50μg.ml^{-1}.

2.9 Bacterial strains

Bacterial strains used.

Strain (*E. coli*)	Genotype	Use/Reference
JM 101	*supE, thi-1, Δ(lac-proAB), F'[traD36, proAB$^+$, lacI^q, lacZΔM15]*	High copy plasmid replication strain. (Yanisch-Perron et al, 1985).
JM 109	*recA1, supE44, endA1, hsdR17, gyrA96, relA1, thi, Δ(lac-proAB), F'[traD36, proAB$^+$, lacI^q, lacZΔM15]*	High copy plasmid replication strain. (Yanisch-Perron et al, 1985).
JM 105	*thi, rpsL, endA, sbcB15, hsdR4, supE, Δ(lac-proAB), F'[traD36, proAB$^+$, lacI^q, lacZΔM15]*	Recombinant gene expression from the *tac* promoter (*trp – lac* hybrid), with induction by addition of IPTG. (Yanisch-Perron et al, 1985).
BL21(DE3)	*hsdS, gal, (λcIts857, ind1, Sam7, nin5, lacUV5-T7* gene 1*)*	Recombinant gene expression from the T7 promoter, with induction by addition of IPTG. (Studier and Moffat, 1986).

2.10 Over-night bacterial cultures

20ml of 2xTY growth media (either minus antibiotic or with AMP added to 50μg.ml^{-1}), in a 250ml conical shaker flask, was inoculated with a single colony of a given bacterial strain. The cells were then grown, shaking at 37°C, until A_{600nm} ~ 0.6 – 1.0. The cells were decanted into a sterile 50ml Falcon tube and placed on ice for 15min. Following this, the cells were stored overnight at 4°C. The cells were then pelleted by centrifugation at 3000 xg, for 5min at 4°C. The cells were re-suspended in 20ml of fresh 2xTY media and aliquots of this overnight culture were then used to inoculate larger volumes of growth media for protein expression, plasmid amplification and extraction or for the preparation of Ca^{2+} competent cells.

2.11 Ca^{2+} competent *E. coli*

The protocol used was based on that described by Sambrook et al (1989), in *Molecular Cloning. A laboratory manual.*

5ml from an over-night culture of a given *E. coli* strain, (grown in 2xTY *minus* antibiotic), was used to inoculate 100ml of 2xTY in a 250ml conical shaker flask. Cells were grown, shaking at 37°C, until A_{600nm} reached ~ 0.6 – 1.0. The cells were then transferred to two sterile, 50ml Falcon tubes, and left on ice for 10min. The cells were centrifuged at 3000 xg, for 5min at 4°C, the supernatant carefully removed, and then the cell pellets gently re-suspended in ~ 10ml of 100mM $CaCl_2$ at 4°C. The suspension was left at 4°C for 1hr. Following this incubation the cells were subjected to centrifugation at 3000 xg, for 5min at 4°C, the supernatant removed, and the cell pellets gently re-suspended in ~ 2ml of 100mM $CaCl_2$ 4°C. Ca^{2+} competent cells were stored at 4°C and either used immediately or within 5 days.

2.12 Transformation of *E. coli*

The protocol used is a heat shock method, based on that described by Sambrook et al (1989), in *Molecular Cloning. A laboratory manual.*

100µl of Ca^{2+} competent cells were transferred to a sterile 0.5ml Eppendorf tube at 4°C. 3.0µl of plasmid DNA was added, the solution mixed very gently, and left for 1hr, at 4°C. The cells were then placed in a water bath, at 42°C, and heat shocked for 1min. Following heat shock, the cells were placed on ice for 5min. 500µl of 2xTY media was then added, and the cells were incubated, shaking at 37°C, for 15min. 50µl of the recovered *E. coli,* were transferred onto a 2xTY/AMP (50µg/ml) agar plate and spread using a sterile glass spreader. The agar plate was left for 5min to allow the cell suspension to soak into the media, and then incubated overnight, at 37°C, in an inverted position. Successful transformants were used immediately or stored at 4°C until needed (no longer than 4 weeks).

2.13 Alkali lysis plasmid mini prep

The protocol used was based on that described by Sambrook et al (1989), in *Molecular Cloning. A laboratory manual.*

Stock solutions

SET:	20% (w/w) sucrose;
	50mM Tris, pH 8.0;
	50mM EDTA.
	(The above solution was stored at 4°C).
Alkali lysis:	0.2M NaOH;
	1% (w/v) SDS.
	(The above solution was made up fresh before use).

3M NaAcetate, pH 4.8 (acetic acid), stored at 4°C.

RNase A: $10mg.ml^{-1}$ in dH_2O. (The enzyme was heated to 80°C to inactivate any trace of DNaseI present. It was subsequently stored at minus 20°C).

TE: 10mM Tris, pH 8.0;
0.1mM EDTA.
(The above solution was stored at room temperature).

70% (v/v) Ethanol.

Isopropanol.

A high plasmid copy *E. coli* strain (e.g. JM101, JM109) was transfected with the appropriate plasmid DNA. An overnight culture, (with the appropriate antibiotic added), was grown containing transfected bacteria. 1ml aliquots of the re-suspended cells were then centrifuged at 13,000 xg, for 5min at 4°C. The supernatant was carefully removed and 150µl of SET buffer and 5µl of RNaseI was then added. The mixture was vortexed vigorously and 350µl of alkali lysis solution was added. The solution was gently mixed, by several inversions, until the mixture cleared. The solution was placed on ice for 5min at 4°C. Following this incubation, 250µl of cold 3M NaAcetate, pH 4.8, was added, the solution mixed well, and then placed back on ice for a further 10min. The mixture was then subjected to centrifugation at 13,000 xg, for 10min at 4°C, and the supernatant, containing plasmid DNA, carefully removed to a new tube. This new tube was filled with isopropanol, mixed well and subjected to centrifugation at 13,000 xg, for 5min at room temperature. The supernatant was again carefully removed and 0.5ml of 70% (v/v) EtOH, at room temperature, was added to the precipitate. (A precipitate may not be actually seen as "clean" plasmid DNA is often transparent). The sample was vortexed and centrifuged at 13,000 xg, for 5min at room temperature. The EtOH was then removed and the plasmid DNA pellet re-suspended in 50µl of TE buffer. Plasmid DNA was stored at minus 70°C.

2.14 Recombinant mutant DNaseI/H134Q purification protocol

2.14.1 Optimisation of expression

Ca^{2+} competent JM105 *E. coli* were successfully transformed with pkk223-3[DNaseI/H134Q] and maintained on 2xTY/AMP (50μg.ml^{-1}) agar plates. 5ml from an overnight culture was used to inoculate 100ml of 2xTY/AMP (50μg.ml^{-1}). The cells were grown, shaking at 37°C, until the A_{600nm} ~ 0.6 – 1.0 and induction of synthesis of DNaseI was carried out by addition of IPTG to 1.0mM. 5ml aliquots were removed at various time intervals and the percentage of DNaseI in the soluble protein fraction was analysed.

The cell pellets obtained at each time point were resuspended in 10mM Tris, pH 7.6; 2mM $CaCl_2$; 1.0mM NaN_3; 100μM PMSF; 100μM benzamidine, and subjected to lysis by ultrasonication (3 x 20sec bursts at 4°C). The resulting cell lysate was then centrifuged at 18,000 xg, for 5min at 4°C. The soluble supernatant fraction was removed and the insoluble pellet fraction was resuspended in the same volume of 10mM Tris, pH 7.6; 2mM $CaCl_2$; 1.0mM NaN_3; 100μM PMSF; 100μM benzamidine. 5μl of 5x SDS-sample buffer was added to 20μl samples of soluble, insoluble and pre-lysis whole-cell fractions. These samples were then subjected to SDS-PAGE. The appearance and relative percentage of DNaseI in the soluble and insoluble fractions was subsequently analysed by gel densitometry, performed as described.

2.14.2 Purification protocol

(All purification was performed on Pharmacia Gradifrac™ or FPLC™ systems). Calcium competent JM105 *E. coli* were successfully transformed with pkk223-3[DNaseI/H134Q] and maintained on 2xTY/AMP (50μg.ml^{-1}) agar plates. 10ml from an overnight culture was used to inoculate 1 L of 2xTY/AMP (50μg.ml^{-1}). The cells were grown, shaking at 37°C, until the A_{600nm} ~ 0.6 – 1.0 and induction of synthesis of DNaseI was carried out by addition of IPTG to 1.0mM. The cells were

grown for a further 4hrs and then harvested by centrifugation at 3000 xg, for 10 min at 4°C. The cell pellets were either processed immediately or were flash-frozen with liquid nitrogen in 10ml of 30mM Tris, pH 8.0; 4mM EDTA; 1.0mM NaN_3; 5ml of bacterial cell extract inhibitor cocktail (Sigma), per litre of original bacterial cell culture, and stored at minus 70°C until needed.

Cell pellets were re-suspended at 10% (w/v) of cells, in 30mM Tris, pH 8.0; 4mM EDTA; 1.0mM NaN_3; 5ml.L^{-1} of bacterial cell extract inhibitor cocktail (Sigma). The cell suspension was then lysed by ultrasonication, (5 x 20sec bursts at 4°C). Following centrifugation at 50,000 xg, for 1hr at 4°C, the clarified, soluble cell extract was dialysed overnight against 10mM Tris, pH 7.6; 2mM $CaCl_2$; 1.0mM NaN_3; 100µM PMSF; 100µM benzamidine at a 1:100 volume ratio for sample:dialysis buffer, respectively. The dialysate was then filtered through a 0.22µm filter and loaded onto a DEAE-Sepharose column (V_t ~ 50 ml; 2.6cm x 9.5cm) pre-equilibrated in the same buffer. Unbound proteins were washed through with this buffer and bound proteins were eluted by a gradient of 0 - 0.3M NaCl, over 6 column volumes (300ml), with a flow rate of 1.0ml.min^{-1}. Proteins were detected by A_{280nm} and analysis by SDS-PAGE.

Relevant fractions were pooled, concentrated and dialysed overnight against 10mM Tris, pH 7.6; 2mM $CaCl_2$; 1.0mM NaN_3; 100µM PMSF; 100µM benzamidine, at a 1:100 volume ratio for sample:dialysis buffer, respectively. The dialysate was then filtered through a 0.22µm filter and loaded onto a Cibacron F3GA Blue column (V_t ~ 5.0ml; 1.0cm x 6.5cm), pre-equilibrated in the same buffer. Unbound proteins were washed through with this buffer and specific elution of DNaseI from the resin was achieved with a 1mM – 10mM ATP gradient, over 10 column volumes, with a flow rate of 0.3ml.min^{-1}. Proteins were detected by A_{280nm} and analysis by SDS-PAGE.

Relevant fractions were pooled, concentrated and dialysed overnight against 10mM Tris, pH 7.6; 2mM $CaCl_2$; 1.0mM NaN_3; 100µM PMSF; 100µM benzamidine, at a 1:100 volume ratio for sample:dialysis buffer, respectively. The dialysate was filtered through a 0.22µm filter, concentrated to ~ 2ml, and subjected to size-

exclusion chromatography on a Sephacryl-200 (S200) column (V_t ~ 135ml; 65cm x 1.6cm), pre-equilibrated in the same buffer, with a flow rate of 0.5ml.min^{-1}. Proteins were detected by A_{280nm} and analysis by SDS-PAGE, and the relevant fractions pooled and concentrated and stored at 4°C, in the above buffer, until needed. (See appendix B for details of alternative storage conditions and assay of the activity of DNaseI purified by this protocol).

2.15 Human cytoplasmic gelsolin (HGS) purification protocol

(All purification was performed on Pharmacia Gradifrac™ or FPLC™ systems). Ca^{2+} competent BL21(DE3) *E. coli* were successfully transformed with pMW172[HGS] and maintained on 2xTY/AMP (50μg.ml^{-1}). 10ml from an overnight culture was used to inoculate 1 L of 2xTY/AMP (50μg.ml^{-1}). The cells were grown, shaking at 37°C, until the A_{600nm} ~ 0.6 – 1.0 and induction of synthesis of gelsolin was carried out by addition of IPTG to 1.0mM. The cells were grown for a further 3hrs and then harvested by centrifugation at 3000 xg, for 10 min at 4°C. The cell pellets were either processed immediately or were flash-frozen with liquid nitrogen, in 10ml of 30mM Tris, pH 8.0; 4mM EDTA; 1.0mM NaN_3; 5ml of bacterial cell extract inhibitor cocktail (Sigma), per litre of original bacterial cell culture, and stored at minus 70°C until needed.

The cell pellets were resuspended at 10% (w/v) of cells, in 30mM Tris, pH 8.0; 4mM EDTA; 1.0mM NaN_3; 5ml.L^{-1} of bacterial cell extract inhibitor cocktail (Sigma). The cell suspension was then lysed by ultrasonication, (5 x 20sec bursts at 4°C). Following centrifugation at 50,000 xg, for 1hr at 4°C, the clarified soluble cell extract was dialysed overnight against 25mM Tris, pH 8.0; 0.1mM DTT; 1.0mM NaN_3; 0.2mM EGTA; 100μM PMSF; 100μM Benzamidine, at 4°C. The dialysate was then filtered through a 0.22μm filter and loaded onto a Cibacron F3GA Blue column (V_t ~ 10.0ml; 1.6cm x 5.0cm), pre-equilibrated in the same buffer. Unbound proteins were washed through with this buffer and gelsolin was specifically eluted

with a wash of 1mM ATP, in the above buffer, over 3 column volumes (15ml), with a flow rate of 0.5ml.min^{-1}. Proteins were detected by A_{280nm} and analysis by SDS-PAGE.

For samples from greater than 500ml of original bacterial cell culture, a second round of chromatography, on a Cibacron F3GA Blue column in the presence of calcium, was routinely carried out. Relevant fractions from the first column were pooled, concentrated and dialysed overnight against 25mM Tris, pH 8.0; 0.1mM DTT; 1mM Azide; 1.0mM $CaCl_2$; 100µM PMSF; 100µM Benzamidine, at 4°C, at a 1:100 volume ratio for sample:dialysis buffer, respectively. The dialysate was filtered through a 0.22µm filter and loaded onto a Cibacron F3GA Blue column (V_t ~ 5.0ml; 1.0cm x 6.5cm), pre-equilibrated in the same buffer. Elution of gelsolin from the resin was achieved with a 0.4 – 1.0M NaCl gradient, over 4 column volumes, or a 0.6mM NaCl wash, over 5 column volumes, with a flow rate of 0.5ml.min^{-1}. Proteins were detected by A_{280nm} and analysis by SDS-PAGE.

Relevant fractions were pooled, concentrated and dialysed overnight against 25mM Tris, pH 8.0; 0.1mM DTT; 1mM Azide; 0.2mM EGTA; 100µM PMSF; 100µM Benzamidine, at 4°C, at a 1:100 volume ratio for sample:dialysis buffer, respectively. The dialysate was filtered through a 0.22µm filter, concentrated to ~ 2ml, and subjected to size-exclusion chromatography on a Sephacryl-200 (S200) column (V_t ~ 135ml; 65cm x 1.6cm), pre-equilibrated in the same buffer, with a flow rate of 0.5ml.min^{-1}. Proteins were detected by A_{280nm} and analysis by SDS-PAGE, and the relevant fractions pooled and concentrated and stored at 4°C, in the above buffer, until needed. Gelsolin was routinely stored in a buffer containing EGTA. Long term storage of gelsolin in Ca^{2+} containing buffers has been shown to result in a loss of the Ca^{2+} sensitive actin binding activity (Pope et al, 1989).

2.16 Purification protocol for recombinant full-length T-cap-protein

(All purification was performed on Pharmacia Gradifrac™ or FPLC™ systems). Ca^{2+} competent BL21(DE3) *E. coli* were successfully transformed with pMW172[T-cap-protein/R861-A1223] and maintained on 2xTY/AMP (50μg.ml^{-1}) agar plates. 10ml from an overnight culture was used to inoculate 1 L of 2xTY/AMP (50μg.ml^{-1}). The cells were grown, shaking at 37°C, until the A_{600nm} ~ 0.6 – 1.0 and induction of synthesis of the T-cap-protein construct was carried out by addition of IPTG to 1.0mM. The cells were grown for a further 3hrs and then harvested by centrifugation at 3000 xg, for 10 min at 4°C. The cell pellets were processed *immediately.*

Cell pellets were re-suspended at 10% (w/v) of cells, 20mM Bis-Tris, pH 6.1; 0.25mM EDTA; 5mM NaCl; 1mM NaN3; 5ml of bacterial cell extract inhibitor cocktail (Sigma) per litre of original cell culture. The cell suspension was then lysed by ultrasonication, (5 x 20sec bursts at 4°C). Following centrifugation at 50,000 xg, for 1hr at 4°C, the clarified, soluble cell extract was dialysed overnight against 20mM Bis-Tris, pH 6.1; 0.25mM EDTA; 5mM NaCl; 1mM NaN3; 5ml of bacterial cell extract inhibitor cocktail (Sigma) per litre of dialysis buffer, at a 1:100 volume ratio for sample:dialysis buffer, respectively. The dialysate was then filtered through a 0.22μm filter and loaded onto a DEAE-Sepharose column (V_t ~ 50 ml; 2.6cm x 9.5cm) pre-equilibrated in the same buffer. Unbound proteins were washed through with this buffer and bound proteins were eluted by a gradient of 5 – 300mM NaCl, over 6 column volumes (300ml), with a flow rate of 1.0ml.min^{-1}. Proteins were detected by A_{280nm} and analysis by SDS-PAGE.

Relevant fractions were pooled, concentrated and dialysed overnight against 50mM MES, pH 5.50; 0.25mM EDTA; 5mM NaCl; 1mM NaN3; 5ml of bacterial cell extract protease inhibitor cocktail (Sigma) per litre of dialysis buffer, at a 1:100 volume ratio for sample:dialysis buffer, respectively. The dialysate was filtered through a 0.22μm filter and loaded onto a Mono-S/(30μm) column (V_t ~ 6.0ml; 1.6cm x 2.0cm), pre-equilibrated in the same buffer. Unbound proteins were washed through with this buffer and elution of T-cap-protein from the resin was achieved

with a 5mM – 100mM NaCl gradient, over 6 column volumes (36ml), with a flow rate of 0.5ml.min^{-1}. Proteins were detected by A_{280nm} and analysis by SDS-PAGE.

Depending on the degree of proteolytic degradation and the relative yields of full-length T-cap-protein and the major degraded fragment, several further rounds of cation-exchange on Mono-S/(30μm) resins were performed. The gradient parameters used were varied to maximise the purity and yield of the full-length T-cap-protein. However, the final ion exchange step was always that described below.

Relevant fractions were pooled, concentrated and dialysed overnight against, 50mM MES, pH 5.50; 0.25mM EDTA; 5mM NaCl; 1mM NaN3; 5ml of bacterial cell extract protease inhibitor cocktail (Sigma) per litre of dialysis buffer, at a 1:100 volume ratio for sample:dialysis buffer, respectively. The dialysate was then filtered through a 0.22μm filter and loaded onto a HR 5/5 Mono-S/(15μm)/FPLC column (V_t ~ 1.0ml; 1.0cm x 1.30cm), pre-equilibrated in the same buffer. Unbound proteins were washed through with this buffer and elution of T-cap-protein from the resin was achieved with a 60mM – 80mM NaCl gradient, over 15 column volumes (15ml), with a flow rate of 0.25ml.min^{-1}. Proteins were detected by A_{280nm} and analysis by SDS-PAGE.

Relevant fractions were pooled and concentrated to ~ 200μl. The sample was then subjected to size exclusion chromatography on an FPLC/Superose-12™ (Pharmacia) size exclusion column (V_t ~ 24ml; 1.0cm x 32cm), pre-equilibrated in either ATP-F-Buffer or 100mM Tris, pH 8.0; ATP-G-Buffer, with a flow rate of 0.5ml.min^{-1}. Proteins were detected by A_{280nm} and analysis by SDS-PAGE, and the relevant fractions were pooled and concentrated and stored at 4°C, in the above buffer until needed.

2.17 Determination of protein concentration

2.17.1 Individual proteins

For the individual proteins, gelsolin, actin, DNaseI, full-length T6-potein and myosin S-1 head, concentrations were calculated using the extinction coefficients listed below:

Actin[1],	$\varepsilon_{290nm} = 24.9\ mM^{-1}.cm^{-1}$.
Gelsolin[1],	$\varepsilon_{280nm} = 150\ mM^{-1}.cm^{-1}$.
DNaseI[1],	$\varepsilon_{280nm} = 34.4\ mM^{-1}.cm^{-1}$.
Full length T-cap-protein[2]	$\varepsilon_{280nm} = 19.2\ mM^{-1}.cm^{-1}$
Myosin S-1 head[3],	$\varepsilon_{280nm} = 88.8\ mM^{-1}.cm^{-1}$.

[1]Webber et al, 1994; [2]Gill and von Hippel, 1989; [3]Combeau et al, 1992.

2.17.2 Protein complexes

The concentrations of the various protein complexes, actin:DNaseI binary complex (A:D), gelsolin:actin binary complex (G:A), gelsolin:actin$_2$ ternary complex (G:A$_2$) were determined by using the Bicinchoninic acid (BCA) protein assay (Pierce®) protocol, usually with a primary TCA precipitation step to avoid any interfering substances (e.g. DTT, EGTA, EDTA). Bovine serum albumin (BSA) or a sample of known concentration of the individual proteins was used as the reference standard. Reagents were as described for the standard Bicinchoninic acid (BCA) protein assay (Pierce®), with the method modified as described below.

Trichloroacetic acid (TCA) precipitation reagents

0.15% (w/v) Sodium Deoxycholate

72% (w/v) TCA

5% (w/v) SDS in 0.1M NaOH

Method

50µl of the protein sample to be assayed (either unknown or standard) was added to a 1.5ml Eppendorf tube. 950µl of dH_2O was then added followed by 100µl of 0.15% (w/v) sodium deoxycholate. The solution was mixed by inversion and incubated at room temperature for 15min. 100µl of 72% (w/v) TCA was then added, the solution vortexed and subjected to centrifugation at 3000 xg for 15min at room temperature. The supernatant was carefully removed and the insoluble protein pellet solubilised in 50µl 5% (w/v) SDS; 0.1M NaOH. 1.0ml of working BCA reagent was then added to the tube, the sample vortexed and incubated at 37°C for 30min. Following this incubation the samples were quickly removed and the absorbance at 562nm measured for all the samples.

Typically, the range of standards used was 100, 75, 50, 25, 12.5, 6.25µg. A dilution series of 1:1, 1:2, 1:4, 1:8, 1:16 of the unknown protein solution was used, treated in the manner described above. Plots of A_{562nm} against µg of standard protein, and µl of unknown sample were performed. To try and minimise the errors inherent in this method of protein concentration determination, the ratio of the gradients from the two plots ($Abs_{562nm}.\mu l^{-1}$ / $Abs_{562nm}.\mu g^{-1}$ = $\mu g.\mu l^{-1}$) was used to calculate the unknown sample concentration.

2.18 Sodium dodecylsulphate polyacrylamide gel electrophoresis (SDS-PAGE)

SDS-PAGE was performed as described by Laemmli (1970). Modifications are described below. The BioRad Mini-PROTEAN II™ gel system was used, with gels typically 11% (w/v) acrylamide.

Gel solutions

Acrylamide/Bis 146g acrylamide

4g bis-acrylamide

made up to dH_2O to 500ml.

(The above solution was filtered through a Whatman No. 1 filter, and stored at room temperature).

1.5M Tris, pH 8.8.

0.5M Tris, pH 6.8.

10% SDS (w/v).

10% (w/v) Ammonium persulphate (APS) made up fresh before use.

TEMED, stored at 4°C.

dH_2O saturated isobutanol.

0.1% (w/v) bromophenol blue in dH_2O, stored at 4°C.

Running buffers

10x running buffer: 30g Tris-base;

144g Glycine;

10g SDS;

made up to 1L with dH_2O.

5x SDS-Sample buffer: 4ml dH_2O;

1ml 0.5M Tris, pH 6.8;

1ml glycerol;

1.6ml 10% (w/v) SDS;

0.4ml β-mercoptoethanol or 100mM DTT;

0.2ml 0.1% (w/v) bromophenol blue.

(Non-reducing sample buffer contained the same ingredients minus the DTT or β-mercoptoethanol).

Separating gel mixtures.

	7.5%	10%	12%	15%	18%	20%
dH_2O	4.85ml	4.05ml	3.35ml	2.35ml	1.35ml	0.75ml
1.5M Tris, pH 8.8	2.5ml	2.5ml	2.5ml	2.5ml	2.5ml	2.5ml
10% SDS	100µl	100µl	100µl	100µl	100µl	100µl
acrylamide	2.5ml	3.3ml	4ml	5ml	6ml	6.6ml
10% APS	50µl	50µl	50µl	50µl	50µl	50µl
TEMED	5µl	5µl	5µl	5µl	5µl	5µl

Stacking gel mixture; 4% (w/v) acrylamide.

dH_2O	3.05ml
0.5M Tris, pH 6.8	1.25ml
10% SDS	50µl
acrylamide	650µl
10% APS	25µl
TEMED	5µl

Running conditions: 45min at a constant 200V.

R250 Coomassie Blue stain: 1g of R250 Coomassie Blue;
180ml dH_2O;
180ml Methanol;
40ml Acetic acid.

The dye was dissolved in the above solutions, while gently stirring, and was then filtered through a Whatman No. 1 filter. Gels were typically stained for 20min and then subjected to exhaustive destain.

Destain: 100ml Methanol, (10% v/v);
100ml Acetic acid, (10% v/v);
made up to 1L with dH_2O.

2.19 Non-denaturing polyacrylamide gel electrophoresis

2.19.1 First dimension native-PAGE.

The protocol used was based on an electrophoretic procedure for detecting actin-binding proteins described by Safer (1989). Modifications for the BioRad Mini-PROTEAN II™ system are described below. Typically 7% acrylamide (w/v) gels were used.

Gel solutions

10x native gel buffer:	250mM Tris, pH 9.0;
	1.94M Glycine.
Running buffer:	50ml 10x native gel buffer;
	0.2mM ATP (100mM stock in dH_2O);
	0.5mM DTT (1M stock in dH_2O);
	made up to 500ml with dH_2O.

Depending on the proteins being analysed, further additions were included in the running buffer.

0.2mM $CaCl_2$;
0.25mM EGTA;
0.2 - 2.0mM $MgCl_2$.

Sample buffer: 50% (v/v) Glyerol in running buffer (with appropriate additions).

Gel mixture (7% acrylamide).

dH_2O	6.54ml
Native buffer	1.0ml
100mM ATP	20µl
1M DTT	5µl
acrylamide	2.33
10% APS	100µl
TEMED	3µl

($CaCl_2$, EGTA, and $MgCl_2$ were added to the appropriate concentrations and the volume of dH_2O adjusted accordingly).

Running conditions: Constant 200V for various times (see below).

Method

Double sets of 0.75mm spacers were used during gel set up. A four well, 50µl sample volume, comb was also used during the gel set up. Samples were first incubated under the appropriate conditions, then a 25µl sample was mixed 1:1 with the appropriate sample buffer. This was incubated for 5min at room temperature, and

then loaded carefully into the sample wells of the gels. A tracking dye containing Xylene cyanol and bromophenol blue was also added to an unused sample well to follow the electrophoretic progress. Gels were typically run until the green Xylene cyanol band had migrated to the bottom, ~ 40 – 50min. This gave a migration distance for G-Actin of ~ 60% (with respect to the bottom of the gel). The conditions for each given set of individual proteins/protein complexes were determined empirically, and adjusted accordingly.

2.19.2 Second dimension SDS-PAGE

After the first dimension native-gel had been run, the entire lane of interest was excised from the gel, using a razor blade. The edges of the lane were trimmed to remove the "smile" section of the gel that commonly appeared during running of the native gels (see results for examples). The gel lane was then placed horizontally ~ 5mm from the top of a clean glass gel plate. The gel lane was then incubated in ~ 5 – 10ml of SDS-PAGE 1x running buffer, and ~ 1ml of 10% SDS, for 15min at room temperature.

The excess liquid was carefully removed, (with a tissue and thin pasteur), and the gel piece was then clamped between two glass plates and an 11% (w/v) acrylamide SDS-separating gel carefully poured underneath. After this had set, a 4% (w/v) acrylamide SDS-stacking gel was poured round the gel piece, completely covering it. A protein standards lane was placed in the stacking gel. Following acrylamide polymerisation second dimension SDS-PAGE, staining and destaining were performed as described.

2.20 SYPRO™ Red (Molecular Probes Inc.) fluorescent protein stain protocol

2.20.1 Staining protocol

The SYPRO™ Red protein stains are a set of fluorescent protein stains developed for the detection of low levels of protein (~ 2ng, Molecular Probes Inc.) on SDS or non-denaturing polyacrylamide gels. The SYPRO™ Red protein stain is supplied as a 5000x stock solution in dimethylsulphoxide, (DMSO).

Method

SDS-PAGE/Native-PAGE were carried out as normal. Gels were placed in clean gel boxes (R250 Coomassie Blue binds to the proteins and masks SYPRO™ Red staining) and rinsed for 5min in dH_2O. Following this 50 ml of a 1:5000 dilution, in 7.5% (v/v) acetic acid, of SYPRO™ Red protein stain was added, per gel. The gels were then incubated for 1hr, at room temperature in the dark. (The staining solution can be used for up to five times if protected from light).

The gel was then rinsed several times with dH_2O to remove any excess stain. The gel was then visualised on a Molecular Dynamics Chemifluorescence imager set to Blue fluorescence, 100 micron pixel size, 800 PTM Voltage. The image was saved to disc and subsequently analysed in ImageQuant™. Following analysis in ImageQuant™ the gels were be re-stained with R250 Coomassie Blue to visualise the proteins normally.

2.20.2 Gel densitometry using SYPRO™ Red (Molecular Probes Inc.) fluorescent protein stain

SDS-PAGE was carried out as described. Gels were stained with SYPRO™ Red as described. The gel was then visualised on a Molecular Dynamics Chemifluorescence imager set to Blue fluorescence, 100 micron pixel size, 800 PTM Voltage. The image was saved to disc and subsequently analysed in ImageQuant™ v.1.1 for the MacIntosh. The gel was displayed in inverted false colour to make the band

boundaries easier to see. Rectangular scan profiles were then placed around the protein bands of interest and the integrated volume intensity calculated using the Local Background setting in ImageQuant™.

The intensity responses were calibrated. SDS-PAGE was performed with 11% (w/v) polyacrylamide gels loaded with 0, 0.1, 0.25, 0.5, 1.0, 1.5, 2.0, 3.0, 4.0, 5.0, 6.0, 7.0, 8.0, 10.0μg of each respective protein, either applied separately or together. The gels were stained and the intensity analysed. The colour-intensity response was linear for all proteins (DNaseI, G-Actin, gelsolin and T-cap-protein), in the concentration range of 0 – 6μg, and amounts of protein within this level (typically 2 - 3.0μg) were used as internal reference standards for stoichiometric analysis of complex components.

The SYPRO™ Red stain intensity showed less protein to protein variability than R250 Coomassie Blue. However, the limit detection level for protein that we observed, (for DNaseI, G-Actin, gelsolin and T-cap-protein), with SYPRO™ Red, was not significantly better than R250 Coomassie Blue (~ 0.1μg). Nevertheless, the mechanics and logistics of the quantification procedures for SYPRO™ Red were very much better than those available for R250 Coomassie Blue staining analysis.

2.21 Size-exclusion chromatography

2.21.1 FPLC/Superose-12 size-exclusion chromatography

An FPLC/Superose-12™ (Pharmacia) size exclusion column (V_t ~ 24ml; 1.0cm x 32cm) was used extensively during experiments performed to analyse complex formation between gelsolin and G-Actin, G-Actin and DNaseI, that between G:A_2 ternary complex and DNaseI, and during experiments analysing the formation of the putative "minifilament" complex.

ATP-F-Buffer

5mM Tris, pH 8.0; 0.5mM DTT; 0.2mM $CaCl_2$; 0.2mM ATP; 1.0mM NaN_3; 100mM KCl; 2mM $MgCl_2$.

ATP-G-Buffer

5mM Tris, pH 8.0; 0.5mM DTT; 0.2mM $CaCl_2$; 0.2mM ATP; 1.0mM NaN_3.

100mM Tris, pH 8.0; ATP-G-Buffer

100mM Tris, pH 8.0; 0.5mM DTT; 0.2mM $CaCl_2$; 0.2mM ATP; 1.0mM NaN_3.

The column was equilibrated in either ATP-F-Buffer, ATP-G-Buffer, 100mM Tris, pH 8.0; ATP-G-Buffer (modified by the further addition of 0.6mM EGTA and/or 0.2mM $CaCl_2$). Calcium was added to the buffers to ensure the activation and subsequent actin binding activity of gelsolin. Due to interactions between the resin and proteins, in buffers with low ionic strengths, ATP-G-Buffer was not used extensively. Instead under conditions where depolymerising conditions were required, 100mM Tris, pH 8.0; ATP-G-Buffer was substituted. Proteins were applied to the column in a sample volume, up to a maximum of 200µl, with an automated injection valve/sample loop. The column was run at 0.5ml.min^{-1} and the elution profiles monitored by A_{280nm} and subsequent analysis by SDS-PAGE. Fraction size was typically 400µl over the dynamic range of the column. The column was calibrated, in the appropriate buffer, with protein standards (see table 2.1 and fig. 2.2).

Protein	Theoretical Mr. (kDa.)	Retention Vol. (ml)	log_{10} Mr.
Ribonuclease A	13.7	15.37	4.14
DNaseI	29	14.36	4.46
Ovalbumin	43	12.95	4.63
BSA	67	11.98	4.83
Aldolase	158	11.68	5.2
Catalase	232	11.2	5.37
Ferritin	443	9.91	5.65

Table 2.1. ***Calibration standards for FPLC/Superose-12 column, in ATP-F-Buffer; 0.2mM $CaCl_2$.*** The column was calibrated with the proteins indicated. ~ 200µg of each protein was applied and the column run with ATP-F-Buffer; 0.2mM $CaCl_2$, with a flow rate of 0.5ml.min^{-1}. V_t = 24ml; 30.7cm x 1.0cm. Void volume ~ 7.25ml (calculated from the retention volume of Blue dextran, Mr > 2,000kDa.).

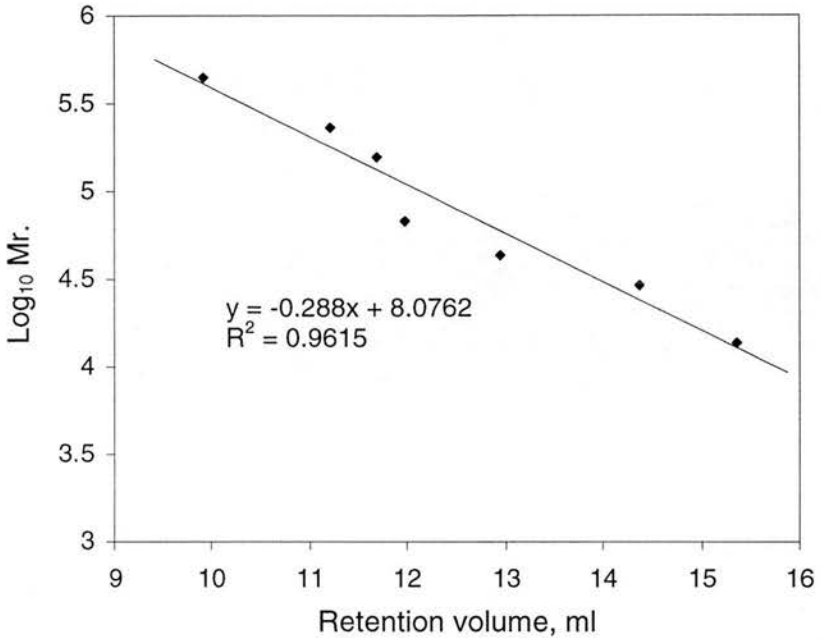

Fig. 2.2 ***Calibration standard curve for FPLC/Superose-12 column, in ATP-F-Buffer; 0.2mM $CaCl_2$.*** The retention volume for the proteins was plotted against the $\log_{10}$ of the proteins Mr. and a linear regression performed on the data. The inset indicates the equation of calibration, with the R^2 value listed below. The column was calibrated with the proteins indicated in table 2.1.

2.21.2 Preparative Sephacryl-200 (S200) size-exclusion chromatography

(All purification was performed on Pharmacia Gradifrac™ or FPLC™ systems). A Sephacryl-S200 (S200) size exclusion column (V_t ~ 135ml; 65cm x 1.6cm) was used for the purification of large amounts (~ 5 – 10mg) of the gelsolin:actin$_2$ ternary complex, (G:A_2), the gelsolin:actin binary complex (G:A), and the actin:DNaseI binary complex, (A:D) for use in further binding experiments.

The column was calibrated with protein standards in ATP-G-Buffer, with a flow rate of 0.5ml.min^{-1}. Protein standards used: Ferritin (Mr. = 443kDa), Catalase (232kDa), Aldolase (158kDa), BSA (67kDa), Ovalbumin (43kDa), and Ribonuclease A (13.7kDa). Plots of $\log_{10}$ Mr. against elution volume were linear throughout this

range. Proteins were detected by A_{280nm} and subsequent analysis by SDS-PAGE, performed as described.

Protein samples were concentrated to ~ 2ml and then applied to the S200 column, pre-equilibrated in ATP-G-Buffer. No more than ~ 10mg of total protein applied to the column during any given chromatographic run. The column was run with a flow rate of 0.5ml.min^{-1}. Fraction size was typically 1.0ml over the dynamic range of the column.

2.21.3 Gelsolin:actin complex formation and purification.

For large scale preparation of G:A_2, typical concentrations used were ~ 6μM gelsolin and 12μM G-Actin, with ~ 5 – 10mg of total protein. Such incubations were carried out in ATP-G-Buffer, to avoid any actin polymerisation. (At such actin concentrations, well in excess of the monomer critical concentration, the presence of salt results in the initiation of polymerisation). The complex mixture was then concentrated to ~ 2ml and subjected to size exclusion on an S200 column, (V_t ~ 135ml; 65cm x 1.6cm), in ATP-G-Buffer.

2.21.4 Purification of the gelsolin:actin binary complex, (G:A)

Due to problems with an incomplete dissociation of G:A_2, in the presence of EGTA, to form G:A complex and free G-Actin we used an alternative method for the large scale production of G:A, (amounts ~ 3 – 5mg).

The protocol used was based on that described by Selve and Wegner (1986). Modifications are described below.

Method

(All purification was performed on Pharmacia Gradifrac™ or FPLC™ systems). DNaseI was used to prepare a DNaseI-Sepharose affinity column. ~ 5mg of pre-purified DNaseI was concentrated to ~ 5mg.ml^{-1} and then applied to a Sephadex-G25

(Coarse) desalt column, (Vt ~ 80ml; 2.6cm x 15cm), pre-equilibrated in 100mM $NaHCO_3$, pH 8.3; 150mM NaCl, with a flow rate of $1ml.min^{-1}$. Elution was monitored by A_{280nm} and the relevant fractions pooled and concentrated to approximately $5mg.ml^{-1}$. This protein solution was added to an 80% slurry of NHS-activated Sepharose 4® (N-hydroxysuccinamide-Sepharose 4, Pharmacia), in the same buffer, at a ratio of 0.5:1 (coupling media:protein solution, respectively). The mixture was then incubated, with gentle agitation, at room temperature for 4hrs, to allow coupling of DNaseI to the Sepharose resin via the activated NHS group and free primary amino groups.

Following this incubation, excess 200mM Tris, pH 8.0 buffer was added (~ 20 volumes) to quench the reaction, and the mixture left for a further 2hrs. The resin was then washed extensively with ATP-G-Buffer (~ 50 volumes), at 4°C, and the media then loaded into a C 10/10 column® (Pharmacia) (Vt ~ 2 – 3ml; 1.0cm x 4.0cm). The column was then loaded with excess monomeric actin, in ATP-G-Buffer at 4°C, to saturate the coupled DNaseI with actin.

EGTA and $MgCl_2$ were added to 0.6mM and 0.2mM, respectively, to ~ 5mg of G:A_2 ternary complex in ATP-G-Buffer, purified as described. This mixture was left to incubate for 1hr, at 4°C, and then concentrated to ~ 2ml and subjected to size-exclusion chromatography on a S200 column, pre-equilibrated in ATP-G-Buffer; 0.6mM EGTA; 0.2mM $MgCl_2$. The fractions corresponding to G:A were pooled and concentrated to ~ 1ml. $CaCl_2$ was added to 1.0mM and the protein sample then applied to the Actin:DNaseI-Sepharose column, in ATP-G-Buffer. The G:A binary complex, in the presence of Ca^{2+}, re-binds to the actin, complexed 1:1 with the immobilised DNaseI, to form immobilised G:A_2 ternary complex. The column was washed with ~ 10 column volumes of the same buffer and elution of the G:A complex from the affinity column, was achieved by 5.0mM EGTA in ATP-G-Buffer, additionally with 1.0mM $CaCl_2$ and 1.0mM $MgCl_2$.

This protocol gave a much more homogeneous population of G:A (~ 95%) than gel-filtration of G:A_2 complex in the presence of EGTA.

2.21.5 Large scale actin:DNaseI binary complex purification

DNaseI and G-Actin were mixed together, (in a molar ratio of 1:1) in ATP-G-Buffer, and incubated for 30min at room temperature. Typical concentrations used were ~ 6μM G-Actin and 6μM DNaseI (the addition of 3 – 15 % excess DNaseI was included to account for the amount of inactive protein in a given preparation), with ~ 5 – 10mg of total protein. The mixture was then concentrated to ~ 2ml and subjected to size exclusion chromatography on an S200 column, (V_t ~ 135ml; 65cm x 1.6cm), in ATP-G-Buffer.

The same procedure was performed with NBD-Actin for the creation and purification of the A_{nbd}:D binary complex.

2.22 NBD-Actin fluorescence binding assays

Two types of experiments were performed. (a) Gelsolin solutions of fixed concentration were mixed with variable amounts of NBD-Actin or A_{nbd}:D complex. (b) The proportions of the two proteins/complexes, in a series of mixtures, were continuously varied at a constant total protein concentration (the "continuous variation" experiments). Fluorescence measurements were carried out in a Perkin-Elmer LS50B spectrofluorimeter at 20°C, with a Grant LTD6 temperature control unit. The excitation wavelength for both NBD-Actin and the A_{nbd}:D binary complex titration experiments was 475nm and the emission wavelength was 520nm, using a 5nm slit width for both. A quartz fluorescence cuvette with a 1cm-path length and a 400μl working volume was used. The fluorescence intensity is reported in arbitrary units.

Complex formation was studied in both calcium and EGTA. The proteins/complexes were initially mixed together, in the appropriate concentrations, in ATP-G-Buffer or ATP-F-Buffer, containing 0.2mM $CaCl_2$. For conditions containing Ca^{2+}, the

proteins were incubated for 1hr at 20°C, in the dark and then the fluorescence intensity measured.

For conditions in EGTA, the proteins/complexes were mixed together, in the appropriate concentrations, in ATP-G-Buffer or ATP-F-Buffer, containing 0.2mM $CaCl_2$. Following a 5min incubation at 20°C in the Ca^{2+} containing buffer, EGTA and $MgCl_2$ were added to 0.6mM and 0.2mM, respectively. The protein/complex mixtures were incubated for a further 1hr, at 20°C, and then the fluorescence intensity measured.

2.23 Creation of nucleotide-free solutions for use in experiments probing the "minifilament" conformation with the S-1 head.

The protocol used was based on that described by Pollard et al (1992) and De la Cruz and Pollard (1994). Modifications are described below.

200µl of strong anion exchange Dowex 1 resin (Bio-Rad AG1-X2) was extensively washed (15 times 20 volumes) with 5mM Tris, pH 8.0; 0.5mM DTT; 0.2mM $CaCl_2$; 100mM KCl; 2mM $MgCl_2$. The final preparation of washed resin was stored as a 50% slurry in the same buffer at 4°C.

G:A_2 ternary complex and A:D binary complex were added together at a 1:1 molar ratio and incubated for 30min at room temperature, in modified ATP-F-Buffer; 50nM ATP; 0.2mM $CaCl_2$. Myosin S-1, in *nucleotide-free-ATP-F-Buffer* (5mM Tris, pH 8.0; 0.5mM DTT; 0.2mM $CaCl_2$; 100mM KCl; 2mM $MgCl_2$), was then added at a molar ratio of 1:1 (S-1:putative "minifilament" complex). The final concentrations of G:A_2, A:D and S-1 were 3.0µM. Removal of free nucleotide (both ADP and ATP) from this mixture was performed by gently mixing 25µl (50% slurry in nucleotide-free-ATP-F-Buffer) of Dowex 1 beads (Bio-Rad AG1-X2) with the protein solution, followed by an incubation of 5min at 4°C. The Dowex 1 beads were then pelleted by

centrifugation at 18,000 xg, for 5min at 4°C. Following centrifugation the supernatant was carefully removed and the protein mixture was incubated at room temperature for a further 30min, and then subjected to size-exclusion chromatography on an FPLC/Superose-12 column, pre-equilibrated in nucleotide-free ATP-F-Buffer.

3. Probing the disposition of the actin subunits in ternary complex with gelsolin

3.1 Overview

We have used decoration of the gelsolin:actin$_2$ ternary complex (G:A_2) with DNaseI to probe the disposition of the actin monomers in this complex. We have also determined the stoichiometry of the components within this new complex. This new complex has stoichiometry of **G:A_2:D_2**. Furthermore, we have studied the interaction of the actin:DNaseI (A:D) binary complex with gelsolin.

The results are consistent with the actin monomers within G:A_2 having a *different* spatial orientation to those in a filament, or at least, the tight-binding association with DNaseI is sufficient to change that conformation.

3.1.1 Introduction

Gelsolin was first identified as calcium-dependent actin filament destabilising protein found in blood plasma and in the cytoplasm of macrophages (Chaponnier et al, 1979; Yin and Stossel, 1979; Harris et al, 1980). It is a member of a ubiquitous family of severing proteins that is defined by either a three (e.g. fragmin, severin) or a six (e.g. gelsolin, villin and adsevrin) repeat sequence motif spanning 125 – 150 residues that fold up into functionally distinct domains (Weeds and Maciver, 1993; Sun et al, 1999). The six segments of gelsolin (G1 – 6), originally identified on the basis of their sequence homology (Kwiatkowski et al, 1986; Way and Weeds, 1988; Way et al, 1989) have been shown to contain the same basic fold (McLaughlin et al, 1993; Burtnick et al, 1997). (See chapter 1 and figs. 1.7, 1.8 and 1.9 for details).

The activation of gelsolin requires calcium ions and it appears that while gelsolin has several high affinity binding sites for calcium (K_d in the nM range) in the C-terminal half, that may be involved in the activation and opening of the molecule, calcium concentrations in the μM range are required for actin binding, severing and

nucleation activities (Weeds et al, 1986; Way et al, 1989; Hellweg et al, 1993; Ditsch and Wegner, 1995; Pope et al, 1997; Burtnick et al, 1997; Robinson et al, 1999).

Gelsolin has two binding sites for monomeric actin, a calcium-independent site in G1 (K_d ~ 5pM) and a calcium-dependent site in S4 (K_d ~ 1.8μM for G5 alone, but ~ 25nM as the G4 – 6 construct; Pope et al, 1995) and one F-Actin binding site located in G2 (K_d ~ 1 – 5μM; Bryan, 1988; Way et al, 1992). The minimal actin severing domain is G1 – 2 (Way et al, 1992; Sun et al, 1994), while full nucleating ability requires the two actin binding sites in G2 – 6 (Way et al, 1989). The former construct is calcium independent while the latter is calcium dependent, indicating the calcium regulation of actin binding, of all three of the sites is mediated via the C-terminal half of gelsolin. However, it is becoming increasingly clear that the interactions of whole gelsolin, with both filamentous and monomeric actin, compared to the analogous interactions of its various truncated domains and constructs, are probably subtly different (Yin et al, 1988; Way et al, 1989; Pope et al, 1991; Way et al, 1992; Sun et al, 1994; Pope et al, 1995; McGough et al, 1998).

Gelsolin also forms two complexes with monomeric actin (in a calcium dependent manner); a binary (G:A) complex and a ternary ($G:A_2$) complex. However, The spatial orientation of the actin monomers in ternary complex with gelsolin is unknown. It is still unclear whether the actin monomers bound in $G:A_2$ are held in an F-actin like conformation, akin to those found at the barbed-end of the filament (as described by Holmes et al, 1990), or in an altogether different conformation.

Kinetic analysis of polymerisation nucleated in the presence of gelsolin or $G:A_2$ appears to be inconsistent with models where the nucleating species act like the pointed-ends of already formed filaments (Coué and Korn, 1985; Pollard and Cooper, 1986; Ditsch and Wegner, 1994). Evidence has been reported to suggest that $G:A_2$ (at least at low actin or low $G:A_2$ concentrations) does not act like a "true" nucleus, with regard to the nucleation of actin polymerisation in the pointed-end direction (Coué and Korn, 1985). The inference is that $G:A_2$ executes nucleating activity in a manner slightly different to normal actin nucleation and polymerisation,

possibly due to a difference in the disposition of the actin monomers within $G:A_2$, in relation to those at the barbed-end of a filament. Other evidence from cross-linking studies has also suggested that the actin monomer topography within the $G:A_2$ ternary complex is similar, but not identical, to the monomer orientation at the barbed-end of the filament (Doi et al, 1991; Doi, 1992).

We proposed to use DNaseI, binding at the pointed-ends of actin monomers, to probe the disposition of the monomers within the $G:A_2$ ternary complex.

Deoxyribonuclease I (DNaseI) is a high-affinity actin-sequestering protein (Lazarides and Lindberg, 1974; Mannherz et al, 1975; Hitchcock et al, 1976; Hitchcock, 1980) which forms a 1:1 binary complex (A:D) with actin. DNaseI binds to subdomains II and IV of monomeric actin (Kabsch et al, 1990) with a $K_d \sim 0.1 - 1.0$nM (Mannherz et al, 1980). It has also been reported to bind with similar affinity ($K_d \sim$ 1nM) to the pointed-ends of actin filaments (Podolski et al, 1988; Weber et al, 1994), and this leads to a blockage of filament elongation. This inhibition is conferred by the binding of only one DNaseI molecule to the pointed-end of a single strand of the F-Actin two-start helix. (One DNaseI molecule bound per filament, Podolski et al, 1988). The binding of this DNaseI appears to have no significant effect on the affinity of the attached actin for the pointed-end of the filament (Weber at al, 1994). DNaseI has also filament side-binding activity (Hitchcock et al, 1976) but this is of much lower affinity ($K_d \sim 0.1$mM; Mannherz et al, 1980).

Work carried out by Weber and co-workers (Weber et al, 1994) indicated that the binding of two DNaseI molecules was not possible at the pointed-ends of gelsolin capped actin filaments. At higher concentrations of DNaseI, 1 – 100μM (which are three orders of magnitude higher than that required for the blockage of elongation), an increase in the rate of depolymerisation from the pointed-ends of gelsolin capped filaments was observed. The $K_{50\%}$ for this effect was ~ 5μM DNaseI (Weber et al, 1994). The explanation proposed for this was a steric clash between two DNaseI molecules at the pointed-end. This prevented the stable binding of both DNaseI molecules and resulted in an increase in the k_{off} rate for the actin monomer, as a 1:1

binary complex with DNaseI (Weber et al, 1994). Modelling of DNaseI molecules onto the pointed-ends of two subunits in the Holmes filament model (Holmes et al, 1990) indicates that DNaseI would sterically interfere with each other.

Assuming the actin monomers within the G:A_2 ternary complex are held in an F-like conformation, akin to that orientation found at the barbed-end of the actin filament, we should not expect to be able to accommodate the binding of ***two*** DNaseI molecules onto the pointed-ends of the actin monomers within this complex. Thus, we propose to use ability of DNaseI to bind at the pointed-ends of actin monomers, to probe the disposition of the monomers within the G:A_2 ternary complex.

3.2 Formation and verification of the G:A_2 ternary, G:A binary and A:D binary complexes

We designed experiments to add DNaseI to G:A_2 ternary complex, and to add the A:D binary complex to gelsolin. This involved the formation and pre-purification of a variety of complexes: A:D, G:A and G:A_2. It also involved the analysis and verification of the stoichiometry of the individual components within these complexes. The three separate proteins (DNaseI, actin and gelsolin) used in the formation of these various complexes were also purified. DNaseI was purified by a novel protocol.

3.2.1 Purification of individual proteins

3.2.1.1 DNaseI protocol

A partial purification protocol for an inactive DNaseI mutant (H134Q) has been reported (Worrall and Connolly, 1990; Doherty et al, 1993). This gave purity of between 60% and 90%, with variable yields. Professor Bernard Connolly kindly supplied us with ~ 2μg of the recombinant mutant DNaseI, in the pkk223-3™ Pharmacia vector. When this protocol was followed, using JM105[pkk223-3/DNaseI/H134Q], we were unable to obtain purity better than ~ 65%.

We have developed a novel purification protocol that routinely gives ≥ 95% purity for DNaseI preparations, with yields of 10 – 15mg.L^{-1} of original bacterial cell culture.

3.2.1.1.1 Optimisation of expression

JM105 *E. coli* were successfully transformed with pkk223-3[DNaseI/H134Q] and the induction of synthesis of high levels of recombinant DNaseI was obtained upon addition of IPTG to 1.0mM. The appearance of a protein band that migrates at

approximately 30kDa on SDS-polyacrylamide gels corresponded to recombinant DNaseI, see fig. 3.1.

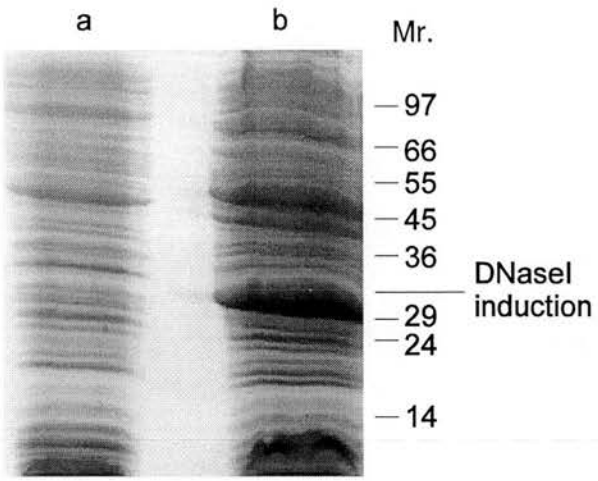

Fig. 3.1. ***SDS-polyacrylamide gel of induction of synthesis of recombinant DNaseI from JM105[pkk223-2/DNaseI/H134Q] by addition of IPTG to 1.0mM.*** Lane a. pre-induction; b. 3hrs post IPTG addition. JM105[pkk223-3/DNaseI/H134Q] in 100ml of 2xTY/AMP (50μg/ml) were grown at 37°C until the A_{600nm} ~ 0.6, and synthesis of DNaseI was induced by addition of IPTG to 1.0mM. Cells were grown for a further 3hrs. 1.0ml aliquots from pre- and post-induction conditions were taken and the resultant cell pellet was resuspended in 100μl of 5 x SDS-sample buffer (see methods) and boiled for 5mins. A 20μl sample was loaded onto the gel, following centrifugation at 15,000 xg for 2min. Mr. of protein standards is given in kilodaltons. (SDS-PAGE was performed as described in methods).

The expression of the protein was optimised. (For protocol details see methods). The time course for the optimisation of expression of recombinant DNaseI is indicated in fig. 3.2(A). The synthesis of this protein increased as a function of time after induction with IPTG. The optimum time for production of soluble protein was 4hrs, see figs. 3.2(A) and (B) at which time it constituted ~ 10 – 15% of the total cellular protein, as judged by densiometric scanning of SDS-polyacrylamide gels (data not shown). Fig. 3.2(B) shows SDS-PAGE analysis of the optimal 4hrs induction time point. The vast percentage of DNaseI is present in the soluble fraction, lane c. After ~ 4 - 5hrs the protein begins to appear in inclusion bodies and the percentage of protein present in the soluble fraction steadily decreases with time, see fig. 3.2(A). After 20hrs the majority of protein was present in inclusion bodies in a non-recoverable form. (Other time point data are not shown for clarity).

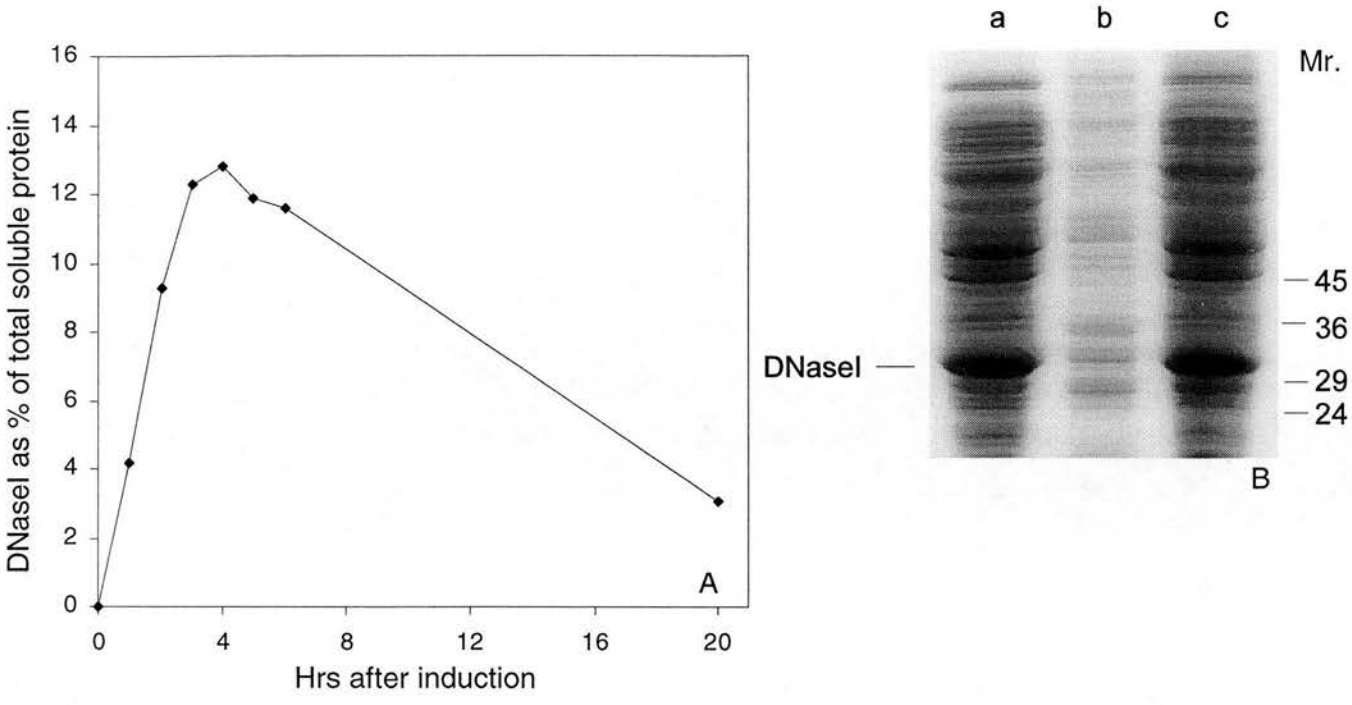

Fig. 3.2. ***Optimisation of induction.*** (A) Graph showing the time course for the optimisation of induction of recombinant DNaseI from JM105[pkk223-2/DNaseI/H134Q] by addition of IPTG to 1.0mM. (B) SDS-polyacrylamide gel analysis of the 4hrs post IPTG addition time point in A. Lane a. 4hrs post IPTG addition, pre-lysis; b. Insoluble fraction, post-lysis; c. Soluble fraction, post-lysis. JM105[pkk223-3/DNaseI/H134Q] in 100ml of 2xTY/AMP (50μg/ml) were grown at 37°C until the A_{600nm} ~ 0.6, and synthesis of DNaseI was induced by addition of IPTG to 1.0mM. 5ml aliquots were removed at various time intervals and the percentage of DNaseI in the soluble protein fraction was analysed. Cell pellets obtained at each time point were resuspended in 10mM Tris, pH 7.6; 2mM $CaCl_2$; 100mM PMSF; 100mM benzamidine, subjected to ultrasonication (3 x 20 sec bursts at 4°C) and the resulting cell lysate centrifuged at 18,000 xg (5min at 4°C). The appearance and relative percentage of DNaseI in the soluble and insoluble fractions was analysed by SDS-PAGE and gel densitometry. (See methods for details).

3.2.1.1.2 Protein purification

JM105[pkk223-3/DNaseI/H134Q] were grown at 37°C in 2xTY/AMP, and protein synthesis induced by the addition of IPTG to 1.0mM. Cells were grown for a further 4hrs and then harvested and processed for purification (see methods for details). Figs. 3.3(A) and (B) show the results of the DEAE-Sepharose anion-exchange chromatography step. Bound proteins were eluted by a gradient of 0 - 0.3M NaCl with DNaseI eluting at ~ 0.1M NaCl, as indicated by the hatched area in fig. 3.3(A). The relevant fractions were pooled, concentrated and following an overnight dialysis

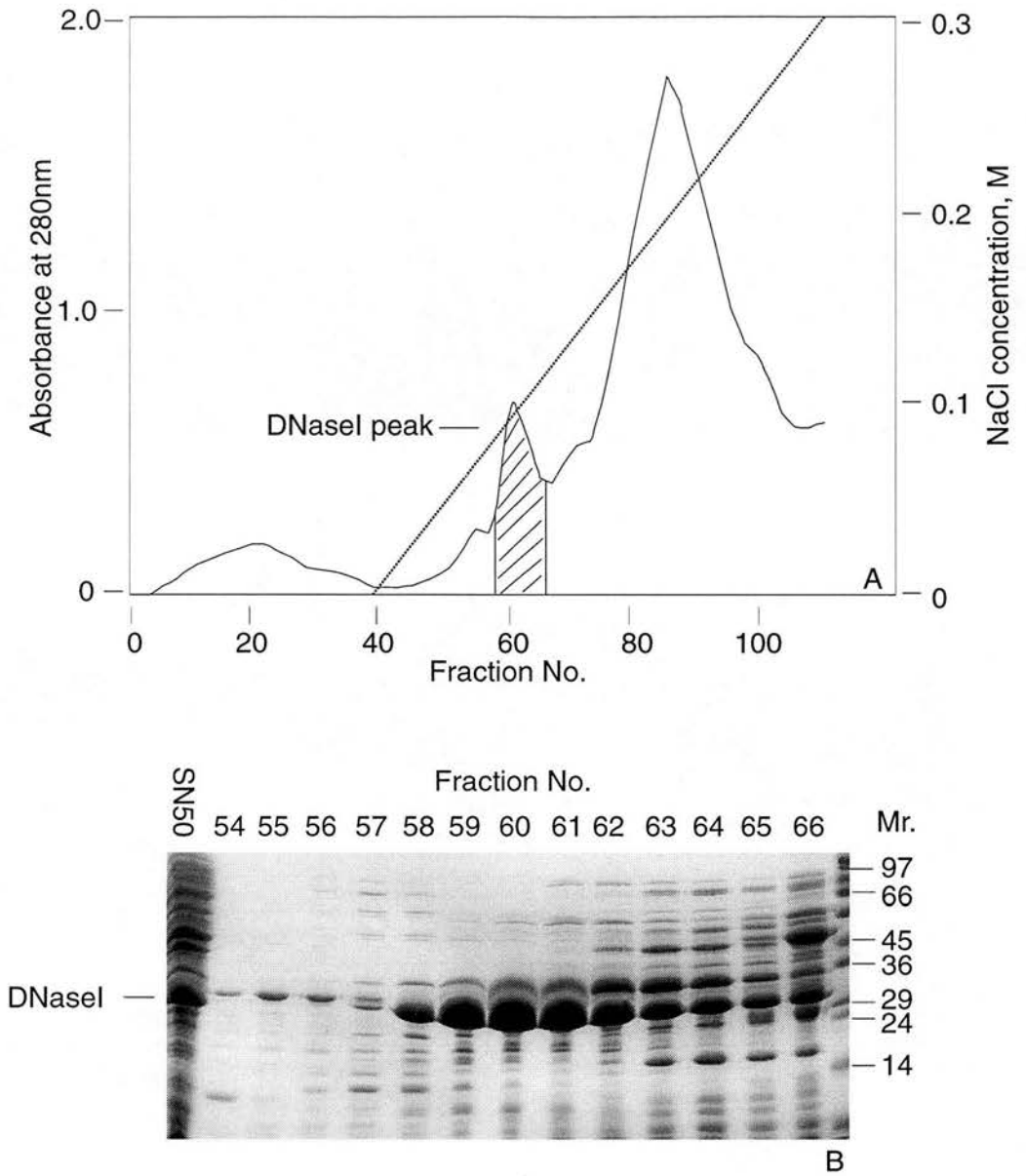

Fig. 3.3. ***DEAE-Sepharose chromatography of recombinant DNaseI.*** (A) Abs_{280nm} monitored elution profile from a DEAE-Sepharose column showing the elution of DNaseI at ~ 0.1M NaCl, indicated by the hatched area. (B) SDS-PAGE analysis of the elution profile in A. (SN50; soluble fraction resulting from centrifugation of cell lysate at 50,000 xg). JM105[pkk223-3/DNaseI/H134Q] were grown at 37°C in 2xTY/AMP (50μg/ml) until A_{600nm} ~ 0.6 and protein synthesis induced by the addition of IPTG to 1.0mM. Cells were grown for a further 4hrs and then harvested by centrifugation at 3000 xg for 10 min at 4°C. Cells were lysed and following an overnight dialysis against 10mM Tris, pH 7.6; 2mM $CaCl_2$; 100μM PMSF; 100μM benzamidine, the soluble clarified fraction was loaded onto a DEAE-Sepharose column (V_t ~ 50 ml; 2.6cm x 9.5cm) pre-equilibrated in the same buffer. Bound proteins were eluted by a gradient of 0 - 0.3M NaCl, over 6 column volumes, and proteins detected by A_{280nm} and analysis by SDS-PAGE. Mr. of protein standards are given in kilodaltons. (SDS-PAGE and chromatography were performed as described in methods).

against 10mM Tris, pH 7.6; 2mM $CaCl_2$; 100mM PMSF; 100mM benzamidine, they were loaded onto a Cibacron Blue F3GA column.

Cibacron Blue F3GA dye is a highly conjugated ligand that shows structural similarities with the co-factors NAD^+, $NADP^+$ and has been used to purify enzymes and proteins that utilise and bind adenyl containing co-factors/ligands (Scopes, 1987). Some proteins combine in a bio-specific way with the ligand. We proposed to attempt to bind DNaseI to the dye - DNaseI binds to DNA so is a possible candidate for specific interaction with the ligand - and attempt specific elution with ATP.

Fig. 3.4(A) shows a typical A_{280nm} monitored elution profile of the purification. The protein bound to the matrix, and specific elution with ATP was achieved only with concentrations above 1mM. Accordingly a gradient of ATP, from 1mM – 10mM was used and this successfully partitioned the protein from its major contaminants, see fig. 3.4(B). Relevant fractions were pooled, concentrated and then subjected to size-exclusion chromatography on a Sephacryl-200 (S200) column. Densiometric scanning of the relevant pooled and concentrated fractions gave final purity for the recombinant protein of $\geq$ 95%. See figs. 3.5(A) and (B). Typical yields of between 10 – 15mg.L^{-1} of original bacterial cell culture were obtained using this protocol.

3.2.1.2 Actin extraction and purification

Actin was extracted from rabbit muscle acetone powder utilising a modified version of a widely used protocol (Spudich and Watt, 1971). (See methods and appendix A for details). Fig. 3.6 indicates the typical purity of G-Actin (as analysed by SDS-PAGE) obtained using this method. Assay of the competence of G-actin, to undergo polymerisation, prepared by this method was carried out by critical concentration assay ($[C_c]$) using 5% pyrene-actin. Incorporation of pyrene-actin into the filament produces an enhancement in the fluorescence intensity; ~ 20 – 25 times that of monomeric actin. The $[C_c]$ of this particular preparation was 0.11μM. $[C_c]$ values routinely obtained with this method of extraction and purification compare favourably with results published by others (Pollard 1986; Pollard and Cooper, 1986;

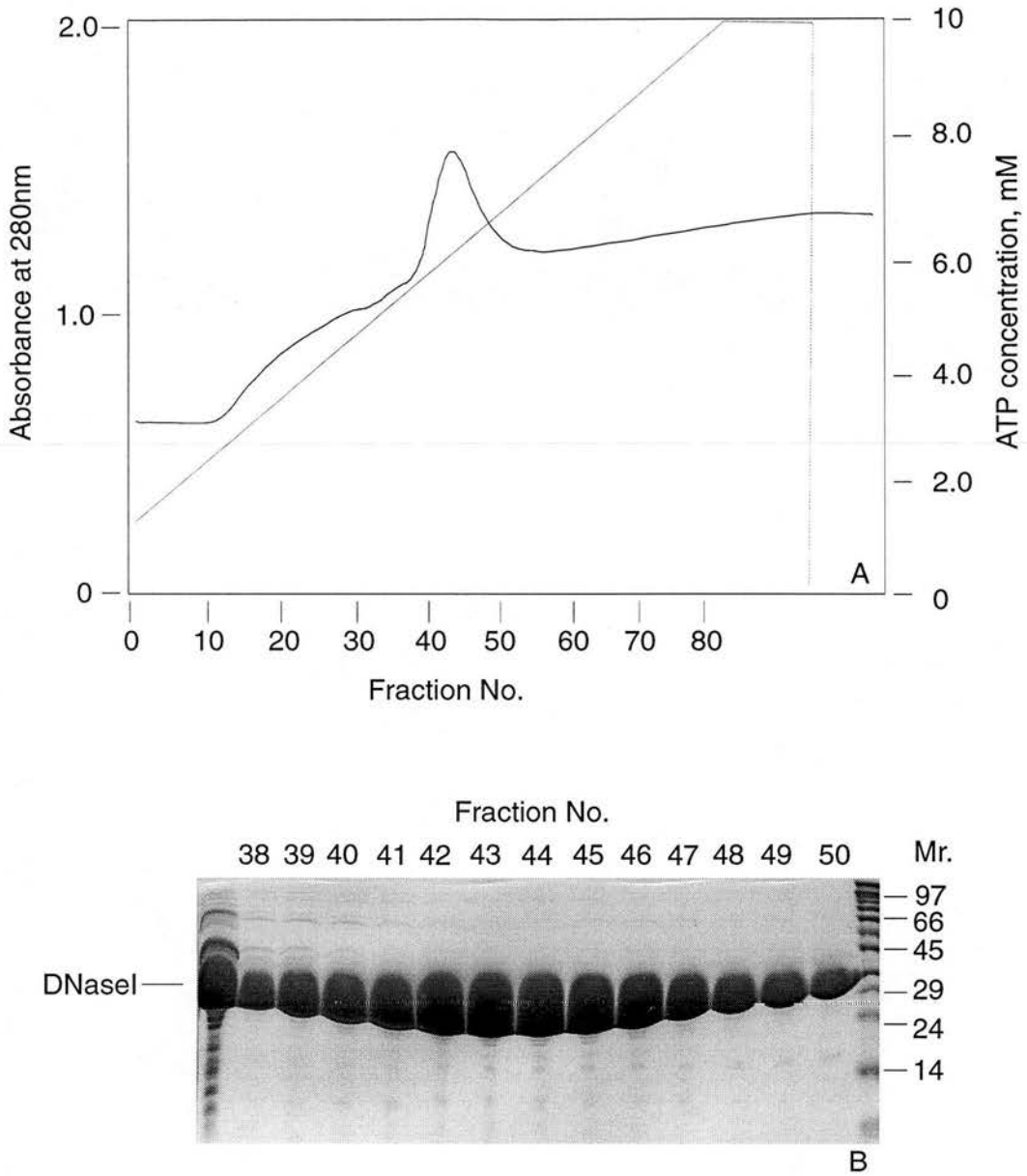

Fig. 3.4. ***Cibacron F3GA Blue chromatography of recombinant DNaseI.*** (A) Abs_{280nm} monitored elution profile from a Cibacron F3GA Blue column showing specific elution of DNaseI by an ATP gradient. (B) SDS-PAGE analysis of the elution profile in A. (The first lane represents the pooled fractions from the DEAE-Sepharose column). Relevant fractions from the DEAE-Sepharose chromatography step were pooled (illustrated by the first lane of the gel) and subjected to an over night dialysis against 10mM Tris, pH 7.6; 2mM $CaCl_2$; 100μM PMSF; 100μM benzamidine. The dialysate was filtered through a 0.22μm filter and loaded onto a Cibacron F3GA Blue column (V_t ~ 5.0ml; 1.0cm x 6.5cm), pre-equilibrated in the same buffer. Specific elution of DNaseI from the resin was achieved with a 1mM - 10mM ATP gradient, over 10 column volumes. (SDS-PAGE and chromatography were performed as described in methods).

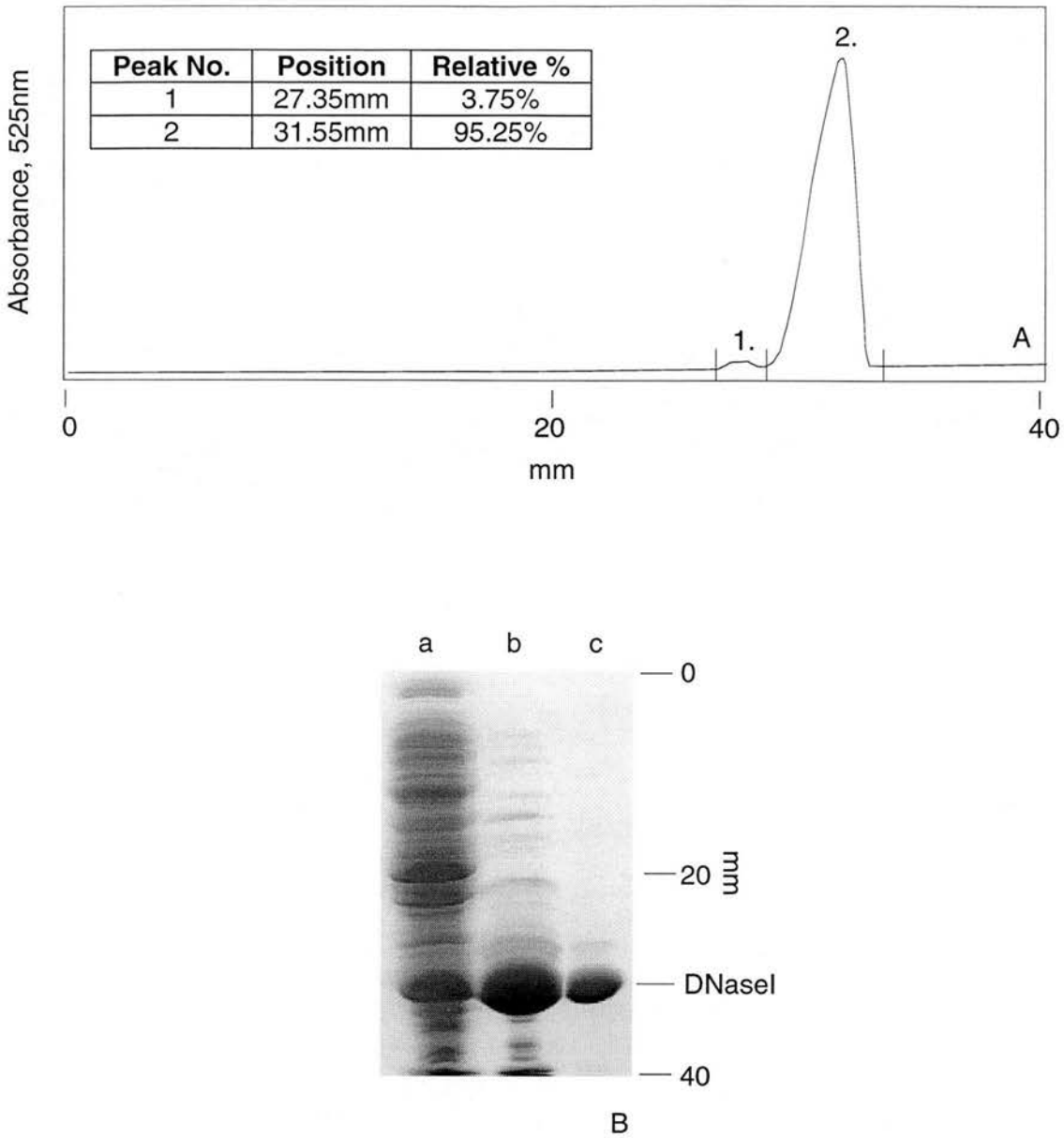

Fig. 3.5. ***Final purity of DNaseI obtained by novel purification protocol.*** (A) Densiometric scan profile, performed on SDS-polyacrylamide gels (similar to that shown in B, lane c) illustrating the final purity of DNaseI preparations. (B) SDS-polyacrylamide gel illustrating the purity of DNaseI at various stages in the purification protocol. Lane a. SN50 fraction (soluble fraction resulting from centrifugation of cell lysate at 50,000 xg); b. pooled fractions from DEAE-Sepharose chromatography; c. final purity, following Cibacron F3GA Blue and S200 size-exclusion chromatography. Final purity of >95% was obtained regularly; see table inset in A. Mr. of protein standards are given in kilodaltons. (SDS-PAGE and gel densitometry were performed as described in methods).

Sheterline et al, 1995). Typical yields were 12 – 15mg of purified G-Actin per g of acetone powder. See methods and appendix A for details of methodology and the assay of the viability of 1M Tris, pH8.0; ATP-G-Buffer for the long-term storage of G-Actin in a stable and active state.

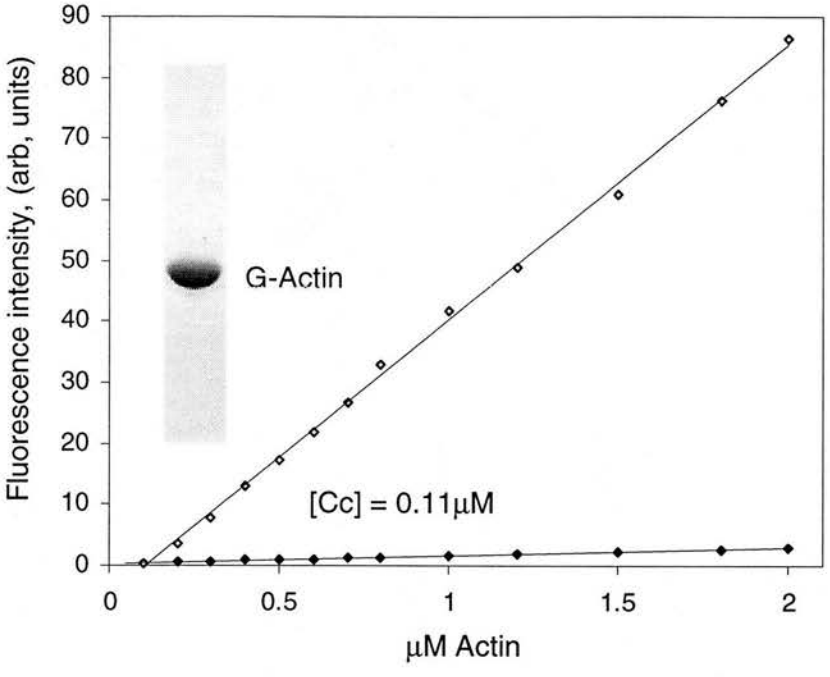

Fig. 3.6. E*xtraction and purification of G-Actin using 1M Tris, pH 8.0; ATP-G-Buffer.* Critical concentration ([C_c]) assay for actin (5% pyrene-labelled) prepared by 1M Tris, pH 8.0; ATP-G-Buffer protocol, performed at 20°C. The excitation wavelength was 366nm, the emission wavelength was 384nm, and a 5nm slit width was used for both. *Open squares* represent the fluorescence intensity of actin incubated in ATP-F-Buffer; *closed squares* represent actin incubated in ATP-G-Buffer. Inset indicates the purity of the G-Actin obtained following extraction and S200 size-exclusion chromatography, as judged by SDS-polyacrylamide gel analysis. *1.0M Tris, pH 8.0; ATP-G-Buffer*: 1.0M Tris, pH 8.0; 0.2mM $CaCl_2$; 0.2mM ATP; 0.5mM DTT; 1.0mM NaN_3. *ATP-G-Buffer*: 5mM Tris, pH 8.0; 0.2mM $CaCl_2$; 0.2mM ATP; 0.5mM DTT; 1.0mM NaN_3. *ATP-F-Buffer*: 5mM Tris, pH 8.0; 0.2mM $CaCl_2$; 0.2mM ATP; 0.5mM DTT; 1.0mM NaN_3; 100mM KCl; 2mM $MgCl_2$. (SDS-PAGE and [C_c] assays were performed as described in methods).

3.2.1.3 Gelsolin Purification Protocol.

Several well-established and documented protocols exist for the purification and over-expression of gelsolin, both from plasma and as recombinant proteins from *E. coli*. Various procedures utilise gelsolins affinity for the Cibacron Blue F3GA ligand (Yamamoto et al, 1989; Ito et al, 1990; Pope et al, 1997). Gelsolin binds to the resin

in the absence of divalent cations, especially Ca^{2+}. Specific elution with 1mM ATP is only achieved in the presence of 0.25mM EGTA. This gives pure gelsolin, after the removal of the ATP by passing the protein down a Sephadex-G25 (coarse) desalt column or long-term dialysis (ca. 48hrs). For larger preparations - over 500ml of original cell culture – a second round of chromatography on a Cibacron Blue F3GA column, in the presence of Ca^{2+} is routinely carried out. Ca^{2+} displaces bound ATP from gelsolin and gelsolin re-binds to the resin. Elution can be achieved by NaCl gradients or salt washes at ~ 0.6M NaCl. These procedures appear to exploit a non-physiological ATP binding site on gelsolin as the ATP is not, as it normally the case, bound co-ordinated with a divalent cation e.g. Mg^{2+}, Ca^{2+}, Mn^{2+}, (Yamamoto et al, 1990; Kambe et al, 1992).

BL21(DE3) *E. coli* were successfully transformed with pMW172[GHS]. Cells were grown in 2xTY/AMP, and the induction of synthesis of high levels of gelsolin was obtained upon addition of IPTG to 1.0mM. Cells were grown for a further 3hrs and then harvested and processed for purification (see methods for protocol details).

Fig. 3.7(A) shows a typical A_{280nm} monitored elution profile from the first round of Cibacron F3GA Blue column chromatography. Gelsolin bound to the matrix and eluted in 1mM ATP, see figs. 3.7(A) and (B). The protein band corresponding to gelsolin migrated with an apparent molecular weight of ca. 86 – 90 kDa on SDS-polyacrylamide gels, see fig. 3.7(B). Fig. 3.7(C) illustrates the purity of gelsolin following processing on the second Cibacron column and an S200 size-exclusion column. Typical purity obtained was ≥95% (as determined by densiometric scanning of appropriate lanes on SDS-polyacrylamide gels similar to that shown in C, lane c, data not shown). Typical yields obtained were between 12 – 18mg.L^{-1} of original bacterial cell culture.

3.2.2 Complex formation between Gelsolin and Actin

Complex formation between gelsolin and actin, in a calcium dependent manner, was confirmed. Gelsolin:$actin_2$ ternary complex (G:A_2) and gelsolin:actin binary complex

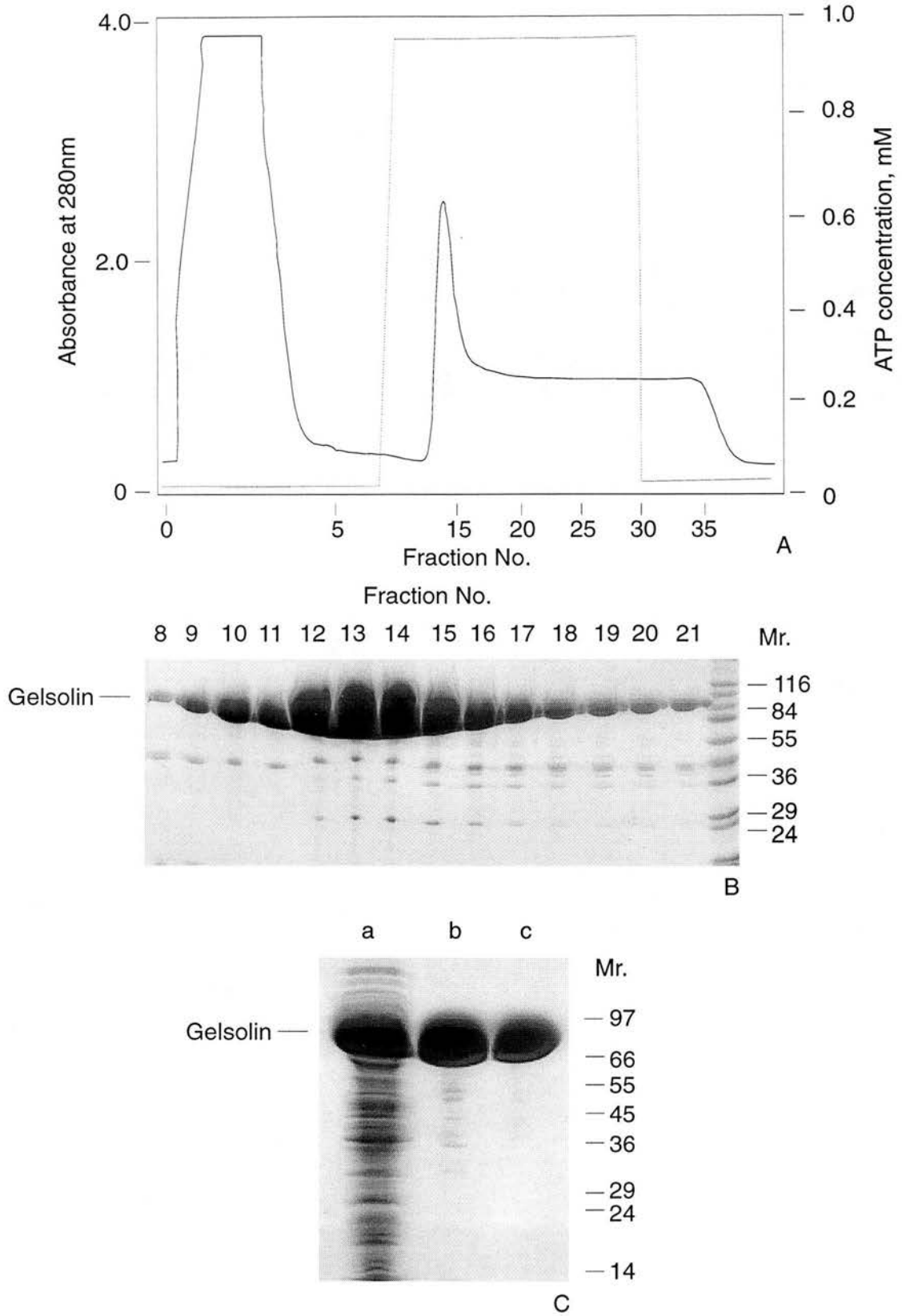

Fig. 3.7. ***Cibacron F3GA Blue chromatography of human cytoplasmic gelsolin.*** (A) A_{280nm} monitored elution profile showing the specific elution of gelsolin by 1mM ATP. (B) SDS-PAGE analysis of the elution profile in A. (C) SDS-polyacrylamide gel illustrating the purity of gelsolin at various stages in the purification protocol. Lane a. SN50 fraction (soluble fraction resulting from centrifugation of cell lysate at 50,000 xg); b. pooled fractions from Cibacron F3GA Blue chromatography performed in 0.6mM EGTA; c. final purity of gelsolin following subsequent purification on a second Cibacron F3GA Blue column (in 0.2mM $CaCl_2$) and an S200 size-exclusion column. >95% purity was regularly obtained. Mr. of protein standards are given in kilodaltons. (SDS-PAGE and chromatography were performed as described in methods).

(G:A) formation was analysed by gel-filtration chromatography. Densitometry confirmed the stoichiometry of the protein components within these complexes.

3.2.2.1 Gel-filtration of complexes.

Complexes between gelsolin and actin were formed by mixing gelsolin and actin in molar ratios between 2:1 and 1:4 (gelsolin:actin, respectively) in buffers containing either 0.2mM $CaCl_2$ (*ATP-G-Buffer*: 5mM Tris, pH8.0; 0.2mM ATP; 0.5mM DTT; 0.2mM $CaCl_2$; 1.0mM NaN_3), 2mM $MgCl_2$ and 100mM KCl (*ATP-F-Buffer*: 5mM Tris, pH8.0; 0.2mM ATP; 0.5mM DTT; 0.2mM $CaCl_2$; 1.0mM NaN_3; 2mM $MgCl_2$; 100mM KCl) or modified G-Buffer containing additionally 0.6mM EGTA; 2mM $MgCl_2$. During the analysis of complex formation in EGTA, gelsolin and actin were first incubated in the calcium-containing buffer for 5min, followed by the addition of EGTA and $MgCl_2$ to 0.6mM and 2mM, respectively. The resultant complex formation was analysed by FPLC/Superose-12 size-exclusion chromatography, performed in ATP-F-Buffer; 0.2mM $CaCl_2$ (see methods for details).

Fig. 3.8(A) shows the elution profiles of the complexes formed in 0.2mM $CaCl_2$ (peak 1) and 0.6mM EGTA (peak 2) compared to those of gelsolin and actin alone (peaks 3 and 4 respectively). The retention volumes (see table 3.1) of these two species give mean apparent Mr. values of 209,kDa (theoretical Mr. 166,kDa) and 149,kDa (theoretical Mr. 124,kDa) for the complexes at peaks 1 and 2, respectively.

The stoichiometry of the components was analysed by densiometric scanning of SDS-polyacrylamide gels, using known amounts of pure actin and gelsolin as internal standards. Fig. 3.8(B) shows the components of peaks 1 and 2 as analysed by SDS-PAGE. The stoichiometry of gelsolin and actin (from several experiments) within these complexes is illustrated in table 3.2. The results gave mean molar ratios for gelsolin:actin of 1:2.1 ($\pm$ 0.13 SD, n=11) in Ca^{2+} and 1:1.2 ($\pm$ 0.084 SD, n= 6) for complexes in EGTA.

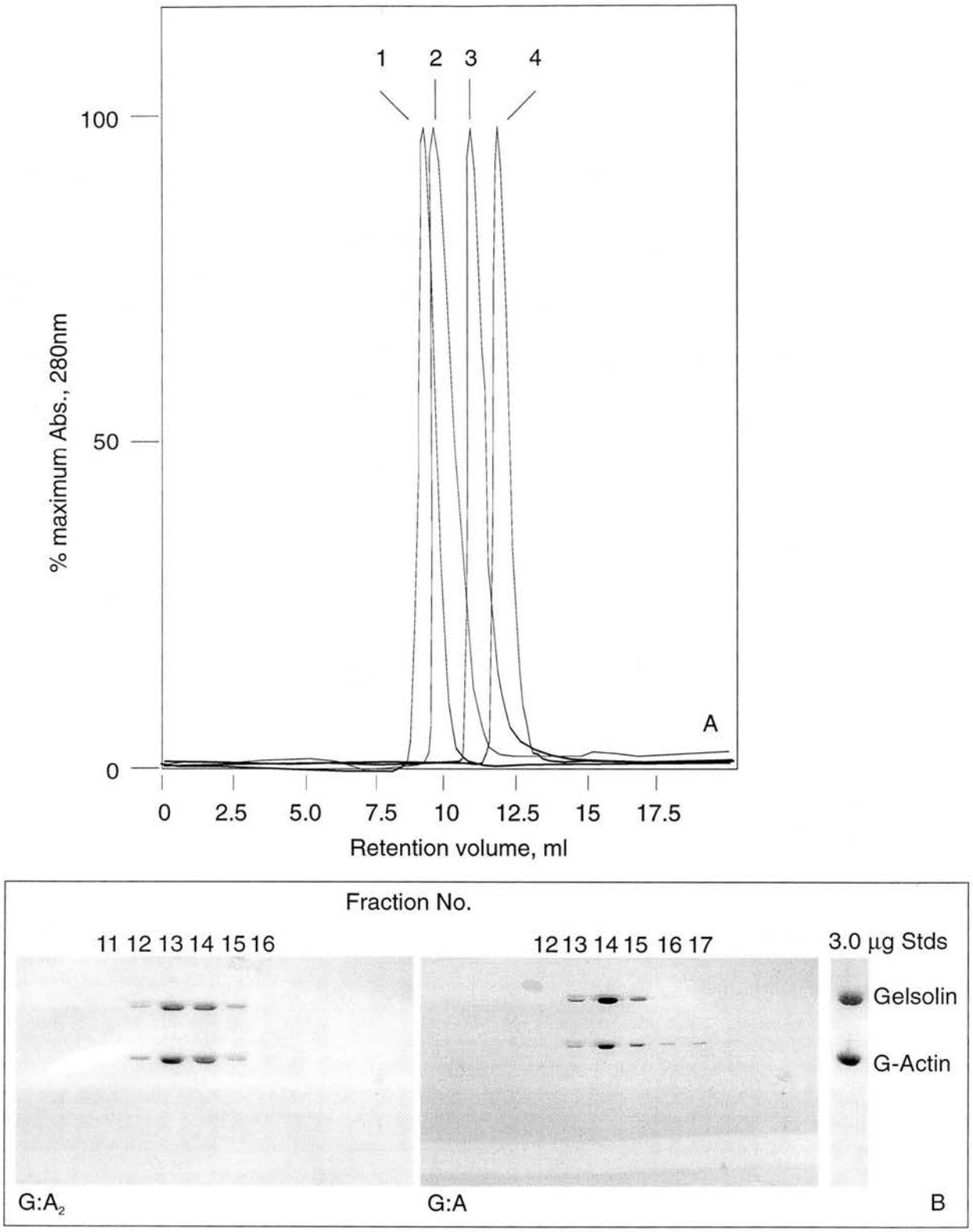

Fig. 3.8. ***Gelsolin:actin complex formation analysed by size-exclusion.*** (A) A_{280nm} monitored elution profiles of G-Actin, gelsolin and gelsolin:actin complexes from an FPLC/Superose-12 size-exclusion column, in ATP-F-Buffer; 0.2mM $CaCl_2$. (B) SDS-PAGE analysis of the peak compositions from A. (G:A and G:A_2 correspond to the binary and ternary complexes respectively). For comparison of different profiles the absorbance values have been normalised to the maximum at the peak. The arrows mark the elution positions of (1) G:A_2 (0.2mM $CaCl_2$); (2) G:A (0.6mM EGTA; 0.2mM $CaCl_2$); (3) gelsolin; (4) G-Actin. (SDS-PAGE and chromatography were performed as described in methods).

Protein species	Retention volume (ml)	Theoretical Mr. (kDa.)	Apparent Mr. (kDa.)
DNaseI	12.79 (± 0.041 SEM, n=9)	29	28.1
G-Actin	11.64 (± 0.062 SEM, n=6)	42	57
gelsolin	10.98 (± 0.051 SEM, n=7)	82	88
actin:DNaseI (A:D)	10.90 (± 0.039 SEM, n=10)	71	92
gelsolin:actin binary complex (G:A)	10.13 (± 0.066 SEM, n=4)	124	149
gelsolin:actin$_2$ ternary complex (G:A$_2$)	9.59 (± 0.037 SEM, n= 12)	166	209

Table 3.1. *Retention volumes (ml) of individual proteins and those of the A:D, G:A and G:A$_2$ complexes.* Data obtained from FPLC/Superose-12 size-exclusion chromatography experiments. The value given for the apparent Mr. is a mean value calculated from the calibration curve using the corresponding mean retention volume. (See methods for details).

Protein complex	Stoichiometry of components
actin:DNaseI (A:D)	1:1.1 (± 0.15 SD, n=5)
gelsolin:actin binary complex (G:A)	1:1.2 (± 0.084 SD, n=6)
gelsolin:actin$_2$ ternary complex (G:A$_2$)	1:2.1 (± 0.13 SD, n=11)

Table 3.2. *Stoichiometry of the protein components within the A:D, G:A and G:A$_2$ complexes.* Data obtained from SDS-PAGE analysis of FPLC/Superose-12 size-exclusion chromatography experiments. (See methods for details).

Complexes that were prepared in 0.2mM $CaCl_2$ eluted at values corresponding to that of the ternary complex even up to molar ratios of actin:gelsolin of 1:2. Uncomplexed gelsolin, in these experiments, eluted at the peak position 3, see fig. 3.8(A). (See discussion for importance and relevance to co-operative binding). In buffers containing EGTA (0.6mM EGTA in the presence of 0.2mM $CaCl_2$ and 0.2mM $MgCl_2$ to prevent the denaturation of the actin) only the binary complex was formed. Even when a molar excess of G-Actin was present in the incubation mix, there was no evidence of ternary complex formation. The excess free G-actin, in such experiments, eluted at the peak position 4, fig. 3.8(A). However, when EGTA was added to preparations of G:A$_2$, and the resultant mixture re-chromatographed in the presence of EGTA, an incomplete dissociation to form G:A and free G-actin was sometimes observed (results similar to Weeds et al, 1986). The G:A binary complex

does not disproportionate into $G:A_2$ and free gelsolin when pre-purified G:A complex (see methods for details of the alternative purification protocol), is re-chromatographed in the presence of Ca^{2+}. Elution volumes give a corresponding Mr. of 149kDa. In contrast, when excess G-actin was added to pre-purified G:A binary complex, in the presence of Ca^{2+} the elution volume of the resultant complex shifted to the higher value corresponding to the molecular weight $G:A_2$ ternary complex.

If gelsolin and actin were mixed together under conditions where the Ca^{2+} concentration is below nM levels no complex formation was observed (results not shown). Similar results have been reported by other workers (Bryan and Kurth, 1984; Coué and Korn, 1985; Wanger and Wegner, 1985; Weeds et al, 1986; Selve and Wegner, 1986; Bryan, 1988; Way et al, 1989; Pope et al, 1997). Calcium concentrations of ~ 5 – 3nM are required for the structural rearrangements that occur upon the activation of gelsolin (Hellweg et al, 1993; Pope et al, 1997; Burtnick et al, 1997; Robinson et al, 1999). Once activated, the Ca^{2+} levels need to be elevated to the μM level (~ 1μM) to allow the binding of actin monomers (Selve and Wegner, 1986; Selve and Wegner, 1987; Schoepper and Wegner, 1991; Lamb et al, 1993; Hellweg et al, 1993; Pope et al, 1995; Ditsch and Wegner, 1995; Pope et al, 1997).

Similar experiments were performed using 100mM Tris, pH 8.0; ATP-G-Buffer as the column running-buffer. (This buffer is essentially the same as ATP-G-Buffer – i.e. low salt – except that the Tris concentration has been increased to raise the ionic strength of the media. Superose resins are prone to interactions with protein samples with low ionic strength buffers). The results obtained were very similar to those carried out in ATP-F-Buffer. The apparent Mr. values obtained during chromatographic runs with this buffer, were in good agreement with the ones described above (data not shown).

For obtaining larger amounts of protein complex, for use in further experiments, size-exclusion chromatography was carried out on a preparative S200 column (V_t ~ 135ml, see methods for details). Similar results to those obtained on the FPLC/Superose-12 column were obtained. Due to the problems with the incomplete

dissociation of G:A_2, to give G:A and free actin in EGTA, an alternative method was used for the preparation of the G:A binary complex (see methods for details).

These results confirm that gelsolin and actin specifically form a ternary complex (G:A_2), in Ca^{2+}, and a binary complex (G:A) in EGTA.

3.2.2.2 Native-gel complex formation

Non-denaturing PAGE showed complex formation for each of the G:A_2 and G:A complexes and second dimension analysis by SDS-PAGE confirmed the identity and stoichiometry of the protein components within each of the complexes.

All densitometry was carried out using SYPRO™-Red (Molecular Probes Inc.) fluorescent stain and a Molecular Dynamics chemi-luminescence imager. Complex formation was further analysed using non-denaturing gels. The proteins to be tested were mixed together in ATP-G-Buffer, in similar ratios as those used in the gel-filtration experiments (see methods for details). F-Buffer was not used routinely to avoid the associated problems that occurred with native-PAGE, due to the presence of high salt (100mM KCl) concentrations in this buffer.

Fig. 3.9(A) shows the migration pattern for G-Actin, gelsolin and the two complexes, G:A_2 and G:A, on a 7% acrylamide (w/v) Native gel (see methods for details). Clear shifts in electrophoretic mobility were seen upon formation of the two complexes. The gel running conditions have to be altered slightly for each individual complex or set of proteins. e.g. Gelsolin alone runs as a broad smear near the top of the gel when Ca^{2+} is included in the gel running buffer. This is not an unexpected feature, as the binding of calcium produces large conformational rearrangements in the tertiary structure of gelsolin (Hellweg at al, 1993; Pope et al, 1997; Burtnick et al, 1997; Robinson et al, 1999). The structural rearrangements and the additional effect of binding Ca^{2+} ions, with the coupled changes in the charge distribution of the molecule, would result in mobility shifts on such non-denaturing gels. Gel running conditions: 0.2mM $CaCl_2$; 0.2mM ATP; 0.5mM DTT were used for G:A_2 complex

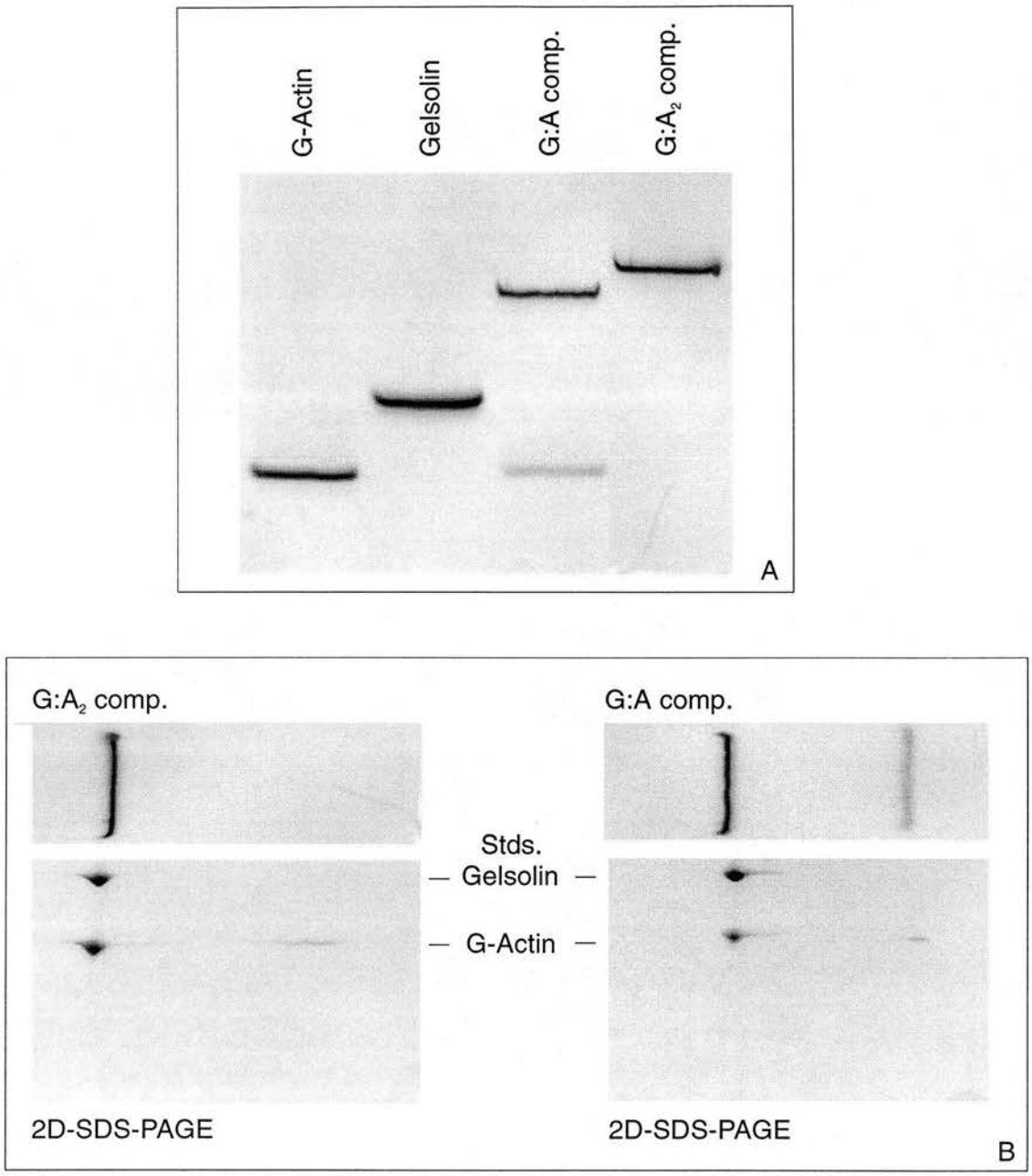

Fig. 3.9. ***Gelsolin:actin complex formation analysed by non-denaturing PAGE.*** (A) Native gel showing the electrophoretic mobilities of G-Actin, gelsolin and gelsolin:actin complexes. (G:Acomp. and G:A_2comp. correspond to the binary and ternary complexes respectively). (B) SDS-PAGE analysis, in a second dimension, of the components of the protein bands in A. Standard migration positions of G-Actin and gelsolin are indicated between the two gels. Gel running conditions; 0.2mM $CaCl_2$; 0.2mM ATP; 0.5mM DTT were used for G-Actin and G:A_2 complex formation; 0.2mM ATP; 0.5mM DTT were used for gelsolin; 0.2mM $CaCl_2$; 0.2mM ATP; 0.5mM DTT; 0.6mM EGTA; 1.0mM $MgCl_2$ were used for G:A complex formation. (SDS-PAGE and native-PAGE were performed as described in methods).

formation. These were changed to 0.2mM $CaCl_2$; 0.2mM ATP; 0.5mM DTT; 0.6mM EGTA; 1mM $MgCl_2$ for G:A complex formation.

SDS-PAGE in a second dimension and subsequent analysis of the components of the protein bands from the native gels, by densiometric scanning, was carried out. Fig. 3.9(B) clearly illustrates the components of the two gelsolin:actin complexes. The stoichiometric values of the respective complex components are shown in table 3.3. Mean values for the molar ratios of gelsolin:actin indicate the formation of the G:A binary complex in EGTA and the formation of the $G:A_2$ ternary complex in Ca^{2+}.

Protein complex	Stoichiometry of components
actin:DNaseI (A:D)	1:1.3 (± 0.06 SD, n=4)
gelsolin:actin binary complex (G:A)	1:1.3 (± 0.05 SD, n=4)
gelsolin:$actin_2$ ternary complex ($G:A_2$)	1:2.1 (± 0.18 SD, n=6)

Table 3.3. *Stoichiometry of the protein components within the A:D, G:A and $G:A_2$ complexes.* Data obtained from non-denaturing-PAGE experiments. SDS-PAGE and stoichiometric analysis was performed as described in methods.

Similarly to experiments performed on size-exclusion columns, incubation mixtures performed in the presence of calcium, that contained an excess of gelsolin (molar ratios of actin:gelsolin of 1:2) the formation of the ternary complex predominated. Very little, if any, binary complex was detected. The uncomplexed gelsolin, in these experiments, migrated at its normal position. (See discussion for importance and relevance of this result to the co-operativity of actin monomer binding for the formation of the $G:A_2$ ternary complex).

In buffers containing EGTA (0.6mM EGTA in the presence of 0.2mM $CaCl_2$ and 1.0mM $MgCl_2$ to prevent the denaturation of the actin) only the binary complex was formed. Even when a molar excess of G-Actin was added to the incubation mix, there was little evidence of ternary complex formation. The excess free G-actin, in such experiments, migrated with a mobility characteristic of free G-Actin, see fig. 3.9(A).

3.2.2.3 Complex formation analysis by fluorescence enhancement measurement

Fluorescence enhancement of NBD-Actin, upon binding to gelsolin, confirmed the stoichiometry of G:A_2 and G:A.

Several workers (Bryan & Kurth, 1984; Doi & Frieden, 1984; Weeds et al, 1986; Way et al, 1989; Way et al, 1990; Pope et al, 1995; Pope et al, 1997) have reported the use of fluorescence enhancement measurements from two fluorescently labelled actin derivatives to follow complex formation with gelsolin; NBD-Actin (Lys - 373) and Pyrene-Actin (Cys - 374) (see methods for protocol details). The maximum fluorescence enhancement observed when NBD-Actin binds to gelsolin (formation of G:A_2) is approximately 110 – 130 % (Weeds et al, 1986; Way et al, 1989; Pope et al, 1997). Several experiments were carried out using NBD-Actin to follow complex formation with gelsolin. Experiments were carried out in ATP-G-Buffer, containing 0.2mM $CaCl_2$ or 0.6mM EGTA; 0.2mM $CaCl_2$; 0.2mM $MgCl_2$ or in ATP-F-Buffer; 0.2mM $CaCl_2$, (see methods for details).

Fig. 3.10(A) shows the titration of NBD-Actin in the absence or presence of a constant amount of gelsolin, 80nM, in 0.2mM $CaCl_2$ (ATP-G-Buffer).

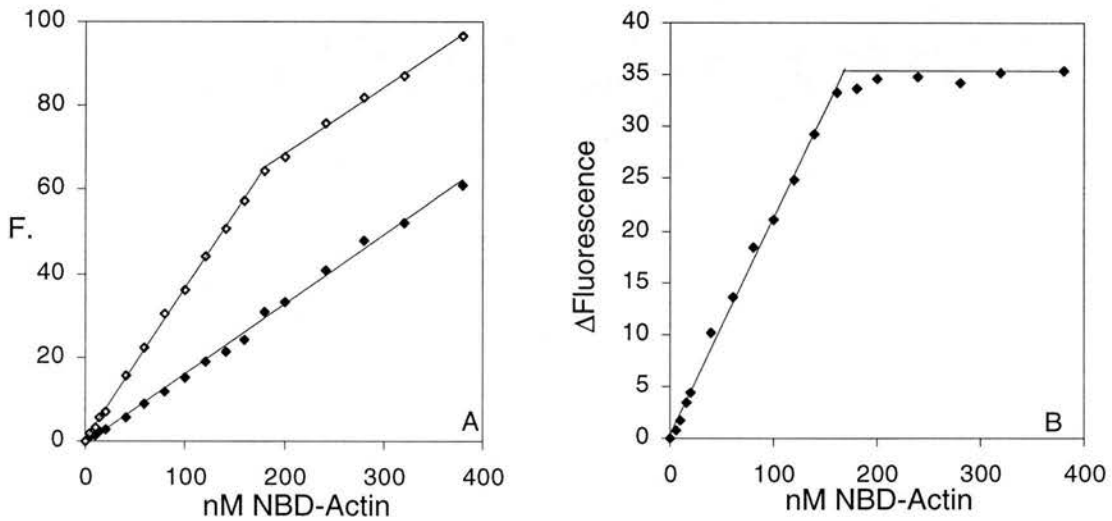

Fig. 3.10. ***Fluorescence titration at constant gelsolin concentration with NBD-Actin, in 0.2mM $CaCl_2$ (ATP-G-Buffer).*** (A) *Closed squares* indicate the fluorescence intensity of NBD-Actin alone; *open squares* indicate the fluorescence intensity of NBD-Actin with added 80nM gelsolin. (B) Difference between fluorescence intensities in (A). (λex=475nm, λem=520nm; 5nm slit for both). The solid line is a linear regression and gives maximum enhancement at 2.1 actin/gelsolin. (Titration was performed as described in methods).

Each data point represents a separate reaction mixture and not serial additions of titrant. Fig. 3.10(B) shows the difference between the two fluorescence profiles, in A, which is due to the enhancement in fluorescence intensity of NBD-Actin upon complex formation with gelsolin. Fig. 3.10(B) clearly indicates that the fluorescence rises linearly as the concentration of NBD-Actin increases, up to an inflexion point. At this point there is an abrupt transition to a plateau level. The position of this inflexion point occurs at a stoichiometry of gelsolin:actin of 1:2 respectively. Mean values for gelsolin:actin were 1:2.1 (± 0.15 SD, n=5) indicating the formation of the $G:A_2$ ternary complex, in Ca^{2+}.

These data also demonstrate that both binding sites on gelsolin contribute equally to the fluorescence signal enhancement. Fig. 3.11 shows the emission spectra of NBD-Actin alone and those with the addition of gelsolin in the presence or absence of Ca^{2+}. An enhancement of ca. 60 – 70% is seen over NBD-actin alone in the presence of gelsolin and EGTA. A further 60 – 70% enhancement is seen in 0.2mM $CaCl_2$. Binding of NBD-Actin to each site on gelsolin contributes equally to the fluorescence enhancement signal.

Fig. 3.12(A) shows the fluorescence measurements from a continuous variation experiment performed in 0.2mM $CaCl_2$ (see methods for details). The total protein concentration is maintained at 400nM and both gelsolin and NBD-Actin are varied in a continuous fashion (Blake et al, 1967; Weeds et al, 1986; Way et al, 1989). The fluorescence shows a very sharp discontinuity at a molar ratio that corresponds to that stoichiometry of the component proteins within the resultant complex. The inflexion point has a mean molar ratio for gelsolin:actin of 1:2.1 (± 0.17 SD, n=9). Similar continuous variation experiments were carried out in the presence of 0.6mM EGTA. The EGTA fluorescence profile is shown in fig. 3.12(B). This biphasic profile also has a sharp inflexion point that corresponds to a mean stoichiometry for gelsolin:actin of 1.1 (± 0.13 SD, n=4).

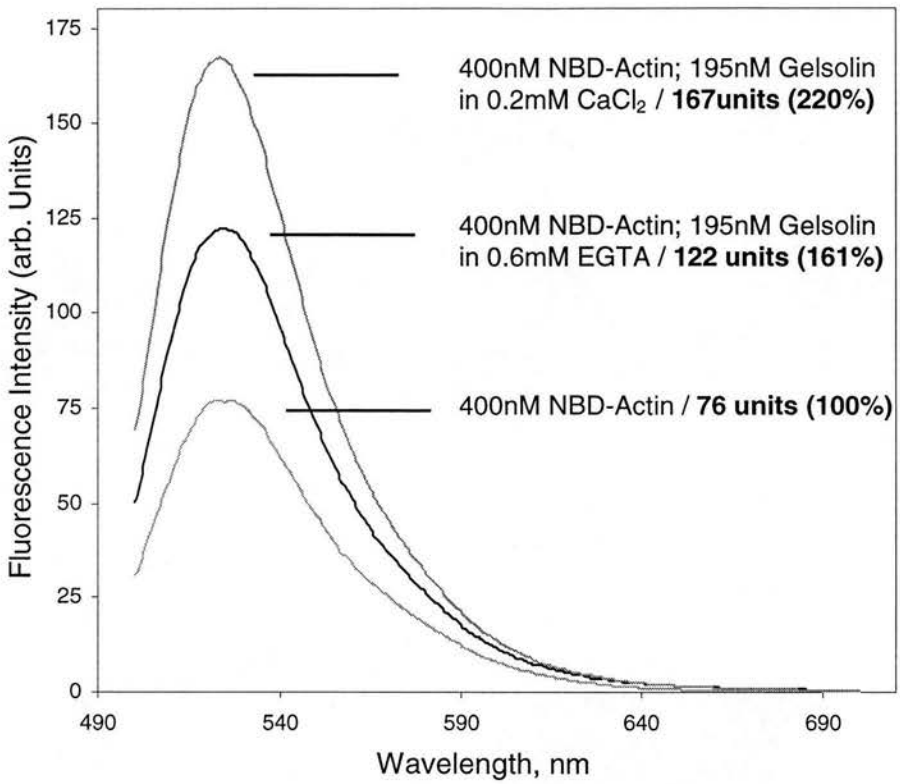

Fig. 3.11. ***The effect on the emission spectra of NBD-Actin upon complex formation with gelsolin.*** The emission spectra (the excitation wavelength used was 475nm, with a 5nm slit width for both excitation and emission) of 400nM NBD-Actin, in 0.2mM $CaCl_2$, and those with added 195nM gelsolin, in the presence or absence of calcium, are shown. (Molar ratio is ~ 2:1 for actin:gelsolin). The equal contribution by each actin-binding site on gelsolin to the fluorescence enhancement is illustrated by two equivalent step-wise increases in fluorescence. Proteins were mixed together, at the appropriated concentrations, in the calcium containing buffer and incubated at RT for 30min, and then the emission spectra measured. For experiments in EGTA the protein mixture was first incubated at RT for 5min, in the calcium-containing buffer, and $MgCl_2$ and EGTA were then added to the appropriate concentrations. Solution conditions for calcium containing buffers: *ATP-G-Buffer*; 5mM Tris, pH8.0; 0.5mM DTT; 0.2mM ATP; 0.2mM $CaCl_2$; 1.0mM NaN_3. Solution conditions for EGTA containing buffers: 5mM Tris, pH8.0; 0.5mM DTT; 0.2mM ATP; 0.2mM $CaCl_2$; 1.0mM NaN_3; 0.2mM $MgCl_2$; 0.6mM EGTA.

Similar experiments were performed in ATP-F-Buffer (additionally contains 100mM KCl and 2mM $MgCl_2$). The results obtained were very similar to those carried out in ATP-G-Buffer (data not shown). However, care has to be taken to make sure that the free G-Actin concentration is below the [C_c] when using ionic conditions that induce actin polymerisation. NBD-Actin gives a fluorescence enhancement of ~100% when

the monomer becomes incorporated into the filament (Detmers et al, 1981). This can often create anomalous fluorescence values and give confusing data.

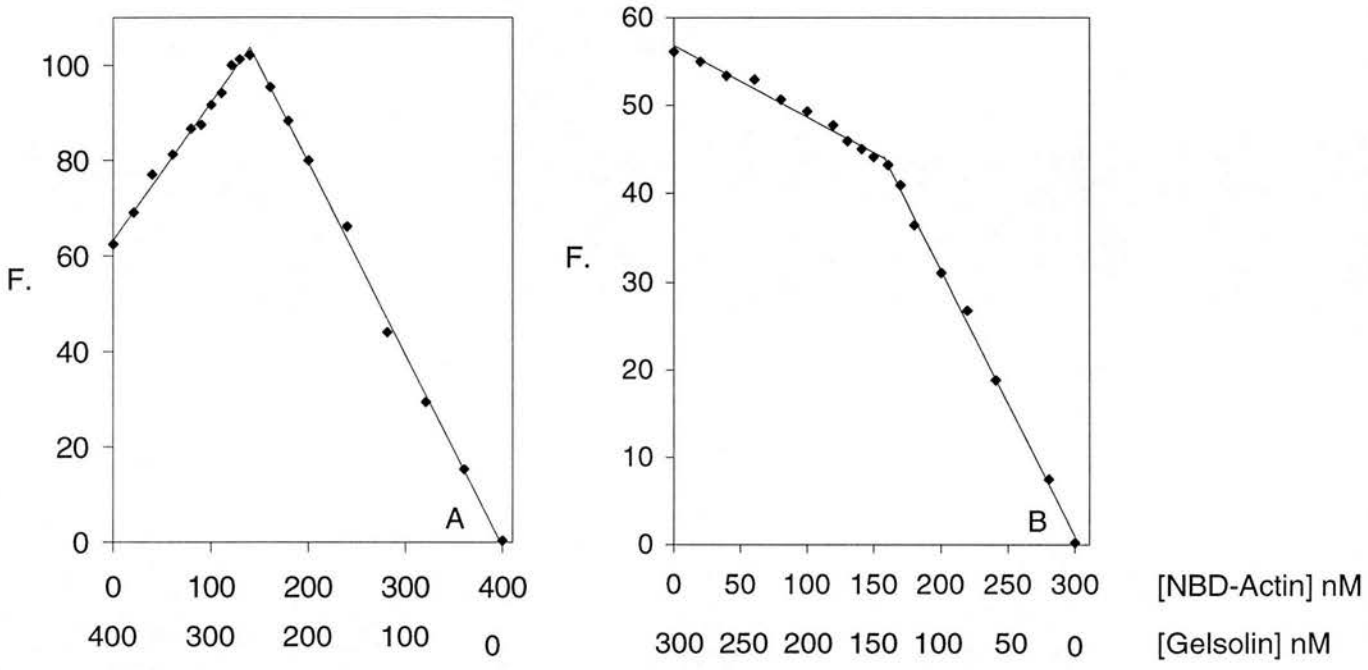

Fig. 3.12. ***Fluorescence titration at constant total protein concentration with continuous variation of both NBD-Actin and gelsolin.*** (A) Experiment using 400nM total protein in 0.2mM $CaCl_2$ (ATP-G-Buffer) with the transition point at 139nM gelsolin and 261nM NBD-Actin (the solid line is a linear regression; inflection point at actin/gelsolin = 1.9). (B) Experiment with 300nM total protein concentration in 0.6mM EGTA (in the presence of 0.2mM $MgCl_2$) with the transition point at 158nM gelsolin and 141nM NBD-Actin (the solid line is a linear regression; inflection point at actin/gelsolin = 0.9). (Titrations were performed as described in methods).

The data obtained from the fluorescence analysis provides further supportive evidence – by a third and completely different physical method - for the formation of $G:A_2$ ternary and G:A binary complexes between gelsolin and actin in Ca^{2+} and EGTA, respectively.

3.2.3 Complex formation between DNaseI and G-Actin.

3.2.3.1 Gel-filtration analysis of complex formation.

In the analysis of the orientation of the actin monomers within the G:A_2 ternary complex we wanted to add A:D binary complex to gelsolin to test the binding of this complex to gelsolin. We purified the A:D binary complex and confirmed its stoichiometry.

Actin and DNaseI were mixed together at molar ratios of 1:1, in ATP-F-Buffer or 100mM ATP-G-Buffer, and then subjected to size-exclusion chromatography. Fig. 3.13(A) shows the elution profile from an FPLC/Superose-12 size-exclusion run of the actin:DNaseI complex (peak 1) compared to G-actin and DNaseI alone, peaks 2 and 3 respectively. The retention volume of peak 1 has a mean apparent Mr. of 92kDa (theoretical Mr. = 71kDa) corresponding to the formation of the actin:DNaseI binary complex (see table 3.1).

SDS-PAGE analysis of the elution profile of peak 1 in fig. 3.13(A) is shown in fig. 3.13(B). It confirmed the presence of both proteins (actin and DNaseI) in peak 1. The stoichiometric analysis of this complex, by densiometric scanning of appropriate gel lanes, is illustrated in table 3.3. The results indicate a molar ratio for actin:DNaseI is 1:1 within this complex.

3.2.3.2 Native-gel analysis of actin:DNaseI binary complex formation.

Formation of complex was similarly analysed using non-denaturing gels (see methods for details). Fig. 3.14(A) shows the protein band migration pattern of DNaseI, G-actin and the A:D complex on a 7% (w/v) acrylamide native gel. Gel running conditions were carried out in the absence of Ca^{2+}, for DNaseI samples. DNaseI binds Ca^{2+} ions - the cation helps to stabilise the molecule and protects against proteolytic degradation (Price et al, 1969; Suck et al, 1984; Suck and Oefner,

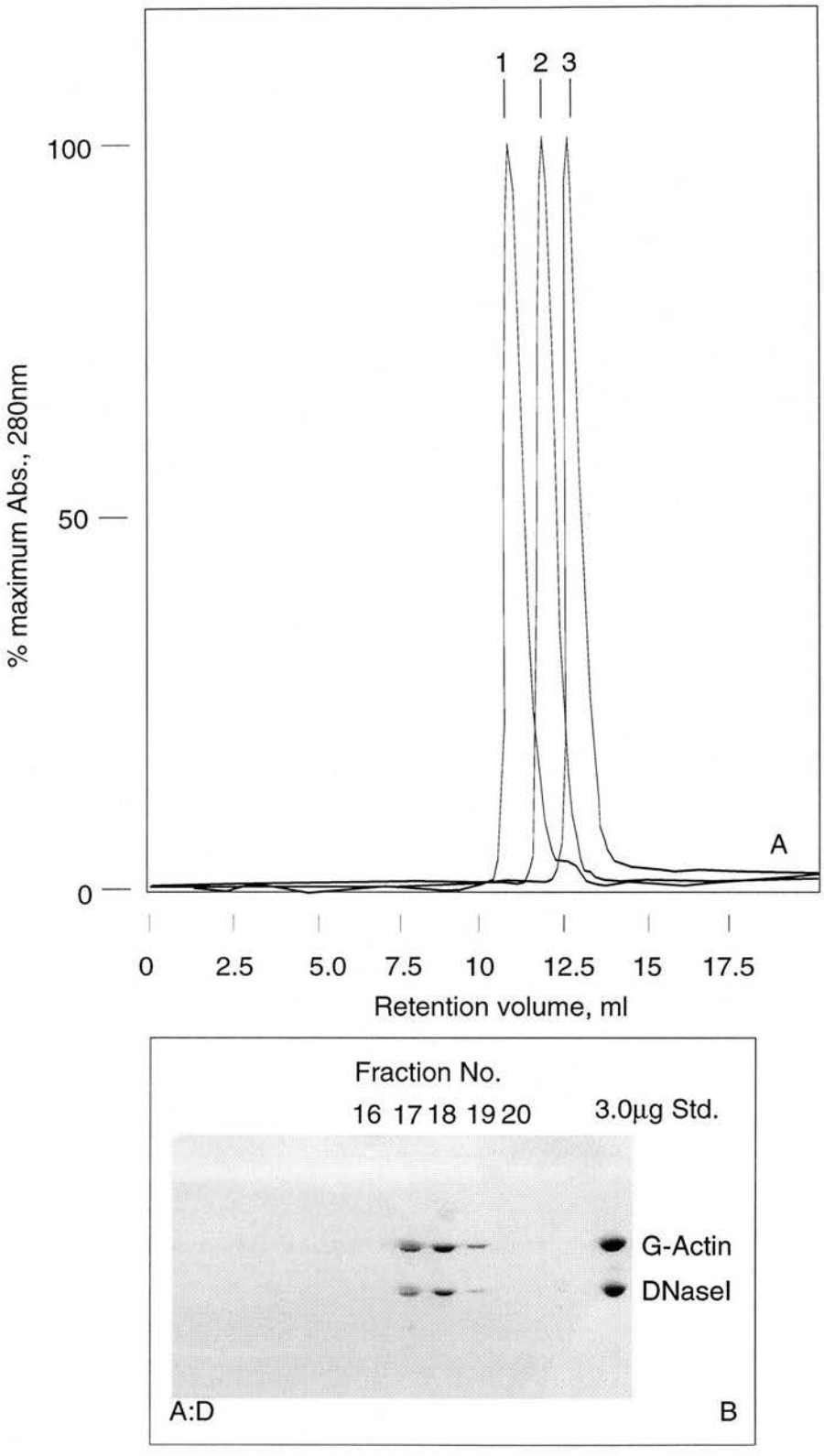

Fig. 3.13. ***Actin:Dnasel complex formation analysed by size-exclusion.*** (A) A_{280nm} monitored elution profiles of DNaseI, G-Actin and the actin:DNaseI complex from an FPLC/Superose-12 size-exclusion column. (B) SDS-PAGE analysis of the peak composition from A. (A:D corresponds to the actin:DNaseI binary complex). For comparison of different profiles the absorbance values have been normalised to the maximum at the peak. The arrows mark the elution positions of (1) A:D; (2) G-Actin; (3) DNaseI. (SDS-PAGE and chromatography were performed as described in methods).

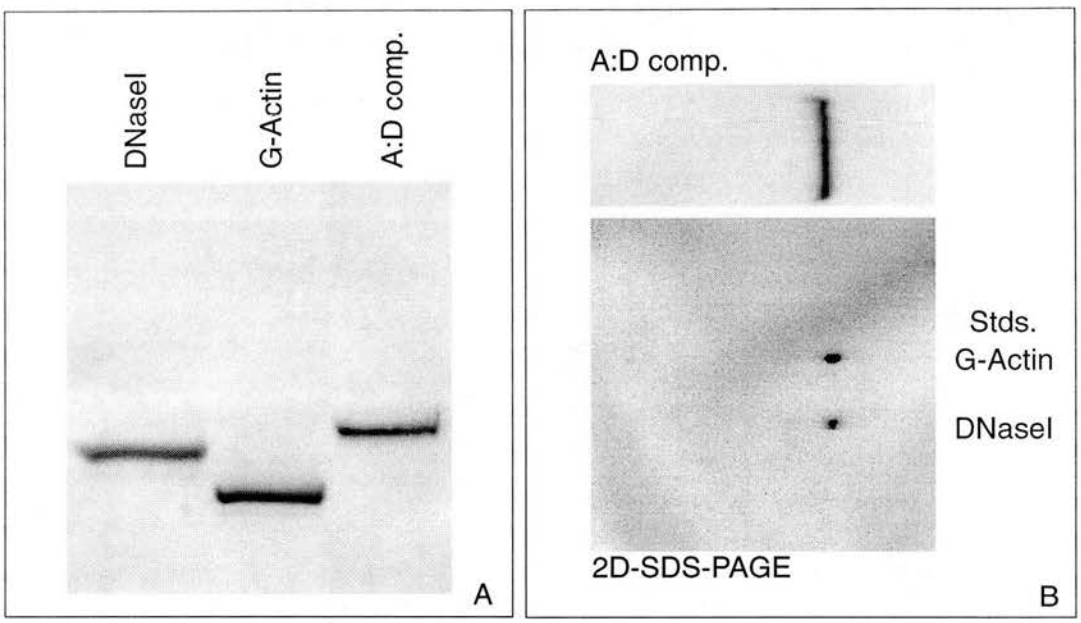

Fig. 3.14. ***Actin:DNaseI complex formation analysed by non-denaturing PAGE.*** (A) Native gel showing the electrophoretic mobilities of DNaseI, G-Actin, and the actin:DNaseI complex. (A:D corresponds to the actin:DNaseI binary complex). (B) SDS-PAGE analysis, in a second dimension, of the components of the protein bands in A. Standard migration positions of G-Actin and DNaseI are indicated beside the gel. Gel running conditions: 0.2mM $CaCl_2$; 0.2mM ATP; 0.5mM DTT were used for G-Actin and A:D complex formation; 0.2mM ATP; 0.5mM DTT were used for DNaseI. (SDS-PAGE and native-PAGE were performed as described in methods).

1986) – and this sometimes resulted in strange mobility shifts and smearing of the protein bands in DNaseI samples, on the non-denaturing gels.

A distinct shift in the electrophoretic mobility of the 1:1 molar ratio incubation sample of A:D was observed. Second dimension SDS-PAGE analysis of the band confirmed the presence of both DNaseI and Actin within this shifted complex band, see fig. 3.14(B). Table 3.3 shows the stoichiometric analysis, by densitometry, confirming the 1:1 molar ratios for actin:DNaseI in the binary complex.

3.2.3.3 Fluorescence analysis of the A:D complex

Fig. 3.15 shows the emission spectra of NBD-Actin alone and that of NBD-Actin complexed 1:1 with DNaseI. There is no significant difference between the two spectra. A ΔF_{max} of minus 5% and a slight blue shift in the wavelength, ~ 1 – 2nm, at

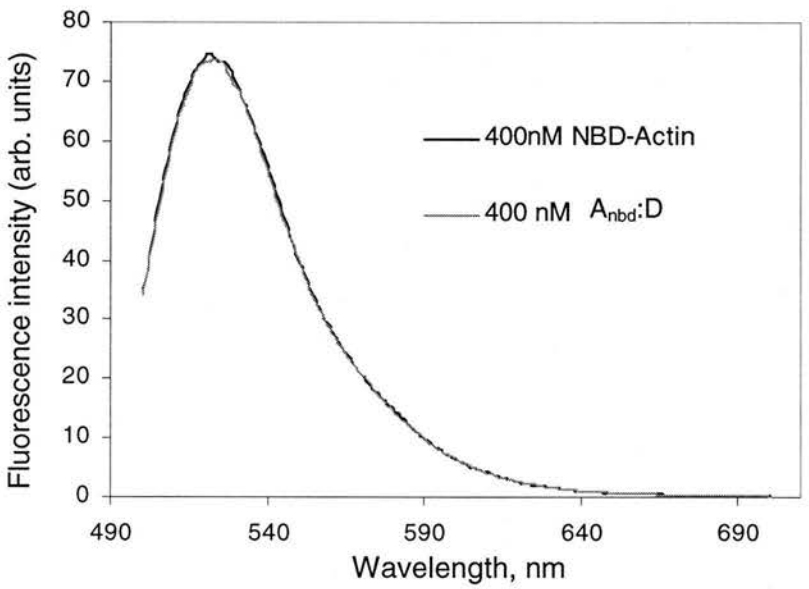

Fig. 3.15. ***The effect on the emission spectra of NBD-Actin upon complex formation with DNaseI.*** The emission spectra (the excitation wavelength was 475nm, with a 5nm slit width for both excitation and emission) of 400nM NBD-Actin, in 0.2mM $CaCl_2$, and that with added 400nM of active DNaseI are shown. (Molar ratio is ~ 1:1 for actin:DNaseI). The two spectra are not significantly different from each other demonstrating the spectral "silence" of the presence of DNaseI bound to the pointed-end of the NBD-Actin monomer. Proteins were mixed together, at the appropriate concentrations, and incubated at RT for 30min in *ATP-G-Buffer:* 5mM Tris, pH8.0; 0.5mM DTT; 0.2mM ATP; 0.2mM $CaCl_2$; 1.0mM NaN_3.

maximal absorbance, upon formation of the binary complex, have been reported but these spectral changes were not observed with every preparation of NBD-Actin or A_{nbd}:D complex (Detmers et al, 1981). The binding of DNaseI to the pointed-end of an NBD-actin monomer has little effect on the emission spectra of that actin. The presence of DNaseI is "silent" with respect to analysis of NBD-Actin by fluorescence enhancement. Conformation of the formation of a tight binary complex, between NBD-Actin and DNaseI, was performed by size-exclusion chromatography and non-denaturing gel analysis. Very similar results to those carried out with the native proteins were obtained (data not shown).

3.2.4 Summary

The results from the preceding sections verify the formation of the G:A_2, G:A and A:D complexes. The techniques applied and the results obtained serve as an illustration of the validity and sensitivity of these methods as sound and complementary ways of elucidating the system of complex formation between gelsolin, actin and DNaseI. (Similar results have been reported by other workers, Detmers et al, 1981; Bryan and Kurth, 1984; Coué and Korn, 1985; Weeds et al, 1986; Way et al, 1989; Way et al, 1990; Pope et al, 1991; Pope et al, 1997). A combination of these three methods served as the basis of the approach to the problem of trying to elucidate the spatial orientation of the actin monomers within G:A_2.

3.3 Probing the actin monomer conformation in the gelsolin:actin$_2$ complex using DNaseI.

3.3.1 Overview

We proposed to use DNaseI as a tool to probe the spatial orientation of the two actin monomers in G:A_2. DNaseI was added to pre-purified G:A_2 and the resultant complex analysed by gel-filtration, non-denaturing gel experiments. Such experiments produced data indicate the formation of a complex, significantly larger than G:A_2, containing **G:A_2:D_2**, respectively. The binding of pre-purified A:D complex (with NBD labelled actin monomers), to gelsolin was also studied. The results also indicated the formation of a larger complex, with a stoichiometry of **G:(A:D)$_2$.**

3.3.2 Binding of DNaseI to the pointed-ends of actin monomers within the G:A_2 ternary complex.

G:A_2 complex was purified: gelsolin and G-actin were incubated in the presence of 0.2mM $CaCl_2$ at a molar ratio of 1:2 (gelsolin:actin, respectively), and then subjected to size-exclusion chromatography on an S200 gel-filtration column (see methods for details)

3.3.2.1 Gel-filtration analysis of "GA_2:D_2" complex formation

Purified DNaseI was added to a solution of G:A_2 complex, in ATP-G-Buffer or ATP-F-Buffer; 0.2mM $CaCl_2$, at a molar ratio of 2:1 (3.0μM G:A_2; 6.0μM DNaseI). This incubation mix included + 3 – 15% DNaseI, to account for the proportion of inactive protein in DNaseI preparations, assayed by a modified [C_c] assay, (see methods and appendix B for details). The mixture was incubated for 30min at RT and any subsequent complex formation analysed by size-exclusion chromatography on an FPLC/Superose-12 column, pre-equilibrated in ATP-F-Buffer; 0.2mM $CaCl_2$ or 100mM Tris, pH 8.0; ATP-G-Buffer.

Fig. 3.16(A) shows the elution profile from FPLC/Superose-12 size-exclusion column chromatography of a "GA_2:D_2" incubation (peak 1), compared to those of G:A_2 and DNaseI alone (peaks 2 and 3 respectively). A significant shift ($P<0.05$) in the retention volume of the "GA_2:D_2" incubation mixture sample mixture was observed, see table 3.4.

The retention volumes for this species give an apparent mean Mr. of 251kDa. This value suggests the formation of a complex between one G:A_2 ternary complex and two DNaseI molecules, $\mathbf{(GA_2):D_2}$. This is in good agreement with the theoretical value of 224kDa (assuming that the complex has a globular shape).

Protein species	Retention volume (ml)	Theoretical Mr. (kDa.)	Apparent Mr. (kDa.)
DNaseI	12.79 (+/- 0.041 SEM, n=9)	29	28.1
gelsolin:actin$_2$ ternary complex (G:A_2)	9.59 (+/- 0.037 SEM, n= 12)	166	209
"GA_2:D_2" complex	9.29 (+/- 0.057 SEM, n=4)	224	251

Table 3.4. *Retention volumes (ml) of DNaseI, G:A_2 ternary complex and the "GA_2:D_2" complex.* Data obtained from FPLC/Superose-12 size-exclusion chromatography. The value given for the apparent Mr. is a mean value calculated from the calibration curve using the corresponding mean retention volume. The significance of the difference between the mean retention volume of G:A_2 and that of (G:A_2):D_2 is $P<0.05$. (See methods for details).

SDS-PAGE analysis of the components of the putative complex peak showed the presence of all three proteins (gelsolin, actin and DNaseI) in the shifted peak, see fig. 3.16(B). DNaseI has shifted from its normal elution volume to that of a much higher molecular weight species, indicative of it having bound to the larger G:A_2 complex. Stoichiometric analysis of the components of the new peak was carried out by densiometric scanning of bands on SDS-polyacrylamide gels, using known amounts of gelsolin, actin and DNaseI as internal standards. Table 3.5 summarises the results from four similar experiments. The stoichiometry of this new complex appears to be $\mathbf{G_2:A_2:D_2}$.

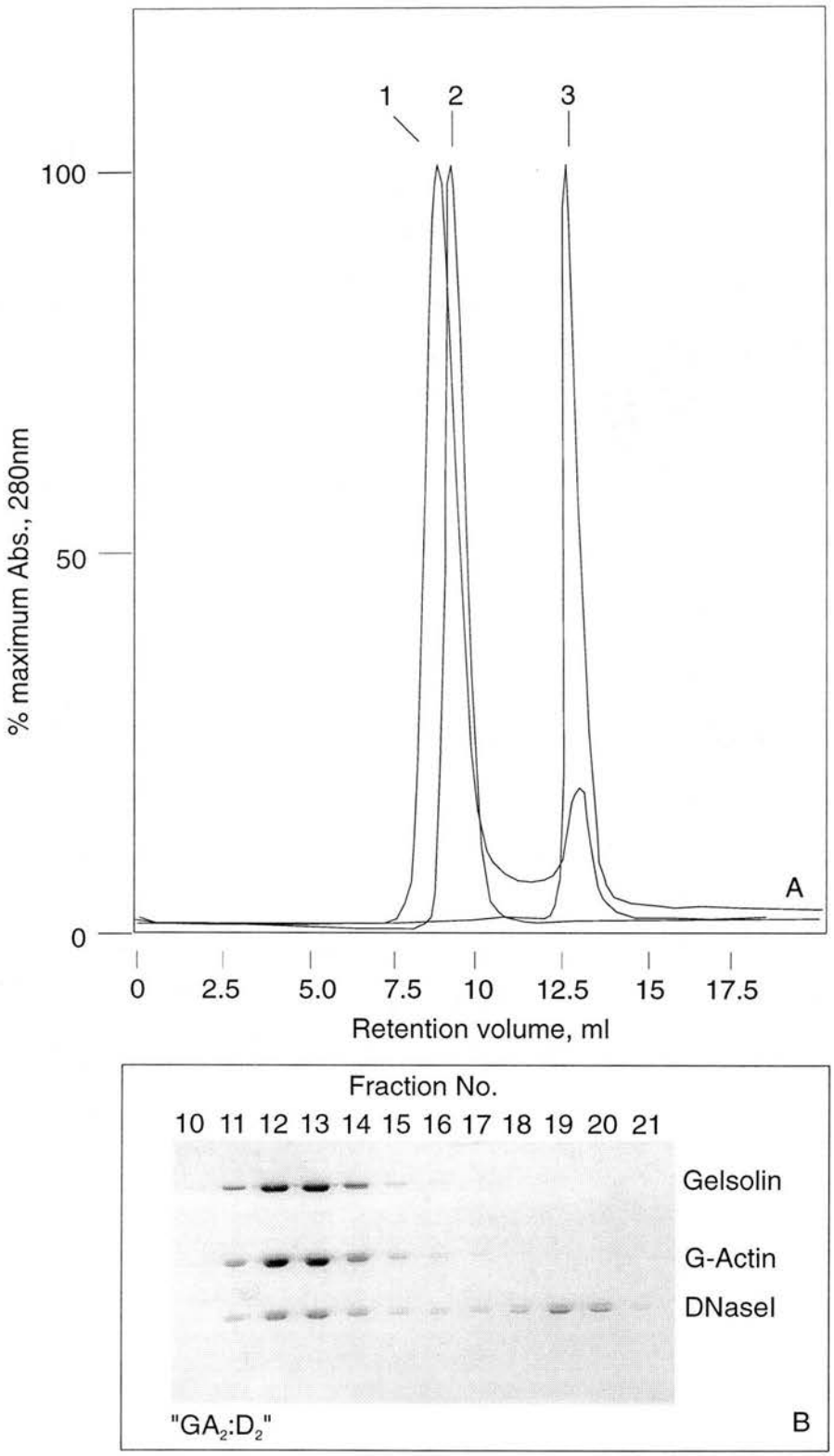

Fig. 3.16. ***Formation of a complex between the G:A$_2$ ternary complex and DNaseI as analysed by size-exclusion.*** (A) A_{280nm} monitored elution profiles of DNaseI, G:A_2 ternary complex and the "GA_2:D_2" complex on an FPLC/Superose-12 size-exclusion column, run in ATP-F-Buffer; 0.2mM $CaCl_2$. (B) SDS-PAGE analysis of the peak composition for the "GA_2:D_2" sample from A. For comparison of different profiles the absorbance values have been normalised to the maximum at the peak. The arrows mark the elution positions of (1) "GA_2:D_2"; (2) G:A_2; (3) DNaseI. The "GA_2:D_2" cpmplex is that formed from an incubation (30min at RT) of pre-purified G:A_2 ternary complex and DNaseI in a molar ratio of 1:2 (3.0µM G:A_2 and 6.0µM DNaseI) in ATP-F-Buffer; 0.2mM $CaCl_2$. (SDS-PAGE and chromatography were performed as described in methods).

FPLC/Sup-12 size exclusion	Mole ratios			
gelsolin:actin	1:2.2	1:2.07	1:2.17	1:2.34
actin:DNaseI	1:1.05	1:1.03	1 :1.13	1:1.05
gelsolin: DNaseI	1:2.3	1:2.13	1:2.4	1:2.28
Native Gels	**Mole ratios**			
gelsolin:actin	1:1.94	1:2.3	1:2.1	1:2.3
actin:DNaseI	1:1.02	1:0.81	1:1.08	1:0.95
gelsolin: DNaseI	1:1.97	1:1.81	1:2.1	1:1.90

Table 3.5. *Stoichiometry of the individual component proteins within the "$(GA_2):D_2$" complex.* The values given in the upper half of the table represent data obtained from 4 similar experiments carried out on FPLC/Superose-12 size-exclusion chromatography columns. Those in the lower half represent data obtained from 4 similar experiments carried out on non-denaturing gels. The densitometry was carried out with the fluorescent SYPRO-Red™ stain (Molecular Probes Inc.) and a chemi-luminescence imager. The gels were then subsequently stained with Coomassie Blue-R250 for visual conformation of the results. (See methods for details).

When 2:1 molar ratio incubations of (A:D):gelsolin (in ATP-F-Buffer; 0.2mM $CaCl_2$), were subjected to size-exclusion chromatography, on an FPLC/Superose-12 column the elution profile produced a peak corresponding to position 1 in fig. 3.16(A). The apparent Mr. of this species was ~ 251kDa indicating the formation of a complex with an apparent stoichiometry of **$G:(A:D)_2$**, see table 3.2 for the retention volume details.

Similarly to the formation of $G:A_2$, when excess gelsolin was included in incubation mixtures of gelsolin and A:D (up to 2:1, respectively), the $G:(AD)_2$ complex preferentially forms with the excess gelsolin eluting at a position corresponding to free uncomplexed gelsolin (peak position 3 in fig. 3.8).

Incubations of both, $G:A_2$ plus DNaseI (molar ratio of 1:2, respectively), and those of gelsolin plus pre-formed A:D binary complex (molar ratio 1:2, respectively), gave a complex that eluted with the same retention volume, and with the same stoichiometry for its protein components; **$G:A_2:D_2$**.

3.3.2.2 Native-gel analysis of "(GA_2): D_2" complex formation

The use of non-denaturing gels provided additional evidence for the formation of a complex between the G:A_2 ternary complex and two DNaseI molecules. Fig. 3.17(A) shows the appearance of a band with a shifted electrophoretic mobility in lanes that contained samples from an incubation (RT for 30min, in ATP-G-Buffer) of G:A_2 and DNaseI at a 1:2 molar ratio (3.0μM G:A_2; 6.0μM DNaseI). (The incubation mix contained additional DNaseI to account for the 3 – 15% of inactive protein in that preparation).

Second dimension analysis, by SDS-PAGE, of the "GA_2:D_2" lane was carried out. As can be seen from the gel in fig. 3.17(B) the shifted band contains all three proteins; gelsolin, actin and DNaseI. The stoichiometry of these three proteins was confirmed as being G:A_2:D_2, by densiometric scanning of stained SDS-polyacrylamide gels, with pure samples of each protein included as internal reference standards. Table 3.5 summarises the results from four similar experiments. Our data indicate the formation of a complex with a stoichiometry of **G:A_2:D_2**.

3.3.2.3 Fluorescence enhancement analysis of "GA_2:D_2" complex formation

Several sets of experiments were conducted to investigate the binding of pre-purified $actin_{nbd}$:DNaseI complex to gelsolin in the presence of Ca^{2+} (here after referred to as A_{nbd}:D). Experiments utilising the fluorescence enhancement of the binding of NBD-Actin to gelsolin were designed to test the formation of the putative **G:(A:D)$_2$** complex. They also exploit the fact that the presence of DNaseI bound to the pointed-end of an NBD-Actin monomer is spectrally "silent" (see fig. 3.15). Experiments were carried out in ATP-G-Buffer, containing 0.2mM $CaCl_2$ or 0.6mM EGTA; 0.2mM $CaCl_2$; 0.2mM $MgCl_2$ or in F-buffer additionally containing 0.2mM $CaCl_2$ or 0.6mM EGTA; 0.2mM $CaCl_2$.

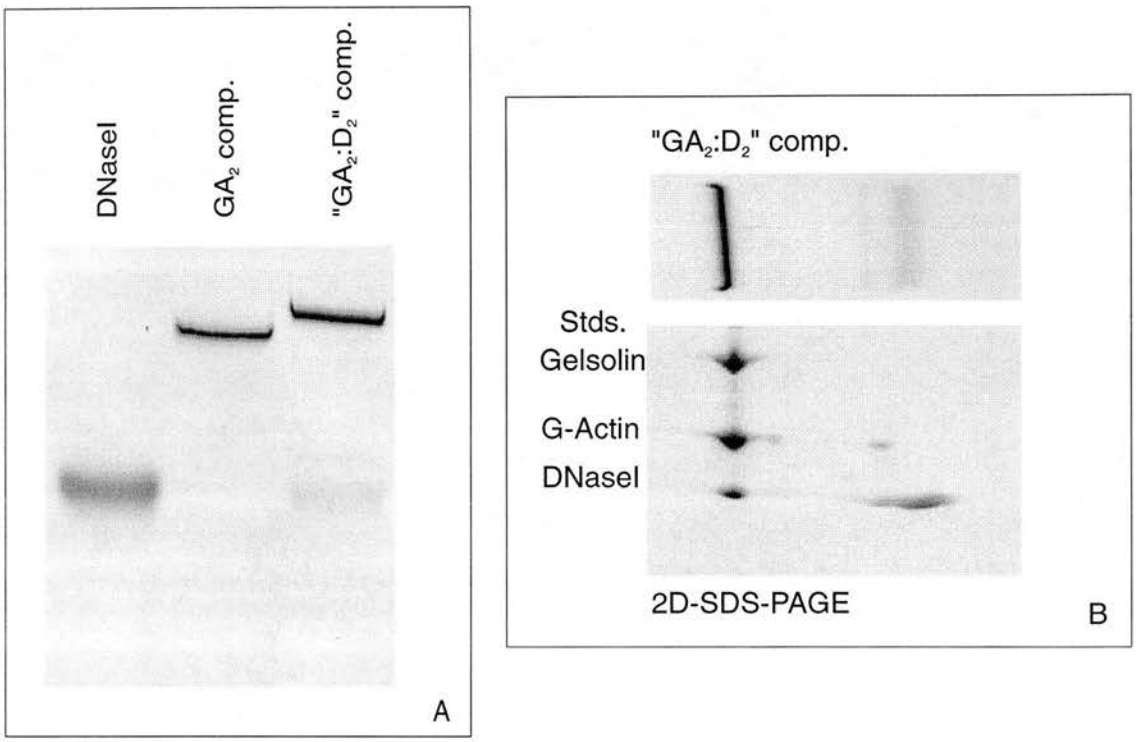

Fig. 3.17. ***Formation of a complex between the G:A_2 ternary complex and DNaseI as analysed by non-denaturing PAGE.*** (A) Native gel showing the electrophoretic mobilities of DNaseI, G:A_2 and the "GA_2:D_2" complex. (B) SDS-PAGE analysis, in a second dimension, of the components of the protein bands in A. "GA_2:D_2" is the complex formed from an incubation (30min at RT) of pre-purified G:A_2 ternary complex and DNaseI in molar ratio of 1:2 (3.0μM G:A_2 and 6.0μM DNaseI) in ATP-G-Buffer. Standard migration positions are indicated beside the gel. Gel running conditions: 0.2mM $CaCl_2$; 0.2mM ATP; 0.5mM DTT was used for G:A_2 and "GA_2:D_2"; 0.2mM ATP; 0.5mM DTT was used for DNaseI. (SDS-PAGE and non-denaturing PAGE were performed as described in methods).

Fig. 3.18(A) shows the titration of pre-formed and pre-purified A_{nbd}:D complex in the absence or presence of a constant amount of gelsolin, 80nM, in 0.2mM $CaCl_2$. (Similarly to those experiments carried out with gelsolin and NBD-Actin alone, each data point represents a separate reaction mixture and not serial additions of titrant). Fig. 3.18(B) shows the difference between the two fluorescence profiles in A. The difference between the titration profiles is again due to the enhancement in fluorescence intensity upon complex formation. Fig. 3.18(B) clearly indicates that the fluorescence rises linearly as the concentration of A_{nbd}:D increases, up to an inflexion point. At this point there is an abrupt transition to a plateau level. The position of this inflexion point occurs at a stoichiometry of 1:2 for gelsolin / A_{nbd}:D respectively. Mean values for the stoichiometry at the inflexion point are 1:2.12 (± 0.17 SD, n=7) apparently indicating the formation of a G:(A_{nbd}:D)$_2$ complex.

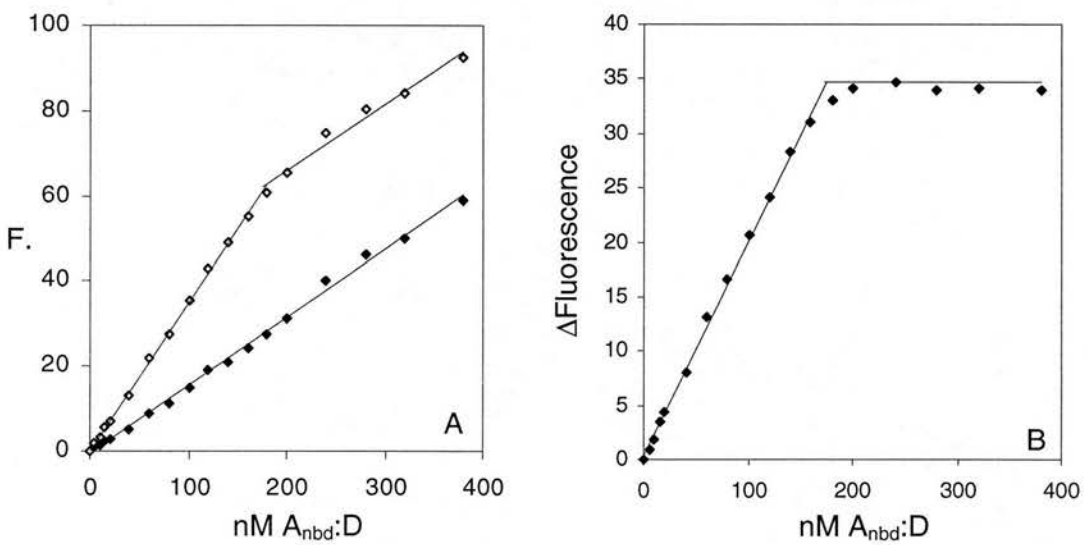

Fig. 3.18. ***Fluorescence titration at constant gelsolin concentration with A_{nbd}:D in 0.2mM $CaCl_2$ (ATP-G-Buffer).*** (A) *Closed squares* indicate the fluorescence intensity of A_{nbd}:D alone; *open squares* indicate the fluorescence intensity of *A_{nbd}:D* with added 80nM gelsolin. (B) Difference between fluorescence intensities in (A). The solid line is a linear regression and gives maximum enhancement at 2.2 (A_{nbd}:D):gelsolin. (λex=475nm, λem=520nm, 5nm slit for both). Titration was performed as described in methods.

The assumption here is that, analogous to the situation of complex formation between gelsolin and NBD-Actin alone, both binding sites on gelsolin contribute equally to the fluorescence signal enhancement of A_{nbd}:D. Fig. 3.19 shows the emission spectra of the A_{nbd}:D binary complex alone (a different preparation of NBD-Actin to that used in fig. 3.11) and those with the addition of gelsolin, in the presence or absence of Ca^{2+}. Very similar levels of enhancement were observed for

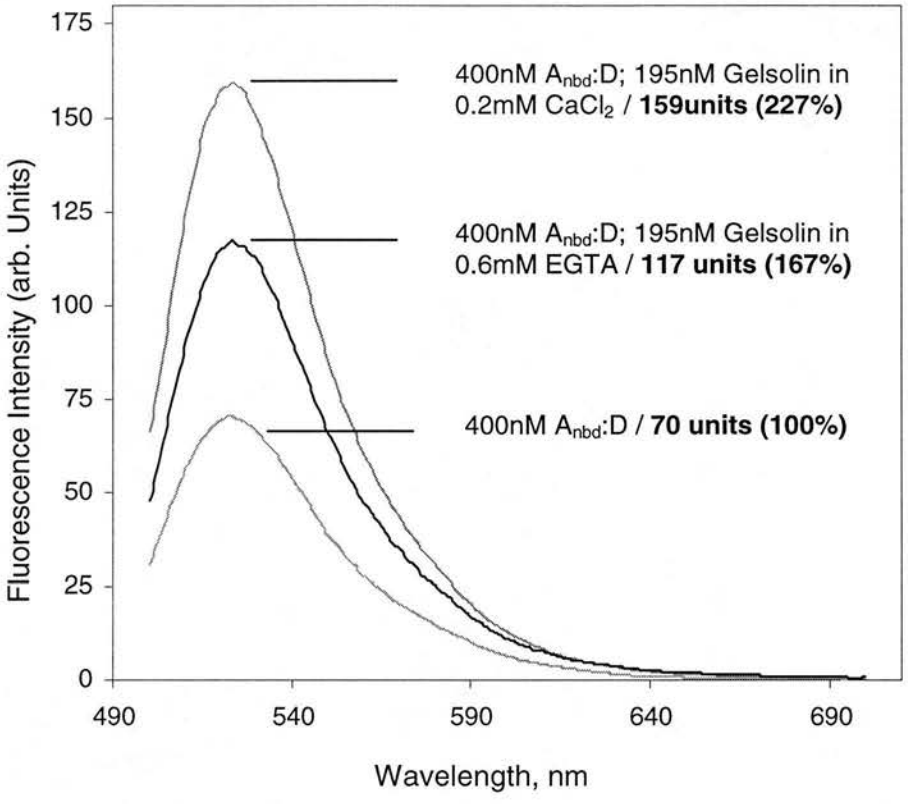

Fig. 3.19. ***The effect on the emission spectra of A_{nbd}:D upon complex formation with gelsolin.*** The emission spectra (the excitation wavelength was 475nm, with a 5nm slit width for both excitation and emission) of 400nM *A_{nbd}:D*, in 0.2mM $CaCl_2$, and those with added 195nM gelsolin, in the presence or absence of calcium are shown. (Molar ratio is ~ 2:1 for *(A_{nbd}:D)* and gelsolin, respectively). The equal contribution by each actin-binding site on gelsolin to the fluorescence enhancement is illustrated by the two equivalent step-wise increases in fluorescence. Proteins were mixed together, at the appropriated concentrations, in the calcium-containing buffer and incubated at RT for 30min. Then the emission spectra measured. For experiments in EGTA the sample was incubated at RT for 5min, in the calcium-containing buffer, and $MgCl_2$ and EGTA were then added to the appropriate concentrations. Solution conditions for calcium containing buffers: *ATP-G-Buffer*, 5mM Tris, pH8.0; 0.5mM DTT; 0.2mM ATP; 0.2mM $CaCl_2$; 1.0mM NaN_3. Solution conditions for EGTA containing buffers: 5mM Tris, pH8.0; 0.5mM DTT; 0.2mM ATP; 0.2mM $CaCl_2$; 1.0mM NaN_3; 0.2mM $MgCl_2$; 0.6mM EGTA.

complex formation between gelsolin and the A_{nbd}:D complex. An enhancement of ~ 60 – 70% was seen in the presence of gelsolin and EGTA, over that observed for A_{nbd}:D alone. A further ~ 60 – 70% enhancement was observed in 0.2mM Ca^{2+}.

Similar results were obtained in ATP-F-Buffer (data not shown). The problem of fluorescent enhancement due to spurious NBD-Actin polymerisation is negated by the presence of DNaseI, bound to the pointed-ends of the actin monomers in the A:D binary complex. This prevents any association between the monomers, thus preventing polymerisation.

Binding of A_{nbd}:D to each site on gelsolin contributes equally to the fluorescence enhancement signal observed upon complex formation. The levels of enhancement are very similar to those obtained with NBD-actin alone. The results from several binding experiments, analysing the interaction between gelsolin and NBD-Actin were compared to those obtained with the A_{nbd}:D binary complex; of which different preparations of NBD-Actin, with different degrees of labelling (~ 40 – 70%) were used. It was found that the two sets were not significantly different from each other, ($P>0.50$). Compare the emission spectra in figs. 3.11 and 3.19.

Fig. 3.20 shows the fluorescence titration measurements from a continuous variation experiment in 0.2mM $CaCl_2$ (see methods for details). The total protein concentration was maintained at 400nM and both gelsolin and the A_{nbd}:D complex were varied in a continuous fashion. The fluorescence again shows a very sharp discontinuity at a molar ratio that corresponds to the stoichiometry of the component proteins within the resultant complex. The inflexion point has a mean molar ratio of 1:2.0 (± 0.16 SD, n=5) for gelsolin:(A_{nbd}:D) binary complex, respectively. A comparison of the levels of fluorescence enhancement and the range of stoichiometries for the complex components (at the inflection point), in experiments using A_{nbd}:D or NBD-Actin alone, indicated no statistically significant differences between them ($P>0.30$).

Similar experiments carried out in ATP-F-Buffer; 0.2mM $CaCl_2$ produced very similar results (data not shown).

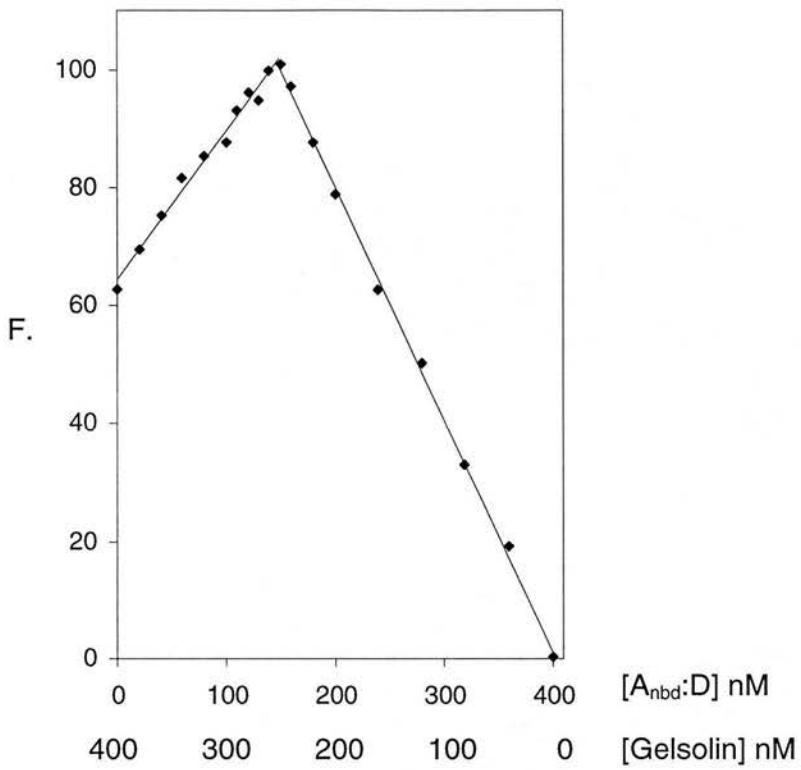

Fig. 3.20. ***Fluorescence titration at constant protein concentration with continuous variation of both gelsolin and A_{nbd}:D.*** Experiment using 400nM total protein in 0.2mM $CaCl_2$ (ATP-G-Buffer) with the transition point at 146nM gelsolin and 254nM A_{nbd}:D (Solid line is a linear regression; A_{nbd}:D/gelsolin = 1.8). (Titration was performed as described in methods).

3.3.3 Summary

The data described in the preceding sections are consistent with the spatial orientation of the two actin monomers in the G:A_2 ternary complex being similar, but not identical, to the orientation of those monomers at the barbed-end of a filament. Our results provide good evidence for the formation of a larger complex between the **G:A_2** ternary complex and ***two*** DNaseI molecules. The association most likely occurs via binding of the two DNaseI molecules to the pointed-ends of the actin monomers. Gelsolin also binds ***two*** A:D binary complexes (in Ca^{2+}). The interaction of A:D with gelsolin, resulting in the formation of the **G:(A:D)$_2$** complex, appears to take place via a similar two-stage binding equilibrium, analogous to that for the

formation of $G:A_2$, with similar affinities (see section 3.5 for details). No experimental evidence was found for an interaction between gelsolin and DNaseI. Data from size-exclusion experiments and non-denaturing gels of 1:1 molar ratio incubations of the two proteins (gelsolin and DNaseI), in a variety of conditions, always produced two distinct and separate populations that corresponded to the two individual uncomplexed proteins (data not shown).

3.4 Analysis of the effect of DNaseI on actin monomer binding to the G:A binary complex

3.4.1 Overview

The results described in the preceding sections appear to indicate that the geometrical arrangement of the two actin monomers in the G:A_2 ternary complex was similar, but not identical, to the orientation of those monomers at the barbed-end of a filament. However, the binding of DNaseI to the pointed-end of one monomer may have a perturbatory effect on the geometrical arrangement of the two actin monomers within the G:A_2 ternary complex. The actin monomers within G:A_2 may normally be held in an F-like conformation, but the high-affinity association between DNaseI and the pointed-end of one of the actin monomer causes a conformational change within the structure of that actin (with respect to uncomplexed actin) that results in a change in the binding interactions with other monomer and/or with gelsolin. I.e. a DNaseI induced disruption to interactions between the actin monomers and/or between gelsolin, may cause a loss of the normal F-like conformation of the actin monomers within G:A_2, and enable the binding of a second DNaseI molecule

We have performed fluorescence enhancement experiments to analyse the interaction between the G:A binary complex and NBD-Actin and also the interaction between G:A binary complex and the A_{nbd}:D complex, in the presence of Ca^{2+}. The results suggest that the equilibrium dissociation constant of A:D binary complex binding to G:A (at the EGTA labile site - G4 - on gelsolin) is equivalent to that of G-Actin alone binding to the G:A binary complex. Our data are consistent with the presence of DNaseI having no effect on the interaction of gelsolin and actin.

3.4.2 The presence of DNaseI has no apparent effect on the dissociation constant of actin monomer binding to the G:A binary complex

We have analysed the binding of NBD-Actin and A_{nbd}:D to the G:A binary complex (in Ca^{2+}) and determined the K_d for each reaction. We have used an alternative

protocol for the purification of G:A binary complex to overcome problem of incomplete dissociation of $G:A_2$, upon addition of EGTA, to give G:A and free G-Actin (see section 3.2.2.1).

3.4.2.1 DNaseI-agarose column purification of G:A binary complex

The protocol used to purify G:A binary complex was based on that described by Selve and Wegner (1986). It utilises the tight binding affinity of DNaseI for the pointed-ends of actin monomers (K_d ~ 0.1nM), and dissociation of the $G:A_2$ ternary complex to give G:A and free G-Actin, upon the addition of excess EGTA (see methods for protocol details).

DNaseI was first covalently coupled to a sepharose matrix (via reaction with NHS-Activated Sepharose 4® Pharmacia). This DNaseI-sepharose column was then equilibrated with G-Actin monomer, in ATP-G-Buffer, resulting in the formation of immobilised A:D binary complex.

EGTA (0.6mM EGTA in the presence of 0.2mM $MgCl_2$) was added to a preparation of pre-formed and pre-purified $G:A_2$ ternary complex. Following incubation (1hr at 4°C) this mixture was subjected to size-exclusion chromatography on an S200 column, pre-equilibrated in ATP-G-Buffer; 0.6mM EGTA; 0.2mM $MgCl_2$. The fractions that contained G:A binary complex were pooled and $CaCl_2$ was then added to 1.0mM (in excess over EGTA), thus enabling G:A complex competent to rebind to monomeric actin. This mixture was then loaded onto the DNaseI-Actin-sepharose column under depolymerising conditions. The G:A complex, in the presence of Ca^{2+}, rebinds to the actin monomers complexed 1:1 with DNaseI on the column, to give immobilised $G:A_2:D$ complexes. Specific elution of essentially only G:A binary complex was achieved with a wash of 5mM EGTA in ATP-G-Buffer (in the presence of 1.0mM $CaCl_2$; 1.0mM $MgCl_2$). This protocol gives a much more homogeneous population of G:A (~ 95%) than gel-filtration of $G:A_2$ in the presence of EGTA.

3.4.2.2 Binding of NBD-Actin by the G:A binary complex, in the presence of calcium

Binding of NBD-Actin to G:A produces a fluorescence enhancement of 60 ~ 70% at saturation (see fig. 3.11 and Weeds et al, 1986; Way et al, 1989; Pope et al, 1997). Fig. 3.21 shows the titration of a constant amount of NBD-Actin (10nM) with G:A binary complex (purified as described). The level of enhancement in the fluorescence signal is directly related to the amount of $G:AA_{nbd}$ ternary complex formed. A non-linear least squares fit of the data gave an apparent K_d of ~ 38nM for this interaction ($G:A + NBD\text{-}Actin \leftrightarrow G:AA_{nbd}$).

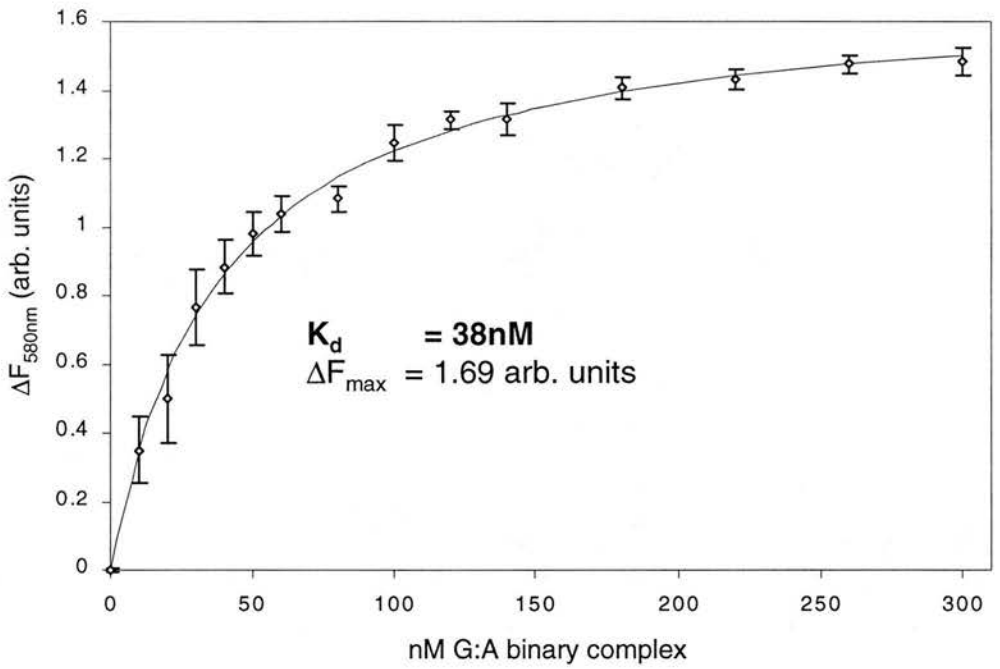

Fig. 3.21. ***Binding of NBD-Actin to the G:A binary complex.*** Fluorescence titration of G:A binary complex against a constant amount of NBD-Actin (10nM), in the presence of 0.2mM $CaCl_2$. The solid line is a non-linear least squares fit of the equation $\Delta F = \Delta F_{max}*[G:A]/([G:A]+K_d)$. The apparent K_d for the interaction ~ 38nM (mean K_d ~ 39nM ± 6 SD, n=3), with a ΔF_{max} ~ 1.69 arbitrary units, (R = 0.997). Titration was performed by adding increasing amounts of G:A binary complex, in ATP-G-Buffer, to 10nM of NBD-Actin in the same buffer, in a total volume of 500µl. Following a 1hr incubation, at 20°C in the dark, the fluorescence intensity was measured. The fluorescence values shown are the mean values calculated after measurement for 90sec, (at 20°C), with a 1sec reading interval. The error bars show 1 SD, calculated from three separate experiments. The excitation wavelength was 475nm, the emission wavelength was 520nm, with a 5nm slit width for both. The level of fluorescence enhancement is directly proportional to the amount of NBD-Actin bound (i.e. the amount of $G:AA_{nbd}$ ternary complex). The fluorescence intensity value of 10nM NBD-Actin was subtracted from each sample

Similar experiments were performed to analyse the binding of A_{nbd}:D to G:A binary complex. Fig. 3.22 shows the titration of a constant amount of A_{nbd}:D (10nM) with G:A binary complex. Similarly to fig. 3.21, the level of fluorescence enhancement is directly related to the amount of GA:(A_{nbd}:D) complex formed. A non-linear least squares fit of the data gave an apparent K_d of ~ 49nM or this binding reaction {G:A + A_{nbd}:D $\leftrightarrow$ GA:(A_{nbd}:D)}.

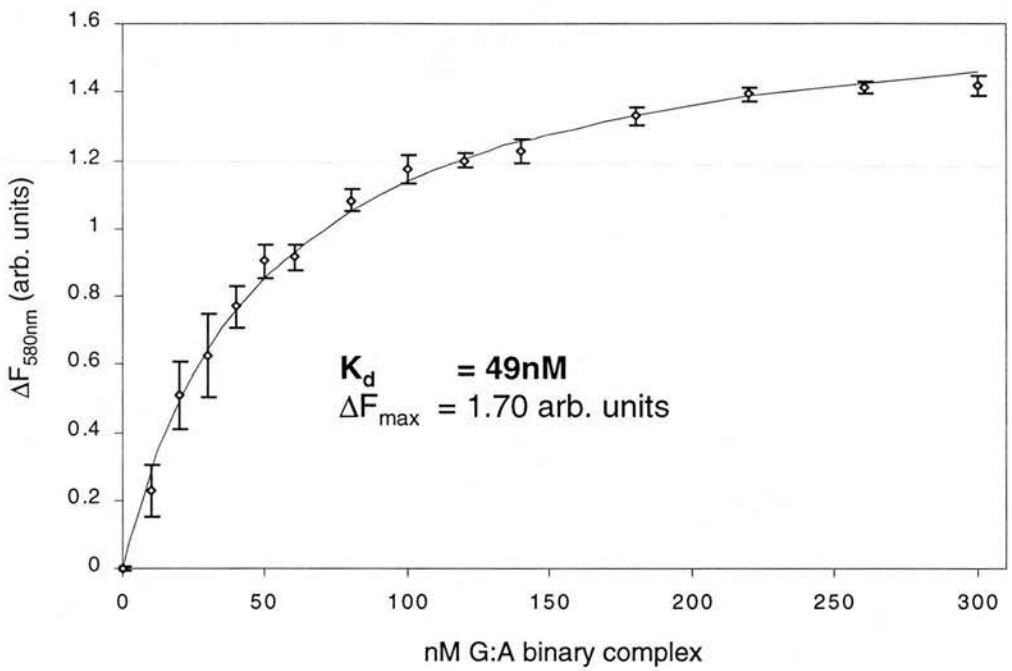

Fig. 3.22. ***Binding of A_{nbd}:D to the G:A binary complex.*** Fluorescence titration of G:A binary complex against a constant amount of A_{nbd}:D (10nM), in the presence of 0.2mM $CaCl_2$. The solid line is a non-linear least squares fit of the equation $\Delta F = \Delta F_{max}*[G:A]/([G:A]+K_d)$. The apparent K_d for the interaction ~ 49nM (mean K_d ~ 50nM ± 6.5 SD, n=3), with a ΔF_{max}~ 1.70 arbitrary units, (R = 0.998). Titration was performed by adding increasing amounts of G:A binary complex, in ATP-G-Buffer, to 10nM of A_{nbd}:D in the same buffer, in a total volume of 500µl. Following a 1hr incubation, at 20°C in the dark, the fluorescence intensity was measured. The fluorescence values shown are the mean values calculated after measurement for 90sec, (at 20°C), with a 1sec reading interval. The error bars show 1 SD, calculated from three separate experiments. The excitation wavelength was 475nm, the emission wavelength was 520nm, with a 5nm slit width for both. The level of fluorescence enhancement is directly proportional to the amount of A_{nbd}:D bound (i.e. the amount of G:A(A_{nbd}:D) complex). The fluorescence intensity value of 10nM A_{nbd}:D was subtracted from each sample

The mean value for the dissociation constant for NBD-Actin binding to G:A was 38nM (± 6 SD, n=3) while that for A_{nbd}:D binding to G:A was 50nM (± 6.5 SD, n=3). A K_d of ~ 39nM for the binding of actin to the EGTA labile site on gelsolin (G4) is in agreement with the ~ 25nM values reported by others (Bryan, 1988; Way et al, 1989; Schoepper and Wegner, 1991; Pope et al, 1995).

The two K_d values show no significant difference from each other ($P>0.15$) and suggests that the equilibrium dissociation constants are equivalent. The maximal level of fluorescence enhancement reached at saturation was virtually identical for both systems; ΔF_{max} ~ 1.69 arbitrary units for NBD-Actin compared to a ΔF_{max} ~ 1.70 arbitrary units for A_{nbd}:D. The extent of enhancement was ~ 60 – 80% over that seen for NBD-Actin and A_{nbd}:D, alone in the absence of G:A binary complex. This data is in good agreement with that reported in section 3.3.2.3.

The apparent equivalence of the two K_d values for the binding of G-Actin or A:D by gelsolin is consistent with DNaseI having no effect on the way G:A binary complex interacts with actin monomers.

3.5 Discussion

3.5.1 DNaseI purification protocol

DNaseI is a highly toxic endonuclease, and as a result does not lend itself to high levels of cytoplasmic expression in *E. coli.* However, the development of an inactive mutant (H134Q; specific activity of the mutant is ~ 0.001% of the native enzyme; Worrall and Connolly, 1990) led to subsequent high level expression in *E. coli* (Doherty et al, 1993). Histidine 134 is essential to enzymatic activity and it plays an integral part in the proposed DNA cleavage mechanism (Price et al, 1969; Suck and Oefner, 1986). Several protocols for the purification of DNaseI have been published (Worrall and Connolly, 1990) but we were unable to achieve purity of >65% when utilising these methods.

Commercially available DNaseI (e.g. Sigma, Worthington, Fluka) has trace contaminants of the proteolytic enzyme Chymotrypsin. Such preparations are commonly pre-purified over hydroxyapatite resins before use, in attempts to avoid further potential problems with protease degradation. However, this procedure does not always remove all the protease activity and the subsequent use of DNaseI in actin:DNaseI binary complex formation and other experiments and assays involving proteolytic sensitive proteins - e.g. gelsolin and actin - often still creates problems with degradation. A further advantage of working with the recombinant protein is that it is always available and cheaper than commercial preparations.

We have established a novel protocol for the purification of the recombinant mutant DNaseI/H134Q, from JM105 *E. coli.* This protocol takes advantage of an apparent specific interaction between the DNaseI enzyme and the ligand Cibacron F3GA Blue. We achieved elution from the Cibacron F3GA Blue resin with an ATP gradient from 1mM – 10mM. Elution could also be achieved with NaCl gradients of 0.15M – 0.5M; however the purity of the protein achieved by salt elution was ~ 85%.

The difference in the ionic strengths between the concentration of ATP (~ 6mM), and the equivalent NaCl concentrations (~ 0.2 - 0.3M) needed to achieve elution, coupled with the extent of partitioning from major contaminants, suggests an apparent specific interaction between DNaseI and the resin. This affinity is possibly not a surprise as the highly conjugated Cibacron F3GA ligand bears structural similarities to the co-factors NAD^+, $NADH^+$ and adenyl containing co-factors and ligands. Bovine pancreatic deoxyribonuclease I (DNaseI) is a glycoprotein that binds to, and subsequently cleaves double stranded DNA to yield 5'-oligonucleotides (Moore, 1981). DNaseI is reported to interact with the DNA helix across the minor groove in a sequence dependent manner (Suck et al, 1984), and its three-dimensional structure, in complex with a fragment of DNA, has been solved to atomic resolution (Lahm and Suck, 1991). The enzyme may be binding to the resin via some specific interaction with the solid phase ligand that might resemble its native DNA substrate.

We routinely obtained purity of ≥95% for the recombinant mutant DNaseI from cultures of JM105 *E. coli* using this protocol and typical yields were 10 – 15mg.L^{-1} of original bacterial cell culture.

3.5.2 1.0M Tris, pH 8.0; ATP-G-Buffer actin extraction and purification protocol

We have developed an alternative method for the extraction and purification of G-actin, altered from the widely used Spudich and Watt protocol, (Spudich and Watt, 1971). Actin was extracted from rabbit muscle acetone powder, in monomeric form, in a low ionic strength buffer (ATP-G-Buffer). Polymerisation was then initiated by addition of KCl to 0.8M followed by very high-speed centrifugation. This pellets essentially *only* actin in F-form. The pellet was then homogenised in a 1M Tris, pH 8.0 buffer (Pinder et al, 1995). This procedure induces rapid depolymerisation of the actin filament, possibly as a result of the Tris acting as a chaotropic agent. Amine salts have been reported to be effective dissociating agents for protein complexes (Keen, 1979). This high Tris concentration buffer seems to perform this function without denaturing the G-actin. 1.0M Tris, pH 8.0; ATP-G-Buffer also allowed us to store G-actin for over 4 months in a stable and active form (compared to 2 –3 weeks

for conventional ATP-G-Buffer). Details of the protocol and the assay of the viability of the buffer for long term storage are given in the methods and appendix A, respectively.

3.5.3 Confirming the formation of the G:A, G:A_2 and A:D complexes

We have analysed the formation of complexes between actin and gelsolin and that between actin and DNaseI. Conformation of the existence of these various complexes was performed by a variety of techniques: gel-filtration, non-denaturing PAGE and by NBD-Actin fluorescence enhancement experiments. Additionally, the stoichiometry of the complexes was verified by gel densitometry.

The experiments reported in the preceding sections show that gelsolin (recombinant expressed human cytoplasmic gelsolin), binds to monomeric actin. No complex formation was observed in the absence of calcium ions (i.e. at less than μM concentrations). G:A_2 ternary complex was formed in the presence of Ca^{2+} and a binary complex, G:A, was formed in EGTA (after first activating gelsolin by the addition of 0.2mM $CaCl_2$, followed by subsequent chelation by EGTA). Chelation of Ca^{2+} results in the dissociation of the actin monomer from the G4 binding site on gelsolin. This G4 binding site is totally calcium dependent. (The removal of calcium only reduces the affinity of the binding site in G1 for actin. K_d in Ca^{2+} ~ 5pM; K_d in the absence of Ca^{2+} ~ 1 – 2nM; Bryan, 1988).

Gel-filtration illustrated that even in the presence of a molar excess of gelsolin (molar ratios of up to 1:2 for actin:gelsolin), the ternary complex predominates in Ca^{2+}. Non-denaturing PAGE analysis of complex formation also confirmed these results, indicating the preferential formation of G:A_2 ternary complex, even in the presence of a molar excess gelsolin (up to 1:2). Weeds and co-workers (Weeds et al, 1986), have reported very similar results and suggested that the two actin-binding sites were coupled in strong co-operative way. The data we report here are in agreement with this

Our data also showed that the fluorescence increment per NBD-Actin monomer bound is approximately the same. Formation of $G:A_2$, in Ca^{2+}, produces an enhancement of ~ 120% (over that observed for NBD-Actin alone) in contrast to the ~ 60 – 70% enhancement observed upon formation of the binary complex, in EGTA, (see fig. 3.11). Similar conclusions can be drawn from the continuous variation experiments. The levels of enhancement upon ternary complex formation, in Ca^{2+}, are approximately twice those seen upon G:A formation in EGTA, see figs. 3.12(A) and (B). Furthermore, the shape of the titration curve and the positions of the sharp inflection point in these experiments, indicates a strong coupling of both sites with tight binding (K_d at least in the nM range, Weeds et al, 1986), and an equal contribution to the enhancement by both binding sites. (See Blake et al, 1967; Pinder and Gratzer, 1982; Weeds et al, 1986, for details of the interpretation of data from such experiments).

Our experiments have also confirmed the formation and stoichiometry of the tight binary actin:DNaseI complex. This complex forms in the presence or absence of Ca^{2+}, with no apparent difference (Pinder and Gratzer, 1982; Weber et al, 1994). However, the addition of EGTA to A:D that had been pre-formed in the presence of Ca^{2+} occasionally resulted in a partial dissociation of the complex. This was observed as small amounts of free actin and DNaseI appearing at the corresponding retention volumes and electrophoretic migration positions for uncomplexed proteins, during size-exclusion and native-PAGE experiments, respectively.

A possible explanation for this observation may be due to the chelation of several Ca^{2+} ions (by EGTA), bound to the DNaseI molecule at two distinct binding-sites. One Ca^{2+} ion is bound at the catalytic site of the enzyme, but the other is found at a site between the two major domains of the molecule (Suck and Oefner, 1986). Binding of calcium at this second site confers a degree of protection against proteolysis; cleavage occurs within a loop that lies between the two domains of DNaseI that form the DNA binding cleft (Suck and Oefner, 1986). Reconstitution of native enzyme activity, in samples of protein cleaved at this site, is possible by the addition of Ca^{2+}.

The removal of this Ca^{2+} from DNaseI in the A:D complex may possibly result in a local conformational change within the DNaseI molecule that then induces a loss of affinity for actin. This phenomenon gave some anomalous results, especially on native gels, during the analysis of the formation of the **G:A_2:D_2** and **G:(A:D)$_2$** complexes but the occurrence was limited and had little effect on our data.

The spectral "silence" of DNaseI bound to NBD-Actin is in agreement with results published by Detmers et al (1981). The protocol used to couple the NBD-probe to G-Actin involves the linkage of NBD to Lys-373, after the Cys-374 residue has been blocked by the action of N-ethylmaleimide (see methods for details). A decrease (maximally 5%) in the fluorescence signal of NBD-Actin complexed with DNaseI (compared to uncomplexed NBD-Actin) is sometimes observed. However, differences in the degree of NBD-labelling within a given preparation of NBD-Actin (~ 40 – 70%) and some spectral interference by small amounts of NBD-Cys-374, (NBD coupled to Cys-374 has a slightly different excitation and emission spectral characteristics than that of NBD-Lys-373), mean this decrease in signal is not always observed (Detmers et al, 1981).

Lys-373 lies at the surface of sub-domain I on the actin monomer (Kabsch et al, 1990). The fluorescence enhancement observed upon the binding of gelsolin to NBD-Actin, is probably due to changes in the polar environment around the NBD probe. The gelsolin:actin binding interaction takes place via a site located between sub-domains I and III of the actin monomer (McLaughlin et al, 1993). This interaction likely cause marked local changes in the solvent environment around the NBD-Probe that lead to enhancement of the fluorescence signal. In contrast to this, the binding of DNaseI takes place via a loop located at the edge of sub-domain II, see fig. 1.10 (Kabsch et al, 1990). This region is far from the site of coupling for NBD, ~ 50Å. There are essentially no changes in the structure of the actin monomer, upon 1:1 complex formation with DNaseI that would affect the structural and/or solvent environment around the NBD probe. This is consistent with the crystallographic data, which suggests that DNaseI does not significantly alter the actin conformation. The

actin monomer has the same structure in the DNaseI crystal (Kabsch et al, 1990) as in the crystal with G1 of gelsolin (McLaughlin et al, 1993), see figs. 1.8 and 1.10.

3.5.4 Decoration of $G:A_2$ with DNaseI suggests a non-filamentous disposition for the actin monomers

The results from our size-exclusion experiments (performed under polymerising conditions) in which DNaseI was added to pre-formed $G:A_2$ (at a molar ratio of 2:1, respectively) showed the formation of a significantly larger complex (relative to $G:A_2$) with an apparent Mr. of 251kDa. The stoichiometry of this larger complex was shown to be $\mathbf{G:A_2:D_2}$. Similarly, in experiments in which we added pre-formed A:D to gelsolin, in the presence of Ca^{2+} (0.2mM $CaCl_2$), a larger complex with the same apparent Mr. (251kDa), and stoichiometry, $\mathbf{G:(A:D)_2}$, was formed. Similar results were obtained from non-denaturing gel experiments.

The fluorescence enhancement data also support the formation of the $\mathbf{G:(A:D)_2}$ complex. Titration of a constant amount of gelsolin with A_{nbd}:D complex, in the presence of Ca^{2+} (0.2mM $CaCl_2$), indicated the formation of a tight complex between gelsolin and A_{nbd}:D, with a stoichiometry of $\mathbf{G:(A_{nbd}:D)_2}$. Similarly, the continuous variation fluorescence titration experiments with gelsolin with A_{nbd}:D indicated the formation of a complex with a stoichiometry of $\mathbf{G:(A_{nbd}:D)_2}$. We found no significant difference between these titration curves and those obtained for the binding to gelsolin of NBD-Actin alone. (Compare the data in figs. 3.10, 3.11 and 3.12 with 3.18, 3.19 and 3.20).

The gel-filtration and native–PAGE experiments seem to illustrate a similar co-operative binding of the A:D binary complex by gelsolin, (analogous to the formation of $G:A_2$ ternary complex). Even in the presence of a molar excess of gelsolin (molar ratios of up to 1:2 for (A:D):gelsolin), we observed the formation of a complex with an apparent Mr. of 251kDa and a stoichiometry of $\mathbf{G:(A:D)_2}$. Non-denaturing PAGE analysis of complex formation also confirmed this result. It seems that the formation of the $\mathbf{G:(A:D)_2}$ complex predominates (up to a molar ratio of 1:2,

for A:D and gelsolin, respectively) in Ca^{2+} (0.2mM $CaCl_2$). This may imply that gelsolin binds A:D by a similar method to the way it binds actin monomers to form the G:A_2 ternary complex. i.e. there is a strong positive coupling between both sites binding sites on gelsolin, with tight binding (K_d at least in the nM range) at both (Weeds et al, 1986; Schoepper and Wegner, 1991). This suggests that the presence of DNaseI, bound to the pointed-ends of the actin monomers in the A:D binary complex, may have little effect on the interaction between the actin monomers and gelsolin.

Our data from fluorescence enhancement experiments analysing the interaction between the G:A binary complex and NBD-Actin and the interaction between G:A binary complex and the A_{nbd}:D complex (in the presence of Ca^{2+}) further support this notion. The mean value for the dissociation constant obtained for NBD-Actin binding to G:A was 38nM (± 6 SD, n = 3) while that for A_{nbd}:D binding to G:A was 50nM (± 6.5 SD, n = 3). A K_d of ~ 39nM for the binding of actin to the EGTA labile site on gelsolin (G4) is in good agreement with the ~ 25nM values reported by others (Bryan et al, 1988; Way et al, 1989; Schoepper and Wegner, 1991; Pope et al, 1995).

The dissociation constants show no significant difference from each other ($P>0.15$) suggesting that the dissociation constants are equivalent. The final level of fluorescence enhancement reached at saturation was virtually identical for both systems. A ΔF_{max} of ~ 1.69 arbitrary units for NBD-Actin compared to a ΔF_{max} of ~ 1.70 arbitrary units for A_{nbd}:D, and the extent of enhancement was ~ 60 – 80% over that observed for NBD-Actin or A_{nbd}:D, in the absence of G:A binary complex. This data is in good agreement with that reported in section 3.3.2.3.

The apparent equivalence of the two dissociation constants for the binding of G-Actin or A:D by gelsolin (at the G4 binding site on gelsolin), is consistent with the presence of DNaseI (bound at the pointed-end of the actin monomer) having no effect on the way G:A binary complex interacts with actin monomers.

The formation of **$G:A_2:(D)_2$** or **$G:(A:D)_2$** is consistent with the actin monomers within $G:A_2$ having a non-filamentous disposition.

Fig. 3.23 illustrates various possibilities for the disposition of the actin monomers in $G:A_2$. If $G:A_2$ has a conformation like that described for condition (A), *F-conformation* in fig. 3.23, we would not have expected to be able to bind ***two*** DNaseI molecules to the exposed pointed-ends of the actin monomers in the ternary complex. This conformation, where the actin monomers are oriented as described in the Holmes filament model (Holmes et al, 1990), prevents the binding of two DNaseI molecules due to a steric clash (Weber et al, 1994). However, our results clearly indicate the formation of a complex between $G:A_2$ and DNaseI with a stoichiometry of $(G:A_2):D_2$ and also the formation of a complex between gelsolin and two A:D binary complexes, with a stoichiometry of $G:(A:D)_2$. i.e. ***two*** DNaseI molecules can be bound to the actin monomers within the $G:A_2$ ternary complex.

Any shift in the spatial disposition of the actin monomers bound to gelsolin, due to the steric effects of DNaseI bound/binding at the pointed-ends (in relation to their disposition in $G:A_2$ without DNaseI bound), may produce changes in the fluorescence spectra of NBD-Actin. The fluorescence emission spectra and enhancement levels of the NBD moiety are very sensitive (significant shifts in the wavelength of maximum absorbance and/or differences in the levels of enhancement) to changes in the polar environment around the probe (Detmers et al, 1981; Way et al, 1989). However, our data showed that the fluorescence enhancement levels for either NBD-Actin alone or the A_{nbd}:D binary complex, binding to gelsolin, are very similar. There was also no significant difference between the fluorescence titration data for NBD-Actin alone binding to gelsolin, and that for A_{nbd}:D binding to gelsolin, (in 0.2mM $CaCl_2$). Furthermore, the dissociation constants for the binding of A:D or G-Actin alone, to G:A, are equivalent (50nM and 39nM, respectively).

This similarity may suggest that the binding of actin monomers by gelsolin takes place via the same equilibrium reaction scheme, whether the monomers are in

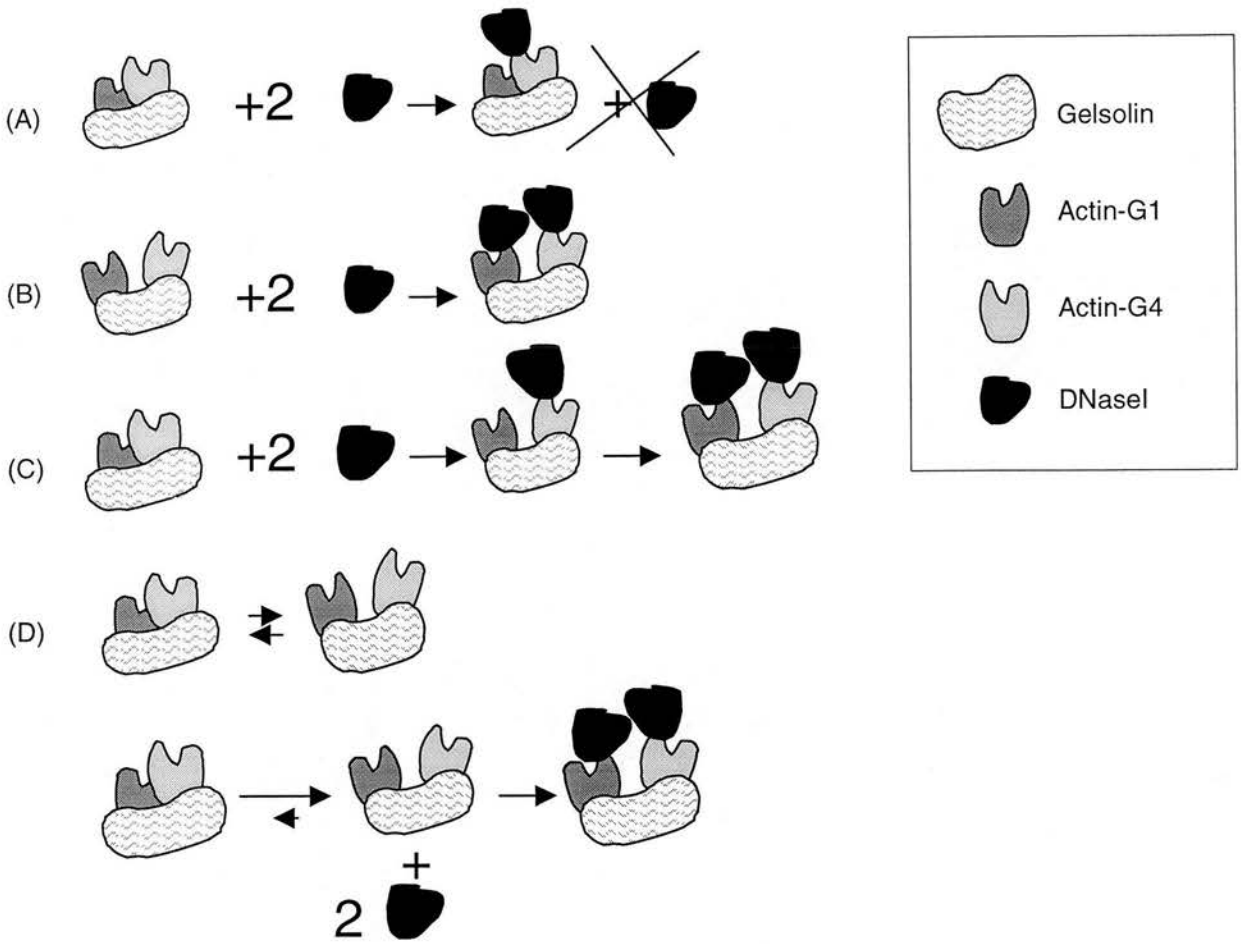

Fig. 3.23. ***Schematic diagram representing the possible conformational orientations of the actin monomers in G:A_2.*** (A) *F-Conformation*. The monomers have a spatial orientation like those at the barbed-end of the filament, as described by the Holmes filament model (Holmes et al, 1990). This conformation prevents the binding of two DNaseI molecules to the exposed pointed-ends, due a steric clash (Weber et al, 1994). (B) *Non-F-Conformation*. The actin monomers are held in a non-filamentous conformation, but in close proximity to each other, by gelsolin. In this orientation there are no steric constraints and two DNaseI molecules could bind to the pointed ends of the actin monomers. (C) *Perturbation.* The actin monomers are held in an F-like conformation. However, the binding of DNaseI to the pointed-end of one monomer disrupts the interaction between the two monomers and/or between gelsolin and the monomers, causing a loss of F-like conformation and enabling the binding of a second DNaseI molecule. This model suggests that the binding of DNaseI to an actin monomer results in a conformational change in the structure of that actin, with respect to uncomplexed actin, that results in a change in it's binding interactions with other monomers and gelsolin. Such a change results in the actin becoming non-viable for adoption of F-like conformation in the G:A_2 complex. (D) *Equilibrium*. In this case the G:A_2 ternary complex is in equilibrium between the two conformations in (A) and (B). The addition of DNaseI to G:A_2 may result in a shift of the equilibrium to favour the non filamentous conformation. The binding of two DNaseI molecules and the resulting steric interference between them, may force the G:A_2 complex to adopt a more open, non-filamentous conformation. Actin-G1; the tight binding actin monomer, on the G1 site on gelsolin. Actin-G4; the EGTA labile, actin monomer, on the G4 site on gelsolin.

complex with DNaseI or not, (analogous to that described below for ternary complex formation between gelsolin and actin). We are proposing that the presence of DNaseI does not impose any steric and/or kinetic constraints on the monomer association with gelsolin, due to the fact that the monomers are normally held in a *non-filamentous* conformation.

Formation of the $G:A_2$ ternary complex has been shown to have two distinct reactions. The binding of the second monomer is ~ 100 – 1000 fold faster than the first, upon activation of gelsolin with >μM levels of Ca^{2+}. $G + A \leftrightarrow G:A$. $k_+ \sim 10^4$ $M.s^{-1}$; $G:A + A \leftrightarrow G:A_2$, $k_+ \sim 2*10^7$ $M.s^{-1}$, $k_- \sim 0.02$ s^{-1} (Schoepper and Wegner, 1991). The kinetic parameters of the two reactions mean that the reverse reaction for the formation of G:A (K_d for G1 and actin is ~ 5pM) essentially does not occur and the concentration of G:A compared to that of $G:A_2$ is negligible. The fitting of kinetic parameters to fluorescence enhancement data, very similar to ours obtained in fig. 3.10, was best achieved by having two tight actin-binding sites (K_d ~ pM, and K_d ~ nM, for G1 and G4 respectively) with strong positive co-operatively between them (Weeds et al, 1986; Selve and Wegner, 1986; Bryan, 1988; Schoepper and Wegner, 1991). As there is no significant difference between the results obtained with NBD-Actin alone and those with A_{nbd}:D then, by analogy, we propose a similar binding scheme for the formation of $G:(A:D)_2$ (see fig. 3.24).

As ***two*** DNaseI molecules are bound to $G:A_2$, and as the formation of $G:(A:D)_2$ is apparently indistinguishable from the formation of $G:A_2$ (at least from our fluorescence enhancement data) we suggest that the actin monomers may be held in an open, non-filamentous conformation, but in *close* proximity to each other. This orientation implies that there may be no steric constraints on the binding of these two DNaseI molecules, such as is illustrated by condition (B) *Non-F-Conformation* in fig. 3. 23.

Our results may also provide an explanation for why the $G:A_2$ ternary complex does not behave as a "true" nucleus for polymerisation, as judged by the kinetic analysis of gelsolin and $G:A_2$ nucleated actin polymerisation. Coué and Korn (1985), showed

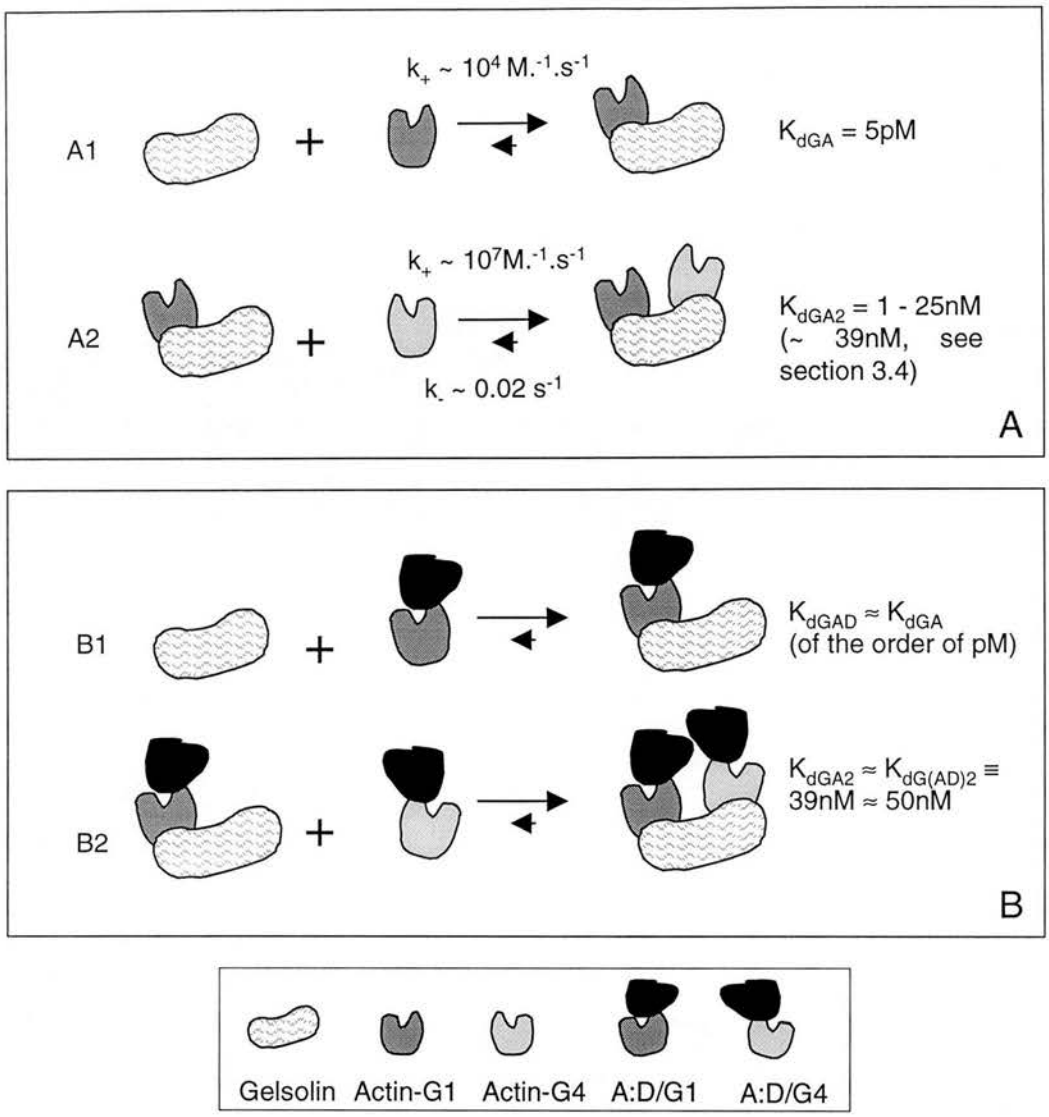

Fig. 3.24. ***Schematic diagram of the two step equilibrium binding scheme for the formation of the G:A_2 ternary complex and the putative (by analogy) binding scheme for the formation of G:$(A:D)_2$.*** (A) Formation of G:A_2 ternary complex takes place via two distinct reactions; A1 and A2. The binding of the second monomer is ~ 100 - 1000 fold faster than the first, upon activation of gelsolin with >μM levels of Ca^{2+} (Schoepper and Wegner, 1991). The kinetic parameters of the two reactions mean that the reverse reaction for the formation of G:A (K_d for G1 and actin ~ 5pM; Bryan, 1988) essentially does not occur (at concentrations used in our experiments) and the concentration of G:A compared to that of G:A_2 is negligible. The fitting of fluorescence enhancement data, very similar to that illustrated in fig. 3.10, was best achieved by having two tight actin-binding sites (K_d ~ pM, and K_d ~ nM, for G1 and G4 respectively) with strong positive co-operatively between them (Weeds et al, 1986). (B) A similar two step (B1 and B2) binding scheme for the formation of G:$(A:D)_2$ is shown. We observed no significant difference between fluorescence enhancement data obtained with NBD-Actin alone and those with A_{nbd}:D (compare the data shown in figs. 3.10, 3.11 and 3.12 with that in figs. 3.18, 3.19 and 3.20). Furthermore, the K_d for the binding of A:D by G:A is equivalent to the K_d of the binding of G-Actin alone by G:A (50nM and 39nM, respectively). By analogy, we propose a similar binding scheme, with similar dissociation constants, for the formation of *G:$(A:D)_2$*. Actin-G1; the tight binding actin monomer, on the G1 site on gelsolin. Actin-G4; the EGTA labile, actin monomer, on the G4 site on gelsolin. A:D/G1; A:D binary complex binding at the tight G1 site on gelsolin. A:D/G4; A:D binary complex binding at EGTA labile G4 site on gelsolin.

G:A_2 greatly accelerated the rate of polymerisation and reduced the nucleation step, but did *not* bypass it altogether, see fig. 3.25 for illustration of this effect. (The lag-phase may be partly due to the exchange of Ca^{2+} for Mg^{2+} at the high affinity site).

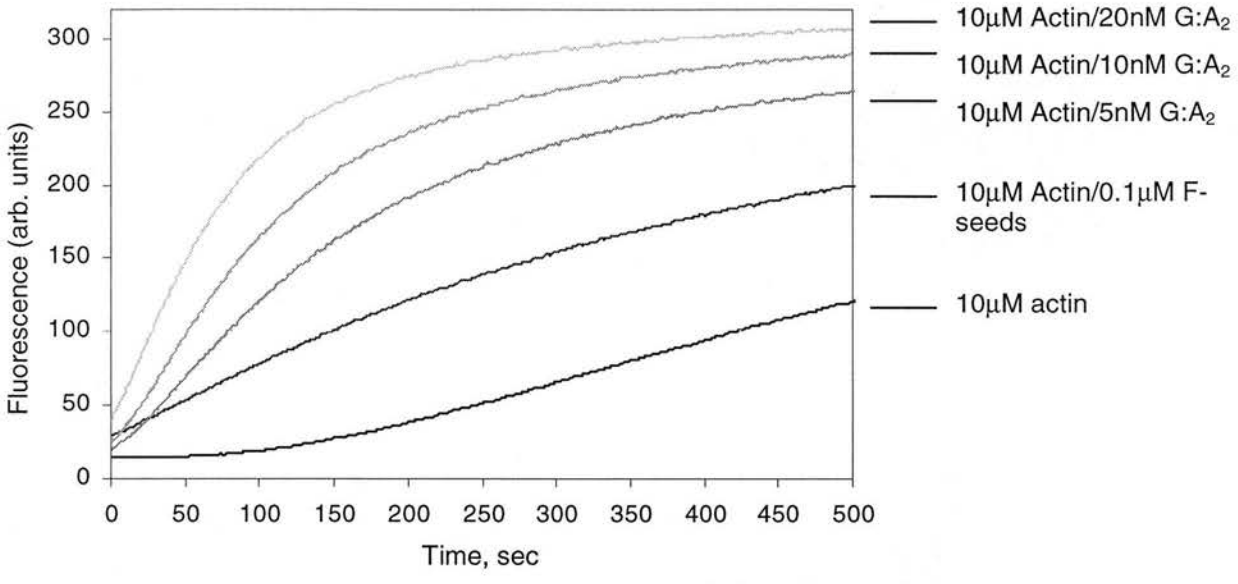

Fig. 3.25. ***Illustration of the nucleating effect of G:A_2 ternary complex on the rate of actin polymerisation, in the presence of 0.2mM $CaCl_2$.*** The time courses of polymerisation of 10μM actin alone (5% pyrene-labelled) or 10μM actin (5% pyrene-labelled) in the presence of 0.1μM F-actin seeds, or 5nM, 10nM or 20nM G:A_2 ternary complex is shown above. Polymerisation was induced by the addition of KCl and $MgCl_2$ to 100mM and 2mM, respectively. Polymerisation was followed by monitoring the increase in fluorescence intensity of pyrene actin. The excitation wavelength was 366nm, the emission wavelength was 384nm, with a 5nm slit-width for both. Buffer conditions: 5mM Tris, pH 8.0; 0.2mM $CaCl_2$; 0.2mM ATP; 0.5mM DTT; 1.0mM NaN_3; 100mM KCl; 2mM $MgCl_2$. The presence of G:A_2 results in an increase in the initial rate of polymerisation, over that of 10μM actin alone, However, although the lag phase is greatly reduced it is *not* abolished completely. Contrast this to the nucleation of polymerisation with 0.1μM F-actin seeds. Under these conditions there is no lag phase and the initial polymerisation rate is the maximum (for these conditions).

Although the initial rate of actin polymerisation is linearly related to the concentration of G:A_2, at low concentrations the rate of polymerisation was less than one would have predicted if all of the G:A_2 present caused nucleated filament growth. i.e. the concentration of the filaments (at least at low actin concentrations) was less than the concentration of G:A_2 used to nucleate polymerisation (Coué and Korn, 1985). The affinity of ATP-G-Actin for G:A_2 (at least at relatively low concentrations of actin, or of G:A_2) may be less than its affinity for an already

formed pointed-end of an actin filament leading to the conclusion that G:A_2 was not acting as a "true" nucleus for actin polymerisation.

This observation could be explained by the actin monomers in G:A_2 being oriented in a non-filamentous conformation. As a result they may then present a different surface for the addition of monomer than that presented by a pointed-end of an already formed filament. In this non-filamentous conformation in G:A_2 may just hold the monomers in very close proximity to each other, whereby the energetics of the nucleation phase is reduced, but it is not by-passed altogether.

However, the ionic conditions used during Coué and Korn's analysis were different to those normally used to initiate and study actin polymerisation. The initiation of actin polymerisation was performed *solely* by the addition of $MgCl_2$ (to 1mM), to actin (in the presence of G:A_2) in ATP-G-Buffer. In similar experiments where actin polymerisation is induced by the addition of physiological concentrations of KCl and $MgCl_2$ (~ 100 – 150mM and 2mM, respectively) to actin in ATP-G-Buffer, the concentration of actin filaments, nucleated in the presence of gelsolin or G:A_2, is *equal* to the concentration of the nucleating species (Janmey and Stossel, 1986; Selve and Wegner 1986; Way et al, 1989; Weber et al, 1994).

The ionic composition of the buffer solution (variations in salt concentration, the type and concentration of mono- and divalent-cations present, and pH) used to initiate actin polymerisation, has *very* marked effects on the kinetics of assembly and disassembly (Frieden, 1982; Brenner and Korn, 1983; Gershman et al, 1984; Pollard, 1986; Zimmerle and Frieden, 1988a/b/c; Wang et al, 1989; Kinosian et al, 1993; Sheterline et al, 1995). Variations in salt concentration and the presence or absence of the divalent-cations Ca^{2+} and Mg^{2+} have also been reported to alter the way gelsolin interacts with both monomeric and filamentous actin (Way et al, 1988; Yin et al, 1988; Way et al, 1989; Pope et al, 1991; Way et al, 1992; Laham et al, 1993; Allen and Janmey, 1994). Thus, the different solution conditions used by Coué and Korn may have caused or amplified the effect they observed for G:A_2.

More direct evidence that the actin subunits in G:A_2 are not held in a filamentous orientation comes from studies of the interaction between gelsolin and a cross-linked actin dimer derived from filaments. Actin filaments can be covalently cross-linked between Cys-374 from one subunit to Lys-191 of a neighbouring subunit, and the actin dimer purified (Knight and Offer, 1978; Elzinga and Phelan, 1984). This cross-link is consistent with the Holmes filament model (Holmes et al, 1990) which indicates that this linkage most likely occurs between two actin monomers that are neighbours across the short-pitch helix. We would predict that gelsolin should bind to both subunits in the dimer in a similar manner to its binding of the terminal actin monomers at the barbed-end of filaments, during capping.

However, this appears not to be the case. Doi and colleagues (Doi et al, 1991; Doi, 1992) showed that although gelsolin did bind to the actin dimer (labelled with NBD) this binding only produced fluorescence enhancement levels indicative of gelsolin having only bound to *one* of the actin monomers. Attempts to covalently link the crosslinked actin dimer to gelsolin, resulted in the linkage of the dimer to only the Ca^{2+} insensitive G1 site in gelsolin and not to G4. While we would not expect the crosslink to hold the dimer in a rigid and inflexible filament conformation, the significance of this result is that when a filament "constraint" – the cross-link – is imposed on actin subunits, gelsolin appears to not be able to bind both monomers. This data is complementary to our own. Doi (Doi, 1992) imposed an F-Actin constraint and did not observe the binding of both G1 and G4 actin-binding sites of gelsolin; we have two binding sites but did not observe results that were consistent with an F-Actin conformation.

A further possible model for actin monomers in ternary complex with gelsolin complex is that illustrated in (C) *Perturbation*, in fig. 3.23. In this perturbation model the actin monomers within G:A_2 are normally in a filamentous conformation. The binding of DNaseI to one of the monomers in G:A_2 may induce some form of conformational change within that actin. This structural rearrangement may then result in change in the way that monomer interacts with gelsolin and/or with the

second neighbouring actin, causing a loss of F-like conformation and enabling the binding of the second DNaseI molecule.

Some support for the idea that DNaseI binding may perturb normal gelsloin:actin interactions comes from the work of Ballweber and colleagues (Ballweber et al, 1997). They have suggested that there is negative co-operativity between the binding sites on G-Actin for DNaseI and gelsolin segment-1 (G1). In the presence of both G1 and DNaseI, the increase in the steady-state critical monomer concentration (due to the sequestration of actin monomers) was found not to be completely additive, unlike the mutually exclusive binding of thymosin-β4 and G1 with actin (Ballweber et al, 1997). This kinetic data suggested a negatively co-operative linkage between the two binding sites, implying that it prevented the formation of a stable ternary complex; DNaseI:actin:G1. DNaseI and G1 bind to two oppositely spaced sub-domains of G-Actin, that bridge an inter-domain cleft (see fig. 1.10 and McLaughlin and Weeds, 1995), and these sites are part of regions of the monomer that are involved in actin-actin interfaces (Holmes et al, 1990; Lorenz et al, 1993). As a result Ballweber et al (1997) suggest that this apparent negative co-operativity may explain the effect of DNaseI increasing the off rate, from the pointed-ends of gelsolin capped filaments (Weber et al, 1994).

Nevertheless, The formation of a ternary complex between actin, DNaseI, and G1 could be demonstrated by gel-filtration and other binding experiments (Weeds et al, 1991). This implied that the affinity of these two proteins were significantly high enough to give a stable ternary complex formation. Formation of the G1:actin:DNaseI ternary complex was also confirmed by us in gel-filtration experiments (data not shown).

Indeed, other evidence suggests that the DNaseI molecule has little, if any, effect on the structure of the actin monomer. The A:D binary complex and G-actin alone appear to have the same affinity for the pointed-ends of actin filaments; K_d in the range of 0.3 – 0.8μM for both species (Podolski et al, 1988; Weber et al, 1994). Crystallographic data also suggests that DNaseI does not significantly alter the

conformation of the complexed actin monomer. Actin has the same structure in the DNaseI crystal, which binds at a loop on the surface of subdomain II (Kabsch et al, 1990), as in the crystal with G1 of gelsolin, which binds to a cleft between domains I and III (McLaughlin et al, 1993). Furthermore, our own data indicates that the dissociation constants for the binding of A:D or G-Actin by the G:A binary complex are equivalent (see section 3.4). The presence of DNaseI appears to have no effect on the actin monomer with regards to its binding interaction with gelsolin. The close similarity of our fluorescence data, for the binding of A_{nbd}:D to gelsolin, compared to that obtained with NBD-Actin alone binding to gelsolin, suggests a similar equilibrium binding scheme. In that case, the presence of DNaseI imposes no steric or kinetic constraints on the binding interaction between gelsolin and actin monomers, and suggests that condition (C) *Perturbation* (fig. 3.23) is unlikely.

The (D) *equilibrium* condition in fig. 3.23 suggests a model where the G:A_2 ternary complex in equilibrium between a closed "F-like" state and a more open "Non-Filamentous" state. Addition of DNaseI to the G:A_2 complex may pull the equilibrium towards the less constrained, and non-filamentous conformation, by simply binding to the pointed-ends of the actin monomers when G:A_2 is in the more open "Non-F-conformation". If the equilibrium, between the open and F-like actin subunit interactions of G:A_2 is very rapid, we could not distinguish this model from the (B) *Non-F-Conformation* model since the binding of actin by gelsolin is so tight. All we can say is that the actin:actin interactions that may exist *between* monomers within G:A_2 are not strong enough to prevent access of DNaseI to both subunits, if they are in a filamentous conformation.

3.6 Conclusion

Our results are not inconsistent with the actin monomers within $G:A_2$ having a different conformation from those at the barbed-end of a filament. The actin monomers are afforded a degree of flexibility, or at least, the tight-binding association with DNaseI is sufficient to change the normal conformation. These results are in agreement with the model (B) *Non-F-Conformation* in fig. 3.23. However, we have no direct evidence to support or discount the possibility of an equilibrium between non- and filamentous conformations for the orientation of the actin monomers in $G:A_2$, like that illustrated in the (D) *Equilibrium* model in fig. 3.23.

Although our results suggest that the actin monomers within isolated $G:A_2$ complexes are not oriented in an F-like conformation (adjacent to each other across the short pitch helix of the filament; Holmes et al, 1990) addition of a third actin subunit, resulting in the formation of a "trimer-nucleus", might stabilise the filament conformation. Therefore, using the A:D binary complex as the third subunit (where further monomer addition is blocked by DNaseI bound at the pointed-end) suggested a possible way in which we could test this idea by forming a *defined* molecular complex.

4. Towards a capped actin-"minifilament"

4.1 Overview

We have performed experiments to test for the formation of an actin-"minifilament", of defined length and composition, capped at both ends by specific binding proteins; with **gelsolin** binding at the barbed-end and **DNaseI** at the pointed-end of the filament. Formation of a putative "minifilament" complex, with a stoichiometry of **G:A_3:D**, is reported. This putative "minifilament" appears to bind rhodamine-phalloidin but not the myosin S-1 head (at least in the presence of ATP).

4.1.1 Introduction

F-actin is not amenable to crystallisation and subsequent determination to atomic resolution, due to the uncontrollable distribution of polymer lengths and their relative flexibility. The crystal structure of the actin:DNaseI binary complex (Kabsch et al, 1990) was used to build a model of the actin filament using data from X-ray diffraction patterns of oriented F-Actin gels (Holmes et al, 1990; Lorenz et al, 1993).

The major problem with this model is that the experimental observations extend to only 7-8 Å, at best, see chapter 1 for details (Holmes et al, 1990; Lorenz et al, 1993; Schmid et al, 1993). Although a unique solution was found, the resolution of the experimental data were insufficient to allow refinement of the input model. Thus, if there had been any conformational changes in surface loops, or even rigid rotations of subdomains within the monomer, the observation to parameter ratio was insufficient to reliably estimate these by least squares fitting of the model to the data. In its favour, the model is consistent with crosslinking and esr-spin probe data and both the EM (Milligan et al, 1990) and X-ray models (Holmes et al, 1990) agree (Mendelson and Morris, 1994).

However, we are far from understanding the atomic contacts that hold the filament together, the interactions involved when myosin uses the actin polymer as a track

during muscle contraction and how the many proteins that control the actin cytoskeleton bind to and interact with the filament.

We propose to take a different approach to attempt to address the resolution problem of the current model: this is to form a **capped-actin-"minifilament"**, with a view to crystallographic studies. This species has a defined length and composition, and contains three actin subunits forming a "minifilament", *blocked* at *both* ends by specific binding proteins with **gelsolin** binding at the barbed-end and **DNaseI** at the pointed-end of the filament, with a stoichiometry of **G:A_3:D**, see fig 4.1.

Gelsolins ability to form a cap at the barbed-end of an actin filament, and formation of stable ternary complexes with two actin monomers, provides us with a tool to control the definition of one end (the barbed-end) of the filament. The GA_2 ternary complex could be combined with a pointed-end capped actin species to give a larger complex, hopefully with the actin monomers in F-conformation. A possible candidate for the capping of the pointed-end is the G-Actin:DNaseI binary complex (A:D), see fig. 4.2.

DNaseI forms a very tight and stable 1:1 binary complex (A:D) with actin (K_d ~ 0.1 – 1.0nM, Mannherz et al, 1980). It also binds to the pointed-ends of actin filaments with similar affinity (K_d ~ 1nM, (Podolski et al, 1988; Weber et al, 1994). This binding leads to a blockage of filament elongation, conferred by the binding of *one* DNaseI molecule to the pointed-end of a single strand of the F-Actin two-start helix (Podolski et al, 1988). The binding of this DNaseI appears to have no significant effect on the affinity of the attached actin for the pointed-end of the filament. Weber and co-workers (Weber et al, 1994) indicated that the binding of two DNaseI molecules was not possible at the pointed-ends of gelsolin capped actin filaments. At DNaseI concentrations in the μM range an increase in the rate of depolymerisation from the pointed-ends of gelsolin capped filaments was observed ($K_{50\%}$ ~ 5μM, Weber et al, 1994). The explanation proposed for this was a steric clash between *two* DNaseI molecules at the pointed-end. This prevented the simultaneous stable binding

of both DNaseI molecules and resulted in an increase in the k_{off} rate for the actin monomer, as a 1:1 binary complex with DNaseI (Weber et al, 1994).

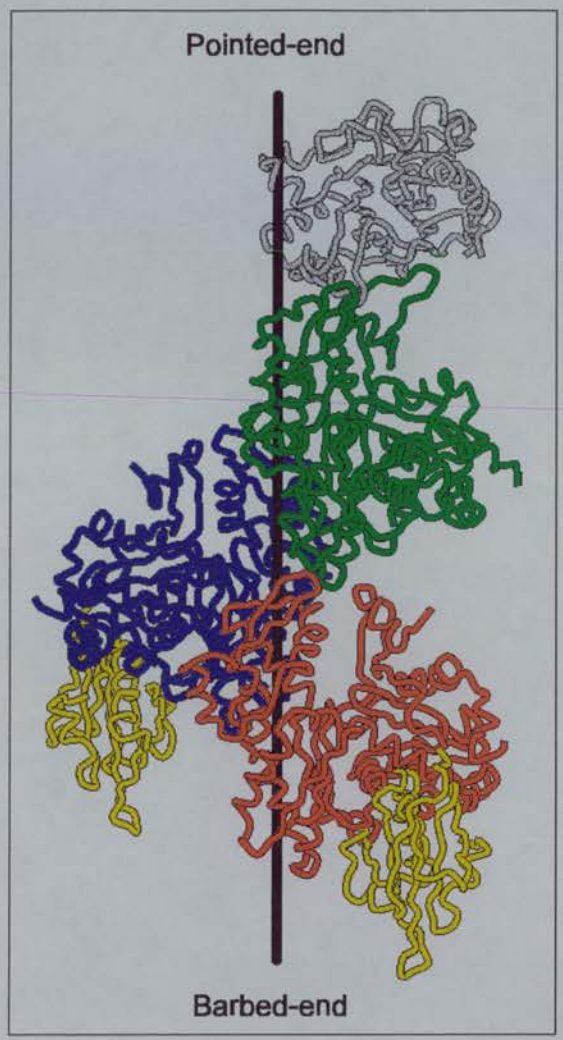

Fig. 4.1. ***Model of the putative "minifilament".*** A schematic representation of a putative model of the capped-actin-"minifilament", with stoichiometry of **G:A_3:D** (gelsolin:$actin_3$:DNaseI), is shown. DNaseI is coloured grey, the three actin monomer subunits, oriented as described by the Holmes filament model (Holmes et al, 1990), are coloured red, green and blue. Only segment 1 (G1) and a putatively positioned segment 4 (G4) – by analogy – from gelsolin are shown, coloured yellow. Kinetic and modelling evidence suggests that only one DNaseI molecule can be bound at the pointed-end (Weber et al, 1994). (The diagram was created using MOLSCRIPT; Kraulis, 1991).

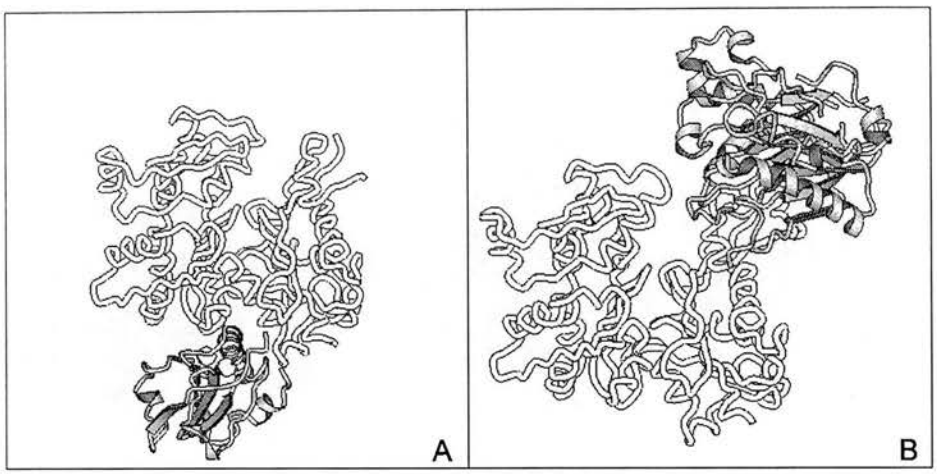

Fig. 4.2. ***G-Actin in complex with two opposite end-opposed binding proteins.*** (A) A schematic view of the actin-gelsolin segment 1 (shaded) complex (the Ca^{2+} ions are shown as spheres) as described by McLaughlin et al (1993. (B) A schematic view of the actin-DNaseI (shaded) complex as described by Kabsch et al (1990). This side-by-side orientation clearly indicates the binding of the two proteins at opposite ends of the actin monomer. (Diagrams were created using MOLSCRIPT; Kraulis, 1991).

Modelling evidence is consistent with this kinetic data. Two actin:DNaseI binary complexes (A:D) cannot be accommodated at the pointed-ends of filaments due to a significant steric clash. Our proposed "minifilament" model (fig. 4.1), with the actin monomers oriented in a filamentous conformation (as described for the filament model, Holmes et al, 1990) acknowledges this argument. It is not possible to accommodate *two* DNaseI molecules at the pointed-ends of the putative "minifilament", giving our model a likely stoichiometry of **$G:A_3:D$**.

Capping and nucleating proteins like gelsolin (and the $G:A_2$ ternary complex) result in an acceleration of the rate of polymerisation by shortening the lag phase (see section 1.3 for details on actin polymerisation and see fig. 3.25 for an example of $G:A_2$ nucleation). The probable explanation for this activity is that the nucleation rate is increased. Despite the apparent lack of F-like character of the orientation of the actin monomers within the $G:A_2$ ternary complex (see results reported in chapter 3), it nevertheless still binds tightly to, and caps the barbed-end of actin filaments, preventing further polymerisation. $G:A_2$ also nucleates actin polymerisation, very

efficiently, in the pointed-end direction. Although polymerisation tales place at the slower growing pointed-end, the overall polymerisation rate is increased because the rate-limiting nucleation step occurs faster; the nuclei are probably more stable and more free pointed-ends are created during gelsolin and $G:A_2$ nucleated polymerisation (Pollard and Cooper, 1986; Ditsch and Wegner, 1994). The final result is the production of large numbers of short filaments with gelsolin capped barbed-ends.

Thus, the nucleating ability of $G:A_2$ probably results in a reduction in the energetics of nucleation (resulting in the formation of more nuclei and thus, more filament ends onto which polymerisation can occur), due to the close proximity, and increased stability of two actin monomers in ternary complex with gelsolin, compared to the "true" actin trimer nuclei. However, the kinetic analysis of such nucleated polymerisation is inconsistent with models where the capping proteins (in this case $G:A_2$ ternary complex) simply orient the actin subunits to be like the pointed-end of an already formed actin filament (Coué and Korn, 1985; Pollard and Cooper, 1986; Ditsch and Wegner, 1994). This is consistent with our results discussed in chapter 3, where our data appear to indicate that the actin monomers in the $G:A_2$ complex are oriented in a different conformation to those at the barbed-end of a filament. Although the kinetics of monomer addition, during nucleated polymerisation, onto the pointed-end of such species is probably different to addition onto the pointed-end of already formed filaments, it nevertheless still requires the formation of some form of "trimer-nuclei" species before rapid elongation takes place. Hence this may be the reason why gelsolin and $G:A_2$ reduce the lag phase but do not bypass it altogether. (The lag phase may also be partly due to the exchange of Ca^{2+} for Mg^{2+} at the high affinity site).

The addition of further actin monomers to the system may alter the orientation of the actin monomers in the $G:A_2$ complex towards a conformation more like that of a filament. Therefore, the addition of a third actin monomer, in the form of A:D binary complex, may result in the formation of a *stable* **$G:A_3:D$** "trimer-nucleus". Gelsolin binds two of the actin monomers tightly, tethering them together preventing the rapid

dissociation observed for the formation of actin dimers during "true" nucleation. Thus, the energetics of formation of this capped actin-"minifilament" may be significantly less, and its relative stability greater, than formation of the "true" actin trimer nucleus.

We propose to use the G:A_2 ternary and A:D binary complexes in an attempt to form a capped "minifilament" with a stoichiometry of **G:A_3:D**, see fig. 4.1. We also propose to use molecules that specifically bind F-Actin and stabilise filaments to probe the putative "minifilament" for filamentous-like conformation, e.g. binding rhodamine-phalloidin or the myosin S-1 head.

4.2 Formation of a putative "minifilament" from G:A_2 ternary and A:D binary complexes

We have performed experiments to test for the formation of a putative capped actin-"minifilament" from the G:A_2 ternary complex and A:D binary complex under polymerising conditions. Gel-filtration experiments appear to indicate the formation of a significantly larger complex (as compared to G:A_2), with stoichiometry of **G:A_3:D**.

4.2.1 Gel-filtration analysis of the formation of a putative "minifilament"

Complex formation between the G:A_2 ternary complex and the A:D binary complex was analysed by FPLC/Superose-12 size-exclusion chromatography (see methods for details). The concentrations of the two complexes were calculated by BCA protein assay (Pierce®). G:A_2 and A:D were mixed together in ATP-F-Buffer; 0.2mM $CaCl_2$, at a molar ratio of 1:1 (at 3.0μM for both complexes) and incubated at room temperature for 1hr. (Calcium was included in the buffers to ensure the activation and to maintain the monomer binding activity of gelsolin). The sample was then loaded onto an FPLC/Superose-12 column, pre-equilibrated in ATP-F-Buffer; 0.2mM $CaCl_2$.

Fig. 4.3(A) shows the elution profile from a 1:1 molar ratio incubation of GA_2 and AD (peak 1) compared to those of G:A_2 and A:D alone (peaks 2 and 3 respectively). A significant shift ($P<0.05$) in the retention volume of the 1:1 GA_2:AD sample was observed, indicative of the formation of a larger species (as compared to G:A_2). The retention volumes of the various protein complexes are shown in table 4.1, and the corresponding apparent Mr. value, 271kDa., suggests the formation of a complex between *one* G:A_2 ternary complex and *one* A:D complex (a complex with an apparent stoichiometry of **G:A_3:D**).

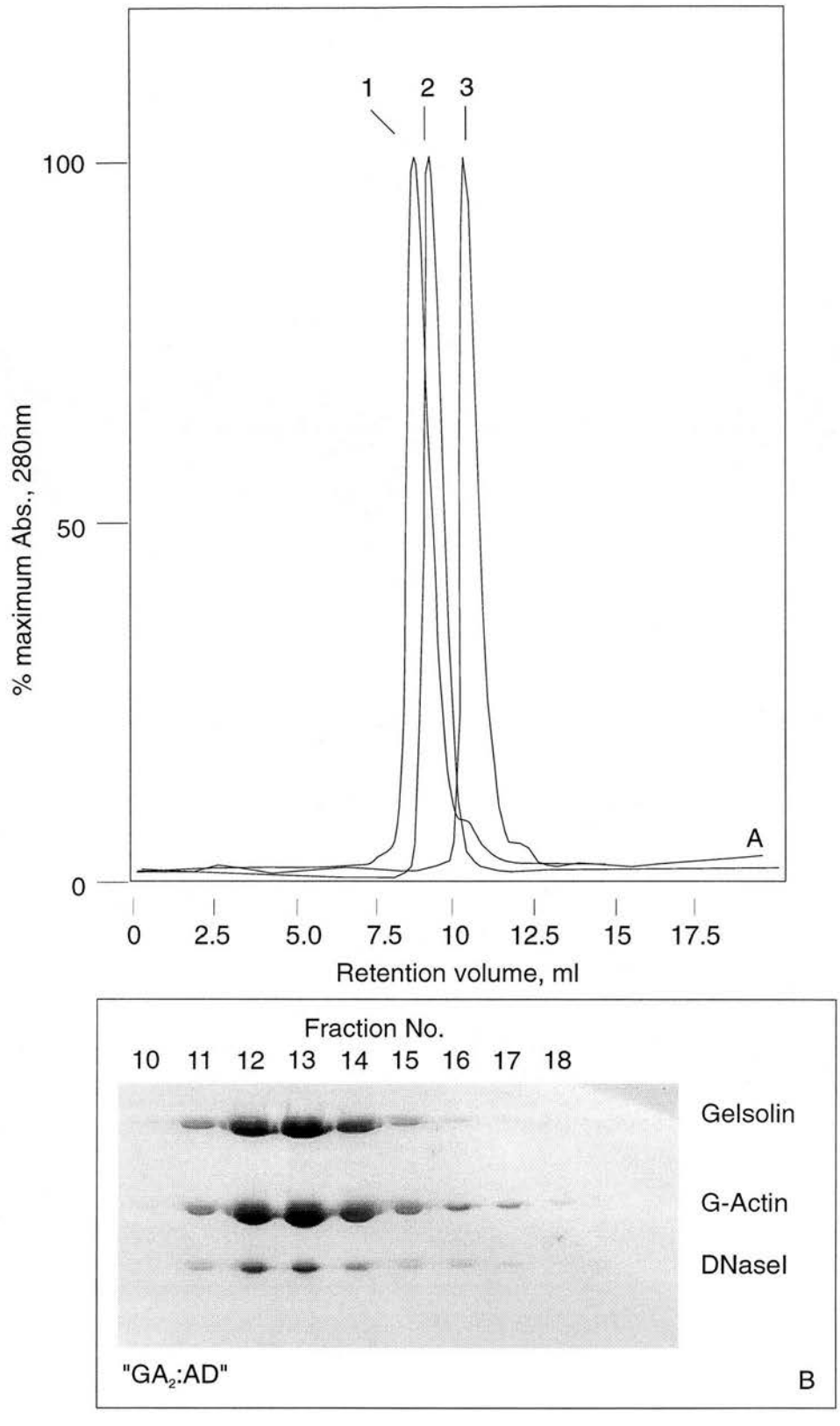

Fig. 4.3. ***Formation of a complex between G:A$_2$ ternary complex and A:D binary complex analysed by size-exclusion.*** (A) A_{280nm} monitored elution profiles of A:D, G:A_2 ternary complexes and the "GA_2:AD" complex from an FPLC/Superose-12 size-exclusion column. (B) SDS-PAGE analysis of the "GA_2:AD" peak from A. For comparison of different profiles the absorbance values have been normalised to the maximum at the peak. The arrows mark the elution positions of (1) "GA_2:AD"; (2) G:A_2; (3) A:D. The "GA_2:AD" sample represents the complex formed from an incubation of pre-purified G:A_2 ternary complex and A:D binary complex, mixed at a 1:1 molar ratio, in ATP-F-Buffer; 0.2mM $CaCl_2$. Proteins were mixed together (at 3.0μM for each complex), and incubated for 1hr at RT, in ATP-F-Buffer; 0.2mM $CaCl_2$ before being loaded onto an FPLC/Superose-12 column, pre-equilibrated in ATP-F-Buffer; 0.2mM $CaCl_2$. (SDS-PAGE and chromatography were performed as described in methods).

Protein species	Retention volume (ml)	Theoretical Mr. (kDa.)	Apparent Mr. (kDa.)
actin:DNaseI (A:D)	10.90 (± 0.039 SEM, n=10)	71	92
gelsolin:actin binary complex (G:A)	10.13 (± 0.066 SEM, n=4)	124	149
gelsolin:actin$_2$ ternary complex (G:A$_2$)	9.59 (± 0.037 SEM, n= 12)	166	209
GA$_2$:AD "minifilament" complex	9.17 (± 0.026 SEM, n=8)	237 (1:1 binding interaction).	271

Table 4.1. ***Retention volumes (ml) of the A:D, G:A and G:A$_2$ complexes and that of the putative "minifilament".*** Data obtained from FPLC/Superose-12 size-exclusion chromatography experiments. The value given for the apparent Mr. is a mean value calculated from the calibration curve using the corresponding mean retention volume. The significance of the difference between the mean retention volume of G:A$_2$ and that of "GA$_2$:AD" (the putative "minifilament") is $P<0.05$.

The peaks from such elution profiles were always very sharp and relatively symmetrical, with only a slight trailing-edge (see peak 1, fig. 4.3A). The width of the peak and the relative peak area for elution profiles of the putative "minifilament" did not significantly alter when compared to those of G:A$_2$ and A:D alone. The trailing-edge appears primarily to contain small amounts of the A:D binary complex (see fig. 4.3B). This section of the elution profiles frequently represented less than 10% of the total protein present in such experiments, and it never accounted for more than 15 %.

SDS-PAGE analysis of the components of the putative "minifilament" complex indicated the presence of all three proteins (gelsolin, actin and DNaseI) in the shifted peak, see fig. 4.3(B). The A:D binary complex has shifted from its normal elution position to one indicative of a much larger species. The stoichiometry of the components of the new peak was determined by scanning of the densities of bands on SDS-polyacrylamide gels, using known amounts of gelsolin, actin and DNaseI as internal standards. Table 4.2 summarises the results from 4 similar experiments. The stoichiometry of this new complex appears to be **G:A$_3$:D**.

FPLC/Sup-12 size exclusion	Mole Ratios			
gelsolin:actin	1:2.7	1:3.1	1:2.7	1:3.2
DNaseI:actin	1:2.9	1:2.8	1:2.8	1:3.3
gelsolin:DNaseI	1:1.1	1:1.25	1:1.3	1:1.3

Table 4.2. ***Stoichiometry of the individual component proteins within the putative "minifilament" complex.*** The values given in the table represent data obtained from 4 similar experiments carried out on FPLC/Superose-12 size-exclusion columns. The central fraction from the elution profile was subjected to SDS-PAGE, with standard amounts of each of the three proteins added as internal references, and the relative amounts of each determined by gel densitometry. (Chromatography, SDS-PAGE and stoichiometric analysis were performed as described in the methods).

4.2.2 Native-gel analysis of putative "minifilament" formation

Non-denaturing PAGE was also used to analyse complex formation between G:A_2 and A:D. Fig 4.4(A) shows the standard migration positions for the A:D binary, the G:A binary, the G:A_2 ternary complexes and that of a 1:1 molar ratio incubation of G:A_2 and A:D (under polymerising conditions). It should be noted, that this is a composite figure, created from several different gels. This was necessary, due to the differences in the running conditions used for each individual complex or set of proteins (see legend to fig 4.4), in order to illustrate the standard migration positions of the various protein complexes.

G:A_2 and A:D were mixed together at a 1:1 molar ratio (5.2μM), and incubated at room temperature for 1hr, in ATP-F-Buffer; 0.2mM $CaCl_2$. Native-gel sample buffer (50% glycerol; ATP-F-Buffer; 0.2mM $CaCl_2$) was added 1:1 (v/v) to the incubated sample prior to loading onto the gel. The electrophoretic pattern for the "GA_2:AD" sample contained multiple bands with a high degree of smudging, see fig. 4.4(A). However, there appears to be a slight shift in the electrophoretic mobility of a major band within the "GA_2:AD" sample (in relation to the normal migration position of the G:A_2 complex).

SDS-PAGE in a second dimension of the "GA_2:AD" sample lane is shown in fig. 4.4(B). The 1:1 incubation mix of GA_2 and A:D always produced a smudged ladder of protein bands. Densiometric analysis of the various constituent proteins present

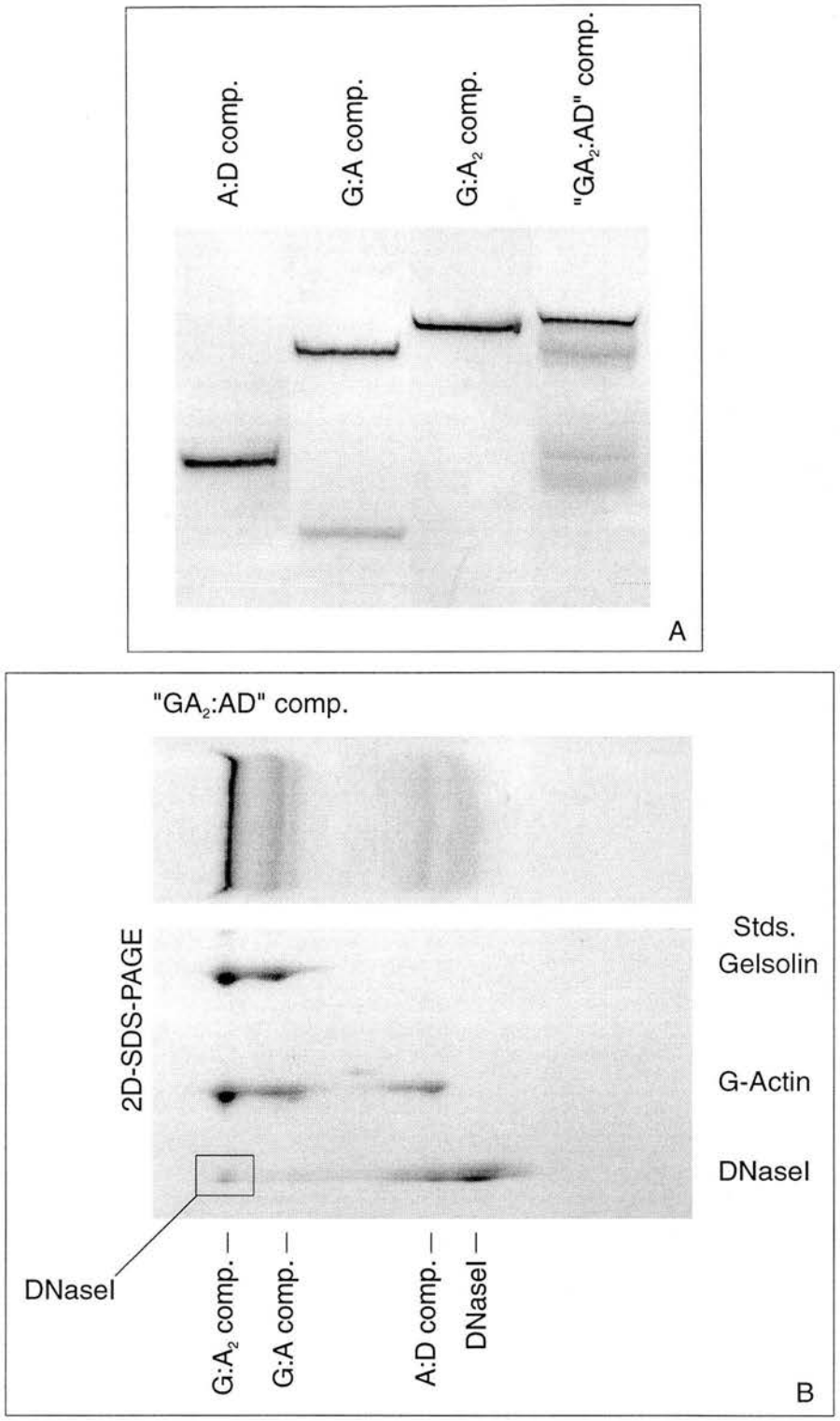

Fig. 4.4. ***Native-PAGE analysis of putative "minifilament" formation.*** (A) Native gel showing the electrophoretic mobilities of the A:D binary, G:A binary, G:A_2 ternary complexes and the migration pattern of "GA_2:AD"comp. "GA_2:AD"comp. represents the mobility pattern formed from an incubation of pre-purified G:A_2 ternary complex and A:D binary complex mixed at a molar ratio of 1:1, in ATP-F-Buffer; 0.2mM $CaCl_2$. Proteins were mixed together at a concentration of 5.2μM (for each complex) and incubated for 1hr at RT before loading. (B) SDS-PAGE analysis, in a second dimension, of the components of the protein bands in A. Standard migration positions of G-Actin, gelsolin and DNAseI are shown beside the gel. The positions of several of the protein complexes are indicated below the gel. The figure shown in A is a composite image created from several lanes from different gels (the running conditions required for each complex/set of proteins are slightly different), however, G:A_2 and "G:A_2:AD"comp. were run on the *same* gel. Gel running conditions: 0.2mM ATP; 0.5mM DTT were used for A:D; 0.2mM $CaCl_2$; 0.2mM ATP; 0.5mM DTT; 0.6mM EGTA; 1.0mM $MgCl_2$ were used for G:A; and 0.2mM $CaCl_2$; 0.2mM ATP; 0.5mM DTT; 2mM $MgCl_2$ were used for G:A_2 and "GA_2:AD"comp. complex formation. (SDS-PAGE and native-PAGE were performed as described in methods).

within these bands was performed on similar lanes from native-gels (data not shown). The major species within the shifted band from samples of 1:1 molar ratio incubations of GA_2 and A:D appears to be G:A_2 ternary complex. However, a small amount of DNaseI was found within these shifted band/s, see the inset box in fig. 4.4(B). This may represent the formation of a small amount of the "minifilament" complex, but we were unable to verify this due to the very small amounts of DNaseI present. However, it may also represent the formation of a small amount of a complex with stoichiometry G:A_2:D, formed due to the binding of A:D binary complex, at the EGTA labile site on gelsolin (see discussion).

G:A binary and A:D binary complexes were also observed, as was a substantial amount of free uncomplexed DNaseI. Several other unidentified protein complexes and small amounts of the individual uncomplexed proteins (gelsolin, actin, DNaseI), were also frequently observed on such native-gel lanes.

We observed little evidence of "minifilament" complex formation in native-PAGE experiments. Several factors related to the limit of resolution of such native-gels, may explain these observations. The resolving power of such non-denaturing gels (where the electrophoretic mobility of a given protein or complex is resolved as a well defined, narrow band) decreases both as a function of the amount of total protein and with the number of individual proteins (or complexes) present in the reaction sample (Safer, 1989). The resolution limit of total protein per gel lane was typically observed to be 10 – 12μg. Protein added in excess of this amount (even for samples of a single protein, of very high purity), often gave ill-defined and broadly smeared mobility profiles. Samples containing several different proteins and/or protein complexes often showed reduced resolution and separation of the components. The distance migrated during the run (under the same solution conditions), compared to samples containing only the individual proteins/complexes, was often altered. Evidence of significant amounts of complex dissociation and break down was also a feature in such sample profiles.

Changes in concentration and the ionic composition of the running buffers, sample buffers and the initial incubation solution conditions, has very marked effects on the electrophoretic mobility of proteins and protein complexes on such native-gels. Addition or removal of the divalent cations Ca^{2+} and Mg^{2+} has drastic effects on the resolution and migration positions of gelsolin and DNaseI (see section 3.2.2.2 for an example). The buffer conditions used in the 1:1 molar ratio incubation of G:A_2 and A:D were 5mM Tris, pH8.0; 0.5mM DTT; 0.2mM ATP; 2mM $MgCl_2$; 100mM KCl; 1.0mM NaN_3; 0.2mM $CaCl_2$. Native gel sample buffer (50% glycerol; ATP-F-Buffer; 0.2mM $CaCl_2$), possesses the same ionic conditions and buffer ingredients as the incubation buffer. However, the running buffer does not (0.2mM $CaCl_2$; 0.2mM ATP; 0.5mM DTT; 2mM $MgCl_2$). Attempts to run such non-denaturing gels under polymerising conditions by the inclusion of salt (~50mM KCl) in the running and gel buffers resulted in the generation of very high currents (~ 300 – 900mAmps). The heat generated, as a consequence of the high current, leads to the rapid and severe denaturation of the protein samples, the gel and damage to the electrophoresis apparatus. The sudden changes in the ionic conditions and shifts in charge distribution of the solution that may occur during the running of such "GA_2:AD" samples, may have compromised any complex formation.

The relatively harsh solution conditions experienced by proteins during electrophoresis, rapid changes in the ionic constituents and the existence of multiple equilibrium systems in the 1:1 incubation sample of G:A_2 and A:D may explain the electrophoretic profile seen in fig. 4.4(A).

4.3 Testing the conformation of the actin monomers in the putative "minifilament"

Using F-Actin specific binding molecules, rhodamine-phalloidin and the myosin S-1 head from rabbit skeletal muscle, we have tested the putative "minifilament" for filament-like properties.

4.3.1 Rhodamine-phalloidin fluorescence enhancement binding assay

Phallotoxins are a family of toxic peptides from the mushroom *Amanita phalloides*. Phalloidin (a bicyclic heptapeptide) and the closely related compound phallacidin, are the two major representatives of this family (Faulstich and Wieland, 1996). The toxic effect is due to a very tight (K_d ~ 4nM) and specific binding to actin filaments (Wulf et al, 1979; Estes et al, 1981; Vandekerckhove et al, 1985). The binding of phalloidin to actin filaments results in their stabilisation, and this stability is conferred by the toxin preventing the dissociation of actin monomers from both the pointed and barbed-ends of filaments (Estes et al, 1981; Coluccio et al, 1984; Sampath and Pollard, 1991). Phalloidin also appears to decrease the rate of association of monomers at the barbed-end by ~ 50% (Coluccio et al, 1984; Sampath et al, 1991). The probable binding site for phalloidin lies at a subunit interface between three actin monomers (Faulstich et al, 1993; Lorenz et al, 1993) and provides a rationale for phalloidin's high F-Actin binding specificity and its ability to stabilise actin filaments (Wieland et al, 1978; Le Bihan et al, 1991). There is also evidence that phalloidin inhibits the dissociation of actin subunits from actin filaments below the critical concentration (Cano et al, 1992).

A fluorescent derivative, rhodamine-phalloidin (Wulf et al, 1979: Faulstich et al, 1983) has been used to visualise and quantitate actin filaments in cells (Cooper, 1987). A 6 - 12 fold fluorescence enhancement is observed upon binding to actin filaments and the dissociation equilibrium constant for this derivative binding to F-actin ranges between 40 – 400nM (Huang et al, 1992; Cano et al, 1992).

We have used a modified version of a fluorescence enhancement assay described by Huang et al (1992) and attempted to use it to probe the actin monomer conformation within the putative "minifilament". This assay is based on a titration of polymerised actin against a constant concentration of rhodamine-phalloidin and measuring the fluorescence enhancement. The fluorescence enhancement is directly proportional to the amount of bound fluorophore and can be readily used in Scatchard analysis for the binding stoichiometry and equilibrium dissociation constant (Huang et al, 1992).

Fig. 4.5 illustrates the fluorescence enhancement obtained upon the binding of rhodamine-phalloidin to F-Actin (0.15μM rhodamine-phalloidin in the presence of 1.2μM Actin, in ATP-F-Buffer; 0.2mM $CaCl_2$). A 7 – 8 fold fluorescence enhancement, over that of rhodamine-phalloidin alone, was observed. No enhancement was seen when rhodamine-phalloidin and actin were incubated together under depolymerising conditions (ATP-G-Buffer), or when either F-Actin or rhodamine-phalloidin were incubated alone under polymerising conditions (ATP-F-Buffer; 0.2mM $CaCl_2$), (data not shown).

Titration of F-actin against a constant concentration of rhodamine-phalloidin (0.32μM) is shown in fig. 4.6(A). Under our experimental conditions (0.32μM rhodamine-phalloidin in ATP-F-Buffer; 0.2mM $CaCl_2$, in a total volume of 500μl, with a 1hr incubation at 22°C) the maximum fluorescence change we obtained was **189.5 units** (arbitrary fluorescence units). This corresponds to the complete binding of 0.32μM rhodamine-phalloidin, and gave a calibration factor of **592.2 units.μM^{-1}**, which was then used to calculate the amount of rhodamine-phalloidin bound at any level of fluorescence enhancement.

Fig. 4.6(B) illustrates the Scatchard analysis of the data presented in fig. 4.6(A). This gave an apparent dissociation constant for rhodamine-phalloidin of ~ 43nM and a binding stoichiometry of ~ 0.94 (phalloidin:actin monomer). The mean K_d values obtained for rhodamine-phalloidin, from two different suppliers, are shown in table 4.3. Our values obtained for the dissociation constant (mean K_d ~ 57nM), and the binding stoichiometry (~ 1:1, phalloidin:actin monomer), are in good agreement with

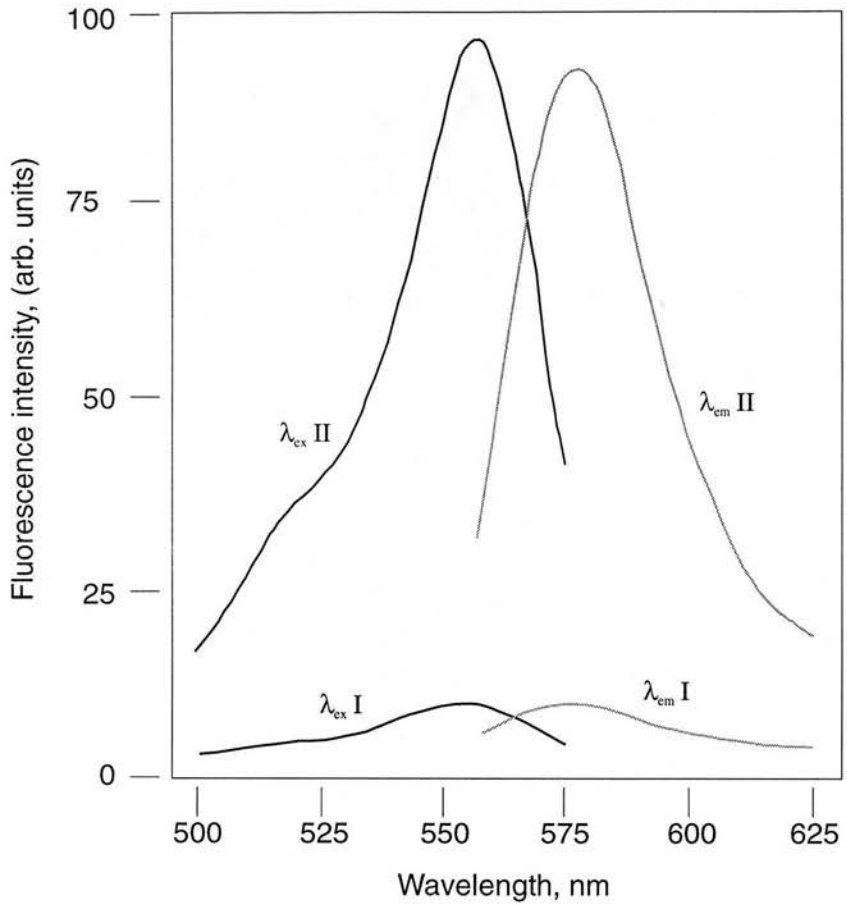

Fig. 4.5. ***Fluorescence enhancement of rhodamine-phalloidin upon binding to F-Actin.*** The fluorescence excitation and emission spectra of 0.15μM rhodamine-phalloidin (λ_{ex} I and λ_{em} I) and 0.15μM rhodamine-phalloidin in the presence of 1.2 μM F-Actin (λ_{ex} II and λ_{em} II), are shown. A 7 - 8 fold enhancement in the fluorescence intensity was observed upon the complete binding of rhodamine-phalloidin to actin filaments. 250μl of 0.3μM rhodamine-phalloidin (100μM stock in ethanol), in ATP-F-Buffer; 0.2mM $CaCl_2$ was added either to 250μl of ATP-F-Buffer; 0.2mM $CaCl_2$ or to 250μl of 2.4μM actin in the same buffer. The samples were left for 1hr at 22°C, in the dark, and then the fluorescence intensity measured. Spectra were recorded in a 1cm cell with a total volume of 500μl. The excitation spectra were recorded with an emission wavelength of 580nm and emission spectra with an excitation wavelength of 550nm, with a band width of 5nm for both.

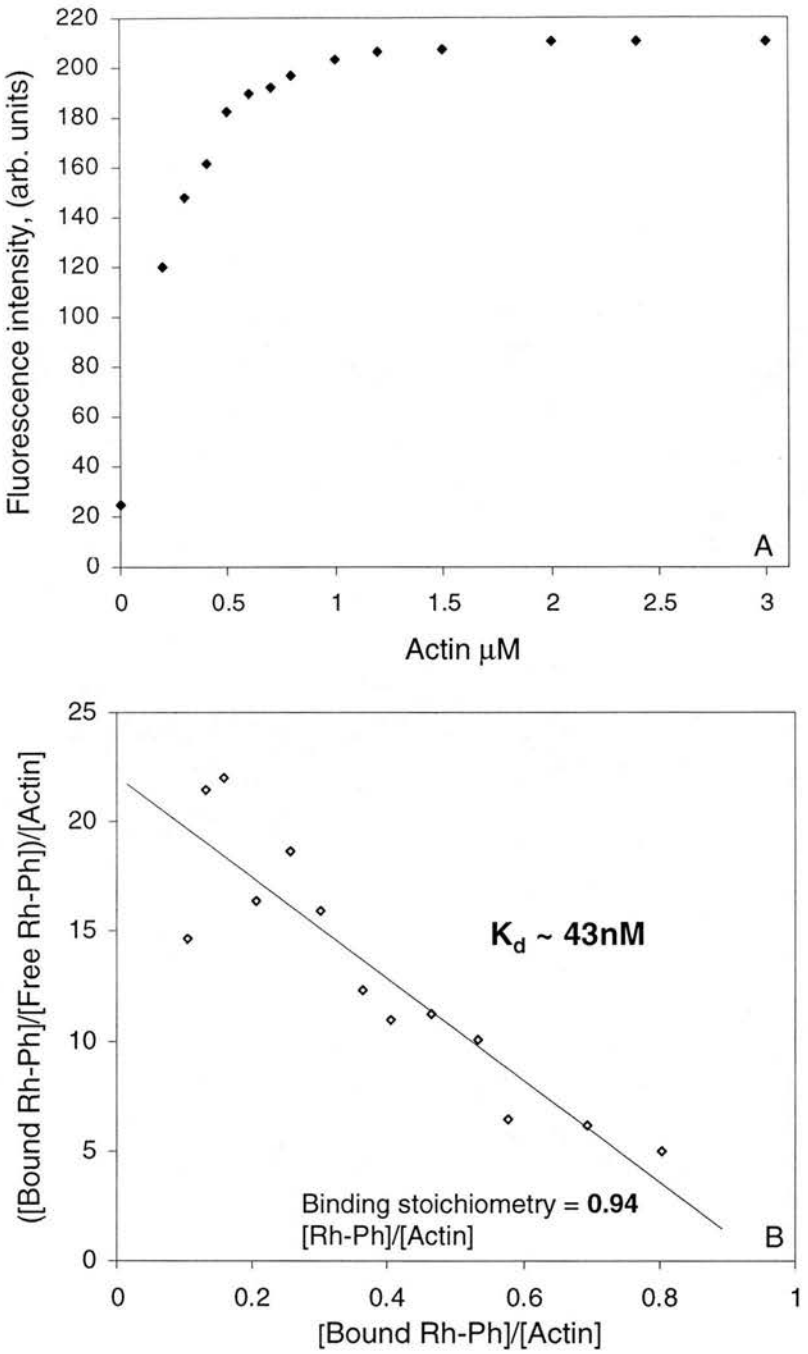

Fig. 4.6. ***Equilibrium dissociation constant of rhodamine-phalloidin binding to actin filaments, determined by a fluorescence enhancement assay.*** (A) Fluorescence titration of actin against 0.32μM rhodamine-phalloidin. (B) Scatchard analysis of the fluorescence data presented in A. The solid line is a linear regression (R^2 = 0.864) and gives an apparent K_d ~ 43nM. 250μl of 0.64μM rhodamine-phalloidin (100μM stock in ethanol), in ATP-F-Buffer; 0.2mM $CaCl_2$, was added to 250μl of various amounts of actin in the same buffer. The samples were incubated for 1hr, at 22°C in the dark, and then the fluorescence intensity of each sample was measured. The excitation wavelength was 550nm, the emission wavelength was 580nm, with a 5nm slit width for both. The maximum value of fluorescence enhancement obtained for 0.32μM rhodamine-phalloidin (Molecular Probes Inc.), under our assay conditions was 189.5 units (arbitrary fluorescence units), corresponding to the complete binding of rhodamine-phalloidin. This gave a calibration factor of 592.2 units.μM^{-1} which was used to calculate the amount of rhodamine-phalloidin bound for any level of enhancement.

results reported by others (Huang et al, 1992; Cano et al, 1992; De la Cruz et al, 1994).

K_d (nM) of Rhodamine-Phalloidin (Molecular Probes Inc.)	K_d (nM) of Rhodamine-Phalloidin (Sigma)
43	71
65	82
49	108
71	132
56	91
	84
Mean K_d = **56.8nM** ± 5.1 (SEM, n=5)	Mean K_d = **94.7nM** ± 9.0 (SEM, n=6)

Table 4.3. ***Equilibrium dissociation constant of Rhodamine-Phalloidin binding to F-Actin.*** The K_d of rhodamine-phalloidin, (obtained from Molecular Probes Inc. and Sigma), binding to F-Actin was determined using the fluorescence enhancement assay, similar to that illustrated in 4.6(A) and (B). 250µl of 0.64µM Rhodamine-Phalloidin (100µM stock solution, in ethanol) in ATP-F-Buffer; 0.2mM $CaCl_2$ was added to 250µl of various amounts of actin in the same buffer. The samples were left for 1hr at 22°C, in the dark, and then the fluorescence intensity of each sample was measured. The excitation wavelength was 550nm, the emission wavelength was 580nm, with a 5nm slit width for both. The K_d was determined by Scatchard analysis of the fluorescence enhancement data. The ΔF_{max} values obtained for 0.32µM rhodamine-phalloidin were 189.5 units and 41 units (arbitrary fluorescence units), for the reagent supplied from Molecular Probes Inc. and Sigma, respectively. This gave a calibration factor of **592.2 units.μM^{-1}** and **128.1 units.μM^{-1}**, respectively.

Rhodamine-phalloidin supplied by Molecular Probes Inc. was superior to that obtained from Sigma, in all respects. Firstly, the K_d values obtained for rhodamine-phalloidin from Sigma are almost double those obtained with reagent supplied from Molecular Probes Inc. (~ 57nM compared to ~ 95nM, respectively). Secondly, the variation and noise levels of the readings obtained during fluorescence measurements were always much greater with the Sigma reagent. Thirdly, the enhancement levels obtained with the Sigma reagent were ~ 3 - 4 fold, in contrast to the ~ 8 fold levels seen with the Molecular Probes Inc. reagent. However, it should be noted that this high quality is reflected by the slightly higher cost of a small amount of the reagent from Molecular Probes, in comparison to that supplied by Sigma. Assays performed on the putative "minifilament", described in the following sections, were carried out using the higher quality reagent from Molecular Probes Inc.

4.3.2 Rhodamine-phalloidin binding to the putative "minifilament"

We have performed experiments to investigate rhodamine-phalloidin binding to the putative "minifilament".

Our postulated model of the "minifilament" contains three actin monomers (see fig. 4.1) oriented in a filamentous conformation. This "minifilament" model feasibly contains a binding site for the phalloidin molecule. The model for the binding site for phalloidin on the filament was constructed from a least squares fit of the monomer crystal structure using X-ray diffraction pattern data of oriented F-Actin gels in the presence of phalloidin (Lorenz, et al, 1993). Although a unique solution was found for the binding site of phalloidin, similarly to the situation for the actin filament model (Holmes et al, 1990) the experimental observations extend to only 7 - 8 Å at best (Lorenz, et al, 1993). Also, the orientation of the bound phalloidin was achieved solely by rotations of its position so it did not penetrate into one of the actin monomers and where it satisfied the biochemical constraints for the residues that possibly contribute to the binding site. Such biochemical constraint data was obtained from cross-linking analysis (Faulstich et al, 1993) and from the generation of point mutants in yeast actin that do not bind rhodamine-phalloidin (Drubin et al, 1993).

These studies indicate that the binding site for phalloidin appears to lie between the two strands of the filament. The small toxin molecule makes contacts with three different actin subunits at this subunit interface site, see fig. 4.7. This multiple subunit contact provides a rationale for the ability of phalloidin to stabilise these monomer-monomer interactions and the resultant increase in the overall stability of the filament. This stabilisation of the monomer-monomer interactions also provides a possible explanation for the reduction in monomer dissociation from the filament (Coluccio et al, 1984; Sampath and Pollard, 1991). Our proposed model of the "minifilament" contains three monomers (compare figs. 4.1 and 4.7), oriented in a filamentous conformation, and so feasibly contains one binding site for a phalloidin molecule. The binding of phalloidin to the "minifilament" may provide extra stability

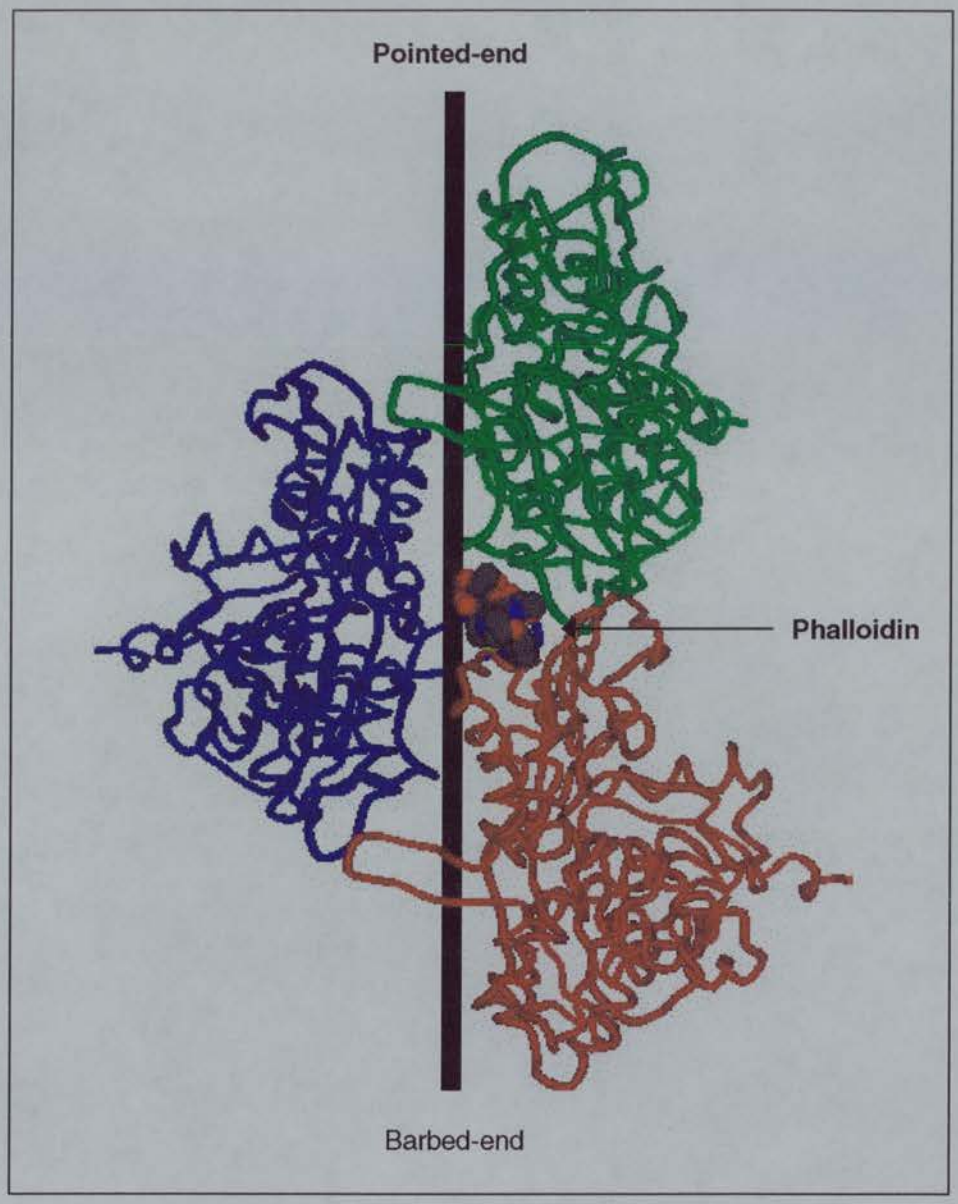

Fig. 4.7. ***Putative model of the phalloidin binding site on F-Actin.*** A schematic representation of the putative model of the phalloidin binding site on the actin filament is shown (as described by Lorenz et al, 1993). Phalloidin binds at a subunit interface and makes contacts with three actin monomers, providing a rationale for the stabilising effects of phalloidin upon filaments. Only three actin monomers are shown (coloured red, green and blue) and they are oriented in a filamentous conformation, as described by the Holmes and Lorenz models (Holmes et al, 1990; Lorenz et al, 1993). The three actin monomers are coloured and oriented in the same way as those in our putative "minifilament" model shown in fig. 4.1. The "minifilament" could theoretically provide a binding site for phalloidin, and in a similar manner to actin filaments, any binding may confer extra stability on the "minifilament".

and help prevent the dissociation of the complex, similar to its stabilising effects on actin filaments.

4.3.2.1 Binding of rhodamine-phalloidin to the putative "minifilament" as analysed by size-exclusion chromatography.

G:A_2 and A:D, in ATP-F-Buffer (in the presence of 0.2mM $CaCl_2$) were added together in a 1:1 molar ratio, at a concentration of 6.0μM for each complex. The "GA_2:AD" mixture was incubated at room temperature for 15min and then rhodamine-phalloidin was added 1:1 (v/v), from a 6.0μM stock in ATP-F-Buffer; 0.2mM $CaCl_2$, giving a 1:1 molar ratio for GA_2:AD/rhodamine-phalloidin, with a final concentration of ~ 3.0μM of each of G:A_2, A:D and rhodamine-phalloidin. Following a further 45min incubation at room temperature, the "GA_2:AD" sample was concentrated and then subjected to size-exclusion chromatography on an FPLC/Superose-12 column, pre-equilibrated in ATP-F-Buffer; 0.2mM $CaCl_2$.

We noted that a small, but significant, proportion of the added rhodamine-phalloidin co-concentrated with the "GA_2:AD" protein fraction (prior to the loading of samples onto the Superose-12 size-exclusion column) in such experiments. The initial concentration of the rhodamine-phalloidin added was 3.0μM. We recovered approximately 2.50 – 2.70μM rhodamine-phalloidin from the flow-through after concentration. (Similar levels of recovery were obtained in 3 other similar experiments; mean concentration of the sample recovered from the flow-through was ~ 2.6μM ± 0.1 SD, n = 4) Correspondingly, approximately 0.3 – 0.5μM rhodamine-phalloidin appears to have co-concentrated with the "minifilament" (~ 10 – 16% of the total rhodamine phalloidin added). The Mr. cut-off of the concentrator membrane was ~ 15,kDa, compared to the Mr. of rhodamine-phalloidin, which is approximately 1,250Da. Thus, the small toxin molecule is unlikely to have been retained by the concentrator membrane. In contrast, concentration of samples from experiments performed with 1:1 molar ratio incubations of rhodamine-phalloidin and either 3.0μM G:A_2 or 3.0μM A:D individually, invariably resulted in the recovery of almost all (~ 98%) of the added 3.0μM rhodamine-phalloidin.

This co-concentration was initially suggestive of a specific binding interaction between rhodamine-phalloidin and a larger protein species containing actin in a filamentous conformation; i.e. the putative "minifilament".

Fig. 4.8(A) shows the elution profile of a 1:1 molar ratio incubation of GA_2:AD (similar to that shown in fig. 4.3A), from a Superose-12 size-exclusion column, compared to that of a similar incubation performed in the presence of rhodamine-phalloidin. There is no apparent difference in the retention volumes for the two samples; however, a slight *leading-edge* was observed in samples incubated in the presence of rhodamine-phalloidin, see fig. 4.8. This leading-edge feature was *only* observed in gel-filtration experiments performed on "GA_2:AD" samples, in the presence of rhodamine-phalloidin. Similar experiments performed on the G:A_2 or A:D complexes individually (at 3.0μM), incubated under the same conditions in the presence of 3.0μM rhodamine-phalloidin showed no evidence of co-purification (or co-concentration) of the phalloidin ligand with the protein complexes. The proteins used in the experiment shown in fig. 4.8 were obtained from different preparations to those used in the experiments illustrated in fig. 4.3(A). The "GA_2:AD" sample contained the equivalent amount of ethanol, ~ 1% (v/v), present in the sample containing rhodamine-phalloidin. A comparison of the elution profiles shown in figs. 4.3A and 4.8(A) indicated that the added ethanol (at least at a concentration of 1%, v/v) was not the cause of the changes in the elution profile (the appearance of a leading-edge) of the putative "minifilament".

SDS-PAGE analysis of the protein components of the elution profiles in fig. 4.8(A) is shown in fig. 4.8(B). The upper gel illustrates the protein peak components from the "GA_2:AD" incubation sample while the lower gel shows the protein components from a similar sample incubated in the presence of 3.0μM rhodamine-phalloidin. Rhodamine-phalloidin appears to have caused a change in the way protein species partition during size-exclusion chromatography. In the presence of rhodamine-phalloidin the leading-edge fractions 9, 10 and 11 (see lower gel in fig. 4.8B) appear to contain relatively more of all three of the component proteins (gelsolin, actin and DNaseI), compared to the corresponding fractions in the upper gel profile. The

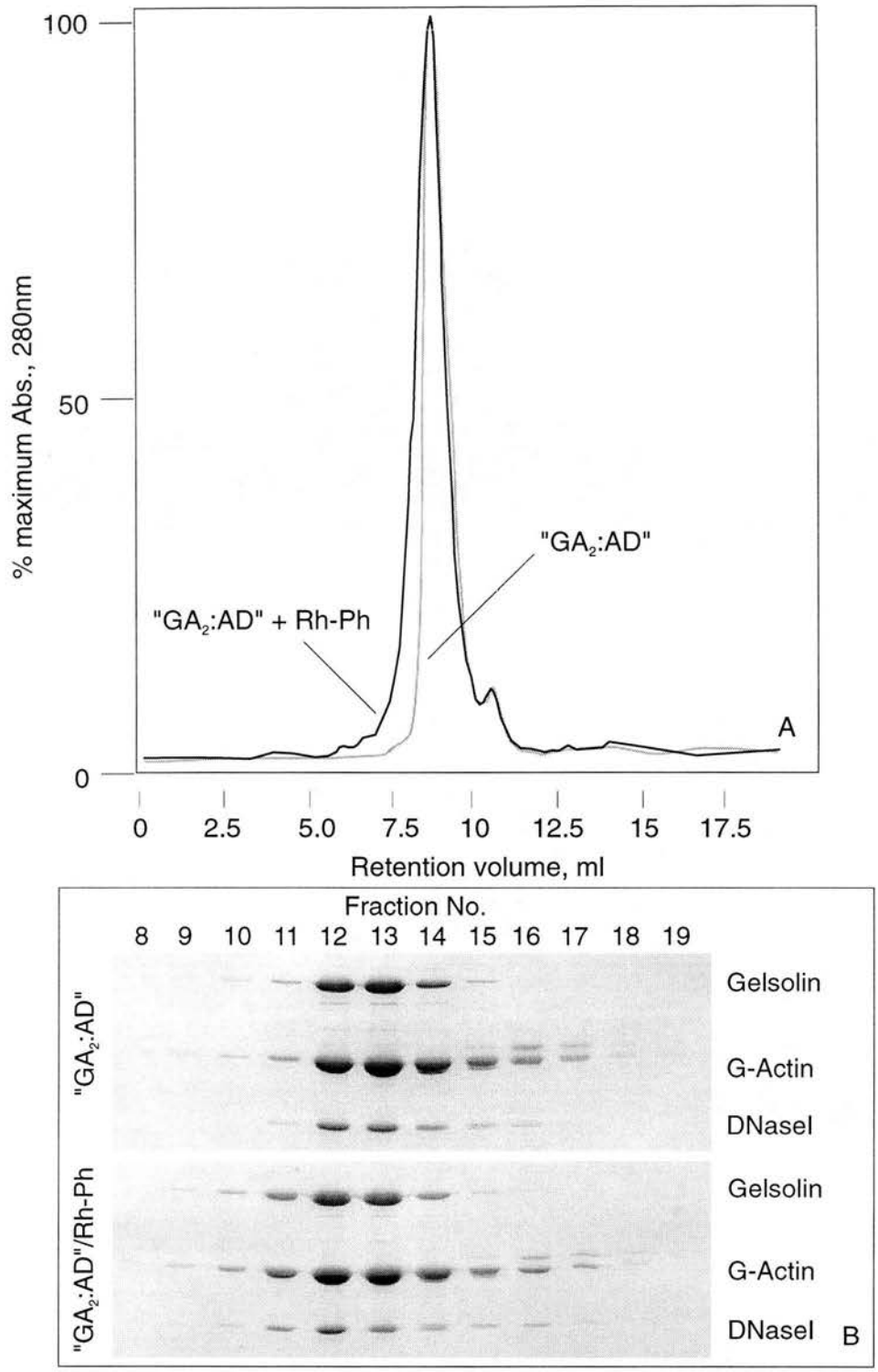

ig. 4.8. *Rhodamine-phalloidin causes a change in the elution profile of the putative "minifilament" omplex.* (A) A_{280nm} monitored elution profiles of the putative "minifilament" complex in the absence or presence of odamine-phalloidin, from an FPLC/Superose-12 size-exclusion column. (B) SDS-PAGE analysis of the two ofiles shown in A. The upper gel shows the SDS-PAGE analysis of the "GA_2:AD" complex profile while the lower presents the "GA_2:AD" complex profile in the presence of rhodamine-phalloidin. A leading-edge to the elution ofile of the putative "minifilament" was observed in the presence of rhodamine-phalloidin. "GA_2:AD" is the mplex formed from an incubation of pre-purified G:A_2 ternary complex and A:D binary complex, mixed at a olar ratio of 1:1 in ATP-F-Buffer; 0.2mM $CaCl_2$. Proteins were mixed together at 3.0μM, incubated for 1hr at RT id concentrated before being loaded onto an FPLC/Superose-12 column, pre-equilibrated in the same buffer. cubation in the presence of rhodamine-phalloidin was performed as follows; G:A_2 and A:D, in the above buffer, ere added together 1:1, (at a concentration of 6.0μM for each). The "GA_2:AD" mixture was incubated at room mperature for 15min and then rhodamine-phalloidin was added 1:1 (v/v) to give a final concentration for all mponents of 3.0μM. Following a further 45min incubation, at room temperature, the sample was concentrated id subjected to size-exclusion chromatography on an FPLC/Superose-12 column, pre-equilibrated in ATP-F-ıffer; 0.2mM $CaCl_2$. (SDS-PAGE and chromatography were performed as described in methods).

relative molar ratios of the proteins present in the peak, both in the absence and presence of rhodamine-phalloidin, did not change. The stoichiometry (as analysed by gel densitometry), of the proteins in both elution profile peaks was ~ 1:3:1, for gelsolin:actin:DNaseI respectively (see table 4.4).

FPLC/Sup-12 size-exclusion	Mole Ratios	
	"GA_2:AD"	"GA_2:AD"/Rh-Ph
gelsolin:actin	1:3.1	1:2.8
DNaseI:actin	1:3.3	1:3.1
gelsolin:DNaseI	1:1.4	1:1.2

Table 4.4. ***Stoichiometry of the individual protein components in the putative "minifilament" is not changed by the presence of rhodamine-phalloidin.*** The values given in the table represent data obtained from gel densitometry (with standard amounts of each of the three proteins added as internal references), performed on the SDS-polyacrylamide gels of the FPLC/Superose-12 size-exclusion elution profiles illustrated in fig. 4.8. (Chromatography, SDS-PAGE and densitometry were performed as described in the methods).

The apparent increase in the relative amounts of protein in the leading-edge fractions of the "GA_2:AD" sample, incubated in the presence of rhodamine-phalloidin, may reflect a direct and specific interaction between the proteins/complexes and the F-Actin binding ligand. The complex/es partitioning within this leading-edge section of the elution profile possibly represent a sub-population of "minifilament" species that has been stabilised by the binding of rhodamine-phalloidin. Our proposed model of the "minifilament" contains three monomers and providing the actin monomers are oriented in a filamentous conformation, phalloidin may bind to the complex (see figs. 4.1 and 4.7). This binding may confer extra stability upon the "minifilament" complex and result in a "stiffening" of this stabilised species. This "stiffening" could conceivably result in an increase in the apparent size and shape of the molecule, with regard to the way the complex partitions during gel-filtration, producing the leading-edge seen in such experiments.

4.3.2.2 Assay of the binding of rhodamine-phalloidin to the putative "minifilament" using fluorescence enhancement.

We have attempted to confirm the binding of rhodamine-phalloidin to the putative "minifilament" and to quantify this interaction using fluorescence enhancement. As described above, we noted that a small, but significant, proportion of the added rhodamine-phalloidin co-concentrated with the "GA_2:AD" protein fraction (prior to the loading of samples onto the Superose-12 size-exclusion column) in experiments similar to those described in fig. 4.8. Approximately 0.3 – 0.5μM rhodamine-phalloidin appeared to co-concentrate with the "minifilament" (~ 10 – 16% of the total rhodamine phalloidin added) suggesting a specific binding interaction.

Fig. 4.9 illustrates the co-purification of rhodamine-phalloidin with the leading-edge fractions of a 1:1 molar ratio incubation (3.0μM for each) of rhodamine-phalloidin and "minifilament" following concentration and size-exclusion chromatography on a Superose-12 column (see legend to fig. 4.8 for details).

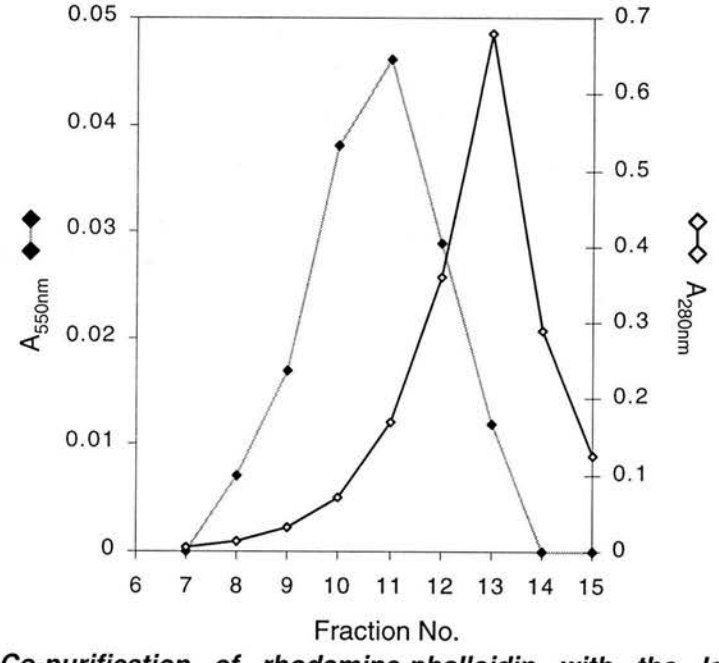

Fig. 4.9. ***Co-purification of rhodamine-phalloidin with the leading-edge fractions of the putative "minifilament" elution profile.*** The absorbance intensities at 280nm measuring total protein (open squares) and 550nm measuring rhodamine-phalloidin (closed squares), were measured for fractions 7 – 15, from a Superose-12 size-exclusion column elution profile, of a 1:1 molar ratio incubation (3.0μM for each), of "minifilament" and rhodamine-phalloidin. (For details see legend to fig. 4.8A). Rhodamine-phalloidin co-purifies with the leading edge fractions. The Mr. of the species present in this section of the elution profile is very much larger than the ~ 1250Da for rhodamine-phalloidin. This implies a specific binding interaction with a protein species containing actin monomers in a filamentous conformation.

We have used the absorbance at 550nm to follow the presence of rhodamine-phalloidin in these leading-edge fractions. Unlike the assay described in section 4.3.1, we were unable to obtain a reliable estimate for the extent (if any) of the fluorescence enhancement of the rhodamine-phalloidin putatively binding to the "minifilament" in these leading-edge fractions. Thus, using fluorescence intensity measurements may have resulted in an over estimation of the amount of binding. The rhodamine-phalloidin peaks close to fraction 11 (see fig. 4.9) and this corresponds well with increase in the amounts of protein observed in these leading-edge fractions, as observed on SDS-polyacrylamide gel analysis performed on such elution profiles (see fig. 4.8B, fraction Nos. 9, 10 and 11).

Table 4.5 shows the mean fluorescence enhancement levels obtained from several experiments where we titrated a fixed amount of rhodamine-phalloidin (0.32μM), against 3.0μM of G:A_2 or 3.0μM of A:D individually, or against increasing amounts of putative "minifilament" complex, under polymerising conditions (ATP-F-Buffer; 0.2mM $CaCl_2$). Following incubation, at 22°C for 1hr in the dark, the fluorescence intensity was measured

Protein species	ΔF_{580nm} (arbitrary units)
3.0μM G:A_2 ternary complex	0.9 (± 0.28 SD, n=4)
3.0μM A:D binary complex	0.7 (± 0.21 SD, n=3)
GA_2:AD/"minifilament"	
0.5μM	11.3 (± 4.2 SD, n=3)
1.0μM	14.6 (± 5.5 SD, n=4)
2.0μM	25.5 (± 8.2 SD, n=4)
3.0μM	44.7 (±10.2 SD, n=3)
4.0μM	36.0 (± 10.4 SD, n=4)
6.0μM	49.2 (± 11.1 SD, n=5)
7.5μM	66.2 (± 9.7 SD, n=4)
9.0μM	55.5 (± 9.1 SD, n=3)
10.0μM	65.7 (± 9.4 SD, n=3)

Table 4.5. ***The G:A_2 ternary and A:D binary complex alone do not give fluorescence enhancement.*** The table shows the mean fluorescence enhancement values of 0.32μM rhodamine-phalloidin with 3.0μM of G:A_2 or 3.0μM of A:D individually, and those of 0.32μM rhodamine-phalloidin with increasing amounts of the putative "minifilament" complex observed after a 1hr incubation at 22°C, in ATP-F-Buffer; 0.2mM $CaCl_2$. (The excitation wavelength was 550nm, the emission wavelength was 580nm, with a 5nm slit width for both).

Significant amounts of fluorescence enhancement were observed *only* in the presence of "GA_2:AD" (compared to that for 0.32μM rhodamine-phalloidin alone or in the presence of G:A_2 or A:D alone). Incubation of 3.0μM G:A_2 or 3.0μM A:D individually in the presence of 0.32μM rhodamine-phalloidin (in ATP-F-Buffer; 0.2mM $CaCl_2$), produced virtually no fluorescence enhancement. Mean ΔF values of 0.9 (± 0.28 SD, n = 4) for 3.0μM G:A_2 and 0.7 (± 0.21 SD, n = 3) for 3.0μM A:D alone were obtained, see table 4.5. We would postulate that neither of these two individual species (G:A_2 and A:D) would contain a binding site for phalloidin (see fig. 4.11) and the results are consistent with there being no binding. The partial co-purification and the significant levels of fluorescence enhancement for rhodamine-phalloidin in the presence of "minifilament" (1:1 molar ratio incubation, under polymerising conditions of G:A_2 and A:D) is suggestive of a specific binding interaction.

Using the fluorescence enhancement assay for the titration of 0.32μM rhodamine-phalloidin with F-Actin (see figs. 4.5, 4.6 and table 4.3) we were able to define an enhancement calibration constant (592.2 arbitrary fluorescence units.μM-1) and use it to calculate the amount of binding for any level of enhancement (Huang et al, 1992). We were unable to determine an accurate calibration factor for the binding of rhodamine-phalloidin to the putative "minifilament", and so were unable to employ this specific method in the analysis of the apparent binding. Despite this and the fact that the fluorescence intensity values obtained during the titration of rhodamine-phalloidin with "minifilament" were prone to large levels of fluctuation and large errors (see table 4.5), we have determined an approximate equilibrium dissociation constant for the putative binding interaction between the "minifilament" and rhodamine-phalloidin.

The general trend for the data presented in table 4.5 appears to be an increase in the level of fluorescence enhancement as we increase the amount of added "minifilament". Correspondingly we have assumed a concomitant increase in the amount of bound rhodamine-phalloidin, analogous to that observed with actin filaments (see fig. 4.6A). A non-linear least squares fit of the data presented in table

4.5 is shown in fig. 4.10. An apparent K_d of ~ 4.6μM was obtained by this analysis (assuming a 1:1 stoichiometric binding between rhodamine-phalloidin and the "minifilament" at saturation). The calculated ΔF_{max} for this interaction is ~ 93 arbitrary units, corresponding to an enhancement of approximately 3 - 5 times. The apparent dissociation constant of ~ 4.6μM, for the binding of rhodamine-phalloidin to the putative "minifilament", is very much weaker than the equivalent interaction between rhodamine-phalloidin and F-Actin, (K_d ~ 57nM, see fig. 4.6 and table 4.3). The affinity of the toxin has decreased by ~ 100 times (two orders of magnitude).

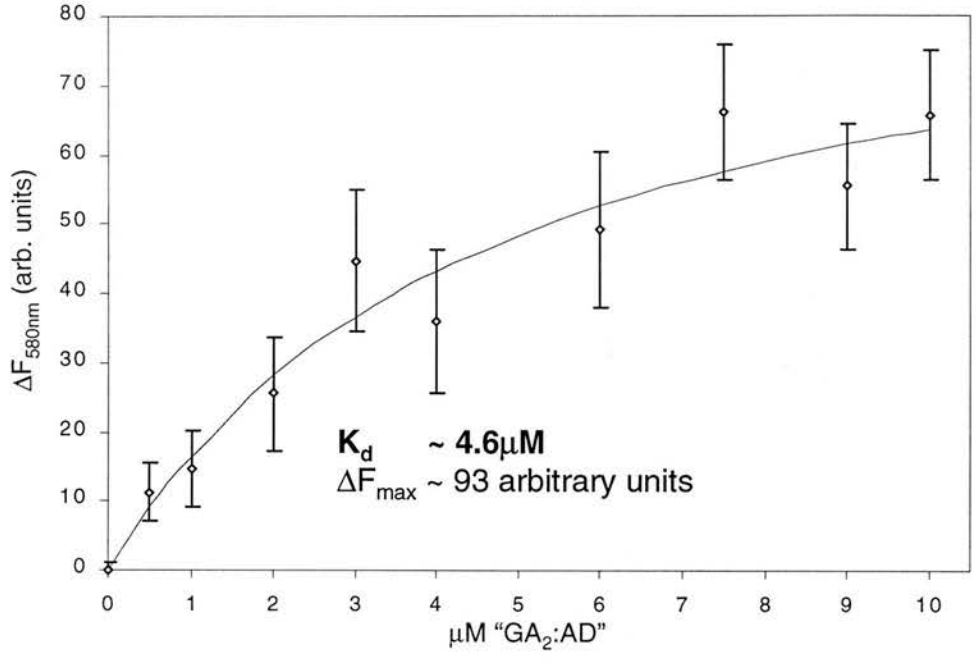

Fig. 4.10. ***Probing the "minifilament" for F-like conformation using rhodamine-phalloidin.*** Fluorescence titration of putative "minifilament" against 0.32μM rhodamine-phalloidin in ATP-F-Buffer, in the presence of 0.2mM $CaCl_2$. The solid line is a non-linear least squares fit of the equation $\Delta F = \Delta F_{max}*[GA_2:AD]/([GA_2:AD]+K_d)$. The apparent K_d for the binding of rhodamine-phalloidin to the putative "minifilament" is ~ 4.6μM, (R = 0.973). Titration was performed by adding 250μl of increasing amounts of "minifilament" (GA_2:AD), in ATP-F-Buffer; 0.2mM $CaCl_2$, to 250μl of 0.64μM rhodamine-phalloidin (100μM stock in ethanol), in the same buffer. The samples were incubated for 1hr, at 22°C in the dark, and then the fluorescence intensity of each sample was measured. The excitation wavelength was 550nm, the emission wavelength was 580nm, with a 5nm slit for both. The error bars indicate 1SD.

Our results are not inconsistent with the formation of a relatively tight and stable "minifilament" complex with stoichiometry of **G:A_3:D**. There also appears to be an

apparently specific binding of rhodamine-phalloidin to the putative "minifilament". We observed significant levels of fluorescence enhancement of rhodamine-phalloidin *only* in the presence of "GA_2:AD". The dissociation constant for this interaction is approximately 4.6μM. Although this is ~100 weaker than that for rhodamine-phalloidin and F-actin, our data suggest that there is an interaction between rhodamine-phalloidin and a protein species that contains actin monomers oriented in a filamentous conformation.

4.3.3 Myosin S-1 head binding to the putative "minifilament"

We next wanted to test whether we could use the myosin S-1 head's F-Actin specific binding activity to test the putative "minifilament" for filamentous character. We proposed to use the S-1 head and the tight, F-Actin specific binding (in an ATP manner) to probe the conformation of the actin monomer in the putative "minifilament". Binding of the S-1 head to the putative "minifilament" would provide a positive indication that the actin monomer conformation was indeed that of F-Actin.

4.3.3.1 Probing the conformation of the putative "minifilament" with the myosin S-1 head

Dr. John Kendrick-Jones kindly supplied us with a preparation of the myosin S-1 head from rabbit muscle, prepared by papain digestion (see methods for details). This treatment results in the generation of several polypeptide chains of varying lengths, as analysed on SDS-PAGE. Polypeptides of 94kDa and 70kDa correspond to the heavy chains while three polypeptides, with Mr. between 14– 30kDa, correspond to fragments derived from the light chains. Fig. 4.11 shows the standard electrophoretic mobilities of gelsolin, G-Actin, DNaseI and the various polypeptide chains derived from the myosin S-1 head, on an SDS-polyacrylamide gel.

Fig. 4.12 shows the elution profile from an FPLC/Superose-12 size-exclusion column, run in ATP-F-Buffer; 0.2mM $CaCl_2$ of the S-1 head alone (peak 2). Table

4.6 displays the retention volume and the corresponding mean apparent Mr. of the S-1 head compared to the A:D, G:A, G:A_2 and putative GA_2:AD/"minifilament" complexes. The apparent Mr. value of the S-1 head is ~ 180kDa. The substantial difference between the apparent Mr. and the theoretical Mr. (180kDa compared to 120 – 130kDa) is probably due to the asymmetric non-globular shape of the S-1 head (~ 165Å long, ~ 65Å wide and up to 40Å thick, Rayment et al, 1993b).

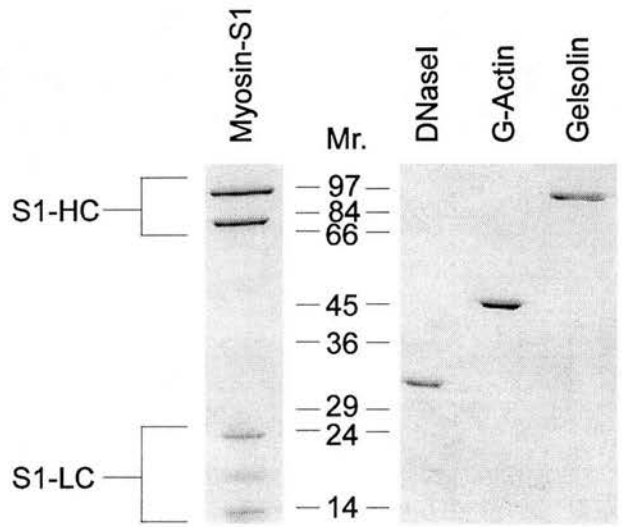

Fig 4.11. ***SDS-polyacrylamide gel showing the standard electrophoretic mobilities of Gelsolin, G-Actin, DNaseI and the polypeptides from the myosin S-1 head.*** The myosin S-1 head, prepared by papain cleavage, produces 5 protein bands present. The two at ~ 94kDa and 70kDa correspond to the polypeptides derived from the heavy chains (labelled S1-HC). Those corresponding to the fragments derived from the light chains have Mr. between 14kDa and 30kDa (labelled S1-LC). Mr. of protein standards are given in kilodaltons. (SDS-PAGE was performed as described in the methods).

G:A_2 ternary complex and A:D binary complex were added together at a 1:1 molar ratio (6.0μM) and incubated for 30min at room temperature, in ATP-F-Buffer; 0.2mM $CaCl_2$. Myosin S-1, in the same buffer was then added at a molar ratio of 1:1 (S-1:"minifilament"). The final concentrations of G:A_2, A:D and S-1 were 3.0μM. This S-1/"minifilament" mixture was then incubated for a further 30min at room temperature, in ATP-F-Buffer; 0.2mM $CaCl_2$. Following the incubation the mixture was subjected to size-exclusion chromatography on an FPLC/Superose-12 column, pre-equilibrated in ATP-F-Buffer; 0.2mM $CaCl_2$.

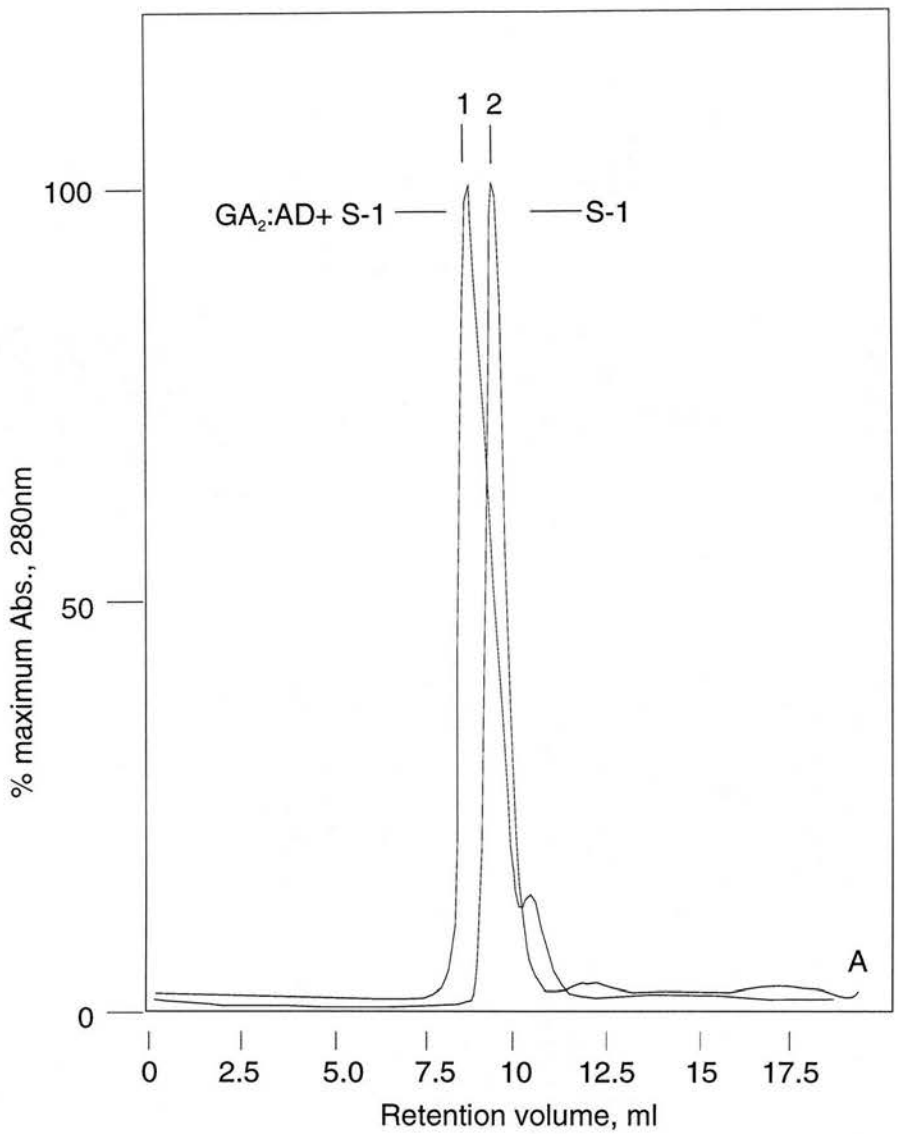

Fig. 4.12. ***Probing the conformation of the putative "minifilament" with the myosin S-1 head.*** A_{280nm} monitored elution profiles of the S-1 myosin head alone, and a 1:1 molar ratio incubation of S-1 and putative "minifilament" complex (GA_2:AD), from an FPLC/Superose-12 size-exclusion column. For comparison of different profiles the absorbance values have been normalised to the maximum at the peak. The arrows mark the elution positions of (1) GA_3:D + S-1: (2) myosin S-1 head. The GA_3:D + S-1 sample was formed in the following manner. G:A_2 ternary complex and A:D binary complex were added together at a 1:1 molar ratio (6.0μM for each complex) and incubated for 30min at room temperature, in ATP-F-Buffer; 0.2mM $CaCl_2$. Myosin S-1, in the same buffer, was then added at a molar ratio of 1:1 (S-1:"minifilament"). The final concentrations of G:A_2, A:D and S-1 were ~ 3.0μM. This s-1:"minifilament mixture was then incubated for a further 30min at room temperature, in ATP-F-Buffer; $CaCl_2$. Following incubation the mixture was concentrated and loaded onto an FPLC/Superose-12 size-exclusion column, pre-equilibrated in ATP-F-Buffer; 0.2mM $CaCl_2$. (SDS-PAGE and chromatography were performed as described in methods).

Protein species	Retention volume (ml)	Theoretical Mr. (kDa.)	Apparent Mr. (kDa.)
actin:DNaseI (A:D)	10.90 (± 0.039 SEM, n=10)	71	92
gelsolin:actin binary complex (G:A)	10.13 (± 0.066 SEM, n=4)	124	149
myosin-S1 head (papain cleavage)	9.79 (± 0.064 SEM, n=4)	120 – 130	180
gelsolin:actin$_2$ ternary complex (G:A$_2$)	9.59 (± 0.037 SEM, n= 12)	166	209
GA$_2$:AD "minifilament" complex	9.17 (± 0.026 SEM, n=8)	237 (a 1:1 binding interaction).	271

Table 4.6. *Retention volumes (ml) of the myosin S-1 head, A:D, G:A and G:A$_2$ complexes and that of the putative "minifilament".* Data obtained from FPLC/Superose-12 size-exclusion chromatography experiments, in ATP-F-Buffer; 0.2mM $CaCl_2$. The value given for the apparent Mr. is a mean value calculated from the calibration curve using the corresponding mean retention volume. The significance of the difference between the mean retention volume of G:A$_2$ and that of "GA$_2$:AD" (the putative "minifilament" peak) is $P<0.05$. Myosin S-1 was produced by papain digestion. This protocol generates heavy-chains with Mr. of 94kDa and 70kDa and three light chain derived fragments with Mr. ranging from 14 – 30kDa. (See methods for details).

Fig 4.12 shows the elution profile from an FPLC/Superose-12 size-exclusion column (in ATP-F-Buffer; 0.2mM $CaCl_2$) of a 1:1 molar ratio incubation of myosin S-1 and "minifilament", (peak 1) compared to that of myosin S-1 alone (peak 2). There was no apparent increase in the retention volume of the 1:1 S-1/"minifilament" incubation compared to that of putative "minifilament" alone. There were also no apparent changes in the shape and width of the elution profile, (compare peak 1 in fig. 4.12 with the peak 1 in fig. 4.3) unlike that observed in similar experiments with rhodamine-phalloidin (see peak 1, fig. 4.8). These data are consistent with there being *no* interaction between the putative "minifilament" and the S-1 head of myosin, in the presence of ATP.

SDS-PAGE analysis of the elution profiles shown in fig. 4.12 appears to confirm this observation. The SDS-polyacrylamide gel illustrated in fig. 4.13(A) shows the protein components of the S-1 head elution profile. The gel below (fig. 4.13B) shows the protein components of the 1:1 S-1/"minifilament" incubation elution profile. The two gels are positioned so that the corresponding fractions collected from each of the

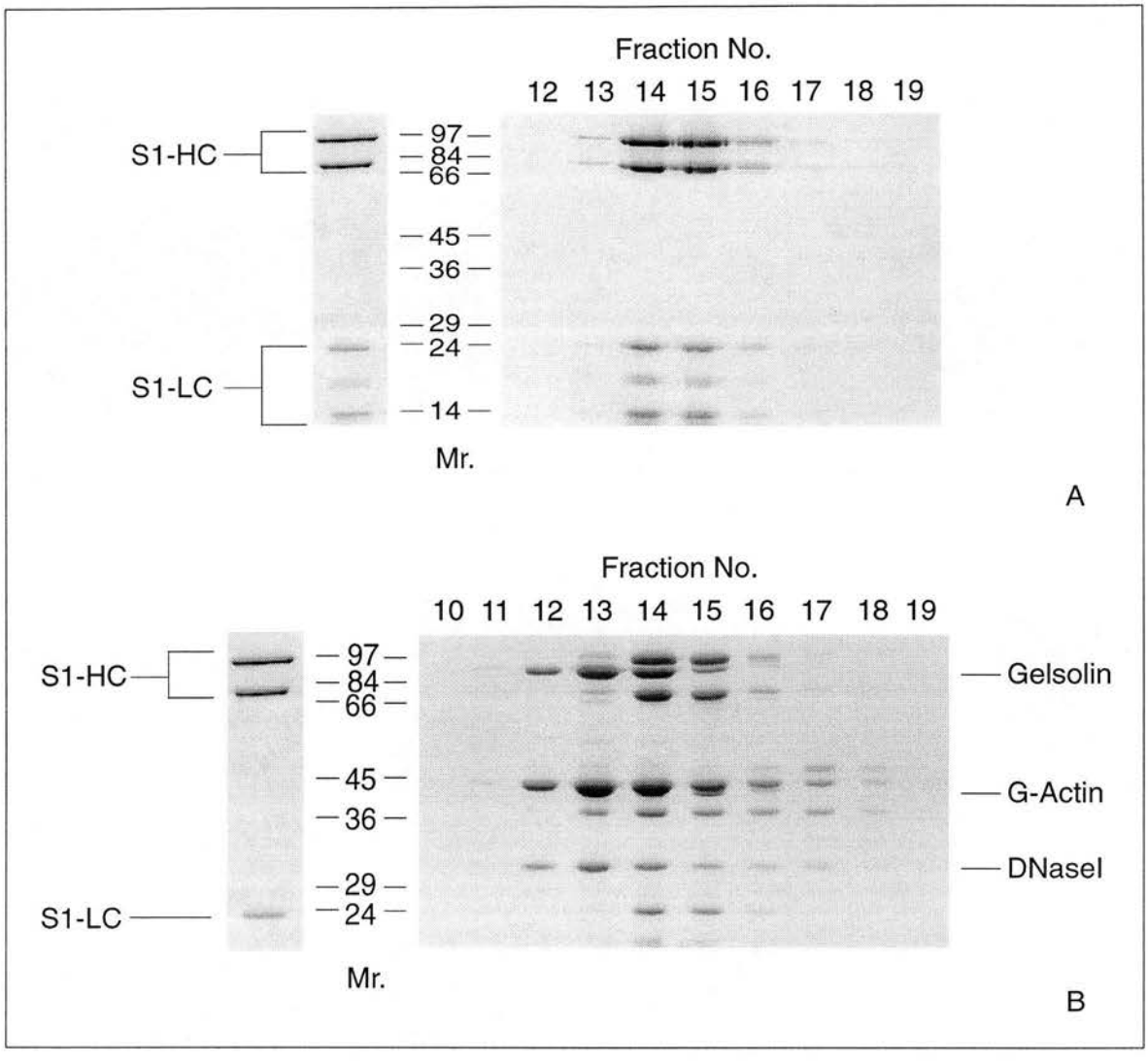

Fig. 4.13. ***Myosin S-1 head does not bind to the putative "minifilament", in the presence of ATP.*** (A) SDS-polyacrylamide gel showing the protein composition of the S-1 elution profile (peak 2) from fig. 4.12. (B) SDS-polyacrylamide gel showing the protein composition of the 1:1 "GA_3:D + S-1" incubation elution profile (peak 1) from fig. 4.12. "GA_3:D + S-1": G:A_2 ternary complex and A:D binary complex were added together at a 1:1 molar ratio (6.0μM for each complex) and incubated for 30min at room temperature, in ATP-F-Buffer; 0.2mM $CaCl_2$. Myosin S-1, in the same buffer was then added at a molar ratio of 1:1 (S-1:"minifilament"). The final concentrations of G:A_2, A:D and S-1 were 3.0μM. This S-1:"minifilament" mixture was then incubated for a further 30min at room temperature. Following the incubation the mixture was concentrated and loaded onto an FPLC/Superose-12 size-exclusion column, pre-equilibrated in ATP-F-Buffer; 0.2mM $CaCl_2$. Preparation of the myosin S-1 head by papain cleavage produces 5 polypeptide bands on SDS-polyacrylamide gels. The two at ~ 94kDa and 70kDa correspond to the polypeptides derived from the heavy chains (labelled S1-HC). Those corresponding to the fragments derived from the light chains have Mr. between 14kDa and 30kDa (labelled S1-LC). Mr. of protein standards are given in kilodaltons. (SDS-PAGE was performed as described in the methods).

two separate chromatographic runs are directly aligned with each other. The S-1 head does not appear to have shifted from its normal elution position. The peak fraction for the elution of S-1 is ~ 14. Comparison of the peak fraction positions of the constituent myosin S-1 polypeptides in fig. 4.13(A) and (B) suggests no shift in the retention volume of S-1. The positions of the three proteins (gelsolin, actin and DNaseI) that constitute the putative "minifilament", with regard to the fractions they appear in, also appear not to have changed. (Compare their positions in figs. 4.3B and 4.14B).

The affinity of myosin for actin filaments increases dramatically in the absence of ATP, and actin and the S-1 head form a very tight rigor complex ($K_a \sim 10^7 - 10^8\ M^{-1}$ for acto-S1, Marston and Weber, 1975; Margossian and Lowey, 1978). We have attempted further experiments to analyse any binding of the S-1 head to the putative "minifilament" in the absence of ATP. The protocol used in the creation of a nucleotide free solution is based on that described by Pollard et al (1992) and De la Cruz and Pollard (1994) (see methods for details).

$G:A_2$ ternary complex and A:D binary complex were added together at a 1:1 molar ratio (6.0μM for each complex) and incubated for 30min at room temperature, in modified ATP-F-Buffer (5mM Tris, pH 8.0; 0.5mM DTT; 0.2mM $CaCl_2$; 0.2mM ATP; 100mM KCl; 2mM $MgCl_2$; <u>50nM ATP</u>). Myosin S-1, in nucleotide-free-ATP-F-Buffer (5mM Tris, pH 8.0; 0.5mM DTT; 0.2mM $CaCl_2$; 100mM KCl; 2mM $MgCl_2$), was then added at a molar ratio of 1:1 (S-1/"minifilament"). The final concentrations of $G:A_2$, A:D and S-1 were ~ 3.0μM. Removal of free nucleotide from this mixture was performed by gently mixing 25μl Dowex 1 beads (Bio-Rad, AG1-X2, stored as a 50% slurry in a nucleotide-free ATP-F-Buffer) with the protein solution, followed by an incubation of 5min at 4°C. (Dowex 1 is a strong anion exchange resin and it binds free nucleotide very tightly). Following removal of the Dowex 1 resin, the proteins mixture was incubated at room temperature for a further 30min, and then subjected to size-exclusion chromatography on an FPLC/Superose-12 column, pre-equilibrated in nucleotide-free ATP-F-Buffer.

This method of free nucleotide removal proved to be unsuccessful in our experiments. We experienced a rapid and extensive protein denaturation upon incubation with the Dowex 1 beads. Denaturation was observed as the appearance of peaks, in A_{280nm} monitored elution profiles from Superose-12 size-exclusion chromatographic runs (performed on samples treated as described above) that were indicative of denatured protein aggregates (data not shown). These denatured aggregates frequently had elution volumes that overlapped with the non-denatured protein complexes and made interpretation of the data almost impossible. The amount of denaturation we observed was very preparation dependent but all of the proteins in the incubation mixture (DNaseI, gelsolin, actin and myosin S-1) appeared to be affected to some degree. However, actin was by far the most predominantly affected protein, with a loss of native protein from the incubation solution of between ~ 40 – 65%. SDS-PAGE analysis of such elution profiles produced a high degree of band smearing and often showed evidence of loss of resolution probably due to the presence of these denatured aggregates.

We have not pursued these experiments further due to the initial problems with denaturation.

4.4 Discussion

4.4.1 Overview

G:A_2 ternary and A:D binary complexes were added together (1:1 molar ratio, at 3.0μM) under polymerising conditions (100mM KCl; 2mM $MgCl_2$ in the presence of 0.2mM $CaCl_2$) and complex formation analysed on size-exclusion columns. Our results are consistent with G:A_2 and A:D having associated together to form a significantly larger species (in relation to G:A_2). This putative capped-actin-"minifilament" appears to have stoichiometry of **G:A_3:D** (gelsolin:actin$_3$:DNaseI).

We observed little evidence of complex formation on Native-PAGE. A possible explanation for this may result from the harsh solution conditions and the rapid changes in charge distribution experienced by the proteins and protein complexes during such electrophoresis experiments (see section 4.3.2 for details), that may have prevented and/or compromised any complex formation.

We performed experiments with rhodamine-phalloidin and the proteolytic myosin S-1 head to specifically probe the actin monomers, within this putative "minifilament", for filamentous conformation. Data from fluorescence enhancement experiments performed with rhodamine-phalloidin, provides some evidence for the specific binding of rhodamine-phalloidin to the putative "minifilament", with a K_d of ~ 4.6μM.

Our results are consistent with there being no binding between the putative "minifilament" and the myosin S-1 head, in the presence of ATP (0.2mM). This may be due to the reduced affinity of myosin for F-Actin in the presence of ATP, and not solely due to the actin monomers lacking filamentous character. Experiments in the absence of ATP proved to be problematic.

4.4.2. $G:A_2$ and A:D associate to form a larger complex, consistent with the proposed capped-"minifilament" model

Data from our size-exclusion experiments, performed on 1:1 molar ratio mixtures of $G:A_2$ and A:D (under polymerising conditions: 100mM KCl; 2mM $MgCl_2$; 0.2mM $CaCl_2$; 0.2mM ATP; 0.5mM DTT; 5mM Tris, pH 8.0; 1.0mM NaN_3), at concentrations in excess (3.0μM for each complex) of the critical monomer concentration of the pointed-end, seem to indicate the formation of a larger complex (in relation to $G:A_2$), with an apparent Mr. of ~ 271kDa. The stoichiometry of the protein components within this larger complex was **1:3:1** (gelsolin:actin:DNaseI, respectively). The apparent molecular weight and stoichiometry of this species is consistent with the formation of the putative "minifilament" complex, most likely via an actin:actin association between the $G:A_2$ ternary and the A:D binary complexes.

The dissociation constant for ATP-G-Actin binding to the pointed-end of a pre-formed actin filament is ~ 0.6 – 0.8μM (Pollard, 1986). If we were simply adding a further actin monomer (in the form of A:D binary complex) to the pointed-ends of the monomers within the $G:A_2$ complex we might have expected that any association between the A:D and the $G:A_2$ complexes (via an actin:actin monomer association occurring between the free ends of these two complexes), would have had a K_d of the order of 0.6 – 0.8μM, or even significantly weaker. Our results discussed in chapter 3 (see section 3.5) indicate the spatial orientation of the actin monomers within the $G:A_2$ ternary complex is different to that of the terminal monomers at the barbed-end of filaments. Therefore, we are probably not dealing with a "true" pointed-end, with regards to the addition of subsequent actin subunits onto the exposed pointed-ends of the $G:A_2$ ternary complex monomers.

However, the addition of a "third" actin monomer, in the form of A:D, may have shifted the conformation of the monomers in $G:A_2$ to be more like those in a filament. Our results (see section 3.4) indicate that the A:D binary complex behaves essentially as an actin monomer with regards to its interaction with gelsolin; the K_d for binding of A:D by G:A is equivalent to the binding of G-Actin alone by G:A. The

presence of DNaseI bound at the pointed-end appears not to alter the crystal structure of the monomer to any great extent; the structure of the monomer in the DNaseI-Actin complex (Kabsch et al, 1990) is the same as that in the G1-Actin complex (McLaughlin et al, 1993; see McLaughlin and Weeds, 1995 for review). The complexed (A:D) monomer also does *not* appear to exhibit different actin:actin interactions with other actin monomers, with regards to its binding at the pointed-ends of filaments, compared to those of uncomplexed G-Actin (Podolski et al, 1988; Pope et al, 1991; Weber et al, 1994). Furthermore, the presence of the DNaseI molecule acts to *prevent* any further monomer addition at the pointed-end.

Thus, adding the "third" A:D monomer may have shifted the conformation of the actin monomers within $G:A_2$ to a more filamentous conformation, resulting in the creation of a "capped-trimer" species, with the three actin subunits in an F-like conformation; i.e. putative "minifilament".

There are multiple equilibrium interactions possible in such 1:1 mixtures of $G:A_2$ and A:D. As well as the proposed actin:actin interaction between the $G:A_2$ and A:D complexes (giving rise to the formation of the putative "minifilament"), there is also a possible exchange reaction. The apparent equivalence of the K_d values for the formation of the GA:(A:D) and $G:A_2$ complexes (50nM and 39nM, respectively; see section 3.4) implies that, at equilibrium in 1:1 molar ratio mixtures of $G:A_2$ and A:D, a significant amount of exchange of the actin monomer (bound at the EGTA site in gelsolin, G4), for the A:D binary complex, would occur. Significant levels of exchange occurring at this G4 actin-binding site has previously been demonstrated in mixtures of NBD-Actin and unlabeled $G:A_2$ ternary complex (Schoepper and Wegner, 1991; Khaitlina and Hinssen, 1997). Such an exchange of G-Actin for A:D would then result in the formation of significant amounts of the $G:A_2$:D complex and the corresponding amount of free G-Actin.

However, we did not observe any evidence of significant amounts of free G-Actin in our size-exclusion experiments. During all of our chromatographic analysis, conducted on 1:1 molar ratio incubation mixtures of $G:A_2$ and A:D, we detected little

of either of the two individual complexes. The elution profiles obtained from such gel-filtration experiments always contained a *single* sharp and relatively symmetrical peak, with only a small trailing-edge. This trailing-edge (containing only very small amounts of A:D binary complex) accounted for no more than ~ 10% of the total protein partitioning on the column (see section 4.2.1). These profiles also all showed a significantly shifted retention-volume, indicative of the formation of a larger protein complex with a mean apparent Mr. of ~ 271kDa with a stoichiometry of 1:3:1 (gelsloin:actin:DNaseI, respectively). Furthermore, the peak-areas for this new complex did not significantly change, in relation to the peak-areas obtained for the individual G:A_2 or A:D complexes alone. No peak broadening, that would suggested the inefficient separation of the two smaller complexes (G:A_2 and A:D) from each other was observed. These profiles are indicative of the partitioning of a stable and predominantly *mono-disperse* protein-complex species. This size-exclusion data is consistent with the formation of a stable G:A_3:D complex but alone not proof of a putative "minifilament" complex.

These results suggest that the interaction between G:A_2 and A:D is *more* stable than one would have theoretically expected. They suggest that the majority of A:D was bound to the pointed-ends of the monomers in the G:A_2 complex and therefore that the amount of exchange occurring was less than expected; i.e. the "minifilament" has formed with a *higher* than expected stability.

For complex formation to occur the actin:actin binding interaction between A:D to G:A_2 would have to have a K_d below the critical concentration of the pointed-end (K_d <0.6μM). The affinity even possibly approaches a value of similar magnitude to those observed for the binding of A:D by G:A, (~ 50nM), to give the significant amounts of "minifilament" (G:A_3:D) we apparently observe at equilibrium, over the formation of the G:A_2:D complex via the exchange reaction. Our size-exclusion elution profiles, indicating the formation of a larger (in relation to G:A_2) and predominantly mono-disperse complex, with a stoichiometry of 1:3:1 (gelsolin:$actin_3$:DNaseI) for the peak components, are consistent with the formation of the putative "minifilament".

This is an unexpected result, but a significant one, that suggests that the actin:actin interactions that occur between the G:A_2 complex and the A:D complex, during the formation of the "minifilament", are significantly *stronger* (and thus, may be different) than the actin:actin interactions that hold the filament together.

Further evidence for the formation of the "minifilament" comes from experiments with rhodamine-phalloidin. Our data (see section 4.3.2) appear to indicate the binding of rhodamine-phalloidin, an *F-Actin specific* binding molecule, to the putative "minifilament". Incubation of rhodamine-phalloidin (3.0μM) with 1:1 molar ratio mixtures of G:A_2 and A:D (3.0μM for each) resulted in a change in the way the proteins partition during gel-filtration experiments. Although the apparent Mr. (~ 271kDa) of the single peak, and the stoichiometry of the peak components (1:3:1 gelsolin:actin:DNaseI, respectively) did not change, (in relation to those experiments performed in the absence of rhodamine-phalloidin), a slight *leading-edge* appeared in these elution profiles. A small amount of rhodamine-phalloidin co-purified (~ 10 – 16% of the total added 3.0μM) with the proteins/protein complexes present within these leading-edge fractions. Furthermore, the fractions of this leading-edge contained increased amounts of all three proteins (gelsolin, actin and DNaseI), with unchanged stoichiometry, compared with the same fractions obtained from size-exclusion experiments performed in the absence of rhodamine-phalloidin.

These data appeared to indicate a specific interaction between the putative "minifilament" and rhodamine-phalloidin. We only observed these changes in the presence of *both* G:A_2 and A:D; Similar experiments with the two individual complexes alone, showed no evidence of co-purification with rhodamine-phalloidin or shifts in the elution profiles. The results were not inconsistent with the binding of rhodamine-phalloidin, to a sub-population of the putative "minifilament". The protein complex/es partitioning within the leading edge-fractions may have been stabilised by the binding of the phalloidin molecule that then resulted in a "stiffening" of the complex. This decrease in the flexibility of the putative complex may then possibly have resulted in an increase in the apparent size or shape that this species presents, with regards to the partitioning during gel-filtration

chromatography. This binding interaction (rhodamine-phalloidin is an *F-Actin specific* binding molecule) implies that the actin monomers within the protein complex/es partitioning within these leading-edge fractions possess a filamentous conformation. Or at least that the conformation is relatively flexible and could be shifted more towards that of a filamentous conformation, by the binding of rhodamine-phalloidin.

Using fluorescence enhancement experiments we have further characterised the apparently specific binding of rhodamine-phalloidin to the putative "minifilament". We only observed significant fluorescence enhancement in the presence of *both* G:A_2 ternary complex and A:D binary complex (essentially no enhancement was observed with either of the two smaller complexes – A:D or G:A_2 – on their own, see section 4.3.2). Although the noise levels we observed were high, this enhancement further suggested a *specific* interaction between the rhodamine-phalloidin and the new, larger putative "minifilament" complex. The apparent K_d for rhodamine-phalloidin binding to the putative "minifilament" species was ~ 4.6μM. This K_d value is ~100 fold lower than the binding of for rhodamine-phalloidin to actin filaments (K_d ~ 40 - 50nM; Huang et al, 1992; and see our own results described in section 4.3.1).

These results provide further, and again significant, evidence for the formation of a putative "minifilament" complex, with the actin monomers within such a species having filamentous-like conformation. The loss of binding affinity and the noisy fluorescence signals we observed are probably not an unexpected feature of the binding of rhodamine-phalloidin to such a protein complex that, after all, at best only contains the minimal number of actin subunits (three) to bind phalloidin.

A refinement of the actin filament model in the presence of phalloidin (Lorenz, et al, 1993), coupled with other data, from biochemical cross-linking experiments (Faulstich et al, 1993) and yeast point mutations that no longer bind to phalloidin (Drubin et al, 1993), has suggested that the binding site for phalloidin lies at a subunit interface between three actin subunits (see fig. 4.7). It is not difficult to

envision why the very stereo-specific binding of phalloidin at this binding site on F-Actin has the stabilising effects on actin filaments it does.

Although our "minifilament" model theoretically contains only a single rhodamine-phalloidin binding site, this site in the "minifilament" is probably very much more flexible and the very specific orientation required for the tight binding of phalloidin is not as well maintained as in the more stable filament. The three monomers in the putative "minifilament" are unlikely to experience the same strong co-operative effects, arising from the further inter-molecular monomer:monomer interactions, that contribute to the overall stability of the filament (Bremer et al, 1991). Furthermore, due to the symmetry of the filament model (Holmes et al, 1990; Lorenz et al, 1993), and the position of the putative phalloidin binding site at an interface between three subunits (see fig. 4.7), the stoichiometry of rhodamine-phalloidin binding to F-Actin is 1:1, phalloidin:actin monomer (Huang et al, 1992; Cano et al, 1992; De la Cruz and Pollard, 1994; and see also our results in section 4.3.1). Thus, over the whole length of a filament each monomer contributes to *three* separate phalloidin binding sites and thus would be braced by the stabilising interactions arising from these interactions. Our putative "minifilament" model, at best with its single binding site, even with the monomers oriented in a filamentous conformation, would lack these additional co-operative stabilising interactions, arising from further phalloidin binding sites over the whole actin filament.

A gelsolin-induced disruption of the actin:actin contacts that contribute to the phalloidin binding site, may further explain the noisy fluorescence signals we observed and also the markedly reduced affinity (~ 100 fold less than that for actin filaments) of rhodamine-phalloidin for the "minifilament". Allen and Janmey (1994) have reported that gelsolin causes a disruption of the rhodamine-phalloidin binding site on F-Actin filaments. A gelsolin-induced loss of fluorescence enhancement, following severing and capping of rhodamine-phalloidin saturated filaments, was observed. This was explained by gelsolin causing a disarrangement in the normal interactions of residues that were important in the formation of a tight rhodamine-phalloidin binding site, and this caused a loss of affinity of rhodamine-phalloidin for

the filaments. A disruption of these residues (or ones close by) is also probably a pre-requisite for severing, as several proteins that sever filaments either interfere with (gelsolin) or compete for (ADF) the binding site of phalloidin (Maciver et al, 1991).

However, the fact that we observe the binding of rhodamine-phalloidin at all, and detect a specific enhancement in the fluorescence intensity of rhodamine-phalloidin, (*only* observed in the presence of *both* A:D and $G:A_2$) is a significant result. Rhodamine-phalloidin binding a pre-requisite for considering the actin monomers within the $G:A_3$:D complex possessing filamentous conformation; binding is *F-Actin specific*.

Native-PAGE experiments provided little evidence of the formation of the putative "minifilament". However, as we have already discussed (see section 4.2.2), the harsh solution conditions and rapid changes in charge distributions experienced by the proteins and protein complexes during such electrophoresis experiments, may provide a possible explanation for why we did not observe any indication of "minifilament" complex formation by this method.

Similarly, our size-exclusion experiments, in which we used the myosin S-1 head to probe the conformation of the actin monomers within the putative "minifilament", showed no evidence of an interaction. These experiments were carried out in the presence of ATP (~ 0.2mM). In the absence of ATP, actin and myosin form a very tight complex ($K_a \sim 10^7 - 10^8\ M^{-1}$ for acto-S1, Marston and Weber, 1975; Margossian and Lowey, 1978; Sellers and Goodson, 1995). ATP binds rapidly to the S-1 head, as it does with myosin alone, and has the resultant effect of lowering the affinity of actin for myosin to about $10^4 - 10^5\ M^{-1}$ (Chalovich et al, 1984). The presence of ATP may have resulted in any binding interaction, between the S-1 head and the actin monomers within the putative "minifilament", being of such a low affinity that we were unable to detect it during our size-exclusion experiments. In a similar manner to the reduced affinity we observe for the binding of rhodamine-phalloidin to the "minifilament", any increased flexibility of the actin monomers in the "minifilament", compared to a filament, may have further reduced the affinity of

the S-1. As described in section (4.3.3.1) our attempts to perform experiments in the absence of ATP proved to be problematic and we have not pursued them further.

Nevertheless, our data do provide some evidence for the formation of a complex formed by the actin-actin association between the $G:A_2$ ternary complex and the A:D binary complex. This putative "minifilament" appears to have a stoichiometry of 1:3:1 (gelsolin:$actin_3$:DNaseI), and the actin monomers within the complex associate with the F-Actin specific binding molecule rhodamine-phalloidin, with an apparent K_d of ~ 4.6μM. The stability of this complex also appears to be *higher* than one would theoretically predict simply by the association of the actin monomers in A:D and $G:A_2$, further taking into account the apparent lack of filamentous-like conformation of the monomers within $G:A_2$ (see chapter 3).

A possible explanation for the increased stability of the putative "minifilament" arises from a consideration of why gelsolin exhibits such tight barbed-end capping activity. Very tight capping of the barbed-end (gelsolin has a K_{cap} of ~ 10pM, Selve and Wegner 1986) can be achieved by the binding protein having a high on-rate and a low off-rate. However, the on-rate for the capping protein cannot be greater than the on-rate for actin monomer addition to the barbed-end as this appears to already be approaching a diffusion-limited rate (Bonder and Mooseker, 1983; Pollard, 1983; Frieden, 1985; Pollard and Cooper, 1986; Pollard, 1986; Sheterline et al, 1995). Dissociation of the capping protein (from the barbed-end of the filament) can proceed by two mechanisms; alone or complexed to the actin monomer. This dissociation will be determined by the faster of the off-rates of these two dissociation mechanisms. K_{cap} values that are lower than the K_d of the terminal actin monomer for the barbed-end, (~ 0.1μM), imply that the off-rate of the actin monomer *complexed* with the capping protein has a lower off-rate than an uncomplexed terminal actin monomer.

This could be accomplished in two ways. One is that the capping molecule binds tightly to two actin monomers and tethers them together (e.g. gelsolin, villin and severin). Dissociation of the capping molecule complexed with two monomers, from

the barbed-end of a filament (dissociation of actin-dimers), would involve the breakage of more bonds than single monomer dissociation (Holmes et al, 1990; Lorenz et al, 1993), and would thus be more energetically unfavourable. Such actin-dimer dissociation could result in a decrease in the rate of dissociation from the capped-end. The second method involves the capping protein inducing a subtle conformational change in the structure of the terminal actin monomer/s bound to it. This conformational change may then cause a change in the subunit:subunit interactions that occur between the complexed monomer/s and the subsequent monomers at the barbed-end of the filament. These altered interactions then cause a reduction of the off-rate of the complexed actin monomer/s, from the barbed-end of the filament. This could be accomplished by either a purely kinetic effect or by *strengthening* the terminal actin-actin bond at the barbed-end of the filament (Weber et al, 1991).

Some support for a gelsolin-induced conformational change in actin monomers, has come from the work of Prochniewicz and co-workers (Prochniewicz et al, 1996). They studied the effect of gelsolin on the rotational dynamics of capped actin filaments, using time-resolved fluorescence anisotropy with erythrosin-iodoacetamide-Cys-374 actin. Significant changes in the internal dynamics of the whole filament were observed. These changes could not be explained simply by the increase in the number of short length filaments by the severing and capping activity of gelsolin, and they postulate that gelsolin had induced a subtle conformational change in the actin monomers, that was translated along the entire length of the actin filament (Prochniewicz et al, 1996). Similar reports indicating a co-operative translation of filament-end-effects along the entire length of the actin filament have also been described by other workers (Orlova and Egelman, 1995; Orlova et al, 1995; Egelman and Orlova, 1995a/b).

Evidence of a similar nature has been reported by Weber et al (1991). G1 – 3 and G1 alone have K_{cap} values less than the monomer critical concentration of the barbed-end (the K_{cap} for G1 is ~ 10 - 20nM). One explanation proposed for these low K_{cap} values was a capping-protein-induced conformational change in the terminal

complexed actin monomer that had resulted in an increased stability of the terminal actin-actin monomer contacts at the barbed-end of the filament. i.e. G1 had strengthened the longitudinal actin-actin interactions between the capped terminal monomer and the barbed-end, resulting in a reduction of the off-rate of the G1-monomer complex.

Gelsolin (and to a lesser extent the G:A_2 ternary complex) may possibly achieve its extremely tight capping of the barbed-ends of filaments by a combination of the two methods described above. If gelsolin is able to induce a conformational change in the actin monomers bound to it, that then strengthens the longitudinal actin-actin monomer contacts between the terminal gelsolin-bound monomers and any subsequent monomers binding to the pointed ends of G:A_2, it may provide an explanation for the higher than expected stability of the "minifilament". i.e. gelsolin has altered the conformation of the two monomers bound in ternary complex with it. This re-arrangement then results in any subsequent monomer:monomer interactions, between these gelsolin-bound monomers and say that of the A:D bound monomer, being strengthened. In this manner, the off-rate of the A:D monomer may be reduced (compared to the off-rate from the pointed-ends of filament), and the stability of the putative "minifilament" increased.

However, even accounting for a gelsolin-induced strengthening of the terminal longitudinal actin:actin associations, the interactions that take place between the two terminal gelsolin-bound actin monomers in G:A_2, and the two monomers at the barbed-end of the filament, are likely to be different, and more stable, than the actin-actin interactions that may result in the formation of the putative "minifilament". Capping of the barbed-end of a filament involves a dimer:dimer association between the two monomers in G:A_2 and the two terminal barbed-end subunits. One would have expected that the formation of the putative "minifilament", occurring *solely* via actin:actin associations between the free barbed-end of the single monomer in A:D and the free pointed-ends of the monomers in the G:A_2 complex, to be significantly less stable than the binding of G:A_2 to a filament end. Furthermore, as our results described in chapter 3 indicate the monomers in G:A_2 are probably not oriented in a

filamentous conformation, and we are not simply adding monomers to the pointed-ends of already formed filaments. i.e. we would have predicted that the K_d for this interaction would have been larger than the K_d for monomers binding to the pointed-end (~ 0.6μM) of actin filaments. As described above, if this were the case we would have expected to see a significant amount of uncomplexed A:D, $G:A_2$ in our gel-filtration experiments, to have experienced more problems with the exchange of actin for A:D at the EGTA labile (G4) actin-binding site on gelsolin, and to have observed little, if any, rhodamine-phalloidin binding.

This notion of a capping protein-induced conformational change in the complexed actin subunits, that increases the stability of the terminal longitudinal actin:actin interactions may partially explain the high-affinity capping activity of gelsolin and the barbed-end of actin filaments. However, an alternative model where gelsolin forms a contact with a *third* actin monomer (via an interaction with the F-Actin binding site in G2), up the longitudinal axis of the filament, is now emerging from a body of work. This model seems to provide a better explanation for why the "minifilament" might form, with a higher than expected stability, but it also provides an insight as to why the orientation of actin monomers in the $G:A_2$ ternary complex may be non-filamentous. This model will be discussed in detail in chapter 6.

4.5 Conclusion

Gel-filtration and fluorescence enhancement experiments provide evidence consistent with our model for the formation of a capped-actin-"minifilament". This complex appears to have formed from via an actin:actin association between the $G:A_2$ ternary complex and the A:D binary complex. The actin monomer conformation within this putative "minifilament" complex ($G:A_3:D$) may be relatively flexible, but the binding of rhodamine-phalloidin shifts it towards a more filamentous-like and rigid conformation. A model where gelsolin forms a contact with a *third* actin monomer (via an interaction with the F-Actin binding site in G2), up the longitudinal axis of the filament is emerging from a body of work. This model seems to provide an explanation for why the "minifilament" might form, with a higher than expected stability, but it also provides an insight as to why the orientation of actin monomers in the $G:A_2$ ternary complex may be non-filamentous. This model and the implications for the formation and stability of our putative "minifilament" will be discussed in detail in chapter 6.

5. T-cap-protein, a fragment of tensin spanning the sequence containing "insertin", acts as a barbed-end-capper of actin filaments.

5.1 Overview

In an attempt to resolve some of the problems, possibly associated with monomer exchange at the EGTA labile actin-binding site (G4) on gelsolin, we proposed to use an alternative protein as the barbed-end capping species in the analysis of the "minifilament". This protein is a cloned polypeptide fragment derived from the protein tensin, a component of focal adhesions. (We have termed this construct T-cap-protein and its sequence spans amino acid residues R861 – A1223 of whole tensin). T-cap-protein spans the region of tensin that contains the sequence of "insertin", previously identified as a polypeptide possessing a controversial high-affinity barbed-end capping activity. We have developed a novel purification protocol that gives >85% final purity for T-cap-protein. We have studied its interaction with filamentous actin. The results are consistent with T-cap-protein having a tight barbed-end capping activity, with an apparent K_{cap} of ~ 6 - 8nM, *but* with a non-"insertin-like" activity. We also report a novel F-Actin side-binding activity for T-cap-protein, with an apparent K_d of ~ 10μM. However, our results are consistent with T-cap-protein showing no binding interaction with monomeric G-actin, and therefore, it is not useful in the further analysis of the putative "minifilament".

5.1.1 Introduction

Focal contacts (also called adhesion plaques or focal adhesions) are specialised areas of the plasma membrane where cells attach to the underlying substratum (see section 1.4 for details). The protein tensin, originally identified in chicken gizzard extracts (Wilkins and Lin, 1986), appears to be a prime candidate for the role of linking of the actin cytoskeleton to the plasma membrane and the extra-cellular matrix (ECM). Tensin is a large (~ 200kDa) actin cross-linking and capping protein that localises in

the dense plaques of smooth muscle, the Z-line of cardiac muscle and focal adhesions of fibroblasts (Bockholt et al, 1992). Three distinct actin-binding domains have been identified within tensin; two N-terminal proximal domains (ABD-1, one of which contains a region that shares homology with a consensus actin binding sequence commonly found in cross-linking proteins; Matsudaira, 1991) and a central ABD-2 domain, see fig. 5.1. *In vitro* binding experiments indicate that tensin probably binds to the side of F-actin filaments via these ABD-1 domains (Lo et al, 1994c). The barbed–end capping of actin filaments is thought to occur via the central ABD-2 domain (Lo et al, 1994c; Chuang et al, 1995).

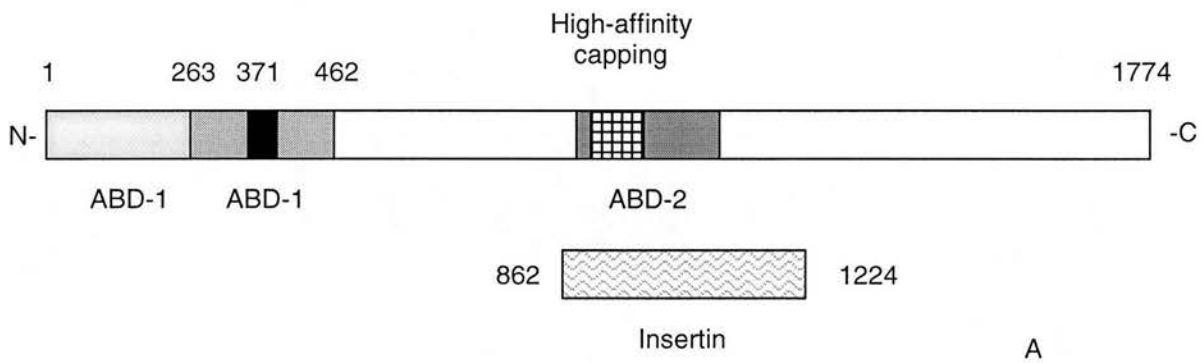


```
α-Actinin     113          LVSIGAEEIVDGNVKMTLGMI-WTILR    138
Filamin       127          LVSIDSKAIVDGNLKLILGLI-WTILH    152
Tensin        371          LENGPSVS-VDYNTSDPL--IRWDSYE    394
                           |         ||       |  | |
Actin-binding consensus    L++I+++++VD++++++LG+I-W+IL+
```

B

Fig. 5.1 ***Tensin has homology with a consensus actin-binding sequence.*** (A) A schematic diagram of tensin, with the 3 proposed actin-binding domains highlighted (2 ABD-1 domains and a ABD-2 domain), is illustrated above. The sequence with very high identity to "insertin" (Wieght et al, 1992) is highlighted below the tensin schematic. The position of the consensus actin-binding sequence, located in the second ABD-1 domain (Lo et al, 1994a) is indicated by the black box insert in the second ABD-1 domain. The high-affinity barbed-end capping domain is indicated by the hatched box insert in ABD-2 (the sequence within this region is not numbered due to a discrepancy in the residues of tensin actually involved in the capping of the barbed-end; see Lo et al, 1994a/c and Chuang et al, 1995). (B) Actin-binding consensus sequence found in the second ABD-1 domain in tensin. The sequence illustrated is emerging as an F-actin binding consensus sequence. This consensus sequence is usually found as a stretch of 25 amino acids conserved within a 250 amino acid domain, commonly found in F-Actin cross-linking domains e.g α-Actinin, filamin, spectrin, dystrophin, plastin/fibrin, APB-120 and APB-280 (Nagafuchi et al, 1991; Bresnick et al, 1991; Hartwig and Kwiatkowski, 1991; Matsudaira, 1991; Van Troys et al, 1999). This region appears to be essential for *in vitro* actin binding (Matsudaira, 1991). The numbering of amino acids used is the same as that for the derived tensin sequence described by Lo et al (1994a).

Tensin appears to be able to form parallel dimers by intermolecular interactions involving sequences localised to the C-terminus (Lo et al, 1994a). The formation of a tensin-dimer, via the C-terminus, would generate a U-shaped structure that could both cross-link and cap two actin filaments. This would enable tensin to act as an adapter, bridging the interactions between the ECM, the actin cytoskeleton and the rest of the focal contact assembly (see fig. 1.3).

Wegner and co-workers (Schröer and Wegner, 1985; Ruhnau et al, 1989) have previously described the purification and characterisation of a small polypeptide (20 – 80kDa) that that co-purified with vinculin. This polypeptide (which they termed "insertin") exhibited barbed-end filament capping activity that retarded, but did *not* completely, inhibit polymerisation (Ruhnau et al, 1989; Gaertner and Wegner, 1991). Subsequent work has demonstrated that "insertin" shares a very high degree of sequence identity to a stretch of amino acid sequence (R861 - A1223) from whole tensin (Wieght et al, 1992; Lo et al, 1994a; Chuang et al, 1995; Teubner et al, 1998). Northern blot analysis with tensin cDNA probes only detected a single mRNA species of 11kb in chick embryo fibroblasts (Davis et al, 1991). Furthermore, amino acid sequence analysis of the derived sequence of tensin from chicken gizzard, indicated the existence of 9 PEST regions (Chuang et al, 1995). PEST regions are amino acid sequences that act as signals for rapid proteolysis, and are common in many rapidly degraded proteins involved in signal transduction (Rogers at al, 1986; Rechsteiner, 1990). Three of these PEST sequences surround the putative "insertin" sequence in tensin (Chuang et al, 1995). This region also contains the high-affinity barbed-end-capping region of tensin (Lo et al, 1994a/c; Chuang et al, 1995). Tensin also shows a high sensitivity to the protease calpain II and both are localised to focal contacts (Lo et al, 1994b), so it now seems highly likely that "insertin" is generated by proteolytic degradation of the highly susceptible protein tensin.

A model in which "insertin" binds to one of the actin monomers at the barbed-end of an actin filament, inhibiting polymerisation at this end, but *still* allowing monomer insertion between the bound protein and the other actin subuint, has been proposed (Ruhnau et al, 1989; Geartner and Wegner, 1991). Lo et al (1994c) provided a

similar monomer insertion model to explain the capping activities (K_{cap} ~ 20nM) of their recombinant tensin, and several bacterially expressed fusion protein constructs that span the sequences of tensin containing the high-affinity barbed-end capping "insertin" domain.

This is in contrast to the findings of Chuang and colleagues (Chuang et al, 1995). Using a set of bacterially expressed fusion proteins, again derived from the sequences of whole tensin containing the high-affinity barbed-end capping "insertin" domain. They report tight capping of the barbed-end (K_{cap} ~ 1 – 3nM). Furthermore, *no* evidence of further monomer insertion was observed.

Both groups have also reported conflicting results with regard to the actual sequences in the "insertin" domain in tensin, that are responsible for the tight capping of the barbed-ends of actin filaments (Lo et al, 1994a/c; Chuang et al, 1995). Two of the sequences reported for chicken cardiac tensin (GenBank accession No. L06662; Chuang et al, 1995 and accession No. M96625; Lo et at, 1994a) show a variation in the determination of the N-terminus and the initiation codon of the full-length protein. The sequence reported by Lo et al (1994a) is missing the first 35 amino acids and the alternative methionine initiation codon of the sequence reported by Chuang et al (1995). These discrepancies are possibly artefacts of the cDNA synthesis and cloning and have led to different residue numbering schemes. Thus, for reasons of clarity, we state here that the numbering of the amino acid residues, used throughout, is based on that scheme described by Lo et al (1994a).

We have cloned a fragment of chicken cardiac tensin (Mary Russell, unpublished results). This construct spans amino acid residues R861 – A1223 of tensin and contains the putative "insertin" sequence. We have expressed this fragment (here termed T-cap-protein) in BL21 (DE3) *E.coli* and purified the full-length polypeptide. Initially this protein was intended as a substitute for gelsolin, as the barbed-end capping protein, in the further experimental analysis of the "minifilament". We have analysed its interaction with actin filaments. Our results are consistent with the *tight* capping of the barbed-ends of actin filaments, an apparent K_{cap} of ~ 6 - 8nM. Our

data are also consistent with T-cap-protein showing *no* evidence of further monomer addition at capped barbed-ends; i.e. no "insertin-like" activity. We further report that this T-cap-protein construct appears to possess a novel F-Actin side-binding activity with an apparent K_d of ~ 10μM. However, as is discussed in the proceeding sections, we found no evidence of an interaction between the G-Actin monomer and T-cap-protein. Thus, it appears that T-cap-protein was not a good alternative for gelsolin, and was not of any use for the further analysis of the putative "minifilament".

5.2 Purification of T-cap-protein.

5.2.1 Purification protocol

We have developed a novel purification protocol for T-cap-protein that gives >85% purity. However, due to problems with *severe* proteolytic degradation, yields of pure protein ranged from 0.2 - 3.0mg, (from 6 litres of original bacterial cell culture), in a very preparation dependent manner.

5.2.1.1 Optimisation of expression

BL21(DE3) *E.coli* were successfully transformed with pMW172[T-cap-protein/R861-A1223] (using the amino acid sequence numbering scheme of tensin as described by Lo et al, 1994a; accession number M96625). Cells were grown in 2xTY and the induction of synthesis of high levels of recombinant T-cap-protein was obtained upon addition of IPTG to 1.0mM. The appearance of a protein band that migrates at approximately 46 – 48kDa on SDS-polyacrylamide gels corresponded to the full- length recombinant T-cap-protein, see fig. 5.2(A). This apparent Mr. (46 – 48kDa) is significantly larger than the expected theoretical Mr. of ~ 38kDa. Examination of the sequence of our protein construct indicated that it contains a higher content of proline residues (14%, see fig. 5.3) as compared to the 5% average of vertebrate proteins (Doolittle, 1986). The high proline content may contribute to the apparent larger Mr. of T-cap-protein on SDS-polyacrylamide gels. Proteins with a higher than average percentage of proline residues have previously been show to have significantly larger than expected apparent Mr. values when analysed on SDS-polyacrylamide gels (Ollo and Maniatis, 1987).

Attempts were made to optimise the expression of the recombinant protein (see optimisation protocol employed in the purification of DNaseI, section 3.2.1.1.1, for general protocol). However, rapid proteolytic degradation of the full-length T-cap-protein was *always* observed upon cell lysis. Often complete degradation of the

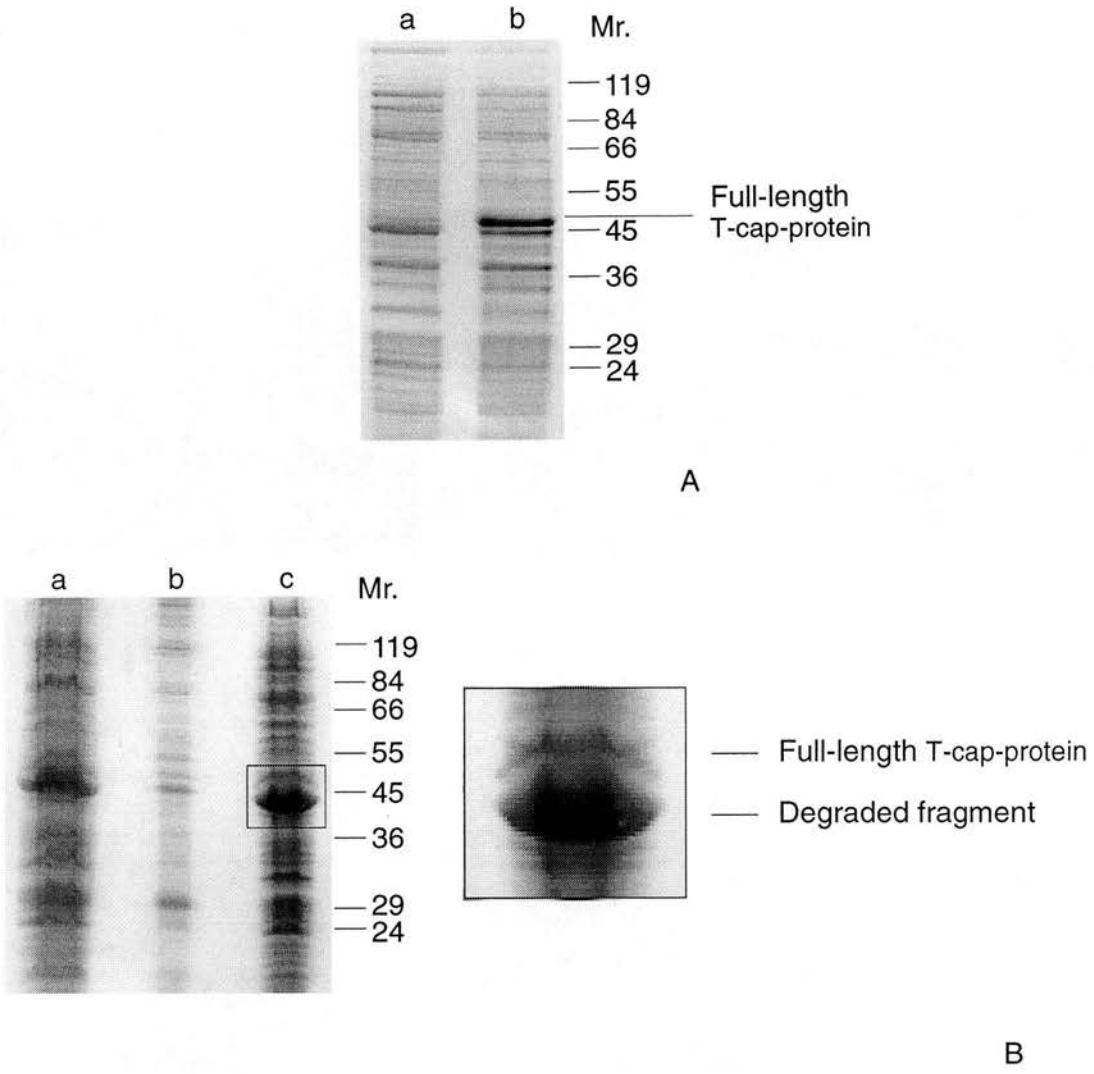

Fig. 5.2. ***SDS-PAGE analysis of induction of synthesis of recombinant T-cap-protein from BL21(DE3)[pMW172/T-cap-protein/R861-A1223].*** (A) SDS-polyacrylamide gel showing the high levels of synthesis of the T-cap-protein from BL21(DE3)[pMW172/T-cap-protein/R861-A1223] by addition of IPTG to 1.0mM. Lane a. pre-induction; b. 3hrs post IPTG addition. BL21(DE3)[pMW172/T-cap-protein/R861-A1223] in 100ml of 2xTY/AMP (50μg/ml) were grown at 37°C until the A_{600nm} ~ 0.6 - 1.0, and synthesis of the recombinant protein was induced by addition of IPTG to 1.0mM. Cells were grown for a further 3hrs. 1.0ml aliquots from pre- and post-induction conditions were taken and the resultant cell pellet was resuspended in 100μl of 5 x SDS-sample buffer (see methods) and boiled for 5mins. A 20μl sample was loaded onto the gel, following centrifugation at 15,000 xg for 2min. Mr. of protein standards are given in kilodaltons. (B) SDS-polyacrylamide gel showing the extensive proteolytic breakdown of the full-length T-cap-protein to give a slightly smaller cleavage fragment as the major protein constituent (Mr. ~ 42kDa). Lane a. Total cell extract, 3hrs post IPTG addition, post-lysis; b. Insoluble fraction, post lysis; c. Soluble fraction, post lysis. The magnified image to the right of the gel shows the two protein bands, full-length T-cap-protein and the major degradation fragment, from the box inset in lane c. The increase in the relative amounts of the full-length and degraded T-cap-protein, when compared to those in A, can clearly be seen. BL21(DE3)[pMW172/T-cap-protein/R861-A1223] in 100ml of 2xTY/AMP (50μg/ml) were grown at 37°C until the A_{600nm} ~ 0.6, and synthesis of the recombinant protein was induced by addition of IPTG to 1.0mM. Cells were grown for a further 3hrs and then a 5.0ml aliquot was resuspended in 20mM Bis-Tris, pH 6.1; 0.25mM EDTA; 5mM NaCl; 1mM NaN_3; 1ml of bacterial cell extract protease inhibitor cocktail (Sigma), subjected to ultrasonication (3 x 20 sec bursts at 4°C) and the resulting cell lysate centrifuged at 18,000 xg (5min at 4°C). The extent of proteolysis was analysed by SDS-PAGE. SDS-PAGE was performed as described in methods.

protein was observed, even in the presence of excess of a cocktail of protease inhibitors (~ 5x the normal recommended concentrations).

```
        10          20          30          40          50          60

MRSFGTSVGT DPLAKPYSPG PLVPAARSTA EPDYTVHEYR ETYTPYSYQP VPEPRSYGSA
PASILPLSAS YSPAGSQQLL VSSPPSPTAP AQSQLPHKGL ESYEDLSRSG EEPLNLEGLV
AHRVAGVQSR EKSPEESTVP ARRRTPSDSH YEKSSPEPGS PRSPTVLSPE VVSTIAANPG
GRPKEPHLHS YKEAFEEMES ASPSSLTSGG VRSPPGLAKT PLSALGLKPH NPADILLHPV
GELEGEAGAD SEEEPRSYVE SVARTATTGR AGNLPAAQPV GLEVPARNGA FGNSFTVPSP
VSTSSPIHSV DGASLRSYPS EGSPHGTVTP PHAVAETAYR SPMVSQTPSA HSSYQTSSPS
SFQA
                                        *
```

Fig. 5.3. ***The amino acid sequence of full-length T-cap-protein[R861 – A1223].*** The proline (P) residues are highlighted in bold type. Out of a total of 364 residues 51 are proline, contributing 14% of the sequence. The underlined portion indicates the sequence of the N-terminus, reported for the smaller degradation fragment (see fig. 5.2B) following N-terminal sequencing. * denotes the likely Endoproteinase Glu-C (or a bacterial enzyme with a similar specificity) cleavage site (E336/T337, Teubner et al, 1998) for the proteolytic fragment. The methionine (M) residue at the start of the sequence is derived from the bacterial initiation codon within the pMW172 vector.

Fig. 5.2(B) shows the degradation of the full-length T-cap-protein, following cell lysis. As a result of this degradation problem, it proved impractical to analyse the relative amounts of protein present in the soluble and insoluble fractions in the course of the optimisation procedure. The synthesis of T-cap-protein increased as a function of time after induction with IPTG. After 3hrs the protein constituted ~ 6 – 9% of the total cellular protein prior to being subjected to lysis, as judged by densiometric scanning of SDS-polyacrylamide gels lanes, similar to that shown in fig. 5.2(A), lane b (data not shown). Therefore, cells were routinely induced for 3hrs and then processed for purification as rapidly as possible. Although the severe degradation hampered the optimisation process, we have developed a working method that provides full-length T-cap-protein at >85% final purity.

5.2.1.2 Protein purification

BL21(DE3)[pMW172/T-cap-protein/R861-A1223] were grown at 37°C in 2xTY/AMP, and protein synthesis induced by the induction of IPTG to 1.0mM. Cells were grown for a further 3hrs and then harvested and processed for purification (see

methods for protocol details). To minimise the extent of proteolytic degradation the cells were processed as quickly as possible immediately after induction, always using freshly transformed BL21(DE3) *E.coli.* Protease inhibitors were included (at ~ 5 times the normal working concentration) in *all* dialysis and chromatography buffers, throughout the purification protocol.

Fig 5.4 shows the results of the DEAE-Sepharose anion-exchange chromatography step. Bound proteins were eluted by a gradient of 5 – 300mM NaCl. Full-length T-cap-protein elutes at ~ 60mM NaCl, see fig 5.4(A). A band that migrates at a slightly lower Mr. than the full-length T-cap-protein, co-purifying with it (Mr. ~ 42kDa on SDS-polyacrylamide gels), was always the major contaminant, see figs. 5.2(B) and 5.4(B).

We have purified this protein to >80% purity, utilising a similar protocol to that employed in the purification of the full-length protein (data not shown). N-terminal sequencing of this protein species gave the sequence, MRSFGT. This is identical to the N-terminal sequence of full-length T-cap-protein suggesting that this smaller species is proteolytically cleaved at the C-terminus (see fig. 5.3). Electro-spray mass spectrometry analysis of this smaller protein species gave a corresponding mass, for the major peak constituent, of 35236.0 Da. Together both pieces of information are consistent with the full length protein having lost 28 amino acids from the C-terminus, with a likely Glu-C cleavage site (or a bacterial protease with a similar specificity) occurring between E336 and T337, see fig. 5.3. Our data is in agreement with the Glu-C cleavage site reported by other workers (Teubner et al, 1998) at the same (relative) position in whole tensin. A high susceptibility of tensin to proteolytic degradation (especially for fusion proteins containing sequences that encompass the putative "insertin" sequence, R861 to A1223), has been reported by others (Wieght et al, 1992; Lo et al, 1994a/c; Chuang et al, 1995; Teubner et al, 1998). Thus, it would appear that this smaller protein is a proteolytic fragment derived from our full-length T-cap-protein.

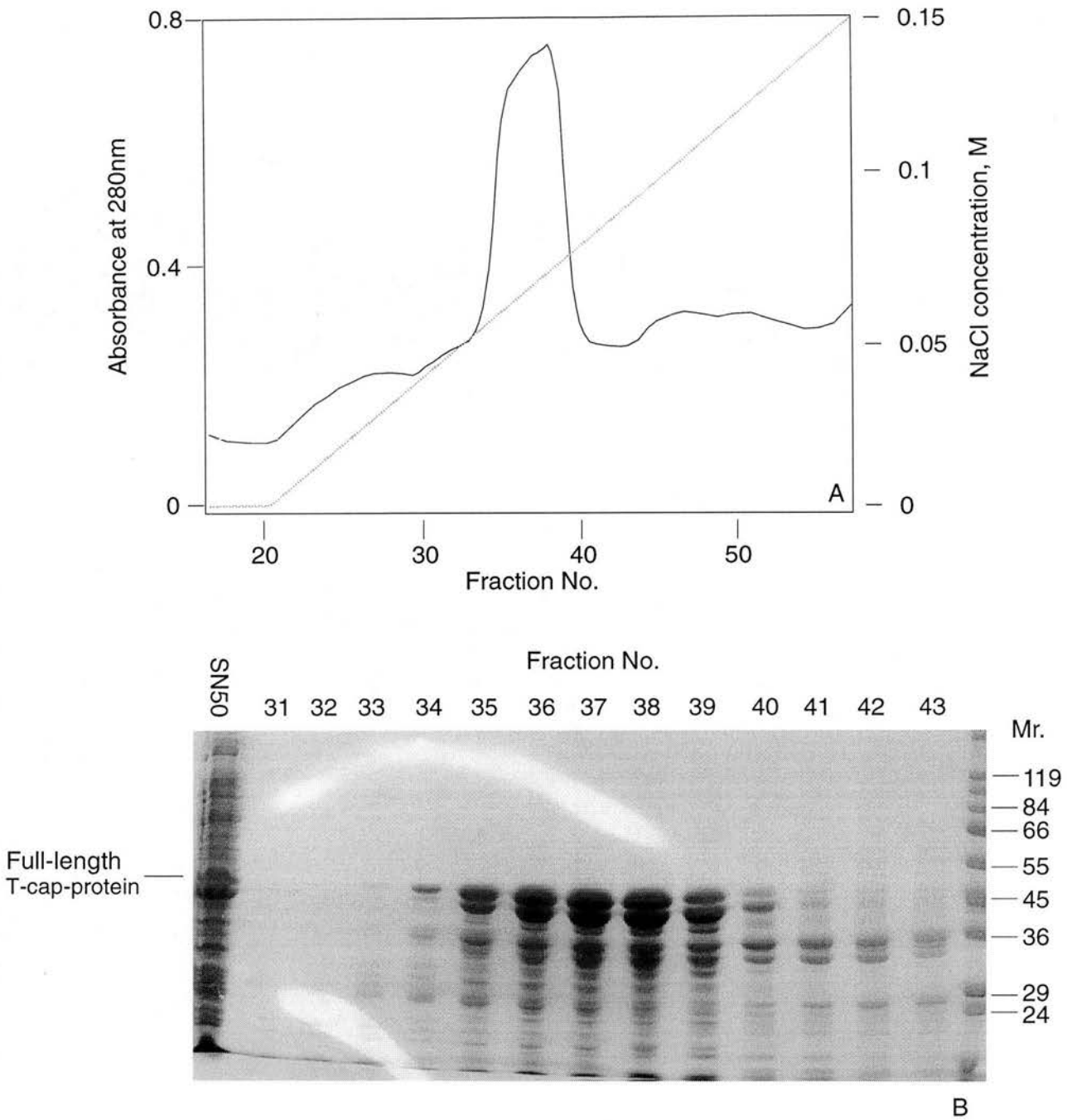

Fig 5.4. ***DEAE-Sepharose chromatography of the recombinant T-cap-protein.*** (A) Abs_{280nm} monitored elution profile from a DEAE-Sepharose column showing the elution of the full-length T-cap-protein at ~ 60mM NaCl. (B) SDS-PAGE analysis of the elution profile in A. (SN50; soluble fraction resulting from centrifugation of cell lysate at 50,000 xg). BL21(DE3)[pMW172/T-cap-protein/R861-A1223] were grown at 37°C in 2xTY/AMP (50µg/ml) until A_{600nm} ~ 0.6 - 1.0 and protein synthesis induced by the addition of IPTG to 1.0mM. Cells were grown for a further 3hrs and then harvested by centrifugation at 3000 xg for 10 min at 4°C. Cells were lysed and subjected to an overnight dialysis against 20mM Bis-Tris, pH 6.1; 0.25mM EDTA; 5mM NaCl; 1mM NaN_3; 5ml of bacterial cell extract protease inhibitor cocktail (Sigma) per litre of dialysis buffer. The soluble clarified fraction was then loaded onto a DEAE-Sepharose column (V_t ~ 50 ml; 2.6cm x 9.5cm) pre-equilibrated in the same buffer. Bound proteins were eluted by a gradient of 5 - 300mM NaCl, over 6 column volumes, and proteins detected by A_{280nm} and analysis by SDS-PAGE. Mr. of protein standards are given in kilodaltons. (SDS-PAGE and chromatography were performed as described in methods).

The relevant fractions, from the DEAE-Sepharose chromatography run, were pooled, concentrated and subjected to an overnight dialysis against a 50mM MES, pH 5.5 buffer. Following dialysis, the soluble fraction was then loaded onto a cation-exchange Mono-S/(30μm) column. Fig. 5.5(A) shows a typical A_{280nm} monitored elution profile of the purification. T-cap-protein bound to the matrix (the theoretical pI for full-length T-cap-protein is ~ 5.7) and elution was achieved with a 5 – 100mM NaCl gradient (see methods). Full-length T-cap-protein elutes at ~ 65mM NaCl.

Fig. 5.5(B) illustrates the analysis of the elution profile by SDS-PAGE. Some success in partitioning full-length T-cap-protein from its major contaminants was achieved on this column. The peak elution fraction of the degraded fragment was ~ F34, while that of the full-length protein was slightly later in the profile, peaking at ~ F36, see fig. 5.5(B). There is however, a high degree of overlap between the two elution positions. Careful pooling of the relevant fractions at this stage was needed to maximise the yield of full-length T-cap-protein. Relevant fractions were pooled, concentrated and dialysed over night against a 50mM MES, pH 5.5 buffer (see methods). Depending on the degree of severity of degradation and the corresponding amounts of full-length T-cap-protein and fragment, several further rounds of Mono-S/(30μm) cation-exchange chromatography, were frequently performed (data not shown). These further stages were very preparation dependent and were not always necessary.

The final ion-exchange chromatography step was always carried out on a HR 5/5 Mono-S/(15μm) column, attached to an FPLC. This semi-analytical column has a highly uniform matrix-bed, due to the smaller 15μm diameter resin beads. This provides higher band resolution, and when attached to an FPLC, chromatographic runs can be performed with very fine and accurate control over the flow-rate and gradient profile parameters (see methods for details).

Fig 5.6 shows the results obtained from such a chromatography step. T-cap-protein bound to the resin and elution was achieved with a very shallow gradient of 60 – 80mM NaCl, over 15 column volumes. Two major peaks were observed on the

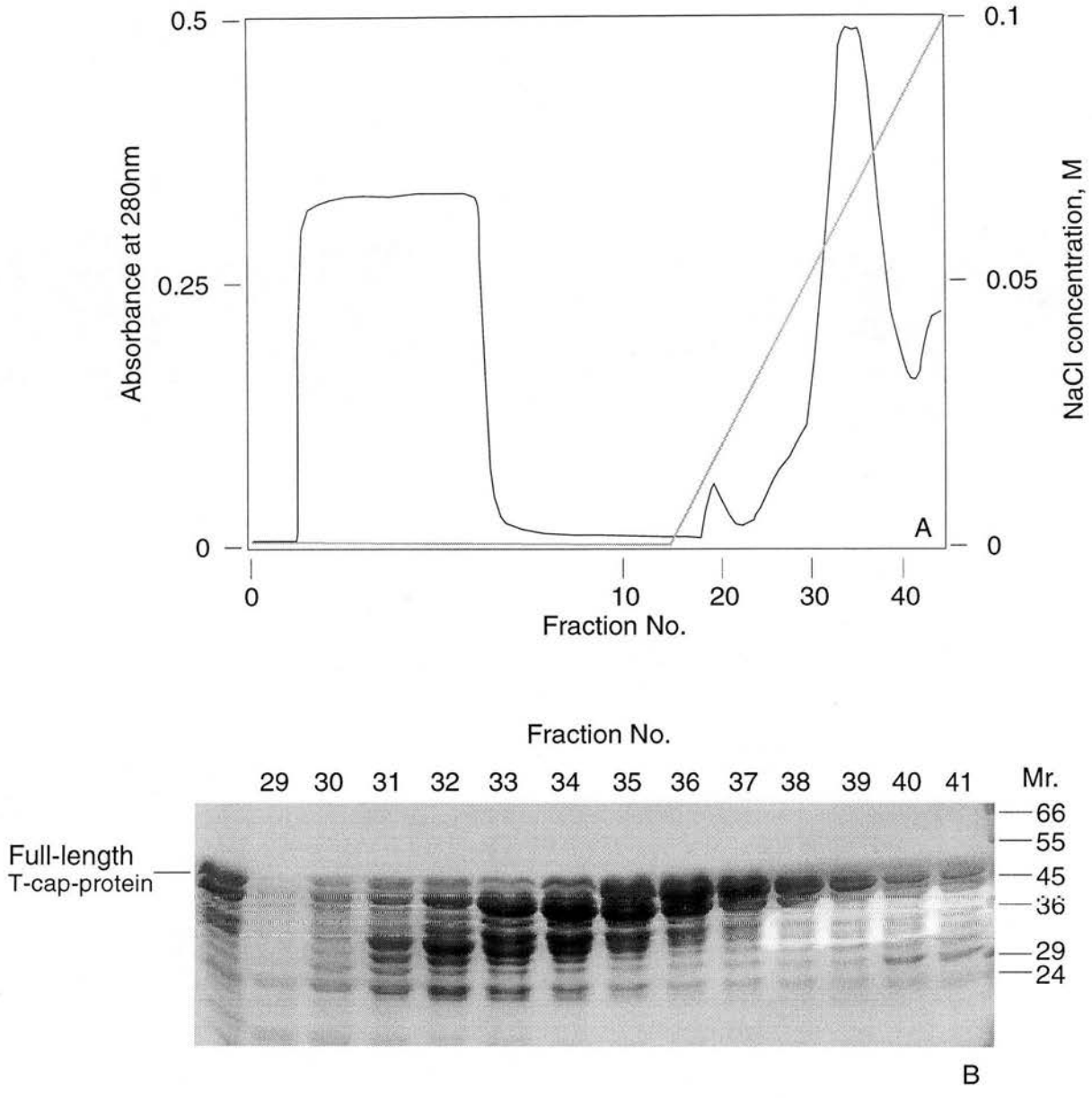

Fig 5.5. ***Mono-S/(30μm) chromatography of recombinant T-cap-protein.*** (A) Abs_{280nm} monitored elution profile from a Mono-S/(30μm) column showing elution of the full-length T-cap-protein at ~ 65mM NaCl. (B) SDS-PAGE analysis of the elution profile in A. The first lane represents the pooled fractions from the DEAE-Sepharose column. Relevant fractions from the DEAE-Sepharose chromatography step were pooled and subjected to an over night dialysis against 50mM MES, pH 5.5; 0.25mM EDTA; 5mM NaCl; 1mM NaN_3; 5ml of bacterial cell extract protease inhibitor cocktail (Sigma) per litre of dialysis buffer. The dialysate was filtered through a 0.22μm filter and loaded onto a Mono-S/(30μm) column (V_t ~ 6.0ml; 1.6cm x 2.0cm), pre-equilibrated in the same buffer. Elution of T-cap-protein from the resin was achieved with a 5mM - 100mM NaCl gradient, over 6 column volumes. (SDS-PAGE and chromatography were performed as described in methods).

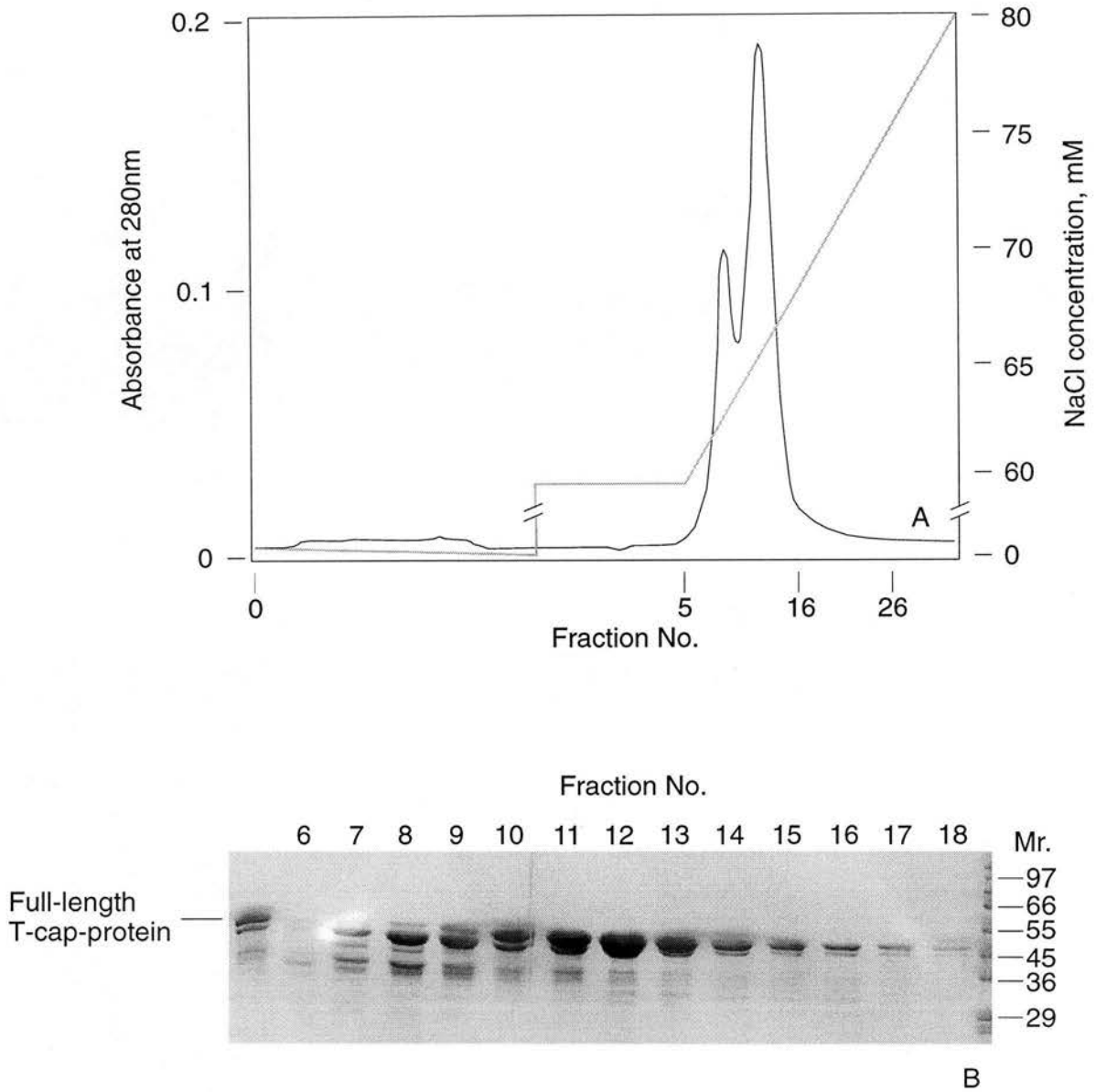

Fig 5.6. ***HR 5/5 Mono-S/(15μm)/FPLC chromatography of recombinant T-cap-protein.*** (A) Abs_{280nm} monitored elution profile from an HR 5/5 Mono-S/(15μm)/FPLC column showing elution of the full-length T-cap-protein at ~ 65mM NaCl. (B) SDS-PAGE analysis of the elution profile in A. The first lane represents the pooled fractions from the previous Mono-S/(30μm) column. Relevant fractions from the previous Mono-S/(30μm) chromatography run were pooled and subjected to an over night dialysis against 50mM MES, pH 5.5; 0.25mM EDTA; 5mM NaCl; 1mM NaN_3; 5ml of bacterial cell extract protease inhibitor cocktail (Sigma) per litre of dialysis buffer. The dialysate was filtered through a 0.22μm filter and loaded onto an HR 5/5 Mono-S/(15μm)/FPLC column (V_t ~ 1.0ml; 1.0cm x 1.30cm), pre-equilibrated in the same buffer. Elution of T-cap-protein from the resin was achieved with a gradient of 60mM - 80mM NaCl, over 15 column volumes with a flow rate of 0.25ml.min^{-1}. (SDS-PAGE and chromatography were performed as described in methods).

A_{280nm} monitored elution profile, see fig. 5.6(A). Analysis of the protein components of this elution profile, performed by SDS-PAGE, is illustrated in fig. 5.6(B). Full-length T-cap-protein eluted at ~ 65mM NaCl (fraction 12) while the smaller degraded fragment eluted earlier at ~ 62mM NaCl (fraction 8).

It is clear from the Mono-S cation-exchange chromatography that the pI of the major contaminant (the smaller proteolytic fragment, Mr. ~ 42kDa on SDS-PAGE) and that of full-length T-cap-protein are very close. Partition of these two protein species was achieved, but the elution concentration of NaCl that separated them differed by only ~ 5mM, see fig. 5.6(A). The pI for the degraded fragment (assuming an intact N-terminus and the loss of 28 amino acids from the C-terminus, via proteolysis at the tryptic cleavage site, see fig. 5.3) is ~ 5.5. The difference in pI is only ~ 0.2 of a pH unit. This apparent closeness of pI values, coupled with problems associated with rapid and extensive proteolysis, made purification very difficult and resulted in the very variable yields. Typically, yields ranged from 0.2 – 3.0mg, from 6 litres of original bacterial cell culture. This is in contrast to the relatively high initial levels of expression obtained (~ 6 – 8mg.L^{-1}) *prior* to cell lysis (see fig. 5.2 A).

Further purification was carried out by subjecting the relevant fractions from the HR 5/5 Mono-S/(15µm) column, to size-exclusion chromatography on an FPLC/Superose-12 size-exclusion column. Fig. 5.7 illustrates the final purity typically obtained for full-length T-cap-protein. Densiometric scanning of similar SDS-polyacrylamide gel lanes gave a final purity for full-length T-cap-protein of >85% (data not shown).

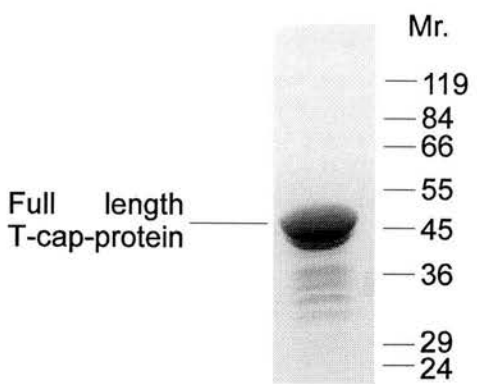

Fig 5.7 ***Final purity of full-length T-cap-protein obtained by a novel purification protocol.*** SDS-polyacrylamide gel lane illustrating the final purity of T-cap-protein. A final purity of >85% was obtained, as determined by densiometric scans of similar gel lanes (data not shown). Mr. of protein standards are given in kilodaltons. (SDS-PAGE and gel densitometry were performed as described in methods).

5.3 *In vitro* characterisation of full-length T-cap-protein's interaction with actin

5.3.1 Interaction of recombinant T-cap-protein with filamentous actin

As described before (see section 5.1.1) tensin has been previously shown to have high-affinity capping activity, reflected in a K_{cap} for the barbed-end of actin filaments in the nM range. There is however, a disagreement as to the "type" of capping activity exhibited (see below). There is also disagreement as to which residues of tensin are responsible for this barbed-end capping activity.

In summary: Lo et al (1994c) report a barbed-end capping affinity for whole tensin of ~ 20nM (comparable to the K_{cap} of ~ 50nM, reported for "insertin" by Ruhnau et al, 1989). Both whole tensin and several GST-tensin fusion constructs retarded but did *not* completely inhibit barbed-end polymerisation, allowing for the insertion of further actin monomers at the barbed-end, following capping ("insertin-like" activity). This feature was illustrated by the protein having no effect on the long-term steady-state critical monomer concentration ($[C_c]$) of F-Actin (measured after 24hr). The residues important in this activity were located between amino acids T880 – R989 (Lo et al, 1994c).

On the other hand, Chuang and colleagues (Chuang et al, 1995) have reported an order of magnitude higher affinity (K_{cap} ~ 3nM), for capping of the barbed-end. Furthermore, they also report a *lack* of "insertin-like" activity; their GST-tensin fusion constructs (containing portions of the amino acid sequence that traverse the "insertin" domain) affected the steady-state critical monomer concentration of F-Actin, shifting it towards that of the pointed-end (0.6 – 0.8μM). In further contrast to Lo et al (1994c), they identified the residues between amino acids R989 – V1121 as being important in the high affinity capping activity.

We have performed experiments to test our T-cap-protein construct (containing residues R861 – A1223 from tensin) for tight capping of the barbed-end and also to test its effect on the steady-state $[C_c]$ values of F-Actin. We have also tested samples

of the partially purified (~ 80% purity) degraded fragment for barbed-end capping activity.

5.3.1.1 The effect of T-cap-protein on nucleated barbed-end actin polymerisation

We have determined the effect of our recombinant T-cap-protein on the initial rate of nucleated actin polymerisation, under conditions (0.5μM G-Actin, 20% pyrene labelled, polymerised by the addition of KCl and $MgCl_2$ to 100mM and 2mM, respectively, in the presence of 0.1μM F-Actin seeds) where monomer addition *only* occurs at the barbed-end. The time course of polymerisation was followed by measuring the increase in the fluorescence intensity of pyrene actin, which is directly proportional to the incorporation of monomers into filaments. (See methods for details of the protocol and see section 5.4 for an explanation of the kinetic considerations).

Fig. 5.8 illustrates the effect of the addition of increasing amounts of full-length T-cap-protein on the rate of nucleated actin polymerisation. It is clear that as the concentration of T-cap-protein increases, the rate of polymerisation decreases correspondingly. At high concentrations of T-cap-protein (~ 250nM and above) very little, if any, polymerisation was observed. This approach to an initial polymerisation rate of zero implies capping of the barbed-ends by T-cap-protein; polymerisation is carried out under conditions that limit monomer addition to the barbed-end *only*.

Figs. 5.9(A) and (B) further illustrate the strong inhibitory effects of T-cap-protein on nucleated polymerisation and show a graphical determination of the K_{cap} (the concentration of capping protein that causes a 50% inhibition in the initial rate of nucleated polymerisation). The initial polymerisation rates from the experiments shown in fig. 5.8 were converted to units of $nM.s^{-1}$ (see methods) and the percentage of inhibition calculated, in relation to the initial rate of polymerisation in the absence of T-cap-protein (that labelled as F-Actin in fig. 5.8).

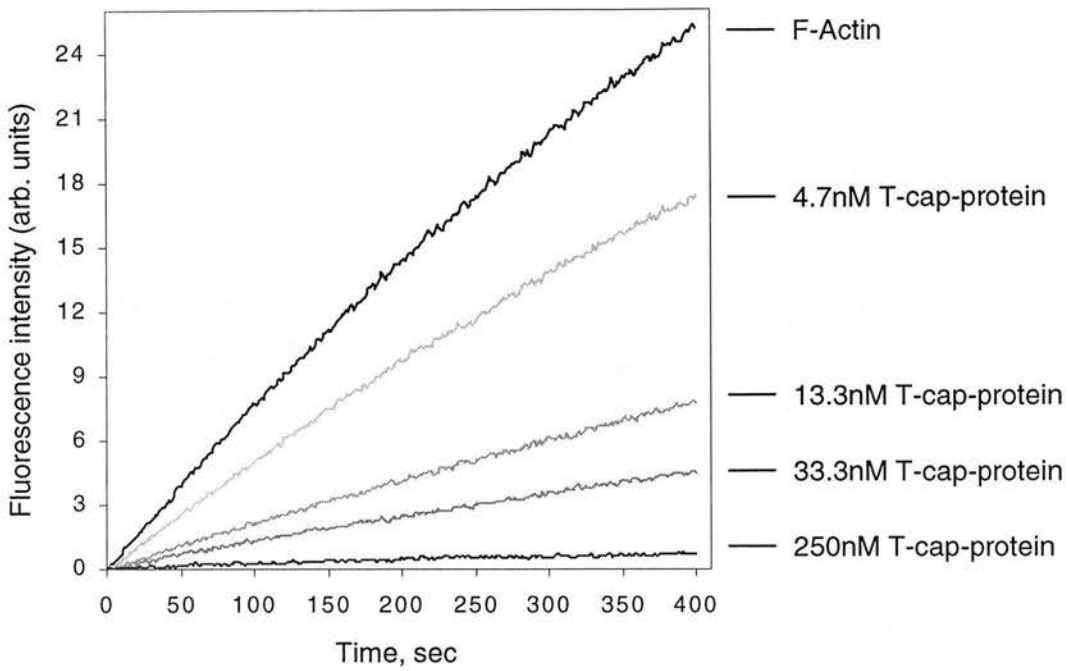

Fig 5.8. ***The effect of full-length T-cap-protein on nucleated actin polymerisation.*** 0.5μM G-actin (20% pyrene-labelled) was polymerised, in the presence 0.1μM F-Actin seeds and in the absence or presence of increasing amounts of full-length T-cap-protein, by the addition of KCl and $MgCl_2$ to 100mM and 2mM, respectively. The time course of polymerisation was measured (at 20°C) by following the increase in the fluorescence intensity of pyrene actin. The excitation wavelength used was 366nm with an emission wavelength of 384nm, with a 5nm slit for both. (Polymerisation assays were performed as described in the methods).

As can be clearly seen from fig. 5.9(A) nM concentrations of T-cap-protein result in extensive inhibition polymerisation, with the final level approaching *complete* inhibition (100%). Under our assay conditions, polymerisation can only occur by the addition of G-Actin monomers onto the *free* barbed-ends of the added F-Actin nuclei. (The rate of spontaneous nucleation and subsequent polymerisation of 0.5mM actin is negligible; Selve and Wegner, 1986; see also discussion). Capping of these barbed-ends by T-cap-protein correspondingly reduces the number of free barbed-ends onto which monomer can add, resulting in a reduction in the initial polymerisation rate. This effect is clearly illustrated in fig. 5.8.

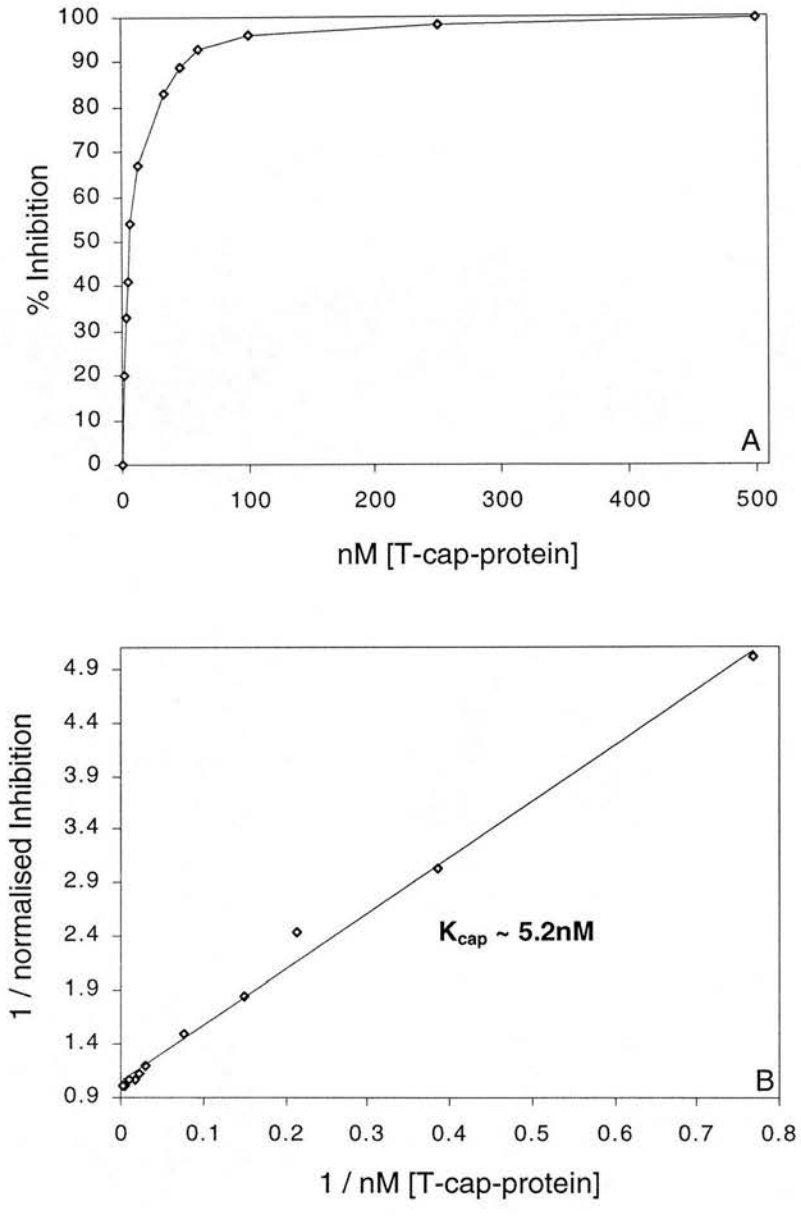

Fig 5.9. ***Effect of full-length T-cap-protein on nucleated actin polymerisation.*** (A) Inhibition of the rate of nucleated, barbed-end limited actin polymerisation by the addition of increasing amounts of T-cap-protein. (B) Graphical determination of the K_{cap} for T-cap-protein, derived from the values in A. K_{cap} is the dissociation constant for T-cap-protein binding to the barbed-end of actin filaments, where this causes a 50% inhibition in the initial rate of polymerisation. Percentage inhibition values were obtained from the experiments shown in fig. 5.8, and have been normalised to 1.0 for 100% inhibition. The initial rate of polymerisation was measured and the units of fluorescence intensity units per second converted to give the rate of monomer addition in $nM.s^{-1}$, (calibrated from steady-state values). The solid line (in B) shows a linear regression (R^2 = 0.993), with the gradient corresponding to the K_{cap}; the value is shown in the inset in B. (Polymerisation assay was performed as described in methods).

Fig. 5.9(B) shows the graphical determination of the K_{cap}. A value of ~ 5.2nM was obtained for the K_{cap} of this particular T-cap-protein sample. The mean K_{cap} values obtained for full-length T-cap-protein and for the degraded fragment were 6.9nM (± 3.1 SD, n=7) and 8.0nM (± 2.6 SD, n=6) respectively (see table 5.1). (The K_{cap} values obtained for the degraded fragment were derived from a similar series of assays to those described above and in fig. 5.8). These very low nM concentrations of T-cap-protein (and the degraded fragment) that cause significant levels of inhibition further suggest that inhibition of polymerisation is due to capping of the barbed-end and *not* via the stoichiometric sequestration of monomers (see section 5.3.1.3).

K_{cap} T-cap-protein (nM)	**K_{cap} degraded T-cap-protein fragment (Mr. ~ 42kDa.) (nM)**
3.8	5.3
4.9	6.9
5.2	6.1
5.8	12.1
6.2	10.1
10.1	7.4
12.3	
Mean = **6.9nM** ± 3.1 (SD, n=7)	Mean = **8.0nM** ± 2.6 (SD, n=6)

Table 5.1 ***Range of K_{cap} values for full-length and degraded T-cap-protein.*** Values for K_{cap} were calculated from data obtained from nucleated polymerisation experiments, similar to those described in figs. 5.8, 5.9(A) and (B). (See methods for protocol details).

There is very little difference between the K_{cap} values obtained for full-length T-cap-protein and those obtained for the degraded fragment (see table 5.1). The loss of the 28 amino acid residues from the C-terminus, likely due proteolysis (see section 5.2.1.2), appears to have no effect on the capping activity of this protein. These residues (T337 – A364 from our T-cap-protein construct) therefore appear not to be important for capping of the barbed-end of filaments. This is in agreement with both Lo et al (1994c) and Chuang et al (1995), neither of whom, despite their conflicting reports, has implicated these residues as being important in the high affinity capping activity of tensin.

5.3.1.2 The effect of full-length T-cap-protein on actin depolymerisation

We have also analysed the effect of full-length T-cap-protein on actin depolymerisation. Fig. 5.10(A) shows the time course of actin depolymerisation (induced by dilution of 3.0μM F-actin - 20% pyrene labelled - to 0.5μM with *ATP-G-Buffer*) in the absence or presence of increasing amounts of full-length T-cap-protein on (see methods for details). The loss of fluorescence intensity is directly proportional to monomer dissociation from the ends of filaments. Under these low-salt conditions actin filaments depolymerised *completely*, from both the pointed and barbed-ends. The rate of depolymerisation is directly dependent on the number of filament ends (both barbed and pointed) from which monomers are able to dissociate (see discussion). Capping of the faster depolymerising barbed-ends will thus result in very marked decreases in the initial rates of depolymerisation (under physiological ionic conditions the ratio of the rate constants of monomer dissociation, from both ends, k_{-b} / k_{-p}, is ~ 5 - 10; Pollard, 1986).

Fig. 5.10(A) clearly shows a steady decrease in the initial rate of depolymerisation as the concentration of T-cap-protein in increases. In a similar manner to the polymerisation experiments, a K_{cap} value of ~ 7.8nM was calculated for full-length T-cap-protein (data not shown), in good agreement with the ~ 5 – 12nM values obtained from analysis of nucleated polymerisation. Although the extent of depolymerisation reached at the end of the time course (400 sec) was increasingly reduced, as the concentration of added T-cap-protein increased, the *final* extent reached was always the same (determined by measuring the fluorescence intensity after ~ 4hrs). The intensity values measured, in all cases, were equal to that of 0.5μM G-Actin (20% pyrene labelled) indicating that depolymerisation had proceeded to completion.

Further evidence of barbed-end capping activity of T-cap-protein can be seen in fig. 5.10(B). In these experiments, depolymerisation was performed by diluting 3.0μM F-Actin (20% pyrene labelled) to 0.5μM with *ATP-F-Buffer* (see methods for details). F-actin alone exhibits a rapid initial rate of depolymerisation, followed by a steady

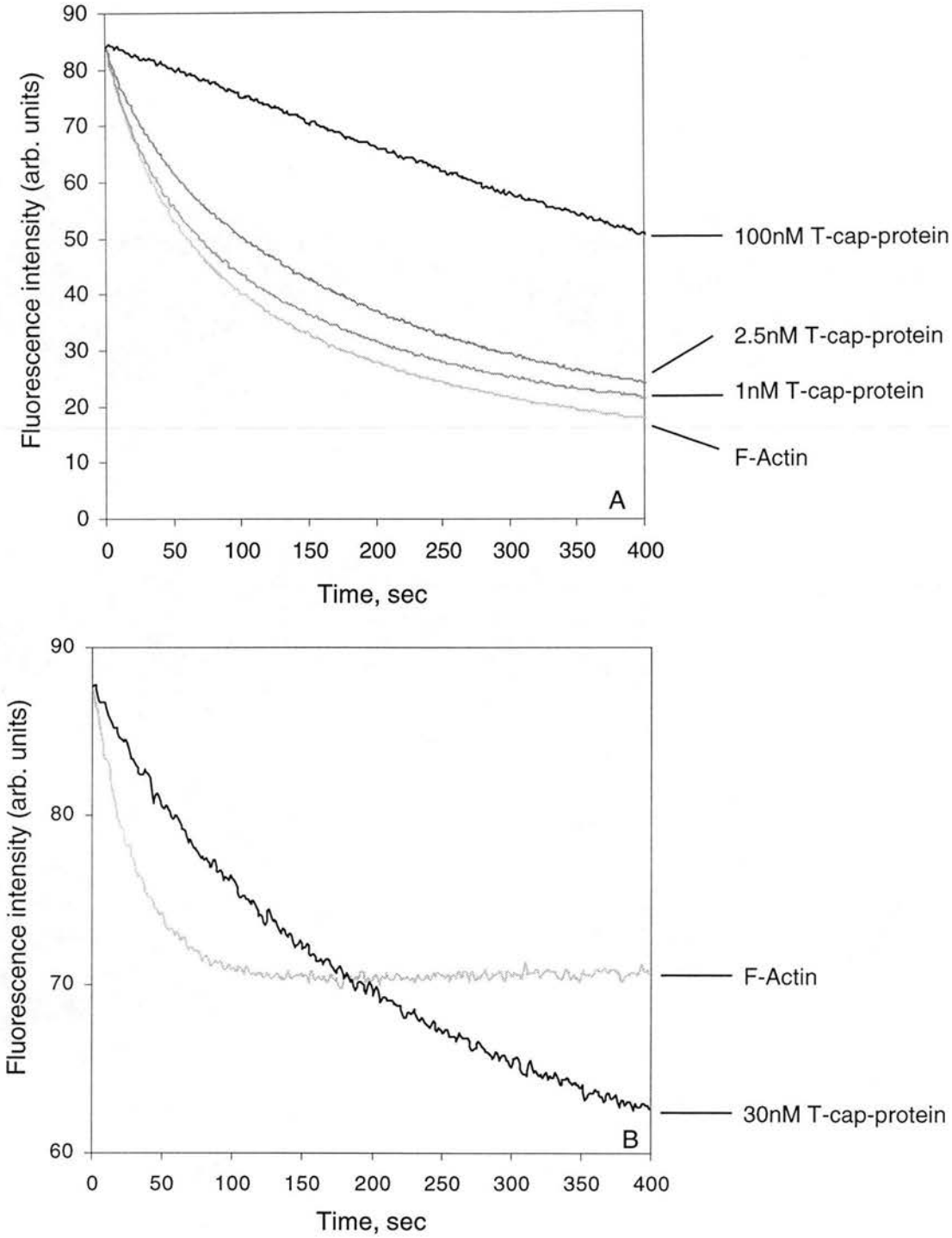

Fig. 5.10. ***Effect of full-length T-cap-protein on the rate and extent of actin depolymerisation***. (A) 3.0μM F-Actin (20% pyrene-labelled) was diluted to 0.5μM, into *ATP-G-Buffer*, in the absence or presence of increasing amounts of full-length T-cap-protein. (B) 3.0μM F-Actin (20% pyrene labelled) was diluted to 0.5μM, into *ATP-F-Buffer*, in the absence or presence of 30nM full-length T-cap-protein. The time course of depolymerisation (at 20°C) was followed by measuring the decay of the fluorescence intensity of pyrene-actin. The excitation wavelength was 366nm and the emission wavelength was 384nm, with a 5nm slit for both. (Depolymerisation assay was performed as described in the methods).

trailing-off to a new plateau level reflecting the attainment of a *new* steady-state (in this instance, 0.5μM total actin), where the concentration of [F-Actin] = $[Actin]_{tot}$ – $[C_c]$. The actin filaments at this concentration are experiencing loss of monomer from the pointed-ends (we are below the critical concentration of the pointed-end; 0.6 – 0.8μM) balanced by the addition of subunits to the barbed-end ($[C_c]_b$ ~ 0.1μM), with the net concentration of *filaments* remaining the same. i.e. the filaments are undergoing treadmilling.

The time course of depolymerisation in the presence of 30nM T-cap-protein showed a very different profile to that of F-actin alone (see fig. 5.10B). The initial depolymerisation rate was much slower and a *lower* fluorescence intensity value was reached at the end of the time course (400sec). Under these assay conditions the F-Actin will depolymerise until it reaches a *new* steady-state, where the concentration of F-Actin present at this new steady-state is determined by the concentration of free monomer and by the ratio of *free* barbed and pointed-ends (especially the number of free barbed-ends). Thus, increased capping of these faster growing barbed-ends, (in this case by T-cap-protein), results in the new steady-state having increasingly *reduced* F-Actin concentrations (reflected by lower fluorescence intensity signals, directly proportional to the amount of F-Actin present, see fig. 5.10B). Eventually, when all of the available barbed-ends are capped, complete depolymerisation will occur (see discussion for details).

Our results are in agreement with those of Chuang et al (1995) who report a tight K_{cap} (~ 1 – 5nM) and similar effects on nucleated, barbed-end limited polymerisation and depolymerisation, with several of their GST-tensin fusion constructs (those containing residues R989 – V1121).

5.3.1.3 The effect of full-length T-cap-protein on the steady-state monomer critical concentration

In an attempt to address the discrepancy in the "capping mode" of tensin (see section 5.3.1) we have conducted a series of extensive monomer critical concentration ($[C_c]$) assays in the presence of increasing amounts of full-length T-cap-protein. All protein samples were incubated for 24hrs (at 20°C in the dark) to ensure that steady-state had been reached (see methods for details).

Figs. 5.11(A), (B), (C), and (D) show the results from a typical $[C_c]$ assay. The steady-state critical monomer concentration increases with the amount of full-length T-cap-protein added. Significant shifts were observed even with the addition of sub-stoichiometric amounts of T-cap-protein. Fig. 5.12 graphically presents the data from figs. 5.11(A) – (D), illustrating the shift in the steady-state critical monomer concentration, from that of the barbed-end (~ 0.1μM) towards that of the pointed-end (~ 0.74μM under these assay conditions).

Further evidence that the effects of T-cap-protein are due to its interaction with the barbed-end and not due to monomer sequestration is provided by these data. The apparent $[C_c]$ values obtained in the presence of 500nM, 800nM and 1200nM T-cap-protein are essentially identical (0.74μM, 0.72μM and 0.74μM, respectively), and equal to that of the pointed-end. If T-cap-protein were acting by stoichiometrically sequestering monomers, thus making them unavailable for polymerisation (similar to the effects observed with DNaseI, see appendix B) the $[C_c]$ would be shifted by the same corresponding concentration of monomers sequestered. If this was the case, at high concentrations (e.g. 800nM and 1200nM) the steady-state critical concentration would be equal to the $[C_c]$ plus the [sequestered monomer] (which, assuming a 1:1 sequestration, is equal to the concentration of added T-cap-protein). i.e. $[C_c]$ ~ 0.9μM in the presence of 800nM T-cap-protein and $[C_c]$ ~ 1.3μM in the presence of 1200nM T-cap-protein. However, as is clearly indicated by the approach to a plateau, equal to the $[C_c]$ of the pointed-end, (see fig. 5.12B), regardless of the addition of concentrations of T-cap-protein in excess of this, this is not the case.

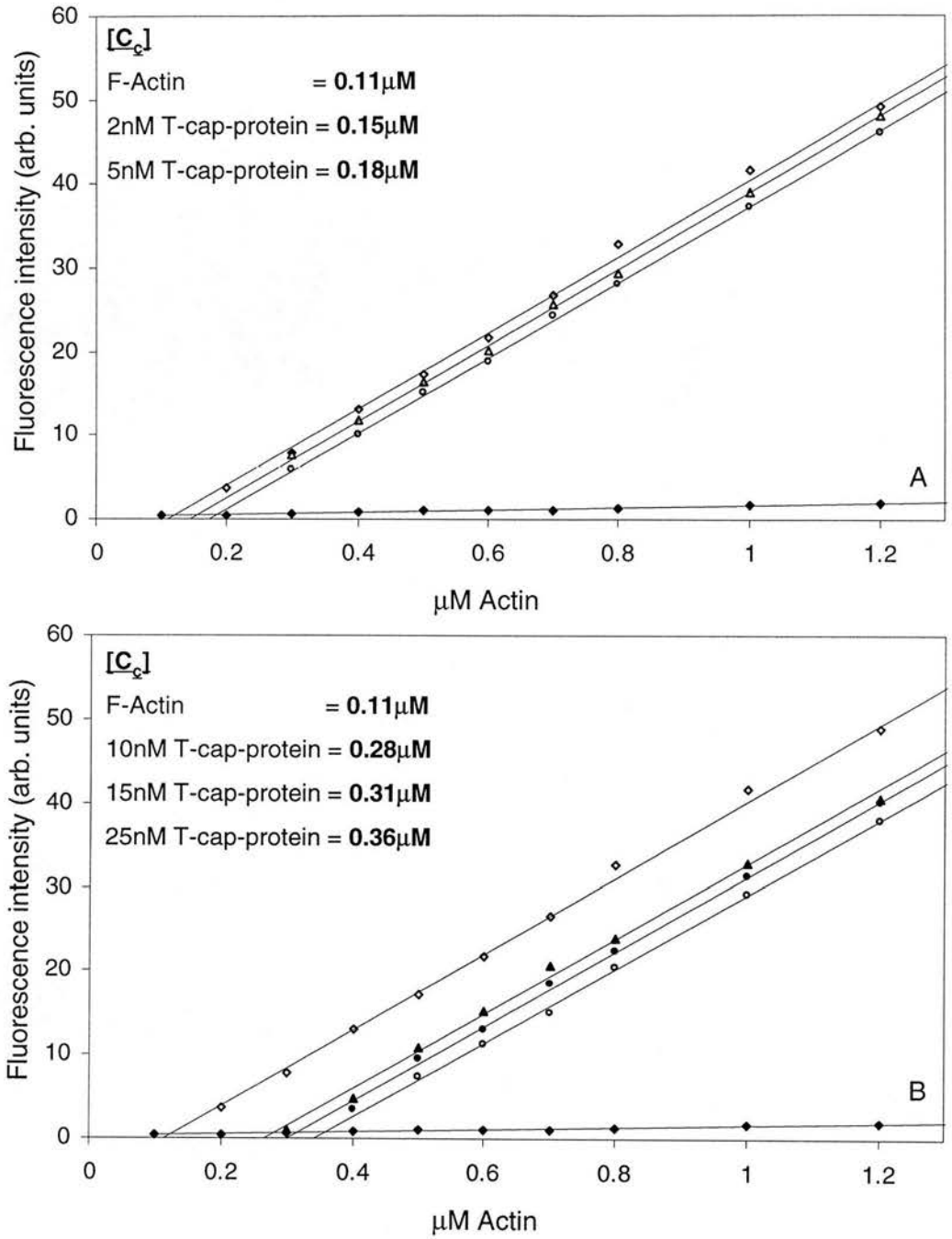

Fig. 5.11(A) and (B). ***Effect of full-length T-cap-protein on the steady-state actin monomer critical concentration ([C_c]).*** The table inset in each of the graphs gives the [C_c] value obtained in each assay. Sub-critical points have been omitted for clarity, and the solid lines are a linear regression of the data. (A) *Closed squares* indicate the fluorescence intensity values for G-Actin alone; *open squares*, F-Actin alone; *open triangles*, 2nM T-cap-protein; *open circles*, 5nM T-cap-protein. (B) *Closed squares* indicate the fluorescence intensity values for G-Actin alone; *open squares*, F-Actin alone; *closed triangles*, 10nM T-cap-protein; *closed circles*, 15nM T-cap-protein; *open circles*, 25nM T-cap-protein. Each point represents a separate incubation mixture. The appropriate amount of T-cap-protein, in ATP-F-Buffer, was mixed with F-Actin (5% pyrene labelled), and then incubated for 24hr, at 20°C in the dark. The fluorescence intensity of each sample was then measured at 20°C. The excitation wavelength was 366nm, the emission wavelength was 384nm, with a 5nm slit width for both. (See methods for protocol details).

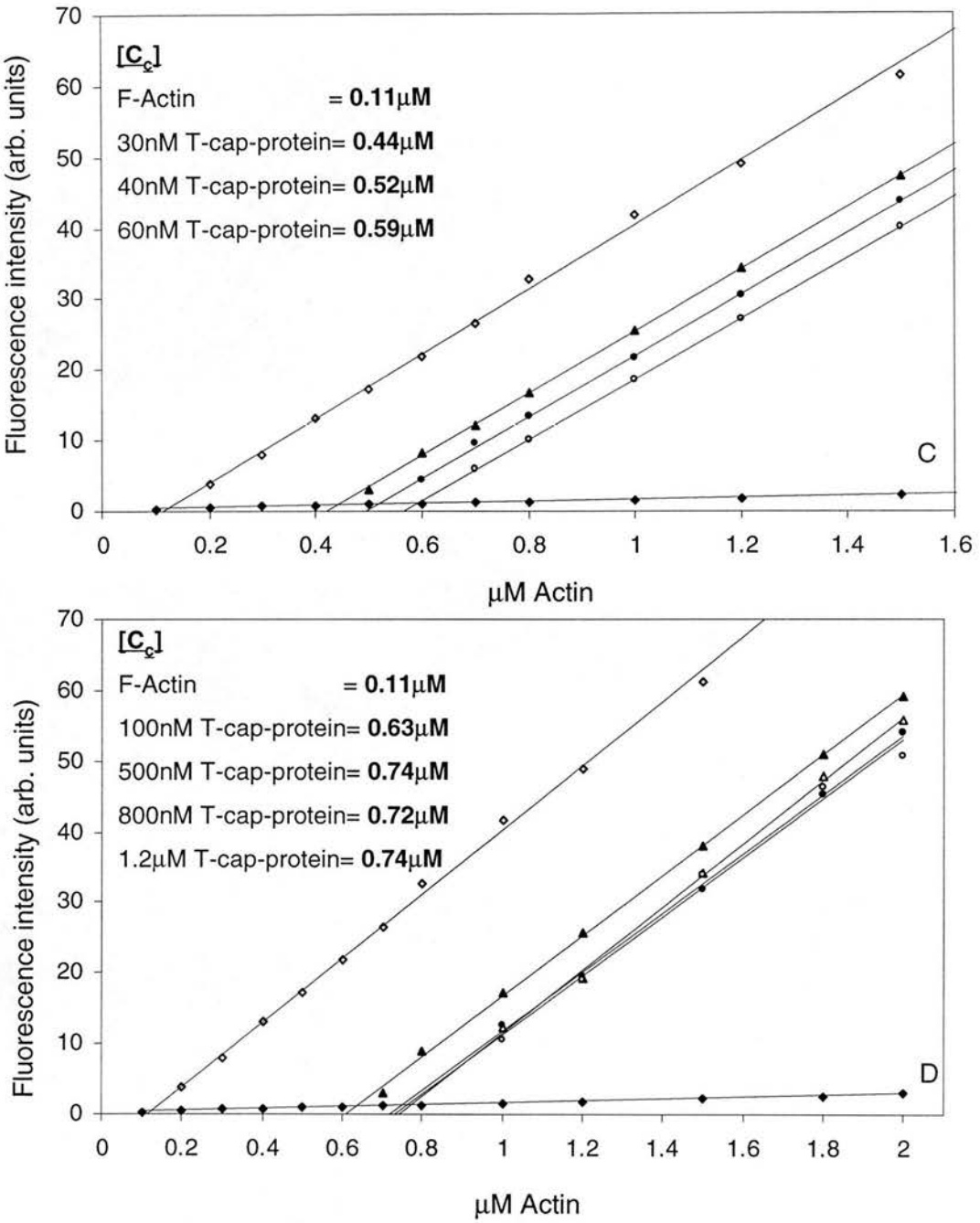

Fig. 5.11(C) and (D). ***Effect of full-length T-cap-protein on the steady-state monomer critical concentration of actin ([C_c]).*** The table inset in each of the graphs gives the [C_c] value obtained in each assay. Sub-critical points have been omitted for clarity, and the solid lines are a linear regression of the data. (C) *Closed squares* indicate the fluorescence intensity values for G-Actin alone; *open squares*, F-Actin alone; *closed triangles*, 30nM T-cap-protein; *closed circles*, 40nM T-cap-protein; *open circles*, 60nM T6-protein. (D) *Closed squares* indicate the fluorescence intensity values for G-Actin alone; *open squares*, F-Actin alone; *closed triangles*, 100nM T-cap-protein; *open triangles*, 500nM T-cap-protein; *closed circles*, 800nM T-cap-protein; *open circles*, 1200nM T-cap-protein. Each point represents a separate incubation mixture. The appropriate amount of T-cap-protein, in ATP-F-Buffer, was mixed with F-Actin (5% pyrene labelled), and then incubated for 24hr, at 20°C in the dark. The fluorescence intensity of each sample was then measured at 20°C. The excitation wavelength was 366nm, the emission wavelength was 384nm, with a 5nm slit width for both. (See methods for protocol details).

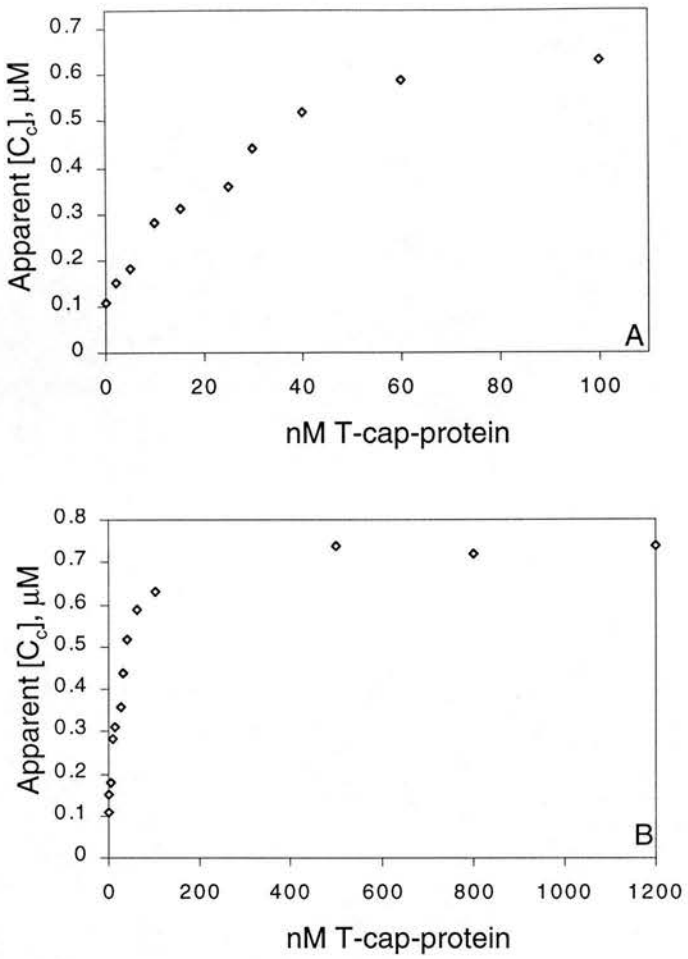

Fig. 5.12. ***Full-length T-cap-protein shifts the steady-state critical monomer concentration towards that of the pointed-end.*** (A) Plot of apparent [C_c] against T-cap-protein concentration, up to 100nM (data obtained from fig. 5.11). (B) Similar plot to that shown in A, with high concentrations of T-cap-protein (those above 100nM,) included. These graphs clearly indicate a shift towards the [C_c] of the pointed-end (~ 0.74µM in this experiment) by addition of increasing amounts of T-cap-protein.

The concentrations of T-cap-protein that produce the increase in the [C_c] are in good agreement with the value of K_{cap} determined from polymerisation assay data. A 50% increase in the *initial* [C_c] value is produced when 50% of the barbed-ends have been capped; i.e. the K_{cap} value (Walsh et al, 1984; see discussion). The initial [C_c] is 0.11µM and a 50% increase gives a figure of ~ 0.17µM. The corresponding amount of T-cap-protein that causes a 50% shift is ~ 5nM, see figs. 5.11(A) and 5.12(B).

Our data is in agreement with the observations of Chuang et al (1995). These workers have report a similar shift towards the critical concentration of the pointed-end, upon addition of sub-stoichiometric amounts of several of their GST-tensin constructs. We did not observe any evidence of an "insertin-like" activity; our assays *always* illustrated significant shifts in the steady-state critical monomer concentration, in samples containing nM concentrations of T-cap-protein.

5.3.1.4 Full-length T-cap-protein has an apparent novel filament side-binding activity

Three distinct actin-binding domains have been identified within tensin; two N-terminal proximal ABD-1 domains and a central ABD-2 domain which our T-cap-protein span (see fig. 5.1, and see Lo et al, 1994a; see Lo et al, 1994b and Taylor et al, 1998 for reviews). The amino acid sequence within ABD-1, from L371 to N395 of whole tensin, shares homology with a consensus actin-binding sequence (see fig. 5.1) found in α-Actinin, filamin, spectrin, dystrophin, plastin/fibrin, APB-120 and APB-280 (Nagafuchi et al, 1991; Bresnick et al, 1991; Hartwig and Kwiatkowski, 1991; Matsudaira, 1991). The two ABD-1 domains are most likely responsible for the side-binding of tensin to F-actin. Lo et al (1994c) have reported that GST-tensin fusion constructs, composed of amino acids 1 – 263 and 263 – 463, co-sediment with actin filaments with dissociation constants in the sub-micro molar range (~ 0.5μM). The central ABD-2 domain (the region of tensin with very high sequence identity to "insertin"), is responsible for the barbed-end capping activity. This has been confirmed by our own experiments performed with T-cap-protein (R861 – A1223), described in the preceding sections.

For the first time, we show evidence that ABD-2 also contains an F-Actin binding site. We performed co-sedimentation assay analysis with our T-cap-protein construct (containing the high-affinity ABD-2 barbed-end-capping domain) and our data seem to suggest a novel F-Actin side-binding activity. Fig. 5.13 shows the results obtained from an actin co-sedimentation assay, performed in the presence of increasing amounts of full-length T-cap-protein (see methods for protocol details). It should be noted that the concentration of full-length T-cap-protein used in this assay was

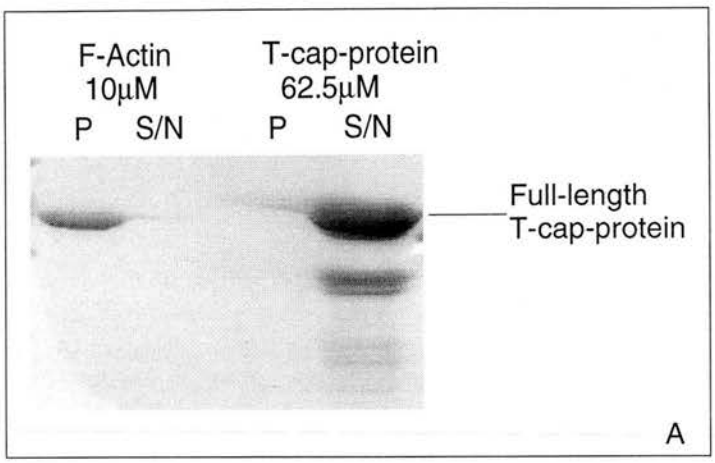

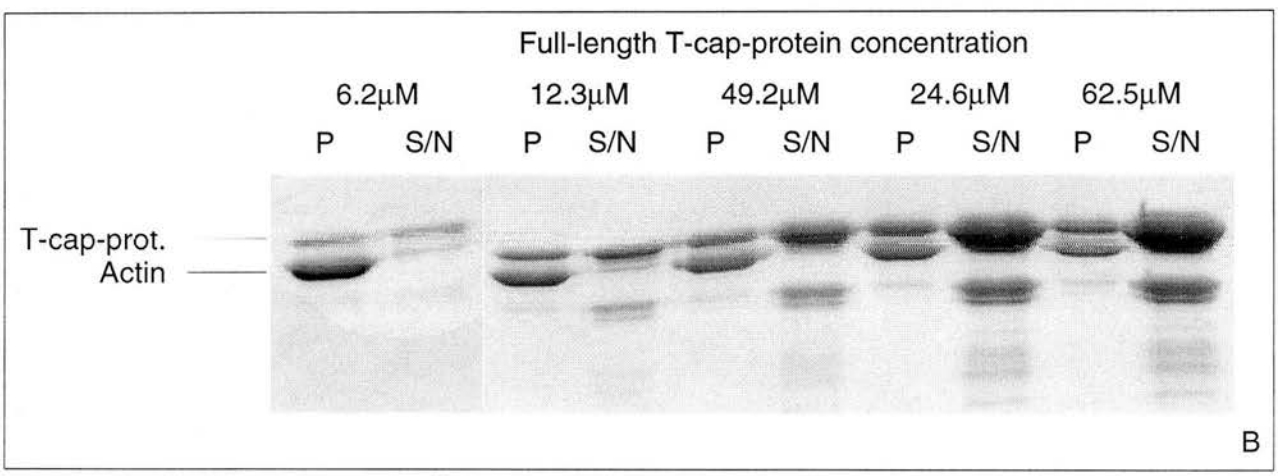

Fig. 5.13. ***Binding of recombinant T-cap-protein to the side of actin filaments.*** (A) SDS-polyacrylamide gel (10%,w/v acrylamide) showing the amounts of T-cap-protein appearing in the pellet and supernatant fractions following centrifugation at 386,000 xg for 15min (at 4°C), in the absence of F-Actin. This is representative of the amount of insoluble T-cap-protein present; i.e. non-specific sedimentation. The corresponding amounts of G-Actin and F-Actin that appear in the in the pellet and supernatant fractions, in the absence of T-cap-protein, are also shown. (B) SDS-polyacrylamide gel (10%,w/v acrylamide) showing the results from an actin co-sedimentation assay performed in the presence of increasing amounts of T-cap-protein. S/N denotes the supernatant fraction; P, denotes the pellet fraction. 10μM Actin was used in all assays. (The co-sedimentation assay was performed as described in the methods).

calculated by analysing the percentage of total protein constituted by full-length T-cap-protein. This was carried out due to the presence of a relatively high amount of contaminants and/or degraded fragments in the T-cap-protein sample used, and was calculated by densiometric scanning (data not shown) of the S/N fraction lane of the 62.5μM T-cap-protein sample (see 5.13A).

As the amount of T-cap-protein increased (added to a constant 10μM F-actin), a concomitant increase in the amount of T-cap-protein co-sedimenting with F-Actin in the pellet fraction was observed (see fig. 5.13B). This appears to be a specific interaction with the sides actin filaments as essentially no T-cap-protein (the faint band seen in the T-cap-protein supernatant fraction of fig. 5.13A represents ~ 1% of the total) sediments in the absence of F-Actin.

Fig. 5.14 shows the binding curve obtained for the apparent specific association of T-cap-protein with F-Actin. The approximate (see below) amount of T-cap-protein in the pellet and supernatant fractions was obtained from densiometric analysis (see methods) of the gel lanes shown in fig. 5.14(B). Least squares, non-linear regression analysis of these data gives an apparent K_d of ~ 10μM for this association, and the B_{max} value is ~ 8.0μM. This gives an apparent stoichiometry of between 1:2 and 1:1 for T-cap-protein:actin, respectively.

We were unable, however, to accurately determine the amounts of both T-cap-protein and actin, present in the supernatant and pellet fractions. Several factors contributed to this problem: the inability to achieve a high degree of separation between G-Actin and T-cap-protein on SDS-polyacrylamide gels (due to the closeness of the Mr. values, ~ 42kDa. for G-Actin compared to ~ 46 – 48kDa. for full-length T-cap-protein), the lateral smudging of the bands in samples containing a high concentration of T-cap-protein, and the existence of a significant amount of degraded polypeptides in the T-cap-protein samples. A degraded fragment (or a contaminant protein in the sample) migrates at a position such that it lies directly under that of G-Actin (Mr. ~ 42kDa., see fig 5.2).

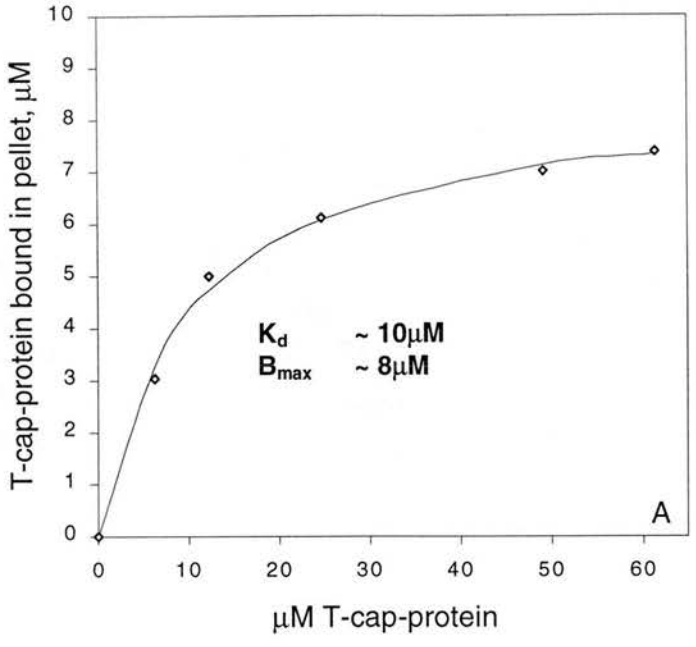

Fig. 5.14. ***Analysis of the apparent F-Actin side-binding activity of full-length T-cap-protein.*** The figure shows a binding curve produced from densiometric analysis of the co-sedimentation assay data shown in fig. 5.13. The solid line is a non-linear least squares fit of the equation [T-cap-protein bound in F-Actin pellet] = B_{max}*[T-cap-protein]/([T-cap-protein]+K_d). The apparent K_d for this interaction is ~ 10µM, with a B_{max} value of ~ 8.0µM. (R = 0.998). This gives a stoichiometry of between 1:2 and 1:1 for T-cap-protein:actin, respectively. (See methods for details of the protocol).

A combination of these problems resulted in severe difficulties in obtaining distinct and well-defined protein band-boundaries during the densiometric analysis (see methods). Therefore, the integrated volume intensity values calculated for each of the protein bands only very rough estimates. As we were also unable to obtain accurate values for the amounts of actin present, in either the pellet or supernatant fractions, the K_d and B_{max} values obtained for T-cap-protein binding to F-Actin are inaccurate, and contain high inherent errors. However, the general trend of an increased binding of T-cap-protein to F-Actin (a *novel* feature) can clearly be seen in the pellet fractions of fig. 5.13(B).

5.3.2 Interaction with G-Actin

As we have described in the preceding sections, our T-cap-protein construct appears to bind tightly (K_{cap} ~ 7 – 8nM) to the barbed-ends of actin filaments. Furthermore, our results seem to suggest that capping of these ends takes place via simple barbed-end capping rather than an "insertin-like" mechanism. We proposed to use T-cap-protein as a replacement for gelsolin (as the barbed-end capping protein) in the creation and further analysis of our putative "minifilament". This was in an attempt to overcome the problems of possible monomer exchange (for the A:D binary complex) at the EGTA labile site (G4) on gelsolin (see section 4.5). Furthermore, as T-cap-protein is approximately half the size of gelsolin (Mr. ~ 38kDa compared to ~ 82kDa for T-cap-protein and gelsolin, respectively) formation of the barbed-end cap by this smaller protein in the analysis of the putative "minifilament", may reduce competition with the surface of the putative "minifilament". This would also possibly reduce the crystallographic problem of crystallisation and solving the structure of this complex.

A pre-requisite for T-cap-protein, as a barbed-end capping protein in the creation of the putative "minifilament", is that it is able to form tight, stable and easily purified complexes with actin monomers. Such complex formation (analogous to the use of the G:A_2 ternary complex) would allow us to control the definition of the barbed-end of the "minifilament". As described before (see chapter 4), the subsequent addition of the A:D binary complex (capping and defining the pointed-end) may then result in the formation of a putative "minifilament" complex. We therefore, initially tested for any interaction between T-cap-protein and G-Actin monomers. Binding studies were performed using size-exclusion chromatography and fluorescence enhancement analysis with NBD-actin. However, the limiting factor in the scope of these experiments was the small amount of pure (~ 85%) full-length T-cap-protein we were able to routinely obtain. This has resulted in the extent and number of these studies being severely limited (see below).

T-cap-protein and G-actin were mixed together in ATP-G-Buffer, at a molar ratio of 1:1 (at a concentration of 3.0μM). Following a 1hr incubation at room temperature the protein mixture was subjected to size-exclusion on an FPLC/Superose-12 column, run in ATP-F-Buffer or 100mM Tris, pH 8.0; ATP-G-Buffer (see below). Fig. 5.15 shows the A_{280nm} monitored elution profile of such an incubation of T-cap-protein and G-Actin, from an FPLC/Superose-12 column. The profile contains two, relatively poorly resolved peaks. The retention volumes (see table 5.2) of the two peaks correspond to the elution positions of the individual *uncomplexed* proteins; T-cap-protein, peak (1) and G-Actin, peak (2). In four similar experiments we conducted no shift in the retention volumes of either of the two proteins was observed; the elution profiles always contained two peaks that corresponded to the retention volumes of *uncomplexed* monomeric G-actin and that of *uncomplexed* full-length T-cap-protein (see table 5.2).

Protein species	Retention volume (ml)	Theoretical Mr. (kDa.)	Apparent Mr. (kDa.)
G-Actin	11.64 (± 0.062 SEM, n=6).	42	57
Full-length T-cap-protein	11.34 (± 0.097 SEM, n=4)	38	64.5

Table 5.2. ***Retention volumes (ml) of G-Actin and full-length T-cap-protein.*** Data obtained from FPLC/Superose-12 size-exclusion chromatography experiments. The value given for the apparent Mr. is a mean value calculated from the calibration curve using the corresponding mean retention volume. (See methods for details).

We did not observe any evidence of complex formation on Superose-12 columns run in either 100mM Tris, pH 8.0; ATP-G-Buffer or ATP-F-buffer, in the presence or absence of Ca^{2+} ions ($CaCl_2$ added to 0.2mM). The 100mM Tris, pH 8.0; ATP-G-Buffer is a buffer that contains no salt (i.e. KCl or NaCl) but the ionic strength is equivalent to that of ATP-F-Buffer. We used this buffer as a substitute for ATP-F-Buffer to prevent any hydrophobic interactions between the partitioning proteins and the Superose resin. It also prevents problems with actin polymerisation, that would be caused by the addition of salt. It gives virtually identical values for protein retention volumes (and thus the same apparent Mr. values) to those obtained for proteins in ATP-F-Buffer.

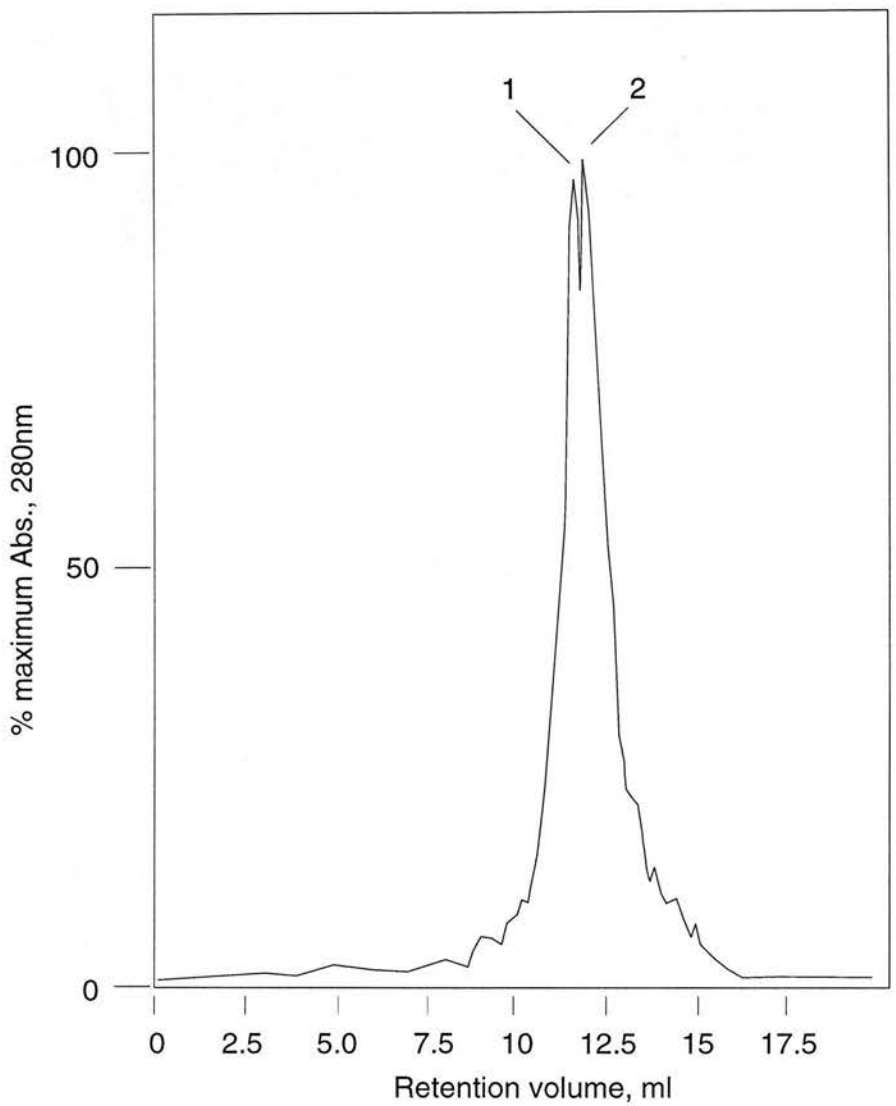

Fig. 5.15. ***Full-length T-cap-protein does not bind to G-Actin.*** A_{280nm} monitored elution profile of a 1:1 molar ratio incubation (in ATP-G-Buffer) of G-Actin and T-cap-protein (3.0μM for each protein), following a 1hr incubation at room temperature, from an FPLC/Superose-12 size-exclusion column, run in 100mM Tris, pH 8.0; ATP-G-Buffer. The arrows mark the elution positions of (1); full-length T-cap-protein and (2); G-Actin when chromatography was performed on the individual proteins alone. No apparent shifts in the retention volumes, of either protein, were observed in samples containing a mixture of the two proteins. (SDS-PAGE and chromatography were performed as described in methods).

The value obtained for the apparent Mr. of T-cap-protein is significantly larger than the theoretical Mr. (64.5kDa compared to 38kDa, see table 5.2). A similar feature was noticed during the analysis of full-length T-cap-protein with SDS-PAGE. The value is close to that theoretically expected for a dimer of T-cap-protein (assuming the protein has a compact globular shape). Full-length recombinant Tensin, from which this T-cap-protein is derived, has been reported to dimerise *in vitro* (Lo et al, 1994a). However, the proposed dimerisation occurred via putative interactions between amino acids in the C-terminus. Our T6-construct contains the amino acids R861 – A1223 from tensin (based on the residue sequence numbering system of Lo et al, 1994a). It does not contain the putative C-terminal residues involved in this dimerisation process.

The relatively high proline content of our T-cap-protein (14%, see fig. 5.3) may account for the larger apparent Mr. Proline has a more restricted set of allowable, non-constrained bond angles than most other amino acid residues. The protein molecule may have a distinctly non-globular hydrodynamic radius, as a direct result of the steric constraints imposed on the protein by this high percentage of proline residues, and this possibly explains its higher than expected apparent Mr. from size exclusion experiments. Further evidence of the non-globular nature of the T-cap-protein was illustrated by data obtained from NMR experiments. These data suggested that the protein had very little secondary structure, and although not completely unfolded, it had a very extended and open conformation (Paul McLaughlin and Mary Russell, unpublished results). This observation may also explain the severe proteolytic degradation observed with this protein. The more open and extended conformation of the peptide backbone would theoretically present more cleavage sites, and allow the proteolytic enzymes easier access to these sites than a compact, folded globular domain would.

Similar results, reflecting no interaction between T-cap-protein and actin monomers, were observed in experiments with NBD-Actin. The position of the covalently linked fluorescent NBD probe, (coupled to lysine-373 of actin) exposed at the surface of subdomain I, provides a method for reporting the binding of other proteins to G-

Actin (see Bryan and Kurth, 1984; Weeds et al, 1986; Way et al, 1989 and see our data described in chapter 3). The binding of other proteins to the barbed-ends of the monomer/s, usually produces an enhancement in the fluorescence emission spectra of NBD-Actin, due to a change in the solvent environment around the probe.

NBD-Actin and T-cap-protein were mixed together at a molar ratio of 1:1 (at a concentration of 3.0μM) in ATP-G-Buffer, and incubated for 1hr at room temperature. Following incubation the emission spectra (scanning from 500nm to 700nm, with an excitation wavelength of 475nm, and with a 5nm slit width for both) was examined for any fluorescence enhancement. In two similar experiments we observed no fluorescence enhancement, over that seen for 3.0μM NBD-Actin alone (data not shown).

We were unable to perform the numerous experiments needed to properly define any possible interaction between our T-cap-protein and G-Actin. This was primarily due to the very small amounts of pure, full-length T-cap-protein we could obtain, and the length of time involved in the purification procedure, to even obtain these amounts. As a result we have not pursued these experiments any further. However, our initial results have suggested that there was no interaction between T-cap-protein and monomeric G-Actin. No other evidence of an interaction between tensin, insertin or any of the fusion proteins derived from tensin, and actin monomers, has been reported in the literature.

Thus, we decided that T-cap-protein was not a good candidate for use as a substitute for gelsolin in the further analysis of the putative "minifilament".

5.4 Discussion

5.4.1 Overview

We have developed a novel working protocol for the purification of our T-cap-protein construct (a fragment of the protein tensin that spans the sequence containing the high affinity barbed-end capping domain "insertin"). This protocol gives a final purity of ~ 85% for the full-length T-cap-protein. Our experiments with the T-cap-protein, a fragment derived from tensin (a protein localised to focal contacts), indicate that it tightly caps the barbed-ends of filaments (K_{cap} ~ 7 – 8nM). The data also indicate that T-cap-protein does not have any "insertin-like" activity; T-cap-protein affects the long-term steady-state critical monomer concentration, shifting it towards that of the pointed-end.

A pre-requisite the use of this T-cap-protein in the further analysis of the formation of the "minifilament" is that it has the ability to form stable and easily purifiable complexes with actin monomers (similar to A:D and G:A_2). However, we did not find any evidence of T-cap-protein binding to monomeric actin, and as a result, using this protein as a substitute for gelsolin as the barbed-end-capping protein in the further analysis of the "minifilament", was not a viable option. Interestingly however, although this T-cap-protein still has function (high-affinity barbed-end capping activity), in a similar manner to β-thymosin, it appears to have little secondary structure and lacks a compact folded core in solution (Czisch, et al, 1993); at least as the isolated T-cap-protein fragment.

5.4.2 Kinetic considerations

A kinetic consideration of the data obtained from our polymerisation, depolymerisation and steady-state critical concentration analysis experiments (described in section 5.3.1), provides good evidence for the interaction of T-cap-protein with the barbed-ends of actin filaments, and for the capping of these ends taking place via a simple *non* "insertin-like" mechanism.

During nucleated actin assembly, the rate of polymerisation d[F-Actin] / dt can be described by the following relationship:

$$d[\text{F-Actin}] / dt = k_{+b}\cdot[G]\cdot[\text{ends}_b] + k_{+p}\cdot[G]\cdot[\text{ends}_p] - k_{-b}\cdot[\text{ends}_b] - k_{-p}\cdot[\text{ends}_p] + \text{spontaneous polymerisation} \quad (1),$$

where k_{+b} is the rate constant of monomer addition to the barbed end, k_{+p} is the rate constant of monomer addition to the pointed end, [G] is the concentration of G-Actin, $[\text{ends}_b]$ is the concentration of barbed-ends and $[\text{ends}_p]$ is the concentration of pointed-ends.

If we consider only the *initial* rates, the loss of monomer from the filament ends can be ignored as, under physiological ionic conditions, the typical ratio of the rate constants for monomer addition, to both ends, k_{+b} / k_{+p}, is ~ 10, and the ratio of the rate constants of monomer dissociation, from both ends, k_{-b} / k_{-p}, is ~ 5 – 10 (Pollard, 1986; Sheterline et al, 1995). Our polymerisation assays were performed with 0.5μM G-Actin (20% pyrene labelled), nucleated by the addition of 0.1μM F-Actin seeds. As a result we can also neglect any spontaneous polymerisation, from equation (1). With actin concentrations below the critical concentration of the pointed-end (0.6 – 0.8μM) the rate of spontaneous polymerisation has been shown to be negligible (Selve and Wegner, 1986). These workers reported that the rate of nucleation for 0.5μM actin was so low that essentially *no* polymerisation was observed for up to 2hrs (as observed by monitoring the increase in fluorescence intensity of pyrene labelled actin). Furthermore, under these conditions (G-Actin concentration is below the critical concentration for the pointed-end, 0.6 – 0.8μM) we can also neglect the rates of polymerisation at the pointed-ends.

This gives the much simpler expression for the initial rate of nucleated polymerisation:

$$d[\text{F-Actin}] / dt = k_{+b}\cdot[G]\cdot[\text{ends}_b] \quad (2)$$

We can calculate the initial rate of polymerisation, the term d[F-Actin] / dt, by measuring the initial increase in the fluorescence intensity of pyrene-labelled actin, directly from the linear portion of time courses of polymerisation (similar to those illustrated in fig. 5.10). Conversion of the Fluorescence units.s^{-1}, to units of monomer addition in nM.s^{-1} can be performed by the following method:

$$d[F\text{-}Actin] / dt = (df / dt) \cdot \{[total\ actin] / (fF - fG)\} \quad (3),$$

where fF is the fluorescence of the pyrene-actin when it is *all polymerised*, fG is the fluorescence when *all* the pyrene-actin is *monomeric* and df / dt is the time dependent fluorescence, measured as the rate of change in fluorescence intensity units (arbitrary units). Thus, we can calibrate df / dt (in units of $\Delta F.s^{-1}$) from the mean values of fluorescence enhancement from a range of concentrations of pyrene labelled G-Actin and F-Actin (corrected for the critical concentration), obtained from critical concentration assays, to give d[F-actin] / dt in nM.s^{-1}.

From equation (2) it is evident that the rate of addition of monomers to the barbed-end is directly proportional to the concentration of *free* ends. An idea of the concentration of the barbed-ends in such assays, $[ends_b]$, can be obtained from the difference in the initial polymerisation rates observed with nuclei in the absence and presence of nM concentrations of gelsolin (~ 1nM). Gelsolin binds to the barbed-ends very tightly (K_d ~ 10pM, Selve and Wegner, 1986; Bryan et al, 1988), but at these very low concentrations it has a negligible effect on the addition of monomers to the pointed-end, or on the rate of nucleation (Selve and Wegner, 1986). When we performed these calculations on control nucleated polymerisation experiments, in the absence and presence of 0.5nM gelsolin, using the value of $5\mu M^{-1}.s^{-1}$ for k_{+b}, (Pollard, 1986), 0.8μM actin (20% pyrene labelled) and 0.3μM F-Actin nuclei the concentration of free barbed-ends was ~ 0.08nM (data not shown). The significance of this very *low* concentration of filament-ends is that the concentration of barbed-ends is very much less than the amount of barbed-end binding protein added in our experiments (in this case T-cap-protein). This means the vast majority of the capping protein (T-cap-protein) remains free in the solution, uncomplexed with actin. This

means we can make the assumption that the amount of free, uncomplexed T-cap-protein is approximately equal to the total amount added, which simplifies the estimate of the affinity for the barbed-end.

The concentration of free barbed-ends (on which the initial rate of nucleated polymerisation is heavily dependent on, as described by equation 2) is dependent on concentration of the barbed-end binding protein, and its affinity for the barbed-end of the filament. Thus:

$$d[\text{F-Actin}] / dt = k_{+b} \cdot [G] \cdot [\text{free ends}_b] \quad (2),$$

where the term $[\text{free ends}_b]$ is described by equation 4 below

$$[\text{free ends}_b] = ([\text{total barbed ends}] * K_d) / ([\text{Barbed binding protein}] + K_d) \quad (4),$$

where K_d is the equilibrium dissociation constant for binding of the protein to the barbed end (i.e. the K_{cap}). As the concentration of barbed-ends is *very* much lower than the concentration of added capping protein the amount of free capping protein is approximately equal to the total added.

Simply put, under the experimental conditions described above, an increase in the concentration of the barbed-end binding protein will result in a decrease in the number of free barbed-ends. This in turn will result in a reduction of the initial rate of nucleated polymerisation. When all of the barbed-ends are capped, the initial rate of polymerisation will approach a rate of *zero*. The concentration that causes a 50% reduction in the initial rate of polymerisation is equal to the K_{cap}. i.e. the concentration of capping protein (in this case T-cap-protein) where 50% of the barbed-ends are capped.

We routinely obtained nM K_{cap} values for our T-cap-protein construct, with the mean value for full length T-cap-protein being 6.9nM (± 3.1 SD, n=7). Under our assay conditions, any decrease in the initial rate of polymerisation most likely due to a

reduction in the number of barbed-ends, as a direct result of the binding, and subsequent inhibition of further monomer addition, of T-cap-protein.

A similar kinetic consideration of our results obtained from depolymerisation assays and steady-state critical concentration analyses, also supports the notion of a tight interaction with the barbed-end. Similarly to the situation with nucleated polymerisation, if we consider only the initial rate of depolymerisation (regardless of the solution conditions that are used to dilute the starting F-Actin concentration), this rate is again heavily dependent on the concentration of free barbed-ends (due to the differences in the rate constants). If, again, we consider only the *initial* rate we can ignore the reverse reactions; furthermore, our assay conditions involve dilutions below the critical concentration of the pointed-end so monomer addition at this end is not going to occur.

Thus, equations 4 and 5 can be used to describe the initial rate of depolymerisation:

$$d[\text{F-Actin}] / dt = k_{-b} \cdot [\text{free ends}_b] + k_{-p} \cdot [\text{ends}_p] \quad (5),$$

where the term $[\text{free ends}_b]$ is described by equation 4

$$[\text{free ends}_b] = ([\text{total barbed ends}] * K_d) / ([\text{Barbed binding protein}] + K_d) \quad (4)$$

Simply, as the concentration of barbed-end binding protein increases, the number of free barbed-ends decreases. Capping of the faster depolymerising barbed-ends then results in a reduction of the rate of polymerisation. However, unlike the situation that exists for polymerisation (where complete capping of the barbed-ends approaches a final zero level), when all of the barbed-ends are capped the final depolymerisation rate will be solely that of monomer dissociation from the pointed-end (the term $k_{-p} \cdot [\text{ends}_p]$). Such behaviour was reflected in our results (see fig. 10A and B). Similar K_{cap} values in the nM range (~ 8nM) were obtained in our depolymerisation experiments, and these data further suggests a tight, stable interaction with the barbed-end of the filament.

At steady-state actin monomers are in equilibrium between the monomer pool and actin filaments. Filaments at steady-state are treadmilling, with a net loss of monomers from the pointed-end and net addition of monomer at the barbed-ends. The *net* concentration of F-Actin and G-actin, at steady-state, remains constant. Therefore, the steady-state concentration of F-Actin, at any given total actin concentration, is determined by the concentration of *free* monomer and by the ratio of *free* barbed and pointed-ends.

$$[\text{F-Actin}] = [\text{Actin}]_{tot} - [C_c] \quad (6),$$

where $[C_c]$ is the steady-state critical monomer concentration, and is defined by the relationship:

$$[C_c] = (k_{-b}\cdot[\text{free-ends}_b] + k_{-p}\cdot[\text{ends}_p]) / (k_{+b}\cdot[\text{free-ends}_b] + k_{+p}\cdot[\text{ends}_p]) \quad (7)$$

Thus, following dilution (under polymerising conditions) of a given concentration of F-Actin, as is described by equations 6 and 7, the *new* steady-state critical monomer concentration is affected by the number of free barbed-ends. Stable, tight capping of increasing numbers of barbed-ends (by a protein that does *not* allow any further monomer addition after capping), has the effect of shifting the steady-state critical monomer from a value close to that of the barbed-end (~ 0.1μM) towards that of the pointed-end (~ 0.6 – 0.8μM).

The critical concentration is *insensitive* to a small extent of capping of the barbed-end because the value for k_+ at the barbed-end is much larger than at the pointed-end. For example, modelled changes in the critical concentration (Walsh et al, 1984; Selve and Wegner, 1986) have indicate that capping of ~ 90% all filaments at the barbed-end is required for a ~ 50% shift towards the critical concentration of the pointed-end. Only after the capping of 70% of the barbed-ends does the steady-state critical concentration start to show sensitivity to the capping, i.e. relatively large shifts in the values towards that of the pointed-end. Similarly, to produce a 50% increase in the *initial* critical concentration, requires the capping of 50% of the

barbed-ends, giving a value equal to the K_{cap} (Walsh et al, 1984). We observed similar shifts in the steady-state critical concentration by the addition of nM concentrations of T-cap-protein (see section 5.3.1.3). For example, an increase of ~ 50% in the *initial* critical concentration, from ~ 0.11μM to ~ 0.18μM, was brought about by the presence of 5nM T-cap-protein. These K_{cap} values are comparable with the values determined from the nucleated polymerisation experiments (~ 7 – 8nM).

In contrast to the high affinity for the barbed-end of filaments, the effect of T-cap-protein on actin assembly and the steady-state monomer critical concentration is consistent with there being no interaction between T-cap-protein and monomeric actin. Preliminary results from size-exclusion and fluorescence enhancement experiments (performed with NBD-Actin) appear to show *no* complex formation between actin monomers and T-cap-protein (see section 5.3.1). This is in agreement with other reports in the literature. No evidence has been reported for the binding of actin monomers by tensin or the numerous sequence-deletion fusion proteins that have been used to study the protein (Schröer and Wegner, 1985; Ruhnau et al, 1989; Lo et al, 1994a/c; Chuang et al, 1995). The kinetic data also support this result; the kinetic effects we observe occur via the interaction of T-cap-protein with the barbed-end and *not* by monomer sequestration.

Equation (2) indicates that the free monomer concentration ([G]) also greatly influences the initial rate of polymerisation (see above). Therefore, a reduction in the free monomer concentration, due to sequestration by T-cap-protein, would also produce a reduction in the initial rates of polymerisation. Our data however, do not support this theory. Addition of sub-stoichiometric amounts of T-cap-protein causes significant inhibition of both assembly and disassembly. Furthermore, the shift in the steady-state critical monomer concentration reach a maximum level, that of the pointed-end (~ 0.74μM). Further addition of T-cap-protein, in excess of this concentration, does not result in any further increase. The $[C_c]$ in the presence of 500nM T-cap-protein is ~ 0.74μM, while that in the presence of approximately 3 times this amount, 1200nM, is also 0.74μM.

5.5 Conclusion

Our data are consistent with the tight, stable capping of the barbed-end, by T-cap-protein. Once bound no further monomer addition, by insertion of subunits between the capping T-cap-protein and the barbed-end, was observed. Thus, our data do not support the "insertin" mechanism of capping, proposed by Ruhnau et al (1989) and Lo et al (1994c), but is in good agreement with similar data reported by Chuang and colleagues (Chuang et al, 1995). Our T-cap-protein construct exhibits a capping activity similar to that shown by gelsolin. However, gelsolin binds to the barbed-end with a very much lower dissociation constant (K_{cap} ~ 10pM; Selve and Wegner, 1986). Gelsolin capping also involves the binding of two actin monomers at the barbed-end (possible reasons for this very tight association are discussed in section 4.5). We have no evidence for the T-cap-protein binding two monomers at the barbed-end, and have assumed throughout that only a single molecule of T-cap-protein binding at the barbed-end was causing the effects we have observed.

Although our T-cap-protein is a tight barbed-end capping protein, its apparent lack of any G-Actin binding activity precludes its usefulness as a substitute for gelsolin (as the barbed-end capping molecule) in analysing the putative "minifilament".

6. Final discussion and conclusions

6.1 Overview and summary

As we have already described, filamentous actin is not amenable to X-ray crystallography because the polymer lengths are not homogenous. A best fit orientation of the monomer crystal structure (Kabsch et al, 1990) to X-ray diffraction data obtained from oriented actin gels has led to the construction of a model of the filament (Holmes et al, 1990; Lorenz et al, 1993). The model is consistent with much independent evidence for associations between the subunits (Mendelson and Morris, 1994) and it continues to be consistent with emerging evidence.

However, the maximum resolution of the fibre diffraction data is ~ 7 - 8Å (Holmes et al, 1990; Lorenz et al, 1993; Schmid et al, 1993), and although a unique solution was found, the resolution of the experimental data were insufficient to allow further refinement of the input model. Thus, we are far from understanding the contacts between the actin monomers in the filament in atomic detail or the molecular details of how the large numbers of actin binding proteins (e.g. gelsolin, myosin, α-Actinin) interact with the filament.

We proposed a different approach in an attempt to try and resolve the resolution problem of the current model; this was to create a capped-actin-"minifilament", with a view to crystallographic studies. This species has a defined length and composition, with the protein gelsolin capping the barbed-end, and the protein DNaseI capping the pointed-end. Both gelsolin (the G:A_2 ternary complex, blocked at the barbed-end), and DNaseI (the A:D binary complex, blocked at the pointed-end) form separate, stable and easily purified complexes with monomeric actin. Thus, we proposed to add the A:D complex to the G:A_2 complex (under polymerising conditions) and test for any association between these two smaller species, resulting in the formation of a putative "minifilament" complex with a stoichiometry G:A_3:D, and hopefully with the actin monomers oriented in a filamentous conformation (see fig. 4.1).

The $G:A_2$ ternary complex is a potent nucleator of actin polymerisation, but it is unclear whether the actin monomers within this species are oriented in a filamentous conformation (akin to the orientation of the terminal monomers at the barbed-end of the filament), or are just held in close proximity to each other, in a more open, non-filamentous conformation. The nucleating ability may just stem from the fact that $G:A_2$ reduces the entropy of nucleation (two monomers are held tightly in close proximity to each other), and that it provides more ends for monomer addition during polymerisation.

Kinetic and modelling evidence has indicated that *two* molecules of DNaseI cannot be bound to the pointed-end an actin filament (Weber at al, 1994). We have probed the spatial orientation of the actin monomers in the $G:A_2$ ternary complex, using the binding of DNaseI. Our results indicate that *two* DNaseI molecules *can* be bound to the pointed-ends of the actin monomers in the $G:A_2$ complex. Furthermore, the presence of DNaseI does not appear to have any influence on the interaction between the complexed monomer and gelsolin. Our results are consistent with the monomers in $G:A_2$ being held in a *non-filamentous* conformation (see chapter 3). Thus it would seem that crystallising $G:A_2$, and solving the complex's structure to atomic resolution (by X-ray crystallography) would not provide us with an insight into the atomic actin:actin interactions between monomers oriented as they are in a filament.

Our experiments with the T-cap-protein, a fragment derived from tensin (a protein localised to focal contacts), indicate that it tightly caps the barbed-ends of filaments (K_{cap} ~ 7 – 8nM, see chapter 5). The data also indicate that T-cap-protein does not have any "insertin-like" activity; T-cap-protein affects the steady-state critical monomer concentration, shifting it towards that of the pointed-end. A pre-requisite the use of this T-cap-protein in the further analysis of the formation of the "minifilament" is that it has the ability to form stable and easily purifiable complexes with actin monomers (similar to A:D and $G:A_2$). However, we did not find any evidence of T-cap-protein binding to monomeric actin, and as a result, using this protein as a substitute for gelsolin as the barbed-end-capping protein in the further analysis of the "minifilament", was not a viable option. Interestingly however,

although this T-cap-protein still has function (high-affinity barbed-end capping activity), in a similar manner to β-thymosin, it appears to have little secondary structure and lacks a compact folded core in solution (Czisch et al, 1993), at least as the isolated T-cap-protein fragment.

Nevertheless, although the actin subunits in the $G:A_2$ ternary complex appear to not be oriented in a filamentous conformation, addition of a "third" actin monomer in the form of the A:D binary complex (where the presence of DNaseI blocks the pointed-end and prevents any *further* monomer addition), to the $G:A_2$ ternary complex may shift the conformation towards a more filamentous one. Our results (described in chapter 4) appear to indicate the formation of a stable putative "minifilament" complex, formed by an association between the actin monomers in $G:A_2$ and A:D, with a stoichiometry of $G:A_3:D$.

This "minifilament" complex binds to rhodamine-phalloidin, with an apparent K_d of ~ 4.6μM, but not to the myosin S-1 head (at least in the presence of ATP). The actin monomers within this "minifilament" complex probably have some degree of flexibility, but their conformation can be shifted towards one more like that of a filament by the binding of rhodamine-phalloidin (an *F-Actin specific* binding molecule).

Furthermore, the stability of this putative "minifilament" also appears to be higher than one would predict. We would predict that the dissociation constant for the binding of further monomers to the pointed-end of the $G:A_2$ complex, to have been close to the critical concentration for monomer addition to the pointed-ends of filaments (K_d ~ 0.6 – 0.8μM), or significantly higher (further taking into account the apparent lack of filamentous character these $G:A_2$ monomers possess). However, our data seem to indicate that the "minifilament" complex is *more* stable than theoretically predicted (see section 4.4.2).

A recent model (McGough et al, 1998; Puius et al, 2000; discussed below in section 6.2) proposes that, during capping, gelsolin is able to make a *longitudinal* contact

with a *third* actin monomer up the long axis of the filament, in addition to the contacts made by G1 and G4 with the two terminal barbed-end monomers, adjacent to each other across the short-pitch helix (see fig. 6.2). This "three-subunit-contact" model provides a rationale for the high stability of our putative "minifilament" and also provides insight as to why the monomers in the $G:A_2$ ternary complex may not be oriented in a filamentous conformation.

Our experiments with the S-1 head were carried out in the presence of ATP and the lack of interaction between it and the putative "minifilament" may be a reflection of the reduced affinity of myosin for F-Actin in the presence of ATP. The *specific* binding of rhodamine-phalloidin ($K_d \sim 4.6\mu M$) to the "minifilament" suggests that the three monomers have filamentous conformation (or at least that the addition of rhodamine-phalloidin shifts the relatively flexible conformation of the monomers within the "minifilament", to be more filamentous). The lack of any association between the myosin S-1 head and the "minifilament" may suggest that the actin subunits do *not* possess a filamentous conformation. Further experimental analysis in the absence of ATP still needs to be carried out. However, the "three-subunit-contact" model may also provide an alternative explanation for why we might not observe *any* binding of the S-1 head to the "minifilament", regardless of whether the actin monomers are oriented in a filamentous conformation or not, and regardless of the absence or presence of ATP.

6.2 A model where gelsolin makes a *longitudinal* contact with a *third* actin monomers provides a possible explanation for the tight capping activity of gelsolin, and also for why the putative "minifilament" species forms with a higher than expected stability

6.2.1 Introduction to the "three-subunit-contact" model

It has been well established that there are three distinct actin-binding sites, unevenly distributed, within the six-fold segmental repeat of gelsolin (G1 – 6), (see chapter 1 for details). Much of this work has been performed by studies on truncated forms of whole gelsolin (following limited proteolysis or using expressed recombinant constructs) and chimeric constructs (see Weeds and Maciver, 1993 and Sun et al, 1999 for reviews). These studies have proved invaluable for the elucidation of gelsolins activity and function. However, they have also suggested that the molecular details of the binding interaction between whole gelsolin and actin monomers (i.e. formation of the G:A_2 complex) and those between gelsolin and the barbed-end of an actin filament (i.e. formation of the tight cap) may be quite different.

As discussed in section 4.4, whole gelsolin (and also its various constructs) may cause a conformational change in the monomer complexed to it. This structural rearrangement may then result in a strengthening of the terminal longitudinal actin:actin bonds between the complexed actin and the barbed-end of the actin filament. Although this provides a possible explanation for high affinity barbed-end capping activity of gelsolin, the molecular details of the interaction between gelsolin (or G:A_2 ternary complex) and the terminal monomers at the barbed-end of a filament, and those between G:A_2 and the A:D complex (resulting in the formation of the "minifilament"), are likely to be different. In the case of G:A_2 binding to the barbed-end of an already formed filament, one set of lateral and two sets of longitudinal bonds form: in the case of G:A_2 binding to A:D, only a single set of longitudinal and lateral bonds form. Thus, despite the loss of a set of longitudinal bonds the A:D binary complex still appears to bind more tightly than we would have predicted for an actin monomer binding at the pointed-end of G:A_2 (further taking

into account the apparent lack of filamentous conformation possessed by the monomers within this G:A_2 ternary complex).

Although we could still explain the increased stability of the putative "minifilament" (G:A_3:D) complex by "action at a distance" (whereby a gelsolin induced conformational change in the complexed monomer results in the strengthening of further longitudinal actin:actin contacts), the possibility remains that gelsolin may make *direct* contact with additional monomers, longitudinally related to those bound by the G1 and G4 domains, possibly with a different domain.

In the proceeding sections we discuss a "three-subunit-contact" model, along with some of its shortcomings, and also discuss why this model provides a possible explanation for the formation of our putative "minifilament" with a higher than predicted stability. This "three-subunit-contact" model also suggests reasons for why the spatial orientation of the monomers within the G:A_2 ternary complex may be non-filamentous and why the myosin S-1 head binding site may not be available.

6.2.2 A "three-subunit-contact" model for the barbed-end gelsolin cap

The residues that are important in the binding of gelsolin to F-Actin (residues, 161 – 172 and 197 – 226 on plasma gelsolin, Sun et al, 1994) are all located within segment 2 (G2) of gelsolin. Furthermore, residues 150 – 160 of G2 have been implicated in providing some form of co-operative contribution to the potent severing activity of G1 (Way et al, 1992). The importance of G2 – 3 for efficient severing activity was confirmed in a chimeric construct containing the first segment (analogous to G1 in gelsolin) from a related non-severing protein gCap39 and G2 – 3 of gelsolin (Yu et al, 1991). This chimera showed severing activity that was absent in the native gCap39 protein. Another chimera containing the G1 domain from gelsolin and the F-actin-binding domain of α-Actinin possessed severing and capping activity not present in the native protein (Way et al, 1992). Furthermore, the domains from gelsolin (G2 – 3) and the F-Actin-binding domains from α-Actinin appeared to compete for a similarly oriented binding-site on the actin filament, each having a

very similar affinity (K_d ~ 4μM, Way et al, 1992). Data from EM images, consistent with these observations, showed that actin filaments could be decorated with G2 – 6 (a construct that severs inefficiently), and indicate an apparent thickening of these filaments, to almost double that of undecorated filaments (Way et al, 1989).

McGough and Way (1995) have produced a molecular model of an actin filament capped at the barbed-end. This model proposes that the G1 – 3 cap would involve *two* subunits related by the *long-pitch* of the filament (McGough and Way, 1995). The orientation of G2 – 3 on the filament was modelled by analogy to the position of the F-Actin-binding domains of α-Actinin on the filament (obtained from reconstruction data from EM images of α-Actinin decorated filaments; McGough et al, 1994), and by assuming that the G2 – 3 and αA1 – 2 domains were competing for a similarly positioned F-Actin-binding site on the filament (Way et al, 1992).

A recent helical reconstruction of cryo-EM images of actin filaments decorated with the G2 – 6 construct (which possesses ~ 10% of the severing activity of whole gelsolin, Way et al, 1989; Way et al, 1992) has provided more direct evidence for the "three-subunit-contact" model (McGough et al, 1998). Three-dimensional reconstruction of these decorated filaments indicates density located at a subunit interface on the filament, bridging two *longitudinally* adjacent actin monomers (up the long-axis of the filament), see fig. 6.1.

McGough et al (1998) suggest that the G2 – 3 domains of the G2 – 6 construct, occupy the density located to the side of the filament. These domains appear to make contacts with two *different* actin subunits *longitudinally* adjacent to each other along the long axis of the filament. The orientation of the G2 – 3 domains on the filament in this reconstruction was found to be similar to the orientation observed for the F-Actin-binding domains of α-Actinin bound to actin filaments (obtained from a similar EM reconstruction study; McGough et al, 1994). Although this analysis seems to establish the general footprint of gelsolin on F-Actin, the resolution of this reconstruction does not permit an unambiguous identification or orientation of the G2 domain from gelsolin on the filament.

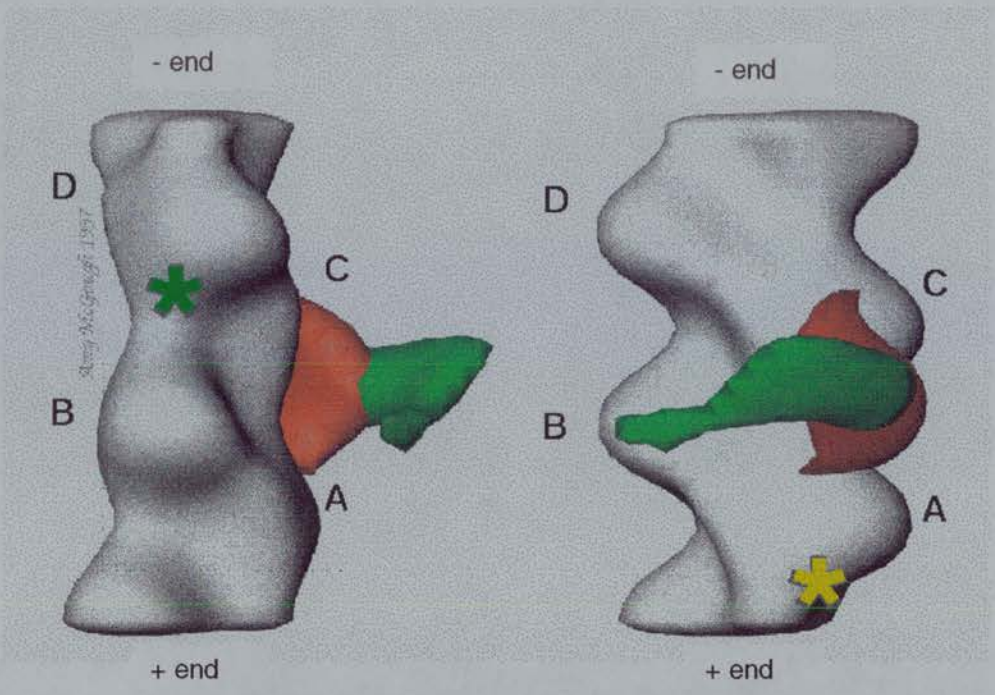

Fig. 6.1. ***Cryo-EM structure of the G2 - 6 domains of gelsolin bound to F-Actin in the presence of 0.5mM $CaCl_2$ (conditions that permit severing).*** The side-on (left-hand image) and face-on (right-hand image) views of a three dimensional reconstruction of an actin filament decorated with the inefficient severing G2 - 6 construct (~ 10% severing activity of whole gelsolin, Way et al, 1989), as described by McGough et al (1998), are shown above. The density attributed to domains G2 - 3 is coloured red, while that attributed to domains G4 - 6 is coloured green. The 2 longitudinally related actin subunits in the filament that G2 - 3 interact with are marked A and C. The yellow asterisk indicates the G1 binding site on monomer A. The green asterisk indicates the G4 binding site (between 50 and 100Å away) located at the base of monomer D, proposed by McGough et al (1998). However, our "minifilament" model (see figs. 4.1 and 6.2) proposes a G4 binding site on monomer B, with G1 and G4 bound to monomers adjacent to each other across the short pitch helix (monomers A and B). *+ end;* indicates the barbed-end of the filament, *- end;* indicates the pointed-end of the filament. (The figure was reproduced from McGough et al, 1998).

However, further supportive evidence for a longitudinal interaction between the G2 domain of gelsolin and a third actin monomer has come from the recent work of Puius et al (2000). These workers have constructed an atomic model of G2 and G1 in complex with filamentous actin. They report the 1.75Å crystal structure of domain 2 from severin (a gelsolin homologue from *Dictyostelium discoideum*; Eichinger and Schleicher, 1992). A structure based alignment of this severin domain 2 and other gelsolin family domains implicated a number of residues in G2 that contributed to the F-Actin binding surface. They assessed the involvement of these residues in the

binding of G2 of gelsolin to filaments by making mutants. Two mutants (with mutations in residues in or near to the long α-helix of G2, RRV168AAA and RLK210AAA) had a lowered affinity for F-Actin; K_d ~ 36μM and ~ 330μM, respectively, compared to ~ 7μM for the wild-type G2 domain (Puius et al, 2000). They suggest that the similarity of the structural fold of the various domains in gelsolin (McLaughlin et al, 1993; Burtnick et al, 1997; Robinson et al, 1999), and the position of these mutated residues in the G2 crystal structure, means that the long helix in G2 was important for the binding of G2 to F-Actin. Residues in gelsolin domain homologues which mediate side-binding activity have been suggested in binding studies where peptides derived from residues in the long helix of G2 or of villin domain 2 displayed a weak affinity for F-Actin (Van Troys et al, 1996; Van Troys et al, 1997). This long helix in G2 was postulated to interact with actin monomers in the filament, in a binding mode similar to that shown by G1 bound to actin monomers (as described by McLaughlin et al, 1993). i.e. the G2 filament binding-site is located in, or very close to, a cleft between subdomains I and III on the actin monomer, in a similar orientation to the binding-site of G1. (See fig. 1.8).

Therefore, Puius et al (2000) have constructed a model of the complex of F-Actin (as described by Holmes et al, 1990) and domains G1 and G2 of gelsolin. This models (see fig. 6.2) the interaction of the G2 domain with the filament by analogy to the end-binding interaction of the G1 domain with the actin monomer (McLaughlin et al, 1993). This G2 orientation appears to agree with data from an immunochemical study that defines a possible interface on the actin monomer, for the binding of gelsolin to the side of actin filaments. This work has identified several regions of the actin monomer, localised to actin subdomain I (residues 1 –10 and 18 – 28), as being important for the binding G2 to the sides of filaments (Feinberg et al, 1995). $G:A_2$ ternary complexes were unable to react with an antibody raised to these N-terminal residues (18 – 28) of the actin monomer, implying that this region was occluded (possibly by G2) in gelsolin:actin complexes, and was thus somehow close to or actively involved in the binding interface between actin and gelsolin.

In summary; the "three-subunit-contact" model (postulated by Way et al, 1992; McGough and Way, 1995; McGough et al, 1998; Puius et al, 2000) proposes that G2 (the F-Actin binding domain) from gelsolin localises the protein to the sides of actin filaments, and once bound it *remains* bound. In conjunction with the side-bound G2 – 3 domains, the G1 domain then severs, disrupting the actin:actin contacts between actin subunits *one* monomer below (longitudinally, down the long axis of the filament) that bound by G2. After severing G1 binds at the end of the filament in a manner akin to that described by McLaughlin et al (1993). A large structural re-arrangement in the C-terminal half of the molecule then allows the second monomer-binding domain (G4) to bind a second monomer, adjacent to that bound by G1 (across the short pitch helix). In this model, the formation of a tight cap (K_{cap} ~ 10pM; Selve and Wegner, 1986) at the barbed-end of the filament has the G2 domain bound to a *third* actin monomer, *longitudinally* related up the long axis of the filament, to the one bound by G1 (see fig. 6.2).

This model provides a possible explanation of why the gelsolin cap is so tight. Loss of this "three-subunit-contact" cap would require the breakage of bonds from *three* intimate gelsolin:actin associations; G1, G2 and G4 are bound to three separate monomers. In addition, binding may be very co-operative, adding additional stability to the interactions. Furthermore, the loss of an actin-trimer species (dissociation of gelsolin complexed to the three monomers it is bound to) from the barbed-ends of filaments would require the breakage of many more bonds in the filament, than would either monomer or dimer dissociation, and would be very energetically unfavourable.

There are, however, criticisms of this model. Although it is clear that G2 localises gelsolin to the filament and is important for efficient severing, the F-Actin-binding domains from other proteins were only *partially* able to functionally replace the G2 – 3 domains from gelsolin. Capping by G1 – 3 is almost as efficient as whole gelsolin (Way et al, 1989; Way et al, 1992) in contrast to the cap formed by the G1:αA1 – 2 hybrid; this cap was significantly less stable than that formed by G1 – 3 (Way et al, 1992). Furthermore, the severing activity of the hybrid was also reduced in

comparison to G1 – 3 and whole gelsolin. The weakened G1:αA1 – 2 hybrid capping and severing activities suggest that the optimal interaction of G1 with the filament and monomer binding site was not achieved, and imply that the F-Actin binding site for G2 – 3 and that of α-Actinin are *not* localised to exactly the same region of the monomer.

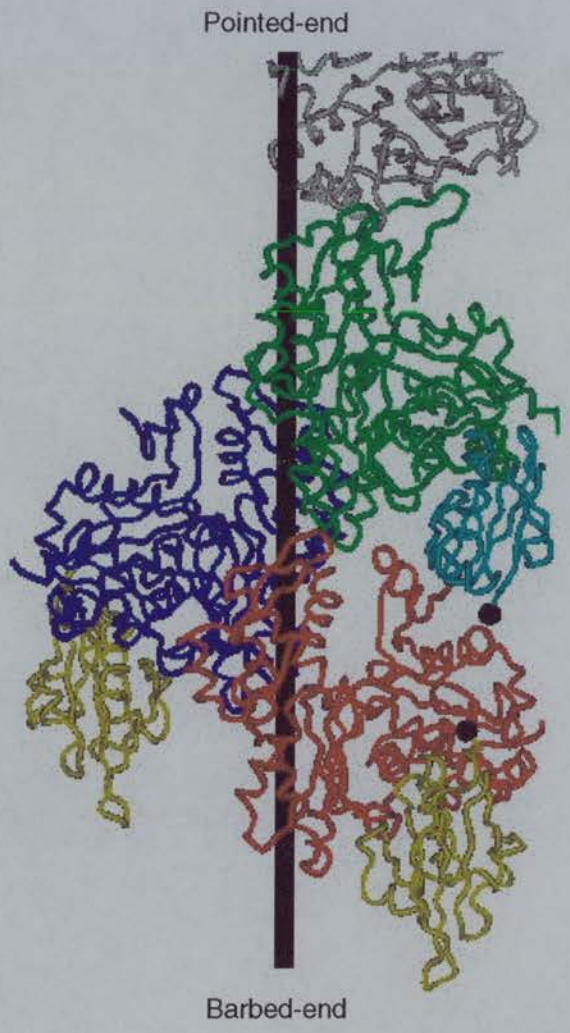

Fig. 6.2. ***"Three-subunit-contact" model of the putative "minifilament".*** A schematic representation of a putative model of the capped-actin-"minifilament", with stoichiometry of G:A_3:D (gelsolin:actin$_3$:DNaseI), is shown. DNaseI is coloured grey, the three actin monomer subunits, oriented as described by the Holmes filament model (Holmes et al, 1990), are coloured red, green and blue. The G1 domain and a putatively positioned G4 domain – by analogy – are shown, coloured yellow (oriented as described by McLaughlin et al, 1993). The *longitudinal* G2 contact with the *third* actin monomer (complexed with DNaseI, here coloured green) is also shown, coloured cyan. The interaction of G2 with this third actin monomer is modelled using a G1 like interaction, as described by the model proposed by Puius et al (2000). The linker sequence between G1 and G2 is not shown. The black spheres indicate the beginning (C-terminus of G1) and end (N-terminus of G2) of this 10-residue linker. (The figure was created using MOLSCRIPT; Kraulis, 1991).

Further evidence for the differences in the localisation of the gelsolin and α-Actinin F-Actin binding site on the filament, arises from the immunochemical analysis of the definition of the possible F-Actin binding gelsolin:actin interface on the monomer (Feinberg et al, 1995). While G2 – 3 did bind, α-Actinin showed no evidence of binding to the peptide derived from residues 18 – 28 of actin. Although McGough et al (1998) report that their reconstruction and difference mapping suggest that these N-terminal residues lie outside the G2 – 3 binding site, the low resolution of their EM reconstruction does not allow for the unambiguous assignment of the position of these actin residues. However, this discrepancy may not be surprising as the N-terminal residues of actin are thought to be relatively mobile (Kabsch et al, 1990; McLaughlin et al, 1993). Furthermore, the conclusions drawn from this study (Feinberg et al, 1995) should be tempered the fact that peptide fragments were used. The actual three-dimensional conformation of these N-terminal residues in the folded actin monomer, may not be at all representative of the conformation of the isolated peptide fragments. Thus, the epitope/s presented by these peptides in isolation, may be completely different to the epitope/s (and thus the three-dimensional conformation) presented by the same region of the polypeptide chain in the native monomer.

Some further objections to the interpretation of the orientation of the F-Actin-binding domain of gelsolin (G2) on a third longitudinally translated actin monomer stem from several anomalies observed during the analysis of the G2 – 6:F-Actin micrographs. To achieve saturation of the actin filaments with G2 – 6 McGough et al (1998) had to add a 4 – 5 molar excess of the construct. This resulted in the micrographs of G2 – 6:F-Actin possessing lots of noise. In addition to the marked length variations observed in the filaments in comparison to undecorated F-Actin (explained by the slow severing of G2 – 6 during the processing time, giving rise to many more shorter filaments) many of the G2 – 6:F-Actin filaments were also "kinky" or curved. Furthermore, during analysis of the images, averaging of the data was halted after eight filaments as it was apparent that further processing was weakening the high radius features, that the authors attribute to the G4 – 6 domains of gelsolin (McGough et al, 1998). Thus, it is possible that the very low level of

resolution and the high levels of noise inherent in the data used to produce these EM images, may have led to artefacts and the mis-assignment of the orientation of gelsolin subunits, with regard to their interaction with the actin filament.

The loss of G1 (a requirement for efficient severing) may have resulted in G2 – 6 adopting an aberrant orientation on the filament. Indeed the change in the structure of some of the filaments (many of the G2 – 6:F-Actin filaments were kinky or curved, McGough et al, 1998) may reflect this aberrant conformational relationship between the filaments and G2 – 6. The rapid severing activity of G1 (in whole gelsolin), and the large structural re-arrangements that then result in G4 binding and subsequent capping, may mean that the conformation of G2 – 3, observed by McGough et al (1998), compared to whole gelsolin bound at the barbed-end, is significantly different.

To allow G2 to bind to the monomer above (longitudinally related up the long axis of the filament) that bound by G1, Burtnick at al (1997) suggest that large and energetically unfavourable re-orientations of the gelsolin structure would have to take place. It is apparent that large scale conformational changes do occur during the transition between the activation (by Ca^{2+} binding to several sites in the C-terminus) and the actin binding, severing and capping activities of gelsolin (Patkowski et al, 1991; Burtnick et al, 1997; Pope et al, 1997; Robinson et al, 1999). However, the C-terminus of G1 and the N-terminus of G2 are only connected by a relatively small (10 residues) linker, unlike the longer ones observed between G2 and G3 (~ 20 – 30 residues) and the ~ 40 - 50 residue linker between G3 and G4. It would seem difficult for G2 to be able to make contact with the F-Actin-binding site on a longitudinally adjacent monomer (adjacent to the one bound by G1), as suggested by orientation of the G2 – 3 domains in the model postulated by McGough and Way (1995) and McGough et al (1998), without some considerable steric strain at the terminal portions of these two domains. However, Puius et al (2000) suggest that the orientation of the G2 domain (with a binding mode similar to the orientation of G1) in their model means that the 10-residue domain linker *could* span the 31Å between the C-terminus of G1 and the N-terminus of G2, without any significant steric strain.

The crystal structure of inactivated gelsolin (Ca^{2+} free) determined by Burtnick and co-workers (Burtnick et al, 1997) showed that all of the six domains (G1 – 6) of gelsolin possess the same basic fold topology. This fold consists of a central five- or six-stranded β-sheet sandwiched between a 3.5 to 4.5 turn α-helix that runs roughly parallel to the strands. Puius et al (2000) have suggested that residues within this long α-helix are important for the binding of both G1 and G2 to the filament (with G2 binding in a similar mode to that exhibited by G1 binding to the actin monomer, as described by McLaughlin et al, 1993). However, if all of the domains possess the same structural fold, why do the other domains from gelsolin not show similar interaction with the filament? The variable length loops that connect the β-sheets and α-helixes in the core of the various domains (Burtnick et al, 1997), may somehow ascribe positive or negative steric determinants for an end- or side-binding activity for the six domains of gelsolin, as suggested by Puius et al (2000). Furthermore, the amino acids that contribute to the formation of this α-helix in the other non-actin-binding domains (G3, G5 and G6) may not possess the residues that "actively" allow the others to bind to the actin-monomer. i.e. an apolar patch of hydrophobic residues exposed on the surface of the long α-helix in G1 (centred around Ile103 in human cytoplasmic gelsolin, see McLaughlin et al, 1993)

Despite the shortcomings of the "three-subunit-contact" model, it nevertheless provides a good model for why gelsolin forms such a tight cap, why our putative "minifilament" forms and also provides a rationale for why the monomers within isolated G:A_2 ternary complexes are not oriented in a filamentous conformation.

As our results appear to indicate (see chapter 3) the orientation of the actin monomers within the G:A_2 ternary complex is non-filamentous. They appear to have some degree of flexibility, with gelsolin holding the monomers in close proximity to one another. This non-filamentous subunit orientation may explain the slightly different kinetics of nucleation exhibited by G:A_2. Thus, in isolated G:A_2 complexes only the G1 and G4 binding sites are occupied with the monomers held in an open non-filamentous conformation; the side-binding G2 site remains unoccupied. Once the G:A_2 complex has bound at the barbed-ends of filaments the strong cap is formed

(and maintained) by the further association of G2 with a third actin monomer, longitudinally related up the long axis of the filament to that bound by G1 (see fig. 6.2). This association then causes the monomers to adopt an F-like conformation. These three monomer contacts (G1, G2 and G4) provide the extra energy and stability needed to form the very strong gelsolin cap.

A similar consideration of this "three-subunit-contact" model provides an explanation for the apparently higher than expected stability of our G:A_3:D/"minifilament" complex (see chapter 4). The actin monomers in the isolated G:A_2 are not in a filamentous conformation, with the G1 and G4 monomer binding-sites occupied, and the G2 filament-binding site unoccupied. However, upon addition of A:D to G:A_2, an end-to-end actin:actin association between A:D and G:A_2, enhanced by a third and possibly co-operative interaction between G2 and the actin monomer in A:D, leads to the formation of the "minifilament" complex. In a similar situation to the formation of a stable barbed-end cap, the third gelsolin:actin contact (with the monomer capped at the pointed-end by DNaseI) results in the increased stability of the G:A_3:D/ "minifilament" complex.

If this third G2 mediated gelsolin:actin interaction leads to the stabilisation of the cap and "minifilament" species why is the formation of gelsolin in complex with three actin monomers (G:A_3) not detected more often? Formation of the **G:A_3** complex *has* been reported during the analysis of the native protein complexes formed between gelsolin and actin, on a Native-PAGE system (Pharmacia PhastGel™ system) (Edgar, 1990), providing some supportive evidence for the "three-subunit-contact" model.

Significant amounts of a complex, with an apparent stoichiometry of G:A_3, was observed in samples taken from incubations of gelsolin (purified from baby hamster kidney cells; BHK gelsolin) with a *large molar excess* of G-Actin (ranging from 4:1 – 14:1, actin:gelsolin). However, this species accounted for only ~ 10% of the total complex formed. There is no evidence of the formation of G:A_3 reported by analytical gel-filtration chromatography, or by other methods, elsewhere in the

literature. However, such experiments are not carried out routinely with the high molar excess of actin needed to produce the complex on native-gels. Thus these studies may not have detected the very small amounts (~ 10% of total) of $G:A_3$ possibly forming. Edgar (1990) suggests that the formation of $G:A_3$ may reflect the simultaneous binding of three actin monomers (in a calcium regulated manner) resulting in the occupation of all of the actin-binding sites in gelsolin (G1, G2 and G4), in an orientation that prevents further monomer addition at the pointed-end of the $G:A_3$ complex.

However, the fact that this complex has not been described elsewhere before, may indicate that this $G:A_3$ complex is an artefact of the gel-system used. Furthermore, as the native-gel cannot be run under polymerising conditions (only the incubation is carried out under these conditions) the details of formation of this putative $G:A_3$ complex and its interaction with both G- and F-Actin cannot properly be assessed. BHK gelsolin may also interact with actin in a different manner to that exhibited by other forms of gelsolin, as has been reported by other workers (Bryan and Kurth, 1984; Weeds et al, 1986; Porte and Harricane, 1986; Laham et al, 1993; Laham et al, 1995). e.g. an apparent Mg^{2+} regulated actin monomer binding activity in pig plasma gelsolin has been reported by Harris (1988).

During $G:A_2$ nucleated polymerisation, the initial formation of a gelsolin-capped trimer species, $G:A_3$, by the addition of a third monomer onto the pointed ends of the monomers in $G:A_2$, resulting in the shift of the monomer conformation towards a filamentous one, may account for the reduced lag-phase observed in such experiments (see section 3.5 and 4.1). However, once this species has formed, with the third monomer bound and stabilised by the interaction with the G2 domain of gelsolin, polymerisation then takes place rapidly onto the pointed-end of the $G:A_3$ species. Thus, $G:A_3$ is rapidly consumed (as fast as the on-rate of monomers at the pointed-ends takes place) and is thus not usually observed as a distinct molecular species during experiments of this nature. However, in our "minifilament" the presence of DNaseI blocks the pointed-end of the putative "minifilament" (defining that end of the complex), and would prevent any further monomer addition.

Thus, the binding of G2 to the third actin in the A:D complex, means that this species is now stabilised (and blocked at both ends preventing any further monomer addition) to such an extent that we are now able to isolate it.

A possible additional feature of this "three-subunit-contact" model is that the interaction of the G2 domain from gelsolin with a third a monomer, longitudinally related to that bound by G1, may occlude the binding site for the myosin S-1 on the putative "minifilament" (see fig. 6.3).

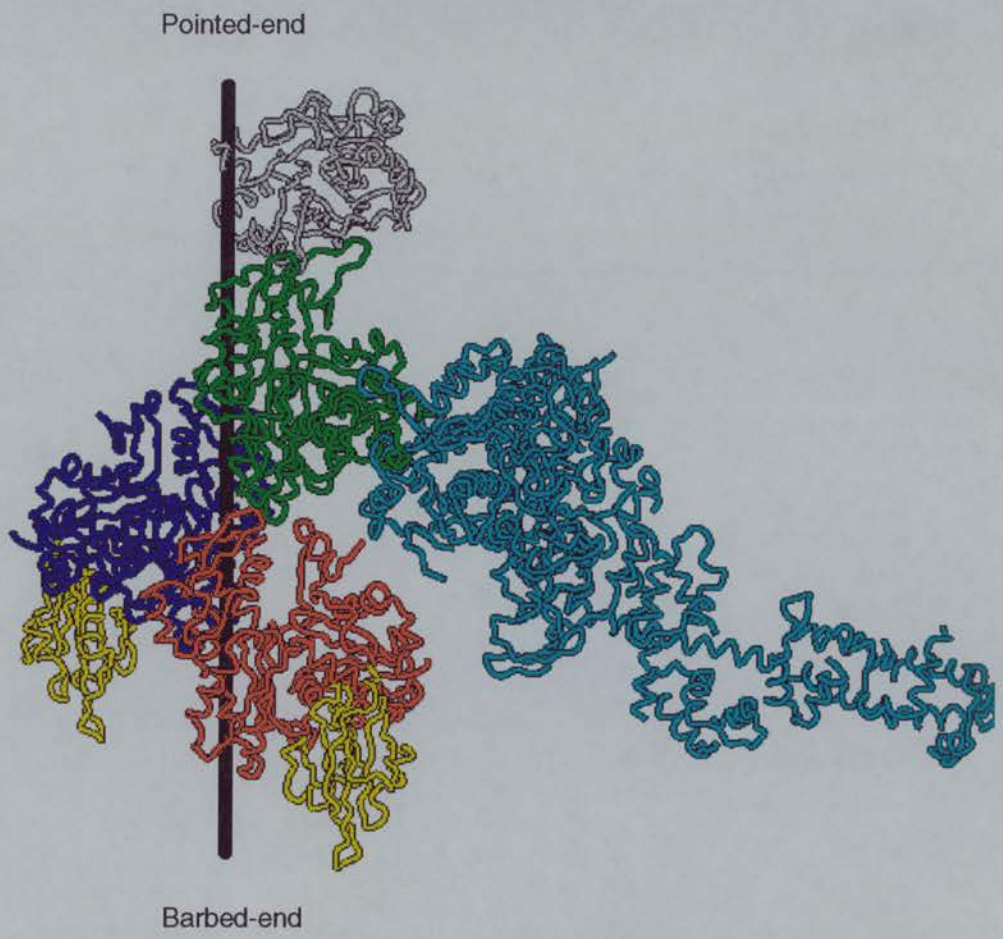

Fig. 6.3. ***Model of the putative "minifilament" with the myosin S-1 head bound.*** A schematic representation of a putative model of the capped-actin-"minifilament", with stoichiometry of **G:A_3:D** (gelsolin:$actin_3$:DNaseI), with the myosin S-1 head bound (oriented as described by Rayment et al, 1993a/b) is shown. DNaseI is coloured grey, the three actin monomer subunits, oriented as described by the Holmes filament model (Holmes et al, 1990), are coloured red, green and blue. Only segment 1 (G1) and a putatively positioned segment 4 (G4) – by analogy – from gelsolin are shown, coloured yellow. The S-1 head is coloured cyan. A comparison of this figure and the schematic model for the proposed G2 contact with the third actin monomer capped by DNaseI (coloured green), shown in fig. 6.2, clearly shows the steric interference that this interaction would have with the binding of the S-1 head. (The figure was created using MOLSCRIPT; Kraulis, 1991).

Each myosin head interacts with two actin monomers, the interaction occurring across a longitudinal subunit interface, giving rise to primary and secondary binding regions on both actin and myosin (Rayment et al, 1993a/b). The primary interaction occurs with residues located in subdomain I of one actin monomer, with secondary interactions occurring with subdomain II of the monomer directly below (see fig. 6.3).

Mutagenesis, cross-linking studies, peptide binding studies and modelling studies have all implicated, amongst numerous others, the N-terminal residues 1 – 28 and the C-terminal residues 341 - 375 of the actin monomer as being important for the myosin interaction (see Sheterline et al, 1995 and Sellers and Goodson, 1995 for a review of the residues involved in the acto-myosin contact site). This area of the actin monomer is important in the binding of G1 (McLaughlin et al, 1993) and is suggested to be a likely site in Puius et al's model for the binding of G2 to F-Actin (Puius et al, 2000). Thus, even in the absence of ATP the S-1 myosin head may not bind to our putative "minifilament" due to an occlusion of its binding site on the actin monomers by the longitudinal G2 domain contact with the A:D actin monomer.

Despite the lack of hard evidence for the Puius et al (2000) model, our "minfilament" would allow a direct test of the hypothesis using the two mutants (RRV168AAA and RLK210AAA, in the long helix of G2), that demonstrated a lowered affinity for F-Actin. If the "minifilament" is indeed forming due to the stabilising effect of the G2 association with a third actin subunit (here complexed with DNaseI), one would predict that similar experiments with gelsolin mutants would show a marked loss of stability of the putative "minifilament" species, as the association between the third (A:D) actin and the mutant G2 (with reduced affinity) would be less stable. This loss of G2 binding affinity would possibly result in the detection of significant amounts of the two smaller complexes during size-exclusion experiments. Furthermore, the loss of this third gelsolin:actin contact, and its stabilising effects, would also possibly result in the loss of the specific rhodamine-phalloidin binding (see section 4.3), as the "minifilament" (with its single putative phalloidin binding site) would no longer form.

6.3 Future directions

Although our experiments, provide evidence for the formation of a capped-actin-"minifilament", of defined length and composition (most likely formed via an actin:actin association between the monomers in the $G:A_2$ ternary complex and the A:D binary complex), with a stoichiometry of $G:A_3:D$ (gelsolin:actin:DNaseI, respectively), verification of the formation of our putative "minifilament" complex by other complementary physical techniques would provide further evidence to support our size-exclusion and rhodamine-phalloidin binding data. Several of these methods include the use of alternative native-PAGE techniques, covalent cross-linking, and possibly analytical ultra-centrifugation methods.

Although the native-gel system (adapted from Safer, 1989) used in the analysis of the spatial orientation of the actin monomers in $G:A_2$ proved to be ill-suited to the analysis of the putative "minifilament", other native-PAGE techniques may possibly be used to demonstrate the formation of the "minifilament". One possible method for this is the adaptation of a Native-Blue electrophoresis technique for our purposes (Schagger & von Jagow, 1991; Schagger et al, 1994). The procedure was developed for the isolation of *native* membrane protein complexes, at a fixed pH of 7.5; however it can also be applied to both acidic and basic water soluble proteins. This system works on the basis of a "charge-shift" method, with the electrophoretic mobility of the proteins determined by the negative charges of bound Coomassie dye. The native gel is then followed by analysis in the second dimension using a Tricine-SDS-PAGE protocol (Schagger & von Jagow, 1987). This native-gel system appears to have a tolerance for the presence of salt in the sample and running buffers (Schagger et al, 1994). Furthermore, the voltage, buffer conditions and gel running times are all significantly different to those used in the system we have used, and thus may allow the use of ionic solution conditions that are similar to F-conditions.

Cross-linking experiments may also provide a further method of verifying the formation and stoichiometry of the putative "minifilament". We have performed some preliminary covalent cross-linking experiments on the putative "minifilament"

with the homo-bifunctional Sulfo-EGS reagent (reacts with primary amine, most often lysine residues); however, our results were inconclusive (data not shown). Nevertheless, further work needs to be carried out to fine-tune the solution conditions required for the cross-linking reaction, and these experiments may provide some useful complementary data for the formation of the "minifilament".

Our size-exclusion experiments performed in the presence of ATP, indicate no binding between the S-1 head and the "minifilament". The "three-subunit-contact" model (discussed above, see section 6.2) provides a possible explanation for way we may see no S-1 binding to the minifilament (G2 occludes the S-1 binding site on the actin monomers within the minifilament), regardless of the presence or absence of ATP. However, we have no direct evidence for this steric hindrance and further experiments with the myosin S-1 head, in the *absence* of ATP, still need to be performed.

Our results (described in chapter 3) appear to indicate that the presence of DNaseI (bound at the pointed-end of the actin monomer in the A:D complex) has no effect on the interaction between gelsolin and actin monomers. Furthermore, our results also seem to indicate that the possible exchange reaction (of G-Actin for A:D binary complex) occurring at the EGTA labile G4 monomer-binding site on gelsolin, creates less of a problem than expected (due to the apparent increased stability of the "minifilament"). Nevertheless, using a gelsolin construct that consists of two G1 – 3 domains in tandem (G1 – 3:G1 – 3), containing two tight (K_d ~ 5pM, Bryan, 1988) G1 subunit binding sites, may increase the stability of the complex and reduce the problems of exchange even further.

Other actin-binding proteins could be used to probe the conformation of the actin "monomers" within our putative "minifilament" complex. Although the proposed position of G2 in "three-subunit-contact" model may sterically occlude the binding sites for several F-Actin specific binding proteins (e.g. α-Actinin, myosin) other binding proteins may be found that are not (or less) affected by the orientation of the G2 domain (e.g. tropomyosin). Such a binding interaction would provide further

evidence of "minifilament" formation, and also confirm the filamentous conformation of the actin subunits implied by our rhodamine-phalloidin experiments.

The putative "minifilament" complex appears to stable enough to perform crystallisation studies with; the complex can be stably re-chromatographed on Superose-12 size-exclusion columns. Although we would have to be careful about interpreting the structure, such an analysis of the putative "minifilament" would hopefully show filamentous actin:actin contacts that could be used to build an atomic resolution model of the actin filament.

7. References

Allen, P.G. and P.A. Janmey. 1994. Gelsolin displaces phalloidin from actin filaments. A new fluorescence method shows that both Ca2+ and Mg2+ affect the rate at which gelsolin severs F-actin. *Journal of Biological Chemistry* 269:32916-32923.

Amos, L.A. 1985. Structure of muscle filaments studied by electron microscopy. [Review] [62 refs]. *Annual.Review.of.Biophysics.&.Biophysical.Chemistry.* 14:291-313:291-313.

Ayscough, K. 1998. Use of latrunculin-A, an actin monomer-binding drug. *Methods in Enzymology* 298:18-25.

Ballweber, E., E. Hannappel, T. Huff, and H.G. Mannherz. 1997. Mapping the binding site of thymosin beta4 on actin by competition with G-actin binding proteins indicates negative co-operativity between binding sites located on opposite subdomains of actin. *Biochemical Journal* 327:787-793.

Blake, R.D., J. Massoulie, and J.R. Fresco. 1967. Polynucleotides. 8. A spectral approach to the equilibria between polyriboadenylate and polyribouridylate and their complexes. *Journal of Molecular Biology* 30:291-308.

Bockholt, S.M., C.A. Otey, J.R.J. Glenney, and K. Burridge. 1992. Localization of a 215-kDa tyrosine-phosphorylated protein that cross-reacts with tensin antibodies. *Experimental Cell Research* 203:39-46.

Bonder, E.M. and M.S. Mooseker. 1983. Direct electron microscopic visualization of barbed end capping and filament cutting by intestinal microvillar 95-kdalton protein (villin): a new actin assembly assay using the Limulus acrosomal process. *Journal of Cell Biology* 96:1097-1107.

Borisy, G.G. and T.M. Svitkina. 2000. Actin machinery: pushing the envelope. [Review] [75 refs]. *Current Opinion in Cell Biology* 12:104-112.

Bremer, A., R.C. Millonig, R. Sutterlin, A. Engel, T.D. Pollard, and U. Aebi. 1991. The structural basis for the intrinsic disorder of the actin filament: the "lateral slipping" model. *Journal.of.Cell Biology.* 115:689-703.

Brenner, S.L. and E.D. Korn. 1983. On the mechanism of actin monomer-polymer subunit exchange at steady state. *Journal of Biological Chemistry* 258:5013-5020.

Bresnick, A.R., P.A. Janmey, and J. Condeelis. 1991. Evidence that a 27-residue sequence is the actin-binding site of ABP-120 ABP-. *Journal of Biological Chemistry* 266:12989-12993.

Bryan, J. and M.C. Kurth. 1984. Actin-gelsolin interactions. Evidence for two actin-binding sites. *Journal.of.Biological.Chemistry.* 259:7480-7487.

Bryan, J. and S. Hwo. 1986. Definition of an N-terminal actin-binding domain and a C- terminal Ca2+ regulatory domain in human brevin. *Journal.of.Cell Biology.* 102:1439-1446.

Bryan, J. 1988. Gelsolin has three actin-binding sites. *Journal.of.Cell Biology.* 106:1553-1562.

Burridge, K., K. Fath, T. Kelly, G. Nuckolls, and C. Turner. Focal adhesions: transmembrane junctions between the extracellular matrix and the cytoskeleton. [Review] [260 refs]. *Annual Review of Cell Biology* 4:K-F

Burridge, K. and L. Connell. 1983. A new protein of adhesion plaques and ruffling membranes. *Journal of Cell Biology* 97:359-367.

Burridge, K. and M. Chrzanowska-Wodnicka. 1996. Focal adhesions, contractility, and signaling. [Review] [385 refs]. *Annual Review of Cell & Developmental Biology* 12:463-518.

Burtnick, L.D., E.K. Koepf, J. Grimes, E.Y. Jones, D.I. Stuart, P.J. McLaughlin, and R.C. Robinson. 1997. The crystal structure of plasma gelsolin: implications for actin severing, capping, and nucleation. *Cell* 90:661-670.

Cano, M.L., L. Cassimeris, M. Joyce, and S.H. Zigmond. 1992. Characterization of tetramethylrhodaminyl-phalloidin binding to cellular F-actin. *Cell Motility & the Cytoskeleton* 21:147-158.

Carlier, M.F. 1991. Actin: protein structure and filament dynamics. [Review] [68 refs]. *Journal.of.Biological.Chemistry.* 266:1-4.

Chalovich, J.M., L.A. Stein, L.E. Greene, and E. Eisenberg. 1984. Interaction of isozymes of myosin subfragment 1 with actin: effect of ionic strength and nucleotide. *Biochemistry* 23:4885-4889.

Chaponnier, C., R. Borgia, E. Rungger-Brandle, R. Weil, and G. Gabbiani. 1979. An actin-destabilizing factor is present in human plasma. *Experientia* 35:1039-1041.

Chen, W.T., J.M. Chen, and S.C. Mueller. 1986. Coupled expression and colocalization of 140K cell adhesion molecules, fibronectin, and laminin during morphogenesis and cytodifferentiation of chick lung cells. *Journal of Cell Biology* 103:1073-1090.

Cheney, R.E., M.A. Riley, and M.S. Mooseker. 1993. Phylogenetic analysis of the myosin superfamily. [Review] [36 refs]. *Cell Motility & the Cytoskeleton* 24:215-223.

Chuang, J.Z., D.C. Lin, and S. Lin. 1995. Molecular cloning, expression, and mapping of the high affinity actin-capping domain of chicken cardiac tensin. *Journal of Cell Biology* 128:1095-1109.

Coluccio, L.M. and L.G. Tilney. 1984. Phalloidin enhances actin assembly by preventing monomer dissociation. *Journal of Cell Biology* 99:529-535.

Combeau, C., D. Didry, and M.F. Carlier. 1992. Interaction between G-actin and myosin subfragment-1 probed by covalent cross-linking. *Journal.of.Biological.Chemistry.* 267:14038-14046.

Cooper, J.A. 1987. Effects of cytochalasin and phalloidin on actin. [Review] [55 refs]. *Journal of Cell Biology* 105:1473-1478.

Cooper, J.A. and D.A. Schafer. 2000. Control of actin assembly and disassembly at filament ends. [Review] [73 refs]. *Current Opinion in Cell Biology* 12:97-103.

Cope, M.J.T., J. Whisstock, I. Rayment, and J. Kendrick-Jones. 1996. Conservation within the myosin motor domain: implications for structure and function. *Structure* 4:969-987.

Coue, M. and E.D. Korn. 1985. Interaction of plasma gelsolin with G-actin and F-actin in the presence and absence of calcium ions. *Journal of Biological Chemistry* 260:15033-15041.

Crawford, A.W. and M.C. Beckerle. 1991. Purification and characterization of zyxin, an 82,000-dalton component of adherens junctions. *Journal of Biological Chemistry* 266:5847-5853.

Critchley, D.R. 2000. Focal adhesions - the cytoskeletal connection. [Review] [57 refs]. *Current Opinion in Cell Biology* 12:133-139.

Cunningham, C.C., T.P. Stossel, and D.J. Kwiatkowski. 1991. Enhanced motility in NIH 3T3 fibroblasts that overexpress gelsolin. *Science* 251:1233-1236.

Czisch, M., M. Schleicher, S. Horger, W. Voelter, and T.A. Holak. 1993. Conformation of thymosin beta 4 in water determined by NMR spectroscopy. *European Journal of Biochemistry* 218:335-344.

Davis, S., M.L. Lu, S.H. Lo, S. Lin, J.A. Butler, B.J. Druker, T.M. Roberts, Q. An, and L.B. Chen. 1991. Presence of an SH2 domain in the actin-binding protein tensin. *Science* 252:712-715.

De La Cruz, E. and T.D. Pollard. 1994. Transient kinetic analysis of rhodamine phalloidin binding to actin filaments. *Biochemistry* 33:14387-14392.

Detmers, P., A. Weber, M. Elzinga, and R.E. Stephens. 1981. 7-Chloro-4-nitrobenzeno-2-oxa-1,3-diazole actin as a probe for actin polymerization. *Journal of Biological Chemistry* 256:99-105.

Ditsch, A. and A. Wegner. 1994. Nucleation of actin polymerization by gelsolin. *European Journal of Biochemistry* 224:223-227.

Ditsch, A. and A. Wegner. 1995. Two low-affinity Ca(2+)-binding sites of gelsolin that regulate association with actin. *European Journal of Biochemistry* 229:512-516.

Doherty, A.J., B.A. Connolly, and A.F. Worrall. 1993. Overproduction of the toxic protein, bovine pancreatic DNaseI, in Escherichia coli using a tightly controlled T7-promoter-based vector. *Gene* 136:337-340.

Doi, Y. and C. Frieden. 1984. Actin polymerization. The effect of brevin on filament size and rate of polymerization. *Journal of Biological Chemistry* 259:11868-11875.

Doi, Y. 1992. Interaction of gelsolin with covalently cross-linked actin dimer. *Biochemistry* 31:10061-10069.

Doi, Y.K., M. Banba, and A. Vertut-Doi. 1991. Cysteine-374 of actin resides at the gelsolin contact site in the EGTA-resistant actin-gelsolin complex. *Biochemistry* 30:5769-5777.

Doolittle R.F. 1986. A Primer on How to Analyse Derived Amino Acid Sequences. AnonymousUniversity Science Books, Sausalito, CA.

Drubin, D.G., H.D. Jones, and K.F. Wertman. 1993. Actin structure and function: roles in mitochondrial organization and morphogenesis in budding yeast and identification of the phalloidin-binding site. *Molecular Biology of the Cell* 4:1277-1294.

Edgar, A.J. 1990. Gel electrophoresis of native gelsolin and gelsolin-actin complexes. *Journal of Muscle Research & Cell Motility* 11:323-330.

Egelman, E.H. and A. Orlova. 1995. New insights into actin filament dynamics. [Review] [79 refs]. *Current Opinion in Structural Biology* 5:172-180.

Egleman, E.H. and A. Orlova. 1995. Allostery, cooperativity, and different structural states in F-actin. [Review] [16 refs]. *Journal of Structural Biology* 115:159-162.

Eichinger, L. and M. Schleicher. 1992. Characterization of actin- and lipid-binding domains in severin, a Ca(2+)-dependent F-actin fragmenting protein. *Biochemistry* 31:4779-4787.

Elzinga, M. and J.J. Phelan. 1984. F-actin is intermolecularly crosslinked by N,N'-p-phenylenedimaleimide through lysine-191 and cysteine-374. *Proceedings of the National Academy of Sciences of the United States of America* 81:6599-6602.

Estes, J.E., L.A. Selden, and L.C. Gershman. 1981. Mechanism of action of phalloidin on the polymerization of muscle actin. *Biochemistry* 20:708-712.

Faulstich, H., H. Trischmann, and D. Mayer. 1983. Preparation of tetramethylrhodaminyl-phalloidin and uptake of the toxin into short-term cultured hepatocytes by endocytosis. *Experimental.Cell Research.* 144:73-82.

Faulstich, H., S. Zobeley, D. Heintz, and G. Drewes. 1993. Probing the phalloidin binding site of actin. *FEBS Letters* 318:218-222.

Faulstich, H. and T. Wieland. 1996. New aspects of amanitin and phalloidin poisoning. [Review] [11 refs]. *Advances in Experimental Medicine & Biology* 391:309-314.

Feinberg, J., Y. Benyamin, and C. Roustan. 1995. Definition of an interface implicated in gelsolin binding to the sides of actin filaments. *Biochemical & Biophysical Research Communications* 209:426-432.

Feramisco, J.R. and K. Burridge. 1980. A rapid purification of alpha-actinin, filamin, and a 130,000-dalton protein from smooth muscle. *Journal of Biological Chemistry* 255:1194-1199.

Frieden, C. 1982. The Mg2+-induced conformational change in rabbit skeletal muscle G-actin. *Journal of Biological Chemistry* 257:2882-2886.

Frieden, C. 1985. Actin and tubulin polymerization: the use of kinetic methods to determine mechanism. [Review] [89 refs]. *Annual Review of Biophysics & Biophysical Chemistry* 14:189-210.

Furukawa, R. and M. Fechheimer. 1997. The structure, function, and assembly of actin filament bundles. [Review] [272 refs]. *International Review of Cytology* 175:29-90.

Gaertner, A. and A. Wegner. 1991. Mechanism of the insertion of actin monomers between the barbed ends of actin filaments and barbed end-bound insertin. *Journal of Muscle Research & Cell Motility* 12:27-36.

Geiger, B. 1979. A 130K protein from chicken gizzard: its localization at the termini of microfilament bundles in cultured chicken cells. *Cell* 18:193-205.

Geiger, B. 1989. Cytoskeleton-associated cell contacts. [Review] [33 refs]. *Current Opinion in Cell Biology* 1:103-109.

Gershman, L.C., J. Newman, L.A. Selden, and J.E. Estes. 1984. Bound-cation exchange affects the lag phase in actin polymerization. *Biochemistry* 23:2199-2203.

Gill, S.C. and P.H. von Hippel. 1989. Calculation of protein extinction coefficients from amino acid sequence data [published erratum appears in Anal Biochem 1990 Sep;189(2):283]. *Analytical Biochemistry* 182:319-326.

Gilmore, A.P. and K. Burridge. 1996. Molecular mechanisms for focal adhesion assembly through regulation of protein-protein interactions. [Review] [35 refs]. *Structure* 4:647-651.

Goode, B.L., D.G. Drubin, and G. Barnes. 2000. Functional cooperation between the microtubule and actin cytoskeletons. [Review] [46 refs]. *Current Opinion in Cell Biology* 12:63-71.

Goodson, H.V. and J.A. Spudich. 1993. Molecular evolution of the myosin family: relationships derived from comparisons of amino acid sequences. *Proceedings of the National Academy of Sciences of the United States of America* 90:659-663.

Harris, H.E., J.R. Bamburg, and A.G. Weeds. 1980. Actin filament disassembly in blood plasma. *FEBS Letters* 121:175-177.

Harris, H.E. 1988. The binary complex of pig plasma gelsolin with Mg2+-G-actin in ATP and ADP. *FEBS Letters* 233:359-362.

Hartwig, J.H. and D.J. Kwiatkowski. 1991. Actin-binding proteins. [Review] [82 refs]. *Current Opinion in Cell Biology* 3:87-97.

Hellweg, T., H. Hinssen, and W. Eimer. 1993. The Ca(2+)-induced conformational change of gelsolin is located in the carboxyl-terminal half of the molecule. *Biophysical Journal* 65:799-805.

Herman, I.M. 1993. Actin isoforms. [Review] [53 refs]. *Current.Opinion.in Cell Biology.* 5:48-55.

Hitchcock, S.E., L. Carisson, and U. Lindberg. 1976. Depolymerization of F-actin by deoxyribonuclease I. *Cell* 7:531-542.

Hitchcock, S.E. 1980. Actin deoxyroboncuclease I interaction. Depolymerization and nucleotide exchange. *Journal.of.Biological.Chemistry.* 255:5668-5673.

Holmes, K.C., D. Popp, W. Gebhard, and W. Kabsch. 1990. Atomic model of the actin filament [see comments]. *Nature* 347:44-49.

Horwitz, A., D. Bozyczko, and C.A. Buck. 1990. The Integrin Family and Neighbours. A. Horwitz, D. Bozyczko, and C.A. Buck, editors. John Wiley & Sons, New York. 1-352.

Huang, Z.J., R.P. Haugland, and W.M. You. 1992. Phallotoxin and actin binding assay by fluorescence enhancement. *Analytical.Biochemistry* 200:199-204.

Hynes, R.O. 1992. Integrins: versatility, modulation, and signaling in cell adhesion. [Review] [180 refs]. *Cell* 69:11-25.

Irwin, N. Molecular Cloning. A laboratory manual. J Sambrook, E.F, Fritsch, and T, Maniati. Molecular Cloning. Alaboratory manual. 2nd. 1989. Cold Spring Harbour Laboratory Press.

Ito, H., H. Yamamoto, Y. Kimura, H. Kambe, T. Okochi, and S. Kishimoto. 1990. Affinity chromatography of human plasma gelsolin with polyphosphate compounds on immobilized Cibacron Blue F3GA. *Journal.of.Chromatography.* 526:397-406.

Janmey, P.A. and T.P. Stossel. 1986. Kinetics of actin monomer exchange at the slow growing ends of actin filaments and their relation to the elongation of filaments shortened by gelsolin. *Journal.of.Muscle Research.&.Cell Motility.* 7:446-454.

Janmey, P.A. and T.P. Stossel. 1987. Modulation of gelsolin function by phosphatidylinositol 4,5- bisphosphate. *Nature* 325:362-364.

Janmey, P.A. and T.P. Stossel. 1989. Gelsolin-polyphosphoinositide interaction. Full expression of gelsolin-inhibiting function by polyphosphoinositides in vesicular form and inactivation by dilution, aggregation, or masking of the inositol head group. *Journal.of.Biological.Chemistry.* 264:4825-4831.

Janmey, P.A., J. Lamb, P.G. Allen, and P.T. Matsudaira. 1992. Phosphoinositide-binding peptides derived from the sequences of gelsolin and villin. *Journal of Biological Chemistry* 267:11818-11823.

Janmey, P.A. 1995. Protein regulation by phosphatidylinositol lipids. [Review] [27 refs]. *Chemistry & Biology* 2:61-65.

Jockusch, B.M., P. Bubeck, K. Giehl, M. Kroemker, J. Moschner, M. Rothkegel, M. Rudiger, K. Schluter, G. Stanke, and J. Winkler. 1995. The molecular architecture of focal adhesions. [Review] [291 refs]. *Annual.Review.of.Cell &.Developmental.Biology.* 11:379-416:379-416.

Kabsch, W., H.G. Mannherz, D. Suck, E.F. Pai, and K.C. Holmes. 1990. Atomic structure of the actin:DNase I complex [see comments]. *Nature* 347:37-44.

Kambe, H., H. Ito, Y. Kimura, T. Okochi, H. Yamamoto, T. Hashimoto, and K. Tagawa. 1992. Human plasma gelsolin reversibly binds Mg-ATP in Ca(2+)-sensitive manner. *Journal of Biochemistry* 111:722-725.

Keen, J.H., M.C. Willingham, and I.H. Pastan. 1979. Clathrin-coated vesicles: isolation, dissociation and factor- dependent reassociation of clathrin baskets. *Cell* 16:303-312.

Khaitlina, S. and H. Hinssen. 1997. Conformational changes in actin induced by its interaction with gelsolin. *Biophysical Journal* 73:929-937.

Kinosian, H.J., L.A. Selden, J.E. Estes, and L.C. Gershman. 1993. Nucleotide binding to actin. Cation dependence of nucleotide dissociation and exchange rates. *Journal.of.Biological.Chemistry.* 268:8683-8691.

Knight, P. and G. Offer. 1978. p-NN'-phenylenebismaleimide, a specific cross-linking agent for F-actin. *Biochemical Journal* 175:1023-1032.

Korn, E.D., M.F. Carlier, and D. Pantaloni. 1987. Actin polymerization and ATP hydrolysis. *Science* 238:638-644.

Kouyama, T. and K. Mihashi. 1981. Fluorimetry study of N-(1-pyrenyl)iodoacetamide-labelled F- actin. Local structural change of actin protomer both on polymerization and on binding of heavy meromyosin. *European Journal of Biochemistry* 114:33-38.

Kraulis, Per. J. Molscript - A Program to Produce Both Detailed and Schematic Plots of Protein Structures. Journal of Applied Crystallography 24, 946-950. 1991.

Kurth, M.C., L.L. Wang, J. Dingus, and J. Bryan. 1983. Purification and characterization of a gelsolin-actin complex from human platelets. Evidence for Ca2+-insensitive functions. *Journal of Biological Chemistry* 258:10895-10903.

Kurth, M.C. and J. Bryan. 1984. Platelet activation induces the formation of a stable gelsolin- actin complex from monomeric gelsolin. *Journal of Biological Chemistry* 259:7473-7479.

Kwiatkowski, D.J., T.P. Stossel, S.H. Orkin, J.E. Mole, Colten, HR, and H.L. Yin. 1986. Plasma and cytoplasmic gelsolins are encoded by a single gene and contain a duplicated actin-binding domain. *Nature* 323:455-458.

Kwiatkowski, D.J., P.A. Janmey, and H.L. Yin. 1989. Identification of critical functional and regulatory domains in gelsolin. *Journal of Cell Biology* 108:1717-1726.

Kwiatkowski, D.J. 1999. Functions of gelsolin: motility, signaling, apoptosis, cancer. [Review] [57 refs]. *Current Opinion in Cell Biology* 11:103-108.

Laemmli, U.K. 1970. Cleavage of structural proteins during the assembly of the head of bacteriophage T4. *Nature* 227:680-685.

Laham, L.E., J.A. Lamb, P.G. Allen, and P.A. Janmey. 1993. Selective binding of gelsolin to actin monomers containing ADP. *Journal.of.Biological.Chemistry.* 268:14202-14207.

Laham, L.E., M. Way, H.L. Yin, and P.A. Janmey. 1995. Identification of two sites in gelsolin with different sensitivities to adenine nucleotides. *European Journal of Biochemistry* 234:1-7.

Lahm, A. and D. Suck. 1991. DNase I-induced DNA conformation. 2 A structure of a DNase I- octamer complex. *Journal.of.Molecular.Biology.* 222:645-667.

Lamb, J.A., P.G. Allen, B.Y. Tuan, and P.A. Janmey. 1993. Modulation of gelsolin function. Activation at low pH overrides Ca2+ requirement. *Journal of Biological Chemistry* 268:8999-9004.

Lauffenburger, D.A. and A.F. Horwitz. 1996. Cell migration: a physically integrated molecular process. [Review] [103 refs]. *Cell* 84:359-369.

Lazarides, E. and K. Burridge. 1975. Alpha-actinin: immunofluorescent localization of a muscle structural protein in nonmuscle cells. *Cell* 6:289-298.

Lazarides, E. and U. Lindberg. 1974. Actin is the naturally occurring inhibitor of deoxyribonuclease I. *Proceedings.of.the.National.Academy.of.Sciences.of.the.United.States.of.America.* 71:4742-4746.

Le Bihan, T. and C. Gicquaud. 1991. Stabilization of actin by phalloidin: a differential scanning calorimetric study. *Biochemical & Biophysical Research Communications* 181:542-547.

(a) Lo, S.H., Q. An, S. Bao, W.K. Wong, Y. Liu, P.A. Janmey, J.H. Hartwig, and L.B. Chen. 1994. Molecular cloning of chick cardiac muscle tensin. Full-length cDNA sequence, expression, and characterization. *Journal of Biological Chemistry* 269:22310-22319.

(b) Lo, S.H., E. Weisberg, and L.B. Chen. 1994. Tensin: a potential link between the cytoskeleton and signal transduction. [Review] [61 refs]. *Bioessays* 16:817-823.

(c) Lo, S.H., P.A. Janmey, J.H. Hartwig, and L.B. Chen. 1994. Interactions of tensin with actin and identification of its three distinct actin-binding domains. *Journal of Cell Biology* 125:1067-1075.

Lorenz, M., D. Popp, and K.C. Holmes. 1993. Refinement of the F-actin model against X-ray fiber diffraction data by the use of a directed mutation algorithm. *Journal.of.Molecular.Biology.* 234:826-836.

Luna, E.J. and A.L. Hitt. 1992. Cytoskeleton--plasma membrane interactions. [Review] [101 refs]. *Science* 258:955-964.

Maciver, S.K., H.G. Zot, and T.D. Pollard. 1991. Characterization of actin filament severing by actophorin from Acanthamoeba castellanii. *Journal of Cell Biology* 115:1611-1620.

Mannherz, H.G., J.B. Leigh, R. Leberman, and H. Pfrang. 1975. A specific 1:1 G-actin:DNAase i complex formed by the action of DNAase I on F-actin. *FEBS Letters* 60:34-38.

Mannherz, H.G., R.S. Goody, M. Konrad, and E. Nowak. 1980. The interaction of bovine pancreatic deoxyribonuclease I and skeletal muscle actin. *European Journal of Biochemistry* 104:367-379.

Margossian, S.S. and S. Lowey. 1978. Interaction of myosin sub-fragments with F-actin. *Biochemistry* 17:5431-5439.

Marston, S. and A. Weber. 1975. The dissociation constant of the actin-heavy meromyosin subfragment-1 complex. *Biochemistry* 14:3868-3873.

Matsudaira, P., J. Bordas, and M.H. Koch. 1987. Synchrotron x-ray diffraction studies of actin structure during polymerization. *Proceedings of the National Academy of Sciences of the United States of America* 84:3151-3155.

Matsudaira, P. and P. Janmey. 1988. Pieces in the actin-severing protein puzzle. [Review] [22 refs]. *Cell* 54:139-140.

Matsudaira, P. 1991. Modular organization of actin crosslinking proteins. [Review] [26 refs]. *Trends in Biochemical Sciences* 16:87-92.

McGough, A., M. Way, and D. DeRosier. 1994. Determination of the alpha-actinin-binding site on actin filaments by cryoelectron microscopy and image analysis. *Journal of Cell Biology* 126:433-443.

McGough, A. and M. Way. 1995. Molecular model of an actin filament capped by a severing protein. *Journal of Structural Biology* 115:144-150.

McGough, A., W. Chiu, and M. Way. 1998. Determination of the gelsolin binding site on F-actin: implications for severing and capping. *Biophysical Journal* 74:764-772.

McLaughlin, P.J., J.T. Gooch, H.G. Mannherz, and A.G. Weeds. 1993. Structure of gelsolin segment 1-actin complex and the mechanism of filament severing [see comments]. *Nature* 364:685-692.

McLaughlin, P.J. and A.G. Weeds. 1995. Actin-binding protein complexes at atomic resolution. [Review] [93 refs]. *Annual.Review.of.Biophysics.&.Biomolecular.Structure.* 24:643-75:643-675.

Mendelson, R.A. and E. Morris. 1994. The structure of F-actin. Results of global searches using data from electron microscopy and X-ray crystallography. *Journal.of.Molecular.Biology.* 240:138-154.

Milligan, R.A. and P.F. Flicker. 1987. Structural relationships of actin, myosin, and tropomyosin revealed by cryo-electron microscopy. *Journal of Cell Biology* 105:29-39.

Milligan, R.A., M. Whittaker, and D. Safer. 1990. Molecular structure of F-actin and location of surface binding sites. *Nature* 348:217-221.

Millonig, R., H. Salvo, and U. Aebi. 1988. Probing actin polymerization by intermolecular cross-linking. *Journal of Cell Biology* 106:785-796.

Moore, P.B., H.E. Huxley, and D.J. DeRosier. 1970. Three-dimensional reconstruction of F-actin, thin filaments and decorated thin filaments. *Journal.of.Molecular.Biology.* 50:279-295.

Moore, S. 1981. Pancreatic DNaseI. In The Enzymes. P.D. Boyer, editor. Academic Press, New York. 281-296.

Nagafuchi, A., M. Takeichi, and S. Tsukita. 1991. The 102 kd cadherin-associated protein: similarity to vinculin and posttranscriptional regulation of expression. *Cell* 65:849-857.

Ollo, R. and T. Maniatis. 1987. Drosophila Kruppel gene product produced in a baculovirus expression system is a nuclear phosphoprotein that binds to DNA. *Proceedings of the National Academy of Sciences of the United States of America* 84:5700-5704.

Orlova, A. and E.H. Egelman. 1992. Structural basis for the destabilization of F-actin by phosphate release following ATP hydrolysis. *Journal.of.Molecular.Biology.* 227:1043-1053.

Orlova, A. and E.H. Egelman. 1995. Structural dynamics of F-actin: I. Changes in the C terminus. *Journal of Molecular Biology* 245:582-597.

Orlova, A., E. Prochniewicz, and E.H. Egelman. 1995. Structural dynamics of F-actin: II. Cooperativity in structural transitions. *Journal of Molecular Biology* 245:598-607.

Patkowski, A., J. Seils, W. Eimer, and T. Dorfmuller. 1991. Conformation of muscle proteins: a laser light-scattering study. *Biochemical Society Transactions* 19:507-508.

Pinder, J.C. and W.B. Gratzer. 1982. Investigation of the actin-deoxyribonuclease I interaction using a pyrene-conjugated actin derivative. *Biochemistry* 21:4886-4890.

Pinder, J.C., J.A. Sleep, P.M. Bennett, and W.B. Gratzer. 1995. Concentrated Tris solutions for the preparation, depolymerization, and assay of actin: application to erythroid actin. *Analytical.Biochemistry* 225:291-295.

Podolski, J.L. and T.L. Steck. 1988. Association of deoxyribonuclease I with the pointed ends of actin filaments in human red blood cell membrane skeletons. *Journal.of.Biological.Chemistry.* 263:638-645.

Pollard, T.D. 1983. Measurement of rate constants for actin filament elongation in solution. *Analytical Biochemistry* 134:406-412.

Pollard, T.D. 1986. Rate constants for the reactions of ATP- and ADP-actin with the ends of actin filaments. *Journal.of.Cell Biology.* 103:2747-2754.

Pollard, T.D. and J.A. Cooper. 1986. Actin and actin-binding proteins. A critical evaluation of mechanisms and functions. [Review] [281 refs]. *Annual Review of Biochemistry* 55:987-1035.

Pollard, T.D., I. Goldberg, and W.H. Schwarz. 1992. Nucleotide exchange, structure, and mechanical properties of filaments assembled from ATP-actin and ADP-actin. *Journal.of.Biological.Chemistry.* 267:20339-20345.

Pollard, T.D. 1993. Guidebook to the cytoskeletal and motor proteins. T. Kreis and R. Vale, editors. Oxford Univ.Press, New York. 3-11.

Pope, B. and A.G. Weeds. 1986. Binding of pig plasma gelsolin to F-actin and partial fractionation into calcium-dependent and calcium-independent forms. *European Journal of Biochemistry* 161:85-93.

Pope, B., J. Gooch, H. Hinssen, and A.G. Weeds. 1989. Loss of calcium sensitivity of plasma gelsolin is associated with the presence of calcium ions during preparation. *FEBS Letters* 259:185-188.

Pope, B., M. Way, and A.G. Weeds. 1991. Two of the three actin-binding domains of gelsolin bind to the same subdomain of actin. Implications of capping and severing mechanisms. *FEBS Letters* 280:70-74.

Pope, B., S. Maciver, and A. Weeds. 1995. Localization of the calcium-sensitive actin monomer binding site in gelsolin to segment 4 and identification of calcium binding sites. *Biochemistry* 34:1583-1588.

Pope, B.J., J.T. Gooch, and A.G. Weeds. 1997. Probing the effects of calcium on gelsolin. *Biochemistry* 36:15848-15855.

Porte, F. and M.C. Harricane. 1986. Interactions of plasma gelsolin with actin. Isolation and characterization of binary and ternary plasma-gelsolin-actin complexes. *European Journal of Biochemistry* 154:87-93.

Price, P.A., S. Moore, and W.H. Stein. 1969. Alkylation of a histidine residue at the active site of bovine pancreatic deoxyribonuclease. *Journal.of.Biological.Chemistry.* 244:924-928.

Prochniewicz, E., Q. Zhang, P.A. Janmey, and D.D. Thomas. 1996. Cooperativity in F-actin: binding of gelsolin at the barbed end affects structure and dynamics of the whole filament. *Journal.of.Molecular.Biology.* 260:756-766.

Puius, Y.A., E.L. Fedorov, L. Eichinger, M. Scheicher, and S.C. Almo. 2000. Mapping the functional surface of domain 2 in the gelsolin superfamily. *Biochemistry* 39:5322-5331.

(a) Rayment, I., H.M. Holden, M. Whittaker, C.B. Yohn, M. Lorenz, K.C. Holmes, and R.A. Milligan. 1993. Structure of the actin-myosin complex and its implications for muscle contraction [see comments]. *Science* 261:58-65.

(b) Rayment, I., W.R. Rypniewski, K. Schmidt-Base, R. Smith, D.R. Tomchick, M.M. Benning, D.A. Winkelmann, G. Wesenberg, and H.M. Holden. 1993. Three-dimensional structure of myosin subfragment-1: a molecular motor [see comments]. *Science* 261:50-58.

Rechsteiner, M. 1990. PEST sequences are signals for rapid intracellular proteolysis. [Review] [53 refs]. *Seminars in Cell Biology* 1:433-440.

Reinhard, M., M. Halbrugge, U. Scheer, C. Wiegand, Jockusch, BM, and U. Walter. 1992. The 46/50 kDa phosphoprotein VASP purified from human platelets is a novel protein associated with actin filaments and focal contacts. *EMBO Journal* 11:2063-2070.

Rich, S.A. and J.E. Estes. 1976. Detection of conformational changes in actin by proteolytic digestion: evidence for a new monomeric species. *Journal of Molecular Biology* 104:777-792.

Robinson, R.C., M. Mejillano, V.P. Le, L.D. Burtnick, H.L. Yin, and S. Choe. 1999. Domain movement in gelsolin: a calcium-activated switch. *Science* 286:1939-1942.

Rogers, S., R. Wells, and M. Rechsteiner. 1986. Amino acid sequences common to rapidly degraded proteins: the PEST hypothesis. *Science* 234:364-368.

Rogers, S.L. and V.I. Gelfand. 2000. Membrane trafficking, organelle transport, and the cytoskeleton. [Review] [46 refs]. *Current Opinion in Cell Biology* 12:57-62.

Rohrschneider, L.R. 1980. Adhesion plaques of Rous sarcoma virus-transformed cells contain the src gene product. *Proceedings of the National Academy of Sciences of the United States of America* 77:3514-3518.

Rouayrenc, J.F. and F. Travers. 1981. The first step in the polymerisation of actin. *European Journal of Biochemistry* 116:73-77.

Ruhnau, K., A. Gaertner, and A. Wegner. 1989. Kinetic evidence for insertion of actin monomers between the barbed ends of actin filaments and barbed end-bound insertin, a protein purified from smooth muscle. *Journal of Molecular Biology* 210:141-148.

Safer, D. 1989. An electrophoretic procedure for detecting proteins that bind actin monomers. *Analytical Biochemistry* 178:32-37.

Sampath, P. and T.D. Pollard. 1991. Effects of cytochalasin, phalloidin, and pH on the elongation of actin filaments. *Biochemistry* 30:1973-1980.

Sato, N., N. Funayama, A. Nagafuchi, S. Yonemura, and S. Tsukita. 1992. A gene family consisting of ezrin, radixin and moesin. Its specific localization at actin filament/plasma membrane association sites. *Journal of Cell Science* 103:131-143.

Schagger, H. and G. von Jagow. 1987. Tricine-sodium dodecyl sulfate-polyacrylamide gel electrophoresis for the separation of proteins in the range from 1 to 100 kDa. *Analytical.Biochemistry* 166:368-379.

Schagger, H. and G. von Jagow. 1991. Blue native electrophoresis for isolation of membrane protein complexes in enzymatically active form. *Analytical.Biochemistry* 199:223-231.

Schagger, H., W.A. Cramer, and G. von Jagow. 1994. Analysis of molecular masses and oligomeric states of protein complexes by blue native electrophoresis and isolation of membrane protein complexes by two-dimensional native electrophoresis. *Analytical.Biochemistry* 217:220-230.

Schaller, M.D., C.A. Borgman, B.S. Cobb, R.R. Vines, A.B. Reynolds, and J.T. Parsons. 1992. pp125FAK a structurally distinctive protein-tyrosine kinase associated with focal adhesions. *Proceedings of the National Academy of Sciences of the United States of America* 89:5192-5196.

Schmid, M.F., J. Jakana, P. Matsudaira, and W. Chiu. 1993. Imaging frozen, hydrated acrosomal bundle from Limulus sperm at 7 A resolution with a 400 kV electron cryomicroscope. *Journal of Molecular Biology* 230:384-386.

Schoepper, B. and A. Wegner. 1991. Rate constants and equilibrium constants for binding of actin to the 1:1 gelsolin-actin complex. *European Journal of Biochemistry* 202:1127-1131.

Schroder, R.R., D.J. Manstein, W. Jahn, H. Holden, I. Rayment, K.C. Holmes, and J.A. Spudich. 1993. Three-dimensional atomic model of F-actin decorated with Dictyostelium myosin S1. *Nature* 364:171-174.

Schroer, E. and A. Wegner. 1985. Purification and characterization of a protein from chicken gizzard, which inhibits actin polymerization. *European Journal of Biochemistry* 153:515-520.

Schutt, C.E., J.C. Myslik, M.D. Rozycki, N.C. Goonesekere, and U. Lindberg. 1993. The structure of crystalline profilin-beta-actin. *Nature* 365:810-816.

Scopes, R.K. 1987. Dye-ligands and multifunctional adsorbents: an empirical approach to affinity chromatography. [Review] [61 refs]. *Analytical.Biochemistry* 165:235-246.

Sellers, J.R. and H.V. Goodson. 1995. Motor proteins 2: myosin. [Review] [2354 refs]. *Protein Profile.* 2:1323-1423.

Selve, N. and A. Wegner. 1986. Rate constants and equilibrium constants for binding of the gelsolin-actin complex to the barbed ends of actin filaments in the presence and absence of calcium. *European Journal of Biochemistry* 160:379-387.

Selve, N. and A. Wegner. 1987. pH-dependent rate of formation of the gelsolin-actin complex from gelsolin and monomeric actin. *European Journal of Biochemistry* 168:111-115.

Sheterline, P., J. Clayton, and J. Sparrow. 1995. Actin. [Review] [2085 refs]. *Protein Profile* 2:1-103.

Shu, W.P., D. Wang, and A. Stracher. 1992. Chemical evidence for the existence of activated G-actin. *Biochemical Journal* 283:567-573.

Spudich, J.A. and S. Watt. 1971. The regulation of rabbit skeletal muscle contraction. I. Biochemical studies of the interaction of the tropomyosin- troponin complex with actin and the proteolytic fragments of myosin. *Journal.of.Biological.Chemistry.* 246:4866-4871.

Stossel, T.P., J.H. Hartwig, P.A. Janmey, and D.J. Kwiatkowski. 1999. Cell crawling two decades after Abercrombie. [Review] [59 refs]. *Biochemical Society Symposia* 65:267-280.

Studier, F.W. and B.A. Moffatt. 1986. Use of bacteriophage T7 RNA polymerase to direct selective high-level expression of cloned genes. *Journal of Molecular Biology* 189:113-130.

Suck, D., C. Oefner, and W. Kabsch. 1984. Three-dimensional structure of bovine pancreatic DNase I at 2.5 A resolution. *EMBO Journal.* 3:2423-2430.

Suck, D. and C. Oefner. 1986. Structure of DNase I at 2.0 A resolution suggests a mechanism for binding to and cutting DNA. *Nature* 321:620-625.

Sun, H.Q., D.C. Wooten, P.A. Janmey, and H.L. Yin. 1994. The actin side-binding domain of gelsolin also caps actin filaments. Implications for actin filament severing. *Journal of Biological Chemistry* 269:9473-9479.

Sun, H.Q., K. Kwiatkowska, and H.L. Yin. 1996. beta-Thymosins are not simple actin monomer buffering proteins. Insights from overexpression studies. *Journal of Biological Chemistry* 271:9223-9230.

Sun, H.Q., M. Yamamoto, M. Mejillano, and H.L. Yin. 1999. Gelsolin, a multifunctional actin regulatory protein. [Review] [74 refs]. *Journal of Biological Chemistry* 274:33179-33182.

Taylor, J.M., A. Richardson, and J.T. Parsons. 1998. Modular domains of focal adhesion-associated proteins. [Review] [145 refs]. *Current Topics in Microbiology & Immunology* 228:K-u

Teubner, A., H.E. Meyer, R. Kaufmann, and A. Wegner. 1998. Derivation of insertin. *Cell Motility & the Cytoskeleton* 39:331-336.

Theriot, J.A. and T.J. Mitchison. 1993. The three faces of profilin. [Review] [24 refs]. *Cell* 75:835-838.

Tsukita, S. and M. Itoh. 1989. A new 400-kD protein from isolated adherens junctions: its localization at the undercoat of adherens junctions and at microfilament bundles such as stress fibers and circumferential bundles. *Journal of Cell Biology* 109:2905-2915.

Turner, C.E., J.R.J. Glenney, and K. Burridge. 1990. Paxillin: a new vinculin-binding protein present in focal adhesions. *Journal of Cell Biology* 111:1059-1068.

Vale, R.D. and R.A. Milligan. 2000. The way things move: looking under the hood of molecular motor proteins. [Review] [77 refs]. *Science* 288:88-95.

Van Troys, M., D. Dewitte, M. Goethals, J. Vandekerckhove, and C. Ampe. 1996. Evidence for an actin binding helix in gelsolin segment 2; have homologous sequences in segments 1 and 2 of gelsolin evolved to divergent actin binding functions? *FEBS Letters* 397:191-196.

Van Troys, M., D. Dewitte, J.L. Verschelde, M. Goethals, J. Vandekerckhove, and C. Ampe. 1997. Analogous F-actin binding by cofilin and gelsolin segment 2 substantiates their structural relationship. *Journal of Biological Chemistry* 272:32750-32758.

Van Troys, M., J. Vandekerckhove, and C. Ampe. 1999. Structural modules in actin-binding proteins: towards a new classification. [Review] [160 refs]. *Biochimica et Biophysica Acta* 1448:323-348.

Vandekerckhove, J. and K. Weber. 1979. Amino-acid sequence analysis of the amino-terminal tryptic peptides of different actins from the same mammal [proceedings]. *Archives.Internationales.de.Physiologie.et.de.Biochimie* 87:210-212.

Vandekerckhove, J., A. Deboben, M. Nassal, and T. Wieland. 1985. The phalloidin binding site of F-actin. *EMBO Journal* 4:2815-2818.

Vandekerckhove, J. 1990. Actin-binding proteins. [Review] [29 refs]. *Current Opinion in Cell Biology* 2:41-50.

Volkmann, N. and D. Hanein. 2000. Actomyosin: law and order in motility. [Review] [97 refs]. *Current Opinion in Cell Biology* 12:26-34.

Walsh, T.P., A. Weber, J. Higgins, E.M. Bonder, and M.S. Mooseker. 1984. Effect of villin on the kinetics of actin polymerization. *Biochemistry* 23:2613-2621.

Wang, F., R.V. Sampogna, and B.R. Ware. 1989. pH dependence of actin self-assembly. *Biophysical.Journal.* 55:293-298.

Wanger, M., T. Keiser, J.M. Neuhaus, and A. Wegner. 1985. The actin treadmill. [Review] [57 refs]. *Canadian Journal of Biochemistry & Cell Biology* 63:414-421.

Wanger, M. and A. Wegner. 1985. Equilibrium constant for binding of an actin filament capping protein to the barbed end of actin filaments. *Biochemistry* 24:1035-1040.

Way, M. and A. Weeds. 1988. Nucleotide sequence of pig plasma gelsolin. Comparison of protein sequence with human gelsolin and other actin-severing proteins shows strong homologies and evidence for large internal repeats. *Journal.of.Molecular.Biology.* 203:1127-1133.

Way, M., J. Gooch, B. Pope, and A.G. Weeds. 1989. Expression of human plasma gelsolin in Escherichia coli and dissection of actin binding sites by segmental deletion mutagenesis. *Journal.of.Cell Biology.* 109:593-605.

Way, M., B. Pope, J. Gooch, M. Hawkins, and A.G. Weeds. 1990. Identification of a region in segment 1 of gelsolin critical for actin binding. *EMBO Journal.* 9:4103-4109.

Way, M., B. Pope, and A.G. Weeds. 1992. Evidence for functional homology in the F-actin binding domains of gelsolin and alpha-actinin: implications for the requirements of severing and capping. *Journal.of.Cell Biology.* 119:835-842.

Weber, A., M. Pring, S.L. Lin, and J. Bryan. 1991. Role of the N- and C-terminal actin-binding domains of gelsolin in barbed filament end capping. *Biochemistry* 30:9327-9334.

Weber, A., C.R. Pennise, and M. Pring. 1994. DNase I increases the rate constant of depolymerization at the pointed (-) end of actin filaments. *Biochemistry* 33:4780-4786.

Weeds, A. and S. Maciver. 1993. F-actin capping proteins. [Review] [60 refs]. *Current.Opinion.in Cell Biology.* 5:63-69.

Weeds, A.G., H. Harris, W. Gratzer, and J. Gooch. 1986. Interactions of pig plasma gelsolin with G-actin. *European.Journal.of.Biochemistry* 161:77-84.

Weigt, C., A. Gaertner, A. Wegner, H. Korte, and H.E. Meyer. 1992. Occurrence of an actin-inserting domain in tensin. *Journal of Molecular Biology* 227:593-595.

Wieland, T. and H. Faulstich. 1978. Amatoxins, phallotoxins, phallolysin, and antamanide: the biologically active components of poisonous Amanita mushrooms. [Review] [404 refs]. *CRC Critical Reviews in Biochemistry* 5:185-260.

Wilkins, J.A. and S. Lin. 1986. A re-examination of the interaction of vinculin with actin. *Journal of Cell Biology* 102:1085-1092.

Winder, S.J. and M.P. Walsh. 1990. Smooth muscle calponin. Inhibition of actomyosin MgATPase and regulation by phosphorylation. *Journal of Biological Chemistry* 265:10148-10155.

Witke, W., A.H. Sharpe, J.H. Hartwig, T. Azuma, T.P. Stossel, and D.J. Kwiatkowski. 1995. Hemostatic, inflammatory, and fibroblast responses are blunted in mice lacking gelsolin. *Cell* 81:41-51.

Worrall, A.F. and B.A. Connolly. 1990. The chemical synthesis of a gene coding for bovine pancreatic DNase I and its cloning and expression in Escherichia coli. *Journal.of.Biological.Chemistry.* 265:21889-21895.

Wulf, E., A. Deboben, F.A. Bautz, H. Faulstich, and T. Wieland. 1979. Fluorescent phallotoxin, a tool for the visualization of cellular actin. *Proceedings.of.the.National.Academy.of.Sciences.of.the.United.States.of.America.* 76:4498-4502.

Yamada, K.M. and B. Geiger. 1997. Molecular interactions in cell adhesion complexes. [Review] [69 refs]. *Current Opinion in Cell Biology* 9:76-85.

Yamamoto, H., M. Terabayashi, T. Egawa, E. Hayashi, H. Nakamura, and S. Kishimoto. 1989. Affinity separation of human plasma gelsolin on Affi-Gel Blue. *Journal.of.Biochemistry* 105:799-802.

Yamamoto, H., H. Ito, H. Nakamura, E. Hayashi, S. Kishimoto, T. Hashimoto, and K. Tagawa. 1990. Human plasma gelsolin binds adenosine triphosphate. [Review] [21 refs]. *Journal.of.Biochemistry* 108:505-506.

Yanisch-Perron, C., J. Vieira, and J. Messing. 1985. Improved M13 phage cloning vectors and host strains: nucleotide sequences of the M13mp18 and pUC19 vectors. *Gene* 33:103-119.

Yin, H.L. and T.P. Stossel. 1979. Control of cytoplasmic actin gel-sol transformation by gelsolin, a calcium-dependent regulatory protein. *Nature* 281:583-586.

Yin, H.L. 1987. Gelsolin: calcium- and polyphosphoinositide-regulated actin-modulating protein. [Review] [27 refs]. *Bioessays* 7:176-179.

Yin, H.L., K. Iida, and P.A. Janmey. 1988. Identification of a polyphosphoinositide-modulated domain in gelsolin which binds to the sides of actin filaments. *Journal of Cell Biology* 106:805-812.

Yu, F.X., D.M. Zhou, and H.L. Yin. 1991. Chimeric and truncated gCap39 elucidate the requirements for actin filament severing and end capping by the gelsolin family of proteins. *Journal of Biological Chemistry* 266:19269-19275.

Yu, F.X., H.Q. Sun, P.A. Janmey, and H.L. Yin. 1992. Identification of a polyphosphoinositide-binding sequence in an actin monomer-binding domain of gelsolin. *Journal.of.Biological.Chemistry.* 267:14616-14621.

Zimmerle, C.T. and C. Frieden. 1986. Effect of temperature on the mechanism of actin polymerization. *Biochemistry* 25:6432-6438.

Zimmerle, C.T. and C. Frieden. 1988. Effect of pH on the mechanism of actin polymerization. *Biochemistry* 27:7766-7772.

Zimmerle, C.T. and C. Frieden. 1988. pH-induced changes in G-actin conformation and metal affinity. *Biochemistry* 27:7759-7765.

Appendix A

Assay for the long term storage of G-Actin in 1M Tris, pH 8.0; ATP-G-Buffer solution

1M Tris, pH 8.0; ATP-G-Buffer

1M Tris, pH 8.0; 0.5mM DTT; 0.2mM $CaCl_2$; 0.2mM ATP; 1.0mM NaN_3.

ATP-G-Buffer

5mM Tris, pH 8.0; 0.5mM DTT; 0.2mM $CaCl_2$; 0.2mM ATP; 1.0mM NaN_3.

Pinder and co-workers (Pinder at al, 1995) have reported that high concentration Tris buffer solutions could be used for the long–term storage (over 6 months), of G-Actin, extracted from platelets. We have developed a protocol (adapted from those of Spudich and Watt, 1971, and Pinder et al, 1995) for the extraction and purification of G-Actin from rabbit muscle acetone powder (protocol details are described in the methods). We have used the actin monomer critical concentration ($[C_c]$) assay (5% pyrene labelled, see methods for details) to test the viability of 1M Tris, pH 8.0; ATP-G-Buffer, at 4°C, for the long-term storage of extracted G-Actin. This is a well documented and sensitive method for reporting the quality of monomeric actin, with regards to its ability to undergo polymerisation. Prior to $[C_c]$ assay and use in other experiments the G-Actin was subjected to size-exclusion on an S200 column (V_t ~ 135ml; 65cm x 1.6cm), in ATP-G-Buffer.

Fig. A.1 shows the elution profile from a similar gel-filtration experiment. Freshly prepared G-Actin always produced a similar profile. A slight leading-edge (arrow 1) followed by a second large sharp peak (arrow 2) were commonly observed. The area under peak 1 of the profile most likely contains an actin-dimer species (probably formed via a disulphide bridge between the Cys-374 residue of one monomer and the corresponding Cys-374 residue of the other) and also higher Mr. aggregates of denatured actin, often found in actin preparations (see Sheterline et al, 1995 for a

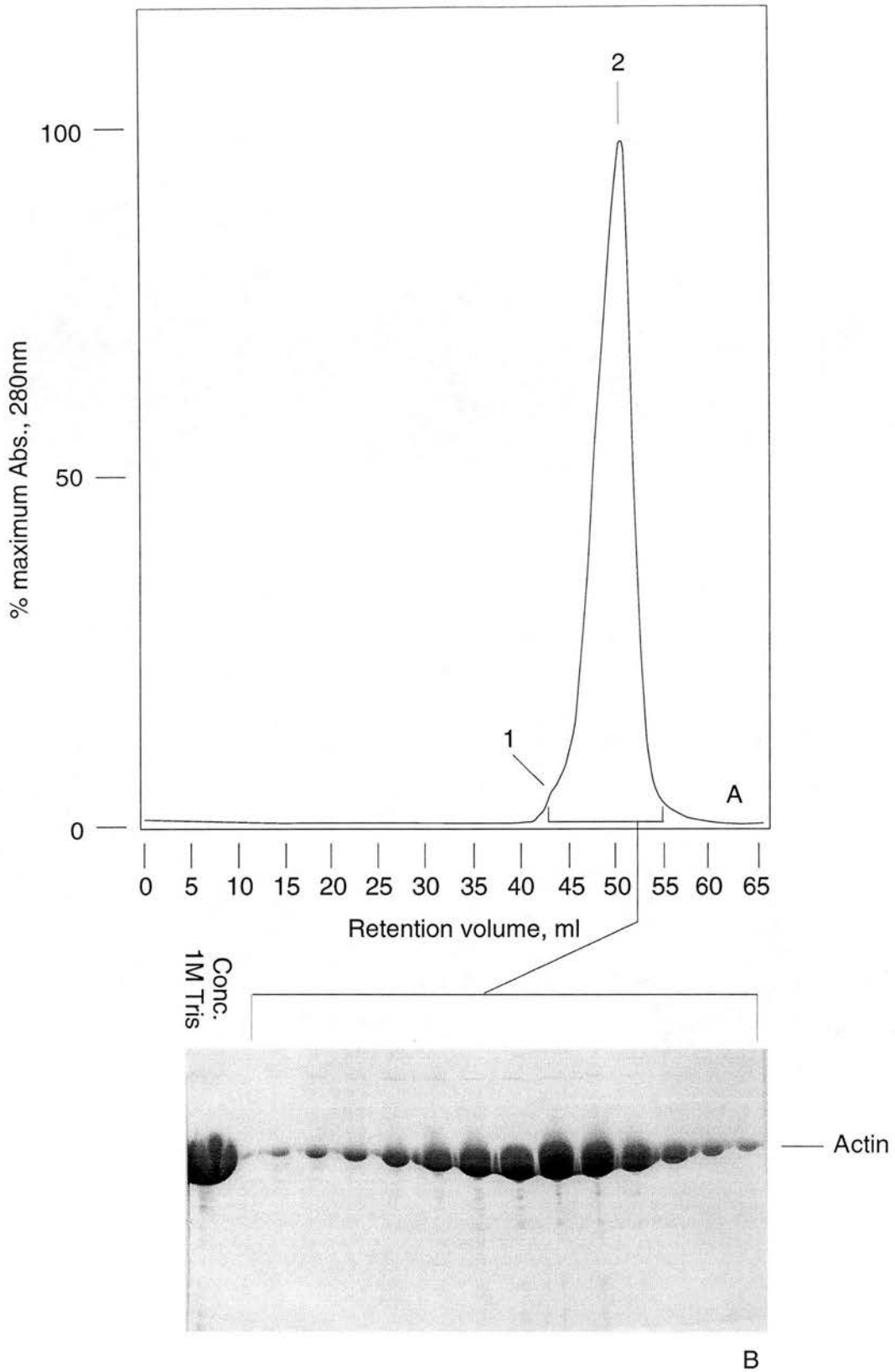

Fig. A.1. ***S200 size-exclusion chromatography of G-Actin prepared using the 1M Tris, pH 8.0; ATP-G-Buffer protocol.*** (A) A_{280nm} monitored elution profile of a 2ml (~ 5mg.ml^{-1}) sample of G-Actin, extracted in1M Tris, pH 8.0; ATP-G-Buffer, from an S200 size-exclusion column (V_t ~ 135ml; 65cm x 1.6cm), run in ATP-G-Buffer at 0.5ml.min^{-1}. (B). SDS-PAGE analysis of the elution profile in A. The arrows mark the elution positions of (1) actin dimer/denatured aggregates; (2) monomeric G-Actin. The column was calibrated with the following protein standards: ferritin (Mr. = 443kDa), catalase (232kDa), aldolase (158kDa), BSA (67kDa), ovalbumin (43kDa) and DNaseI (29kDa). Plots of $\log_{10}$ Mr. against the retention volume for these proteins were linear within this range. The elution volumes for peaks (1) and (2) corresponded to Mr. of 93kDa and 49kDa respectively. These values are in good agreement with the theoretical Mr. (84kDa and 42kDa for the dimer and monomer species, respectively). SDS-page was performed as described in the methods.

review). When pooling fractions of viable G-Actin care was taken to minimise the overlap between these two areas.

Table A.1 shows the [C_c] value taken from 10 different G-Actin preparations following 1, 2, 3, 4 or 6 months storage in 1M Tris, pH 8.0; ATP-G-Buffer. The [C_c] values for freshly prepared G-Actin compare favourably with those published by others, where conventional methods of extraction and purification have been employed in the preparation of G-Actin (Pollard, 1986; Sheterline et al, 1995). [C_c] values for G-Actin, stored in 1M Tris, pH 8.0; ATP-G-Buffer for up to 4 months do not increase significantly, and still compare favourably with those of freshly prepared actin, see table A.1. After 4 months the actin started to deteriorate (as judged by significant increases in the critical concentration).

However, the yield of high quality G-Actin obtained decreased steadily with time. We routinely obtained yields of 12 – 15mg of G-actin (with [C_c] <0.15μM) per gram of acetone powder for fresh preparations. As can be seen from table A.1 the yield drops to ~ 40% after 3 – 4 months. The ratio of the relative amounts of dimer and non-viable denatured aggregate species, to that of viable native G-Actin increased with time. This was reflected by the peak areas at elution positions 1 and 2, in fig. A.1, from S200 gel-filtration experiments performed on such samples, becoming approximately equal.

Steady denaturation of the G-Actin monomer still appears to occur, but at a very much reduced rate, in comparison to storage in ATP-G-Buffer. The high concentration of Tris buffer salts appears to have a stabilising effect on the actin monomer in solution, at 4°C.

We have used 1M Tris, pH 8.0: ATP-G-Buffer routinely for long-term G-Actin storage due to the practicality of obtaining "good" actin with a relatively simple and quick procedure. Other methods for the long-term storage of actin usually involve the flash freezing of F-Actin aliquots in liquid nitrogen. However, although this method allows for reasonable lengths of storage time and recovery, the processing time

(involving rounds of depolymerisation and size-exclusion chromatography under G-conditions) can take up to 4 – 5 days.

	$[C_c]$,μM										Yield ($mg.g^{-1}$ of acetone powder)
Length of storage	**Prep. 1**	**Prep. 2**	**Prep. 3**	**Prep. 4**	**Prep. 5**	**Prep. 6**	**Prep. 7**	**Prep. 8**	**Prep. 9**	**Prep. 10**	**Storage in 1M Tris followed by batch S200 runs in ATP-G-Buffer**
Fresh	0.14	0.12	0.15	0.13	0.11	0.15	0.14	0.14	0.13	0.18	12 – 15
1 Month	0.12	0.14	0.21	0.16	0.14	0.14	0.15	0.21	0.15	0.13	10
2 Months	0.18	0.15	0.25	0.18	0.16	0.17	0.16	0.19	0.17	0.13	8
3 Months	0.21	0.19	0.19	0.20	0.13	0.17	0.19	0.21	0.24	0.15	6 – 7
4 Months	0.16	0.19	0.21	0.19	0.18	0.19	0.20	0.23	0.18	0.19	5
6 Months	0.19	0.18	0.23	0.24	0.25	0.21	0.26	0.27	0.21	0.19	5

Table A.1. ***Assay of the viability of 1M Tris, pH 8.0: ATP-G-Buffer for the long-term storage of G-Actin.*** The critical monomer concentration of G-Actin preparations, following purification by gel-filtration chromatography on an S200 size-exclusion column (V_t ~ 135ml; 65cm x 1.6cm), in ATP-G-Buffer, was used to judge the quality of the G-Actin. $[C_c]$ values range from 0.1μM - 0.2μM, and compare favourably with published values for "good" viable actin (Pollard, 1986). (Protein purification and critical concentration assays were performed as described in the methods).

Appendix B

Activity assay and long-term storage conditions for recombinant DNaseI/[H134Q]

An actin critical concentration assay ($[C_c]$), performed in the presence of 0.5μM recombinant DNaseI, was used as an assay for the relative activity of DNaseI. The amount of inactive protein was compensated for in subsequent experiments by the further addition of the appropriate amount of protein so the final activity was 100%. Fig. B.1 shows the result from a typical $[C_c]$ activity assay performed on a preparation of newly purified DNaseI.

Table B.1 shows the results from various $[C_c]$ activity assays performed on DNaseI stored for differing lengths of time, under different storage conditions.

		Storage conditions	
	Buffer A: *10mM Tris, pH 7.6; 2mM $CaCl_2$; 1mM NaN_3*, stored at 4°C	**Buffer A plus 20% glycerol, stored at –20°C**	**Buffer A plus 20% glycerol, flash frozen in liquid nitrogen, stored at –70°C**
Length of storage		**Activity**	
Fresh	80 – 95%	N/A	N/A
1 month	80 – 95%	60 – 85%	50 – 80%
2 months	50 – 70%	60 – 85%	50 – 80%
3 months	<25%	50 – 75%	50 – 75%
4 months	N/A	50 – 75%	50 – 75%
5 months	N/A	45 – 70%	50 – 70%
6 months	N/A	40 – 65%	40 – 70%

Table B.1. ***Storage conditions for recombinant DNaseI/[H134Q].*** Actin critical monomer concentration activity assays, in the presence of DNaseI (0.5μM), were performed on a variety of samples stored for differing lengths of time and under different conditions. Prior to $[C_c]$ assay protein samples were subjected to high-speed centrifugation and size-exclusion on an S200 gel-filtration column (V_t ~ 135ml; 65cm x 1.6cm), run in ATP-G-Buffer at $0.5ml.min^{-1}$. ($[C_c]$ assay was performed as described in methods).

Short term storage in Buffer A (see table B.1) was viable for 7 – 8 weeks. Longer-term storage required the addition of a cyro-protectant (20% glycerol) and freezing at –20°C or –70°C. Both conditions gave similar results however, the recovery yield of active protein was *very* sample dependent.

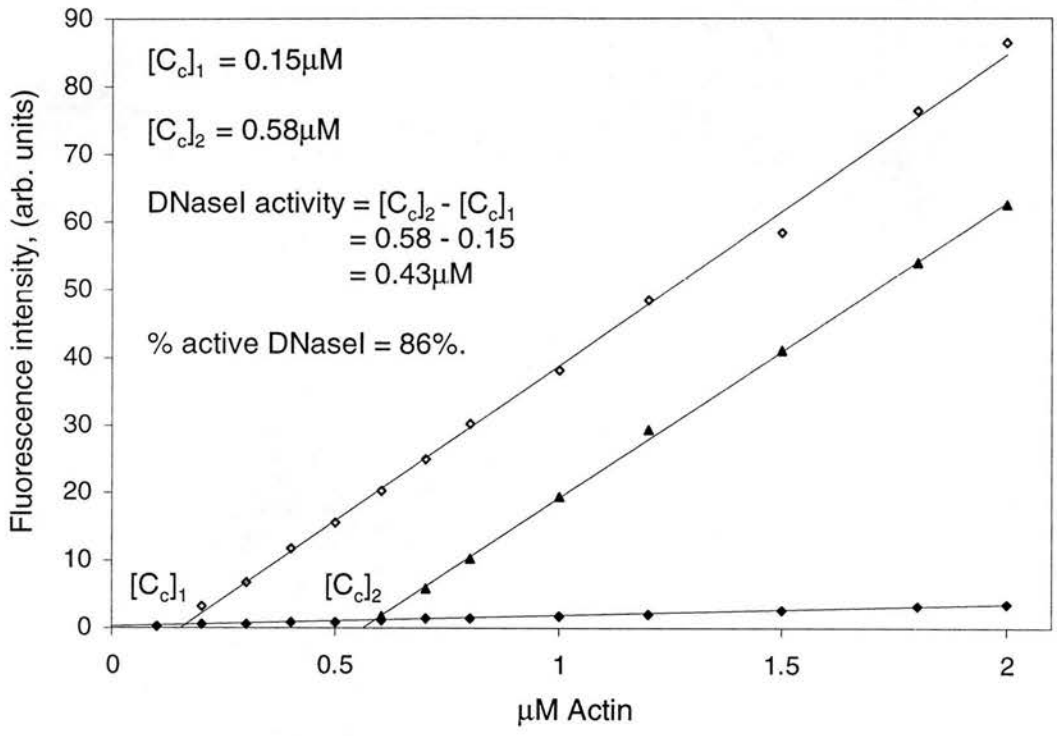

Fig. B.1. ***Assay of recombinant DNaseI/[H134Q] activity.*** Actin critical concentration assay performed at 20°C (5% pyrene-labelled actin) in the absence or presence of 0.5μM recombinant DNaseI/[H134Q]. The excitation wavelength was 366nm, the emission wavelength was 384nm, with a 5nm slit width for both. *Closed squares* represent actin incubated in ATP-G-Buffer; *open squares* represent actin incubated in ATP-F-Buffer; *triangles* represent actin incubated in ATP-F-Buffer, in the presence of 0.5μM DNaseI. DNaseI binds stoichiometrically to the pointed ends of actin monomers (K_d ~ 0.1nM) resulting in its sequestration from the monomers pool available for polymerisation. This results in an increase in the apparent $[C_c]$; the increase directly reflecting the amount of *active* DNaseI present. In this example activity is ~ 86% of the added 0.5μM. (0.58μM - 0.15μM = 0.43μM; 0.43/0.5 = 0.86). $[C_c]$ assay was performed as described in methods.